

## INFORMATION TO USERS

This manuscript has been reproduced from the microfilm master. UMI films the text directly from the original or copy submitted. Thus, some thesis and dissertation copies are in typewriter face, while others may be from any type of computer printer.

**The quality of this reproduction is dependent upon the quality of the copy submitted.** Broken or indistinct print, colored or poor quality illustrations and photographs, print bleedthrough, substandard margins, and improper alignment can adversely affect reproduction.

In the unlikely event that the author did not send UMI a complete manuscript and there are missing pages, these will be noted. Also, if unauthorized copyright material had to be removed, a note will indicate the deletion.

Oversize materials (e.g., maps, drawings, charts) are reproduced by sectioning the original, beginning at the upper left-hand corner and continuing from left to right in equal sections with small overlaps. Each original is also photographed in one exposure and is included in reduced form at the back of the book.

Photographs included in the original manuscript have been reproduced xerographically in this copy. Higher quality 6" x 9" black and white photographic prints are available for any photographs or illustrations appearing in this copy for an additional charge. Contact UMI directly to order.

# U·M·I

University Microfilms International  
A Bell & Howell Information Company  
300 North Zeeb Road, Ann Arbor, MI 48106-1346 USA  
313/761-4700 800/521-0600



Order Number 9236631

**Differential inhibition of the plastoquinone reductase activity by weak organic acids and its relationship to the bicarbonate effect in spinach thylakoids**

Xu, Chunhe, Ph.D.

University of Illinois at Urbana-Champaign, 1992

**U·M·I**  
300 N. Zeeb Rd.  
Ann Arbor, MI 48106



**DIFFERENTIAL INHIBITION OF THE PLASTOQUINONE REDUCTASE ACTIVITY  
BY WEAK ORGANIC ACIDS AND ITS RELATIONSHIP  
TO THE BICARBONATE EFFECT IN SPINACH THYLAKOIDS**

BY

CHUNHE XU

Dipl., Fudan University, 1970  
M.S., Academia Sinica, 1982

THESIS

Submitted in partial fulfillment of the requirements  
for the degree of Doctor of Philosophy in Biophysics  
in the Graduate College of the  
University of Illinois at Urbana-Champaign, 1992

Urbana, Illinois

UNIVERSITY OF ILLINOIS AT URBANA-CHAMPAIGN

THE GRADUATE COLLEGE

APRIL 27, 1992

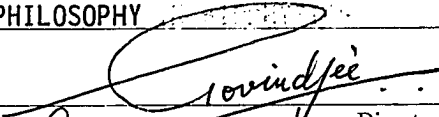
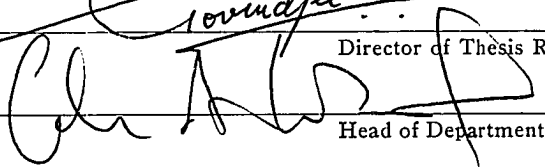
WE HEREBY RECOMMEND THAT THE THESIS BY

CHUNHE XU

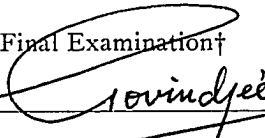
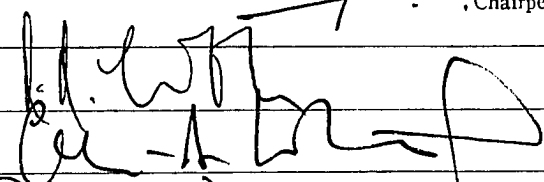

ENTITLED DIFFERENTIAL INHIBITION OF THE PLASTOQUINONE REDUCTASE ACTIVITY  
BY WEAK ORGANIC ACIDS AND ITS RELATIONSHIP TO THE BICARBONATE  
EFFECT IN SPINACH THYLAKOIDS

BE ACCEPTED IN PARTIAL FULFILLMENT OF THE REQUIREMENTS FOR

THE DEGREE OF DOCTOR OF PHILOSOPHY

  
\_\_\_\_\_  
Director of Thesis Research  
  
\_\_\_\_\_  
Head of Department

Committee on Final Examination†

  
\_\_\_\_\_  
Chairperson  
  
\_\_\_\_\_  
  
\_\_\_\_\_  
Peter G. DeBorja

† Required for doctor's degree but not for master's.

© Copyright by Chunhe Xu, 1992

**DIFFERENTIAL INHIBITION OF THE PLASTOQUINONE REDUCTASE ACTIVITY  
BY WEAK ORGANIC ACIDS AND ITS RELATIONSHIP  
TO THE BICARBONATE EFFECT IN SPINACH THYLAKOIDS**

Chunhe Xu, Ph.D.  
Department of Physiology and Biophysics  
University of Illinois at Urbana-Champaign, 1992  
Govindjee, Adviser

Bicarbonate-reversible inhibition of the electron acceptor side of photosystem II (PS II), but not of photosynthetic bacteria, has been known for a long time. In formate treated thylakoids, the  $[Q_A^-]$  decays show a larger slowing down after the second and subsequent flashes than after the first flash. This suggests a blockage of protonation that stabilizes  $Q_B^-$ .

Measurements of the initial binding rate constant of formate/formic acid, when one of the two ( $HCO_2^-/HCOOH$ ) equilibrium species is kept constant by changing the pH of the medium, suggest that acid, not the anion, is the binding species. This conclusion is also consistent with the preliminary data on the observed pH dependence of the binding of (halogenated)-acetates as well as (methyl)acetates.

Several halogenated acetates increase the lifetime of the  $Q_A^-$  reoxidation by  $Q_B/Q_B^-$  as well as the equilibrium  $[Q_A^-]$ . These effects are reversed, in different degrees, upon the bicarbonate addition. The inhibitory activity on the  $Q_A^-$ -to- $Q_B^{(-)}$  electron transfer decreases, whereas the bicarbonate reversibility increases in the following order: (1) trichloroacetic acid > dichloroacetic acid > monochloroacetic acid > acetic acid; (2) monobromoacetic acid  $\geq$  monochloroacetic acid > monofluoroacetic acid > acetic acid. Trichloroacetic acid, with a log P (partition coefficient) of 1.54



and a dipole moment of 2.12 Debye, almost totally blocks the  $Q_A^-$  reoxidation just as DCMU does. A correlation between the inhibitory activity and the geometry as well as the hydrophobicity of the inhibitors is observed, demonstrating the importance of the  $CX_3$  group of these chemicals in affecting the plastoquinone reduction. Furthermore, monochloroacetic acid, with an asymmetric chlorine atom, a log P of 0.32 and a dipole moment of 3.25 Debye, converts, in a bicarbonate-reversible manner, the flash number dependence of  $[Q_A^-]$  with the maxima occurring at even to that at odd flashes. This apparent stabilization of  $Q_B^-$ , caused by MCA, is explained by a combined effect of the shift of the  $Q_A^-Q_B \rightleftharpoons Q_AQ_B^-$  equilibrium towards  $[Q_A^-]$  and an increase of the ratio of  $Q_B^-$  to  $Q_B$  in dark.

## ACKNOWLEDGMENTS

I would like to express my gratitude to Professor Govindjee for his support, encouragement, discussion and criticisms during the course of this thesis. I would like to thank Professor Antony R. Crofts for discussions. Thanks are also due to Drs. Julian Eaton-Rye, Danny J. Blubaugh, Shinichi Taoka and Jin Xiong for their help during this research. Finally, I am grateful to Profs. Jack Widholm, Gregorio Weber, Colin Wraight, Thomas Ebrey, Peter Debrunner, Steven Zimmermann, John Katzenellenbogen and Christos Georgiou for their helpful suggestions. Collaboration with Yong Zhu is also appreciated. The School of Life Sciences Artists' Office was helpful in preparing the figures used in this thesis.

This research was supported mainly by Mcknight Interdisciplinary Grant (1-5-89003) to the University of Illinois at Urbana-Champaign. During 1991-1992, I was supported by a Campus Research Grant (Beckman Award) given to Professor Govindjee. I am thankful to the University of Illinois for a "Dissertation Research Grant" that allowed me to prepare this thesis.

## TABLE OF CONTENTS

CHAPTER	PAGE
<b>I. INTRODUCTION.....</b>	<b>1</b>
A. Background of Photosystem II (PS II).....	1
B. Background for the Bicarbonate Effect in PS II.....	6
C. Objective of this Thesis.....	11
<b>II. MATERIALS AND METHODS.....</b>	<b>15</b>
A. Isolation of Spinach Thylakoids.....	15
B. Growth of <i>Chlamydomonas reinhardtii</i> Cells.....	16
C. Formate Treatment of <i>Chlamydomonas reinhardtii</i> Cells.....	16
D. Heat Treatment of the Cells.....	17
E. Measurements of Oxygen Evolution.....	17
F. Measurement of the Chlorophyll (Chl) <u>a</u> Fluorescence Transient.....	18
G. Measurement of the Decay Kinetics of Chl <u>a</u> Fluores- cence by Using the Double Flash Technique.....	18
H. Calculation of the Concentration of $Q_A^-$ .....	19
I. Fitting of $[Q_A^-]$ Decay Into Exponential Decays.....	20
J. Measurement of the Kinetics of Formate Binding in the Dark-adapted Spinach Thylakoid Suspension.....	20
K. Calculation of Molecular Geometries as well as the Dipole Moment.....	21
L. Calculation of the Hydrophobic Constant ( $\pi$ ) of Acetic and Chloroacetic Acids.....	21
M. Chemicals.....	21
<b>III. FLASH NUMBER DEPENDENCE OF THE DECAY OF <math>[Q_A^-]</math> UPON FORMATE TREATMENT AND THE PROTONATION HYPOTHESIS.....</b>	<b>22</b>
A. Introduction.....	22
B. Materials and Methods.....	23
C. Results and Discussion.....	24
D. A Working Scheme for the Action of Formate at the Plastoquinone Reductase Site.....	33
E. Conclusion.....	37
<b>IV. KINETIC CHARACTERISTICS OF FORMATE/FORMIC ACID BINDING AT THE PLASTOQUINONE REDUCTASE SITE SUGGESTS THAT FORMIC ACID IS THE ACTIVE SPECIES.....</b>	<b>39</b>
A. Introduction.....	39
B. Materials and Methods.....	40
C. Results and Discussion.....	42
1. Determination of the rate constants for binding and unbinding, and the dissociation constant of formate at the plastoquinone reductase site.....	42
2. The binding species: formate or formic acid?.....	45
D. Conclusion.....	53

V.	<b>DIFFERENTIAL EFFECTS ON <math>Q_A^-</math> REOXIDATION AND EQUILIBRIA BY CHLOROACETIC ACIDS EXHIBIT THE IMPORTANT ROLE OF <math>CX_3</math> GROUP</b> .....	55
	A. Introduction.....	55
	B. Materials and Methods.....	55
	C. Results.....	56
	1. Inhibition of the $Q_A^-$ reoxidation and effects on $Q_A^-$ equilibria by acetate and three chloroacetates.....	56
	a. Acetate.....	56
	b. Monochloroacetate.....	62
	c. Dichloroacetate.....	64
	d. Trichloroacetate.....	67
	e. A comparison of the effect of chloroacetates: a hierarchy in the effects on the $Q_A Q_B$ reactions.....	69
	f. Concentration dependence of chloroacetates.....	70
	g. pH dependence.....	73
	2. The inhibition of the $Q_A^-$ reoxidation and effects on $Q_A^-$ equilibria by phenol.....	75
	D. Discussion.....	77
	E. Conclusion.....	89
VI.	<b>DIFFERENTIAL EFFECTS ON <math>Q_A^-</math> REOXIDATION AND EQUILIBRATION BY MONOHALOGENATED ACETATES AND THE BICARBONATE-REVERSIBLE APPARENT STABILIZATION OF <math>Q_B^-</math> BY MONOCHLORO-ACETATE</b> .....	90
	A. Introduction.....	90
	B. Materials and Methods.....	90
	C. Results and Discussion.....	91
	1. Halogenated acetic acids differentially affect the $Q_A^-$ -to- $Q_B$ electron flow and equilibria.....	91
	2. MCA induces apparent stabilization of $Q_B^-$ .....	93
	D. Conclusion.....	98
VII.	<b>PRELIMINARY EXPERIMENTS ON THE EFFECTS ON <math>Q_A^-</math> REOXIDATION AND EQUILIBRATION BY TRIMETHYL ACETATE, PROPIONIC ACID AND AZIDE</b> .....	100
	A. Introduction.....	100
	B. Materials and Methods.....	100
	C. Results and Discussion.....	101
	D. Conclusion.....	106
VIII.	<b>PRELIMINARY RESULTS ON AN ADDITIONAL EFFECT OF FORMATE/FORMIC ACID PRIOR TO <math>Q_A</math> IN PS II</b> .....	107
	A. Introduction.....	107
	B. Materials and Methods.....	108
	C. Results and Discussion.....	109
	1. Experiments with <i>Chlamydomonas reinhardtii</i> .....	109
	2. Experiments with spinach thylakoids.....	112
	D. Conclusion.....	115

<b>IX.</b>	<b>SUMMARY AND GENERAL DISCUSSION.....</b>	<b>117</b>
	A. Heirarchy of Inhibitory Effects: Correlation with Hydrophobicity.....	117
	B. Protonation and Active Inhibitory Species.....	121
	C. General Discussion: Binding Niche.....	127
	D. Final Remarks.....	136
<b>REFERENCES.....</b>		<b>140</b>
<b>APPENDIX:</b>	<b>A. Characteristics of Five New Photoautotrophic Suspension Cultures Including Two <i>Amaranthus</i> Species and a Cotton Strain Growing on Ambient CO<sub>2</sub> Levels by Xu et al. (1988).....</b>	<b>151</b>
	B. Fluorescence Characteristics of Photoautotrophic Soybean Cells by Xu et al. (1989).....	156
	C. Chlorophyll <u>a</u> Fluorescence Measurements of Iso- lated Spinach Thylakoids Obtained by Using Single-Laser-based Flow Cytometry by Xu et al. (1990).....	170
<b>VITA.....</b>		<b>180</b>

## LIST OF TABLES

TABLE	PAGE
3.1. Amplitudes (A) and lifetimes ( $\tau$ ) of three components of the $Q_A^-$ decay after flashes 1-5, in control thylakoids at pH's 6.5 and 7.5.....	31
3.2. Amplitudes (A) and lifetimes ( $\tau$ ) of three components of the $Q_A^-$ decay after flashes 1-5, in 100 mM formate-treated thylakoids at pH's 6.5 and 7.5.....	31
4.1. The on-rate ( $k_F$ ), the off-rate ( $k_{-F}$ ) binding constant, and the dissociation constant ( $K_F$ ) of the binding species (considered to be <i>formate</i> here) in spinach thylakoids.....	46
4.2. The on-rate ( $k_F$ ), the off-rate ( $k_{-F}$ ) binding constant, and the dissociation constant ( $K_F$ ) of the binding species (considered to be <i>formic acid</i> here) in spinach thylakoids.....	46
5.1. Amplitudes (A) and lifetimes ( $\tau$ ) of three components of the $Q_A^-$ decay after <b>flash 1</b> , in control and (chloro)-acetate-treated ( $\pm$ bicarbonate) spinach thylakoids at pH 6.0.....	60
5.2. Amplitudes (A) and lifetimes ( $\tau$ ) of three components of the $Q_A^-$ decay after <b>flash 2</b> , in control and (chloro)-acetate-treated ( $\pm$ bicarbonate) spinach thylakoids at pH 6.0.....	60
5.3. Amplitudes (A) and lifetimes ( $\tau$ ) of three components of the $Q_A^-$ decay after <b>flash 3</b> , in control and (chloro)-acetate-treated ( $\pm$ bicarbonate) spinach thylakoids at pH 6.0.....	61
5.4. Amplitudes (A) and lifetimes ( $\tau$ ) of three components of the $Q_A^-$ decay after <b>flash 4</b> , in control and (chloro)-acetate-treated ( $\pm$ bicarbonate) spinach thylakoids at pH 6.0.....	61
5.5. Dipole moments, the angles between two major planes, log of the partition coefficient and hydrophobic constant of (chloro)acetic acids.....	86
6.1. Amplitudes (A) and lifetimes ( $\tau$ ) of three components of the $[Q_A^-]$ decay in control and halogenated acetate-treated spinach thylakoids at pH 6.0.....	94
9.1. A summary of major results in this thesis.....	118

## LIST OF FIGURES

FIGURE	PAGE
1.1. A diagram showing the primary photochemical reactions and electron flow pathway in oxygenic photosynthesis.....	2
3.1. Effect of formate addition on the Chl <u>a</u> fluorescence yield decay at pH 6.5 in spinach thylakoids.....	25
3.2. Effect of formate addition on the Chl <u>a</u> fluorescence yield decay at pH 7.5 in spinach thylakoids.....	26
3.3. Effect of formate addition on the Chl <u>a</u> fluorescence yield decay at pH 6.0 in spinach thylakoids.....	27
3.4. Time course of formate-induced change in the yield of Chl <u>a</u> fluorescence in spinach thylakoids at 3 different pH's.....	29
3.5. A working scheme showing the formate/formic acid (F) binding mechanism which effects the two electron gate in PS II reaction centers.....	34
4.1. Concentration and time dependence of formate/formic acid binding at pH 6.5, as measured by $[Q_A^-]$ 1 ms after the second actinic flash.....	43
4.2. Concentration dependence of the initial rate constant for formate/formic acid binding.....	44
4.3. pH dependence of the on-rate ( $k_f$ ) and the off-rate ( $k_{-f}$ ) binding constants when formate or formic acid is considered to be the binding species.....	47
4.4. Formic acid concentration dependence of the initial on-rate binding constant of formate/formic acid binding.....	50
4.5. Formate concentration dependence of the initial on-rate binding constant of formate/formic acid binding.....	51
4.6. Lineweaver-Burk plot for the initial binding constant when formate or formic acid is considered to be the binding species.....	52
5.1. Decay of $[Q_A^-]$ after an actinic flash in control and acetate-treated ( $\pm$ bicarbonate) thylakoids at pH 7.5 and 6.0.....	57
5.2. Decay of $[Q_A^-]$ after an actinic flash in control and monochloroacetate-treated ( $\pm$ bicarbonate) spinach thylakoids at pH 7.5 and 6.0.....	62

FIGURE	PAGE
5.3. Decay of $[Q_A^-]$ after an actinic flash in control and dichloroacetate-treated ( $\pm$ bicarbonate) spinach thylakoids at pH 7.5 and 6.0.....	65
5.4. Decay of $[Q_A^-]$ after an actinic flash in control and trichloroacetate-treated ( $\pm$ bicarbonate) spinach thylakoids at pH 7.5 and 6.0.....	68
5.5. A comparison of the $[Q_A^-]$ decay after flash 1 with that after flash 2 in the presence of acetate, monochloroacetate (MCA), dichloroacetate (DCA) and trichloroacetate (TCA) at pH 6.....	71
5.6. Dependence of $[Q_A^-]_{\text{treated}} - [Q_A^-]_{\text{control}}$ on acetate and chloroacetate concentrations at pH 6 and 7.5.....	72
5.7. Dependence of $[Q_A^-]_{\text{treated}} - [Q_A^-]_{\text{control}}$ on the concentration of trichloroacetate at different pH's and after different actinic flashes.....	74
5.8. Decay of $[Q_A^-]$ after an actinic flash in control and phenol-treated ( $\pm$ bicarbonate) thylakoids at pH 7.5 and 6.0.....	76
5.9. Dependence of $[Q_A^-]_{\text{treated}} - [Q_A^-]_{\text{control}}$ on the phenol concentration.....	78
5.10. A comparison of the change in $[Q_A^-]$ with the change in the proportion of the ionic or acidic form of the inhibitors.....	83
5.11. A comparison of the pH dependence of the change of $[Q_A^-]$ with the change in proportion of trichloroacetate or trichloroacetic acid and their ratio.....	84
5.12. Molecular geometry of acetic acid and chloroacetic acids in an apolar solvent.....	87
6.1. $[Q_A^-]$ decays in the monohalogenated acetate-treated thylakoids.....	92
6.2. Flash number dependence of $[Q_A^-]$ at 300 and 400 $\mu$ s after actinic flashes in control and MCA treated ( $\pm$ bicarbonate) thylakoids at pH 6.....	95
6.3. Flash number dependence of $[Q_A^-]$ from 110 $\mu$ s to 100 ms after actinic flashes in control and MCA treated ( $\pm$ bicarbonate) thylakoids at pH 6.....	96



Figure	PAGE
7.1. Decay of $[Q_A^-]$ after flash 1 or 2 in control, trimethyl- acetate-treated and propionic acid treated thylakoids at pH 6.0.....	102
7.2. Effects of formate and azide on the decay of variable Chl <u>a</u> fluorescence yield, measured at pH 6.0 and after the first actinic flash.....	105
8.1. Chl <u>a</u> fluorescence transient in mild-heat and hydroxyl- amine treated <i>C. Reinhardtii</i> cells.....	111
8.2. Effect of formate addition on the Chl <u>a</u> fluorescence yield decay up to 2 ms at pH 6.0 in spinach thylakoids....	113
8.3. Time dependence of formate/formic acid binding at diffe- rent pH, as measured by Chl <u>a</u> fluorescence yield 1 ms after flashes 1 and 2.....	114
9.1. A schematic diagram of a possible folding model of the D-E loop, D and E $\alpha$ -helices of the D1 and D2 polypeptides of <i>Synechocystis sp.</i> PCC 6803.....	124
9.2. Sequence alignment of the L and M subunits from <i>Rh.</i> <i>viridis</i> and the D1 and D2 proteins from spinach chloroplast.....	128
9.3 (A). A schematic diagram of a portion of the D1 and D2 polypeptides of PS II in $Q_A$ -Fe- $Q_B$ region.....	132
9.3 (B). Another view of Fig.9.3. (A).....	133

## ABBREVIATIONS

- Chl: chlorophyll
- D: secondary electron donor to photosystem II
- DBMIB: 2,5-dibromo-6-isopropyl-p-benzoquinone
- DCA: dichloroacetate/dichloroacetic acid
- DCMU: 3-(3,4-dichlorophenyl)-1,1-dimethylurea
- DMQ: dimethylquinone
- FRC: reaction center with formate/formic acid bound
- HEPES: N-2-Hydroxyethylpiperazine-N'-2-ethanesulfonic acid
- MBA: monobromoacetate/monobromoacetic acid
- MCA: monochloroacetate/monochloroacetic acid
- MES: 2-[N-Morpholino]ethane-sulfonic acid
- MFA: monofluoroacetate/monofluoroacetic acid
- PQ: plastoquinone
- PS II: photosystem II
- Q<sub>A</sub>: the one-electron acceptor and primary bound plastoquinone of photosystem II
- Q<sub>B</sub>: the two-electron acceptor and secondary loosely bound plastoquinone of photosystem II
- RC: reaction center
- TCA: trichloroacetate/trichloroacetic acid
- Z: the immediate electron donor to photosystem II reaction center

## CHAPTER I. INTRODUCTION

### A. Background of Photosystem II (PS II)

The conversion of light energy into chemical energy is one of the fundamental processes of life. In oxygenic photosynthesis, absorbed light energy is used to transfer electrons from water to  $\text{CO}_2$ , with the concomitant release of  $\text{O}_2$  and production of carbohydrate ( $\text{CH}_2\text{O}$ ). Two photosystems and two light reactions (I and II) are required for this process to be completed. In this thesis, we focus on photosystem II (PS II), the water-plastoquinone oxido-reductase. The ultimate important oxidation product, oxygen, is a byproduct of the oxidation of water molecules in this system. The reductant produced by PS II is plastoquinol and as, we shall see later, it is the reduction of plastoquinone that is of interest to my work. A schematic model of the PS II reactions, along with the associated PS I, is presented in Fig. 1.1.

The PS II reaction center complex of higher plants (see review in Vermaas and Ikeuchi, 1991) is composed of, among others, three well known proteins D1, D2 and cytochrome (Cyt) b559. The D1 and D2 proteins bind all of the cofactors involved in photochemical charge separation. Photoexcitation of the PS II reaction center complex (D1/D2/Cytb559) creates oxidized reaction center chlorophyll a,  $\text{P680}^+$  ( $E_{m,7} = + 1.12\text{V}$ , Jursinic and Govindjee, 1977; Klimov and Krasnovskii, 1981), and reduced pheophytin within 3 ps (Wasielewski et al., 1989a,b). The charge separation is stabilized by transfer of the electron first to a one-electron acceptor plastoquinone,  $\text{Q}_A$ ,

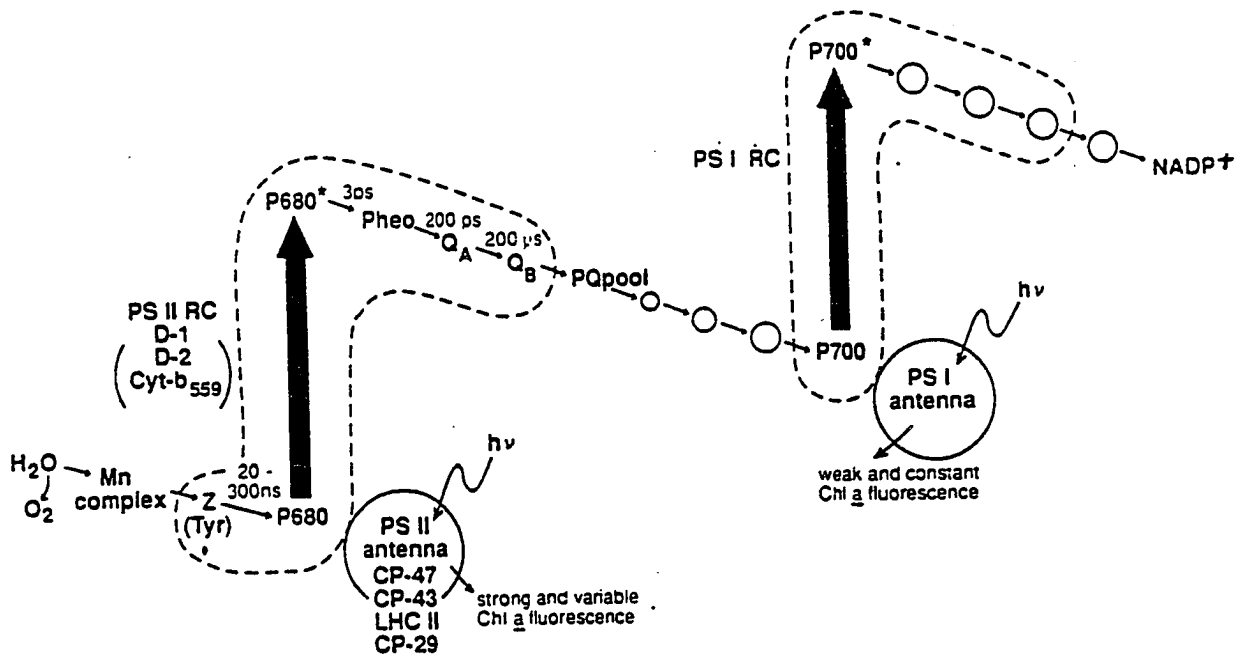
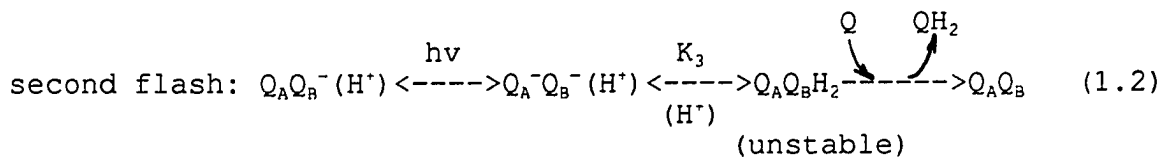
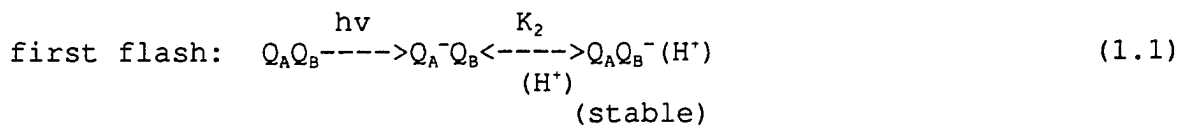


Fig. 1.1. A diagram showing the primary photochemical reactions and electron flow pathway in oxygenic photosynthesis. Dashed lines encircle the components of the two multiprotein reaction center complexes, located in the thylakoid membrane. Electron flow is initiated when photons excite the reaction center chlorophyll a P680 (in PS II) and P700 (in PS I) and/or when excitons from the antenna pigments reach these centers. P680\* and P700\* indicate the first singlet excited states of P680 and P700. The first reaction of P680\* is the conversion of excitonic energy into chemical energy (charge separation). This involves the formation of the cation P680<sup>+</sup> and the anion pheophytin<sup>-</sup> (Pheo<sup>-</sup>) within 3 ps. The P680<sup>+</sup> recovers its lost electron from Z (tyrosine-161 of the D1 polypeptide of PS II). The positive charge on Z is then transferred to an Mn-complex located on the luminal portions of the D1 and D2 polypeptides of PS II. The Pheo<sup>-</sup> delivers the extra electron to a bound plastoquinone electron acceptor Q<sub>A</sub>. The reduced Q<sub>A</sub> transfers its electron to another plastoquinone electron acceptor Q<sub>B</sub>, strongly bound only in its semiquinone form Q<sub>B</sub><sup>-</sup>. After two turnovers of the reaction center P680, Q<sub>B</sub>H<sub>2</sub> exchanges with the plastoquinone (PQ) pool. After four turnovers of the reaction center P680, the Mn complex accumulates four positive charges and oxidizes H<sub>2</sub>O to molecular O<sub>2</sub> and releases 4 H<sup>+</sup>s. Plastoquinol formed in PS II reduces oxidized P700 (P700<sup>+</sup>), formed in PS I, via several intermediates. CP-47, CP-43, LHC-II and CP-29 are pigment-protein antenna complexes of PS II. The role of cytochrome b559 is unknown.

via pheophytin, and then to  $Q_B$ , a two-electron acceptor plastoquinone. The  $Q_B$  operates as a two-electron gate (see e.g. Velthuys and Ames, 1974; Wraight, 1981, 1982). After the initial photoreaction, a tightly bound semiquinone  $Q_B^-$  is formed. A second photochemical reduction of  $Q_A$  then reduces  $Q_B$  to plastoquinol ( $Q_BH_2$ ), which has a weaker binding affinity to the  $Q_B$  site and is displaced within milliseconds by a plastoquinone (PQ) molecule in the PQ pool. The exchange of plastoquinol regenerates the oxidized  $Q_B$  and thus completes the photochemical cycle (see e.g., Crofts and Wraight, 1983; Robinson and Crofts, 1984; Rich and Moss, 1987). The cycle then repeats itself again with a periodicity of two. These reactions in PS II can be summarized as follows, just as in photosynthetic bacteria (Takahashi and Wraight, 1991):



Here,  $K_2$  and  $K_3$  represent equilibrium constants.

The two protons required for the production of plastoquinol appear not to come directly from the external aqueous phase (Ausländer and Junge, 1974). Crofts et al. (1984) proposed for PS II, as already suggested by Wraight (1979) for the  $Q_A Q_B$  complex of photosynthetic bacteria, that an amino acid residue near  $Q_B$  must be protonated to stabilize  $Q_B^-$  before  $Q_B^-$  can accept a second electron from  $Q_A^-$ . Furthermore, the pKa of this group appears to shift from

about 6.4 to approximately 7.9 when  $Q_B$  is reduced to  $Q_B^-$ ; the oxidation of  $Q_A^-$  by  $Q_B^-$  is slowed down when this group is unprotonated (Robinson and Crofts, 1984). The protonation of  $Q_B^-$  was suggested to be the rate-determining step in the reduction of plastoquinone to plastoquinol above pH 7.9, the pK of the state  $Q_A Q_B^-$ .

The crystallization and X-ray diffraction analysis of the reaction center (RC) complex of the photosynthetic purple bacteria, along with the realization that there is an extensive functional and structural homology between RC's of PS II and from purple bacteria, allowed investigators to obtain a better insight into the mechanism of action of PS II (Deisenhofer et al., 1985; Trebst, 1986; Michel and Deisenhofer, 1988). A binding domain for  $Q_B$  was determined to be in a cleft of D1 subunit (equivalent of the L subunit of photosynthetic bacteria), that spans the thylakoid membrane in five hydrophobic  $\alpha$ -helices; the amino acid loop connecting the fourth and fifth transmembrane helices was suggested to contain the  $Q_B$  binding site (Trebst, 1986). On the other hand,  $Q_A$  was suggested to be bound on the D2 subunit that is equivalent of the M subunit of photosynthetic bacteria (see e.g., Barber, 1987), and the non-heme iron was suggested to be equidistant between  $Q_A$  and  $Q_B$ . The suggested  $Q_B$  binding site brings it within the magnetic influence of the non-heme iron.

In photosynthetic bacteria, the  $Q_B$  binding site appears to be more polar than the  $Q_A$  binding site with several ionizable residues located nearby (Allen et al., 1988). Polar residues appear to form

part of a chain to conduct protons from the cytoplasmic surface to the  $Q_B$  site (Allen et al., 1988). L-E212 and L-D213 (glutamic acid 212 and aspartic acid 213 on the L-subunit) in *Rhodobacter sphaeroides* (Paddock et al., 1989) and D1-H252 (histidine 252 on the D1 subunit) in PS II (Crofts et al., 1987; Blubaugh and Govindjee, 1988a) were suggested to be involved in the access of protons. L-E212 and L-D213 in *R. sphaeroides* are two polar residues in the binding site of  $Q_B$ . Using single and double site-directed mutants of L-E212 and L-D213 in *R. sphaeroides*, Takahashi and Wraight (1990, 1991, 1992) have suggested the important role of both L-E212 and L-D213 in the protonation reactions leading to ubiquinol formation.

PS II inhibitors such as DCMU, atrazine (a triazine) and o-phenanthroline are known to compete with plastoquinone for binding at the  $Q_B$  site (Velthuys, 1981, 1982; Wraight, 1981, 1982; also see Diner et al., 1984). Resolution of the crystal structure of *Rhodospseudomonas viridis* reaction center indicated that this type of competition occurs in the binding of the bacterial inhibitors and the ubiquinones at the same site (Michel et al., 1986). In PS II, the inhibitor binding displays a multiplicity of binding sites (Oettmeier, 1992). Although DCMU and o-phenanthroline induce the appearance of a strong axial component ( $g = 6.0$ ) of the Fe(III) EPR signal in spinach PS II membranes (Diner and Petrouleas, 1987a), atrazine produces nearly no modification of this signal, suggesting different binding environments for different herbicides.

Two unusual PS II characteristics suggest significant structural differences between the quinone-binding regions in reaction centers from oxygenic plants and cyanobacteria and those from anoxygenic photosynthetic bacteria: (1) a presumed requirement for bicarbonate to achieve maximal rates of electron flow in normal PS II of plants (see Blubaugh and Govindjee, 1988a) and of cyanobacteria (Cao and Govindjee, 1988; Nugent et al. 1988) but not in photosynthetic bacteria (Shopes et al., 1989; Govindjee, 1991; Wang et al., 1992) and (2) an oxidation of the non-heme iron, which is able to act as an additional electron acceptor (Q400), is seen only in PS II (Petrouleas and Diner, 1986; Zimmermann and Rutherford, 1986; Diner and Petrouleas, 1987a,b), but not in photosynthetic bacteria (Beijer and Rutherford 1987).

We shall now discuss the presumed requirement of bicarbonate on the electron acceptor side of PS II. It manifests itself through a unique bicarbonate-reversible inhibition of PS II reactions by formate, nitrite, NO etc. (see reviews by Govindjee and Van Rensen, 1978; Govindjee and Eaton-Rye, 1986; Blubaugh and Govindjee, 1988a; Diner et al., 1991; Govindjee, 1991; Van Rensen, 1992; Govindjee and Van Rensen, 1992).

#### B. Background for the Bicarbonate Effect in PS II

Warburg and Krippahl (1958, 1960) discovered a stimulatory effect of CO<sub>2</sub> on the Hill reaction. This effect is located on the PS II reactions (see Govindjee and Van Rensen, 1978). There is a major effect on its electron acceptor side (see Blubaugh and



Govindjee, 1988a) although effects on its donor side cannot be discounted (see Stemler, 1982). Treatment of thylakoids with anions such as formate at low pH results in decreased Hill reaction (Stemler and Govindjee, 1973) and in slowing of electron flow between  $Q_A$  and the plastoquinone pool (Govindjee et al., 1976; Jursinic et al. 1976; Siggel et al., 1977), which can be reversed by the addition of bicarbonate. Bicarbonate is unique in the sense that it is the only ion that can restore the activity (see e.g. Good, 1963).

Several observations show that a major bicarbonate-reversible formate effect exists on the electron acceptor ( $Q_A$ -Fe- $Q_B$ ) side of PS II in the  $D_1$  and  $D_2$  proteins of RC II.

(1) There is a dramatic bicarbonate-reversible inhibition, particularly after the second (or third) and subsequent flashes, of the reoxidation of the reduced primary quinone acceptor of PS II,  $Q_A^-$ , as measured by the chlorophyll (Chl) a fluorescence yield decay (Govindjee et al., 1976; Eaton-Rye and Govindjee, 1988a, b), or by the absorbance change at 320 nm (Farineau and Mathis, 1983) in the presence of formate.

(2) Light-induced EPR signals in the  $g=1.6$  to  $g=8$  region, attributed to magnetic interactions between semiquinone forms of  $Q_A$  and  $Q_B$ , and the non-heme iron of the acceptor complex ( $Q_A^-Fe^{2+}Q_B^-$ ,  $Q_A^-Fe^{2+}$ ,  $Q_B^-Fe^{2+}$  and  $Fe^{3+}$ ) (Vermaas and Rutherford, 1984; Bowden et al., 1991; Hallahan et al., 1991), and the Mossbauer spectra of the non-heme  $Fe^{2+}$  (Diner and Petrouleas, 1987b; Petrouleas and Diner, 1990;

Semin et al., 1990), are drastically altered by formate, NO and bicarbonate.

(3) The binding of several herbicides (urea, triazine and phenol-type herbicides), known to interact with the  $Q_B$ -binding protein D1, is drastically affected by the presence of bicarbonate and *vice versa* (Khanna et al., 1981; Van Rensen and Vermaas, 1981). Urea, triazine and phenol-type herbicides decrease the apparent affinity of the thylakoid membrane for bicarbonate (Van Rensen and Vermaas, 1981; Van Rensen, 1982; Vermaas et al., 1982; Snel and Van Rensen, 1983). On the other hand, formate treatment, now known to remove  $CO_2$  (Govindjee et al., 1991a), alters the binding of herbicides (Khanna et al., 1981).

(4) Furthermore, a triazine-resistant mutant of *Amaranthus hybridus* (in which S-264 of D1 was changed to glycine) showed a two fold increase in the dissociation constant of bicarbonate (Khanna et al., 1981). Recent studies on several herbicide-resistant D1 mutants of the cyanobacterium *Synechocystis* 6714 (Govindjee et al., 1990) and of the green alga *Chlamydomonas reinhardtii* (Govindjee et al., 1991b), altered in single amino acids on D1, demonstrate differential, but bicarbonate-reversible, sensitivity to subsaturating concentrations of formate.

As already mentioned, the bicarbonate effect has been well established in PS II of higher plants and cyanobacteria, but not in photosynthetic bacteria. Differences in the amino acid sequence of the reaction center polypeptides of PS II and of bacterial reaction

centers suggested to Michel and Deisenhofer (1988) that the different response to bicarbonate depletion could be due to the provision of the fifth and sixth ligands of the iron atom to binding by the carboxylate group of a glutamic acid residue in bacteria (M-E234 in *R. sphaeroides*) and the absence of this linkage in PSII; in PSII this role might be filled by bicarbonate. However, Wang et al. (1992), on the basis of studies on M-E234V, M-E234N and M-E234G mutants of *R. sphaeroides*, have concluded that this glutamic acid is not essential to normal functioning of bacterial reaction center and that the role of bicarbonate is different from the role of this amino acid. Thus, further research will be necessary to ascertain the reasons for the differences between bacteria and PS II.

Two major, non-exclusive, possible roles for bicarbonate in the function and structure of the acceptor side complex have been suggested:

(1) Bicarbonate may provide a ligand to  $\text{Fe}^{2+}$  in the  $\text{Q}_A\text{-Fe-Q}_B$  complex and keep the D1-D2 proteins in their proper functional conformation, thereby facilitating electron transfer from  $\text{Q}_A^-$  to  $\text{Q}_B$  or  $\text{Q}_B^-$ . Experiments with nitric oxide (NO), that binds to  $\text{Fe}^{2+}$  (Petrouleas and Diner, 1990), suggest (Diner and Petrouleas, 1990) that bicarbonate binds to  $\text{Fe}^{2+}$  in PS II. For other evidences, see earlier discussion on p. 7, this thesis.

(2) Bicarbonate may promote protonation associated with PQ reduction at the  $\text{Q}_B$  site, which explains the larger bicarbonate-reversible formate effect on  $\text{Q}_A^-$  decay after the second and

subsequent actinic flashes than after the first one (Eaton-Rye and Govindjee, 1988a, b; this thesis). This latter concept is reinforced by observations on the effects of formate or bicarbonate on H<sup>+</sup> exchange related to PS II reactions (Khanna et al., 1980; Govindjee and Eaton-Rye, 1986; Van Rensen et al., 1988). The formate inhibition was suggested to destabilize Q<sub>B</sub><sup>-</sup> by preventing the protonation process possibly involving binding to D1-R252 (Crofts et al., 1987; Blubaugh and Govindjee 1988a).

Taking advantage of the consideration of HCO<sub>3</sub><sup>-</sup>/CO<sub>2</sub> equilibrium, Blubaugh and Govindjee (1986) showed that HCO<sub>3</sub><sup>-</sup> is the active species. By studying the pH dependence of the apparent rate constants for formate binding, it will be suggested in this thesis that formic acid, not formate, is the inhibitory binding species. The implication of this observation is not yet fully resolved.

The above discussion has centered around the major role of bicarbonate on the electron acceptor side of PS II. Although a possible donor side effect has not been fully explored, yet certain data on this point deserve mention. Mende and Wiessner (1985) studied the bicarbonate effect in the green algae *Chlomydobotrys stellata* and concluded that bicarbonate depletion affects the donor side of PS II, the oxygen-evolving side. El-Shintinawy and Govindjee (1990) observed a decrease in the rate of oxygen evolution and simultaneous quenching of the variable chlorophyll (Chl) a fluorescence of spinach leaf discs after short-term formate treatment, suggesting an inhibition on the electron donor side of PS II. However, the quenching of variable Chl a fluorescence was

observed even in the presence of hydroxylamine, that blocks O<sub>2</sub> evolution and donates electrons to PS II reaction center, suggesting that there is a site of formate inhibition between the hydroxylamine donation site (Z) and Q<sub>A</sub> (see Fig.1.1). This effect of formate inhibition was also observed by the author in *Chlamydomonas reinhardtii* (see El-Shintinawy et al., 1990). Further research is needed to explore the bicarbonate effect on the donor side of PS II (see e.g., Stemler, 1982); it is, however, not the major concern of my thesis.

### C. Objective of this Thesis

Bicarbonate-reversible inhibition of the electron acceptor side of PS II, but not of photosynthetic bacteria, has been known for a long time. In this thesis, I have explored the inhibitor binding niche on the electron acceptor side by using different small weak organic acids with different sizes and hydrophobicity. Good (1963) had already found that treatment with small monovalent anions (e.g., formate and acetate) increases the dependence of the Hill reaction of thylakoids on bicarbonate. To this list was added, among others, nitrite (see e.g., Eaton-Rye et al., 1986) and azide (Cao and Govindjee, 1990b). Here, I have focussed on formate (Chapters III, IV and VIII) and introduced various halogenated acetates (tri-, di- and monochloroacetate; monobromo- and monofluoroacetate; Chapters V and VI) because of their different size and hydrophobicity. Preliminary data on other chemicals will also be presented for comparison (Chapter VII).

Although it was known that the electron transfer at the  $Q_A$ -Fe- $Q_B$  complex of PS II is significantly and reversibly inhibited by the addition of anions, nothing was known about the kinetic property of formate binding at its binding site and the competitive mechanism of formate/bicarbonate. My first objective was to obtain kinetic parameters of formate binding. When the initial binding rate of formate/formic acid was analyzed, an obvious pH dependence of the inhibition of  $Q_A^-$  oxidation was seen. My results suggest that formic acid, not formate, is the binding species (Chapter IV). In order to obtain further support for the hypothesis that the acidic form is the binding species, several weak organic acids (halogenated acetic acids) were investigated. All of them were found to inhibit the electron flow in the  $Q_A$ -Fe- $Q_B$  complex of PS II and the inhibition was pH dependent as that shown for formate (Chapter V). Thus, I suggest that the acidic forms of weak acid inhibitors are the active species.

An interesting hierarchy of the inhibitory effects of trichloroacetic acid, dichloroacetic acid, monochloroacetic acid, monobromoacetic acid and monofluoroacetic acid on the  $Q_A$ -Fe- $Q_B$  reaction was observed (Chapters V and VI). Furthermore, this inhibition was reversed, but in different degrees, upon bicarbonate addition. The observed correlation between the inhibitory activity, the bicarbonate-reversibility and the geometry as well as the hydrophobicity of the inhibitors demonstrated the importance of the  $CX_3$  group of these chemicals in affecting plastoquinone reduction and the equilibrium between  $Q_A^-Q_B \rightleftharpoons Q_AQ_B^-$ . I mention just two

examples. Trichloroacetic acid, that has a hydrophobic constant ( $\pi$ ) of 1.87 and a dipole moment of 2.12 Debye, not only blocks drastically the reoxidation of  $Q_A^-$ , but dramatically shifts the equilibrium towards  $Q_A^-$ . Here, the bicarbonate-reversibility is low. Monochloroacetic acid, that has an asymmetric chlorine atom, a hydrophobic constant ( $\pi$ ) of 0.65 and a dipole moment of 3.25 Debye, affects, in a bicarbonate-reversible manner, the two electron gate of PS II by converting the flash number dependence of  $[Q_A^-]$  with the maxima occurring at even to that at odd flashes. This apparent stabilization of  $Q_B^-$ , caused by MCA, can be explained by a combined effect on the  $Q_A^-Q_B \leftrightarrow Q_AQ_B^-$  equilibrium and a change in the  $Q_B/Q_B^-$  ratio.

Additional, but preliminary, extension of my work to inhibitors (such as propionic acid and trimethylacetic acid) on the  $Q_A$ -Fe- $Q_B$  reaction is presented in Chapter VII. A brief comment on the effect on the donor side of PS II is presented in Chapter VIII. Finally, in Chapter IX, I have provided a summary and a general discussion of my thesis work in the context of the  $Q_A$ -Fe- $Q_B$  binding niche in the D1 and D2 proteins.

[Three appendices contain additional work done during my tenure as a McKnight student in the laboratories of Profs. Jack Widholm and Govindjee. Appendix A and B, that is not directly related to the theme of the present thesis, is by itself of significance since it deals with the first time culturing and characterization of five new photoautotrophic suspensions of various higher plant species, including two C4 species. Appendix C

contains an attempt to measure Chl a fluorescence of spinach thylakoids by flow cytometry. The usefulness of this method for selecting cell lines and mutants needs further study. These appendices are presented here, at the suggestion of my advisor Prof. Govindjee, for completeness of my work at UIUC, Urbana.]



## CHAPTER II. MATERIALS AND METHODS

### A. Isolation of Spinach Thylakoids

Spinach (*Spinacia oleracea*) leaves were obtained from a commercial source. Selected young leaves were used to obtain thylakoids as described by Eaton-Rye and Govindjee (1988a). Leaf segments were ground in a medium containing 400 mM sorbitol, 50 mM NaCl, 1 mM EDTA (ethylenediaminetetra-acetic acid) and 50 mM Hepes (pH 7.8) for 5 seconds in a Waring blender. The resultant homogenate was filtered through 6 and then 12 layers of cheesecloth. The filtrate was then spun at 5,000 x g for 1 minute, which included the acceleration time, to remove any remaining debris. The filtrate of this step was then spun at 5,000 x g for 10 minutes. After discarding the last supernatant, the pellet was resuspended and osmotically shocked in a medium containing 50 mM NaCl, 5 mM MgCl<sub>2</sub> and 10 mM Hepes (pH 7.8). The suspension was then spun again at 5,000 x g for 10 minutes and resuspended in 0.4 M sorbitol, 15 mM NaCl, 5 mM MgCl<sub>2</sub> and 20 mM HEPES (pH 7.8). The suspension with 1 mM Chlorophyll was frozen rapidly and stored in liquid nitrogen (77K). It was thawed immediately prior to use. All isolation procedures were carried out at 0-4°C.

Chlorophyll concentration was spectrophotometrically determined in 80% acetone (v/v) extracts of thylakoids, as described by Porra et al. (1989).

## B. Growth of *Chlamydomonas reinhardtii* Cells

*Chlamydomonas reinhardtii* cells were grown anaerobically in a Tris-Acetate culture medium (tris-acetate buffer 17 mM, pH 7.3; and 1 mM potassium phosphate, pH 7.0; see Gorman and Levine, 1965) at 25°C. During growth, the cell culture was placed in 125 ml flasks on a gyratory shaker under continuous illumination from 8 daylight fluorescent lamps (15 W) and one tungsten lamp (15 W) (Shim et al., 1990). After four days, dark green cells were collected for assays. Thylakoid isolation was made as described by Diner and Wollman (1980). The description under this section and in the sections below (C-F) is based on our description in El-Shintinawy et al. (1990).

## C. Formate Treatment of *Chlamydomonas reinhardtii* Cells

Formate treatment of cells was carried out as described by Eaton-Rye and Govindjee (1988a,b) for higher plant thylakoids. Samples, containing 250  $\mu$ M Chl, were incubated in the dark for 60 minutes in a CO<sub>2</sub>-free treatment buffer under a stream of N<sub>2</sub> (80%) and O<sub>2</sub> (20%), which had passed through a column of soda-lime and ascarite to facilitate the removal of any trace of CO<sub>2</sub>, and through a water column to prevent evaporation of the sample. A major modification in this study was that a half-diluted culture medium (containing 0.6 mM acetate) was used as a CO<sub>2</sub>-depletion medium after the addition of 25 mM NaHCO<sub>2</sub> and the pH was lowered to 5.8 to enhance the effect under investigation. Usually, for long-term

formate treatment, *Chlamydomonas* cells are incubated for 3 hours at 20°C in the above medium under constant flow of N<sub>2</sub> gas over, not in, the medium. However, we used mostly short-term treatment which was carried out by the infiltration of the freshly harvested cells in the CO<sub>2</sub>-depletion medium under gentle vacuum (about 1 kPa) for 5 minutes. The cells were then resuspended, before measurements, in the half-diluted tris-acetate-phosphate medium with or without 25 mM NaHCO<sub>2</sub> at a pH of 6.5 or 7.5. Bicarbonate-restored samples were prepared by adding 2.5 mM NaHCO<sub>3</sub> to the formate treated samples.

#### D. Heat Treatment of the Cells

Mild heating was done at 45° for 3 minutes; 10 mM freshly prepared hydroxylamine (pH was adjusted to 7.3) was used, when needed, as an artificial electron donor to PS II. The time of treatment with hydroxylamine was 5 minutes.

#### E. Measurements of Oxygen Evolution

Oxygen evolution rates were determined polarographically by using a Yellow Spring Instrument Clark-type electrode. Illumination was provided by a Kodak Carousel 4200 slide projector equipped with a Corning CS3-68 yellow filter. A 1 mM 2,5-dimethyl-p-benzoquinone (DMQ) was used as an artificial electron acceptor and 1 mM ferricyanide was used to keep DMQ in the oxidized state. The 0.5 μM 2,5-dibromo-6-isopropyl-p-benzoquinone (DBMIB) was used as an inhibitor of electron flow between photosystem II and I

(Trebst et al., 1970). A *Chlamydomonas* cell suspension containing 20  $\mu\text{g}$  Chl/ml was used for the oxygen evolution measurements.

#### F. Measurement of the Chlorophyll (Chl) a Fluorescence Transient

Chl a fluorescence transient measurements were made by using a home-built spectrofluorometer, as described by Blubaugh and Govindjee (1988b). The exciting light was provided by a Kodak 4200 projector with the light filtered by two Corning filters (a blue CS 4-76 and a yellow CS 3-73). Fluorescence emission was detected, with a slit width of 3.3 nm, by a S-20 photomultiplier (EMI 9558B) through a Bausch and Lomb monochromator, protected from the exciting light by a red Corning CS 2-61 filter. The photon flux density at the sample was 40  $\mu\text{moles m}^{-2}\text{s}^{-1}$ . Signals were stored and analyzed by a Biomation 805 waveform recorder and an LSI-11 computer.

#### G. Measurement of the Decay Kinetics of Chl a Fluorescence by Using the Double Flash Technique

To monitor the redox state of  $Q_A$ , Chl a fluorescence yields after single-turnover saturating flashes (EG & G FX-124 flash lamp, 2.5  $\mu\text{s}$  duration) were measured by an instrument described elsewhere (Eaton-Rye and Govindjee, 1988a; for earlier instruments, see Delsome, 1971; Jursinic et al., 1976; Robinson and Crofts, 1983). Using weak measuring flashes, the initial "O" (or  $F_0$ ) level of Chl a fluorescence yield of 5 min dark-adapted thylakoids, and the decay of the variable ( $F_v$ ) fluorescence, after saturating flashes,

were measured at 685 nm, using a 10 nm bandwidth interference filter, by a photomultiplier (EMI 9558). The measuring flash was fired at a computer programmed time after each saturating actinic flash; the kinetics of Chl a fluorescence decay was derived from these measurements. Both the actinic and measuring flashes were filtered with Corning blue CS 4-96 glass filters; and the photomultiplier was protected by the Corning red CS 2-61 filter. The  $F_0$  measures the yield when all of the  $Q_A$  is in the oxidized state (see, e.g., Cao and Govindjee, 1990b), and the decay of  $F_v$  reflects the reoxidation of  $Q_A^-$  to  $Q_A$ . For the above measurements, thylakoids, containing 10  $\mu\text{M}$  [Chl], were suspended in 0.4 M sorbitol, 50 mM NaCl and 2 mM  $\text{MgCl}_2$  (Eaton-Rye and Govindjee 1988a). Eighty  $\mu\text{M}$  quinhydrone was added, whenever specified, to the sample to keep all  $Q_B$  in its oxidized state. The pH of the suspension was adjusted by using 20 mM MES (from pH 5.5 to 6.5) or 20 mM HEPES (from pH 7.0 to 7.5).

#### H. Calculation of the Concentration of $Q_A^-$

The concentration of reduced  $Q_A$  was estimated from the above Chl a fluorescence yield data by using the following equation (Joliot and Joliot, 1964; see Mathis and Paillotin, 1981):

$$[F(t) - F_0]/[F_{\text{max}} - F_0] = (1 - p)q/(1 - pq) \quad (2.1)$$

where  $F(t)$  is the Chl a fluorescence yield at time  $t$ ,  $F_0$  is the fluorescence yield when all  $Q_A$  is in the oxidized state,  $p$  is the connection parameter or the probability of the intersystem energy transfer and  $q$  is the fraction of the closed PS II reaction centers

(i.e.,  $q = 1$ , when  $[Q_A^-]$  is maximum). Here  $p$  was taken as 0.5 (Joliot and Joliot, 1964, also cf. Crofts et al., 1984) for calculation of  $[Q_A^-]$  in this study. Therefore,  $q$ , the relative concentration of  $Q_A^-$ , can be represented by the following formula:

$$q = [F(t) - F_0] / \{(F_{\max} - F_0) - 0.5[F_{\max} - F(t)]\} \quad (2.2)$$

#### I. Fitting of $[Q_A^-]$ Decay Into Exponential Decays

The fitting of the  $[Q_A^-]$  decay data into three (and sometimes four) exponential decays was carried out by the GLOBALS UNLIMITED™ global analysis software (Beechem et al., 1991).  $[Q_A^-]$  is given in relative units with 1 being  $[Q_A^-]_{\max}$  obtained in the presence of 6  $\mu\text{M}$  DCMU. Thus, the sum of the analyzed amplitudes (A's) need not add to 1 in our analysis.

#### J. Measurement of the Kinetics of Formate Binding in the Dark-adapted Spinach Thylakoid Suspension

The kinetics of formate binding in the dark-adapted thylakoid suspension was measured by monitoring Chl a fluorescence yield changes after an actinic flash at various times after injecting a known amount of formate (preadjusted to the pH of the suspension medium) with a syringe. The decay of the Chl a fluorescence yield, reflecting oxidation of  $Q_A^-$ , was significantly slowed only after the second and subsequent actinic flashes (see Chapter III). Those centers in which the  $Q_A^-$  oxidation was blocked were considered to be formate bound. The concentration of formate bound PS II RC's was estimated from the fraction of centers showing inhibited  $Q_A^-$  oxidation (measured as above) after the addition of formate. Other details are described under Chapters III and IV.

#### K. Calculation of Molecular Geometries as well as the Dipole Moment

Molecular geometries as well as the dipole moment of acetic acid and its chloride derivatives were calculated by using the MMX molecular mechanics (forcefield), calculation method with the PCMODEL molecular modeling program (Anonymons, 1990). MMX is a subprogram of PCMODEL. The calculation was made in an apolar solvent with a dielectric constant of 1.5 to minimize the energy of the molecular model and to obtain an optimal geometry of the model.

#### L. Calculation of the Hydrophobic Constant ( $\pi$ ) of Acetic and Chloroacetic Acids

The equation given by Hansch (1969) was used in this thesis to obtain hydrophobic constants ( $\pi$ ):

$$\pi = \log P_x - \log P_H \quad (2.3)$$

$P_x$  is the partition coefficient of the derivative of the molecule and  $P_H$  is the partition coefficient of the parent molecule.

#### M. Chemicals

MES, HEPES, monochloroacetic acid, dichloroacetic acid, trichloroacetic acid, monobromoacetic acid, monofluoroacetic acid, trimethylacetic acid, sodium azide and quinhydrone were purchased from SIGMA; Sodium formate and sodium acetate from J.C. Baker; 1-octanol, sodium cyanate and sodium thiocyanate from Aldrich; and liquified phenol from Fisher Scientific. Reagent grade chemicals were used without further purification.

### CHAPTER III. FLASH NUMBER DEPENDENCE OF THE DECAY OF $[Q_A^-]$ UPON FORMATE TREATMENT AND THE PROTONATION HYPOTHESIS

#### A. Introduction

The two-electron gate scheme, developed for anoxygenic photosynthetic bacteria and for oxygenic PS II (for a review, see Crofts and Wraight, 1983), can be easily modified to accommodate formate binding at PS II RC. Both oxidized and fully reduced forms of the secondary PQ acceptor ( $Q_B$  or  $Q_BH_2$ ) bind loosely to the D1 protein of the RC II, whereas the semiquinone form,  $Q_B^-$ , binds tightly. Complete reduction of the bound quinone,  $Q_B$ , requires not only two electrons but transfer of two protons to  $Q_B^{2-}$ . The  $Q_BH_2$  thus formed exchanges rapidly with PQ from the pool and completes the electron flow at this site, the so-called "two electron gate". The steps at which  $Q_B$  protonation occurs in PS II are not really known. Many inhibitors block the electron transport beyond  $Q_A$  by competing with  $Q_B$  at its binding site (Velthuys, 1981, 1982; Wraight, 1981, 1982). However, we have assumed in this thesis that (bicarbonate-reversible) formate and  $Q_B$  bind independently of each other.

The flash number dependence of the halftime ( $t_{50}$ ) of the  $[Q_A^-]$  decay in long-term (hours) formate-treated thylakoid changes with medium pH (Eaton-Rye and Govindjee, 1988a). The  $t_{50}$  reaches maximal level after two flashes at pH 6.5. However, at pH 7.5  $t_{50}$  reaches a much higher maximal level and saturates after 4 - 5 flashes. This was interpreted by a much slower  $Q_A^-$  oxidation rate at pH 7.5 after two turnovers of the two-electron gate. Since the protonation of  $Q_B^-$  is suggested to become the rate-determining step in PQ reduction



above 7.9 (Crofts et al. 1984), bicarbonate was assigned a role in this protonation process (Eaton-Rye and Govindjee, 1988a, b). However, a clear-cut mechanism of formate binding and its effect on  $Q_A-Q_B$  reactions is still not available. Therefore, the objective of this chapter was to reexamine the pH dependence of the so-called "two-electron gate turnover" and its relationship with the protonation of  $Q_B^-$ . For this purpose, we have (a) chosen a shorter and a direct treatment with formate to avoid secondary effects of the longer  $CO_2$ -depletion procedure; (b) analysed the data in terms of the effects on the rates of the reoxidation of  $Q_A^-$  as well as the equilibrium  $[Q_A^-]$ ; and (c) measured the flash number dependence of  $[Q_A^-]$  decay at several selected pH's (5.5, 6.0, 6.5 and 7.5) in formate treated (bicarbonate-depleted) and control (or bicarbonate restored) spinach thylakoids. This has provided me with a better insight into the problem than available from the earlier work of Eaton-Rye and Govindjee (1988a,b). Our results suggest that formate treatment hampers protonation of  $Q_B^-$  since the  $[Q_A^-]$  decay is slowed significantly after the second and subsequent flashes. Thus, I have discussed a working model for formate binding.

The present chapter is based on a paper published by the author (Xu et al., 1991); however, additional analysis has allowed me to obtain a better understanding of the phenomenon studied.

## B. Materials and Methods

Spinach thylakoids were isolated from market spinach as described in Chapter II. Chl a fluorescence yield decay, monitoring

$[Q_A^-]$  decay, was measured and analyzed as also described in Chapter II. Fifteen minutes dark-adaptation of thylakoids was used to ensure that all of the  $Q_A$  was in the oxidized state before measurements began. The reaction medium contained 0.4 M sorbitol, 50 mM NaCl, 2 mM  $MgCl_2$  and MES buffer for pH 6.5.

In contrast to the experiments of Eaton-Rye and Govindjee (1988 a, b) where long-term formate treatment under  $CO_2$ -depletion conditions was used, we have simply added here formate in darkness and measured the effects after 15 min incubation.

### C. Results and Discussion

After the addition of formate to spinach thylakoids, the flash number dependence of the Chl a fluorescence ( $F_v/F_o$ ) yield decay, reflecting the reoxidation of  $Q_A^-$  by  $Q_B/Q_B^-$  and the equilibration of  $Q_A^-Q_B \leftrightarrow Q_AQ_B^-$ , was measured, up to 8 ms. At the 3 pH's (6.0, 6.5 and 7.5) examined, a moderate slowing of the Chl a fluorescence yield decay was found following the first flash excitation of dark-adapted thylakoids, but considerably greater slowing occurred after the second and subsequent flashes (Figs. 3.1, 3.2 and 3.3). Without any analysis of this data, these results are most economically explained by suggesting that protonation is inhibited at the  $Q_B$  site since the electron flow from  $Q_A^-$  to  $Q_B$  (after the first flash) is almost normal (see equations (1.1) and (1.2) in Chapter I). The formate binding at the  $Q_B$  site is, thus, suggested to restrict the availability of the proton for the formation of the plastoquinol,

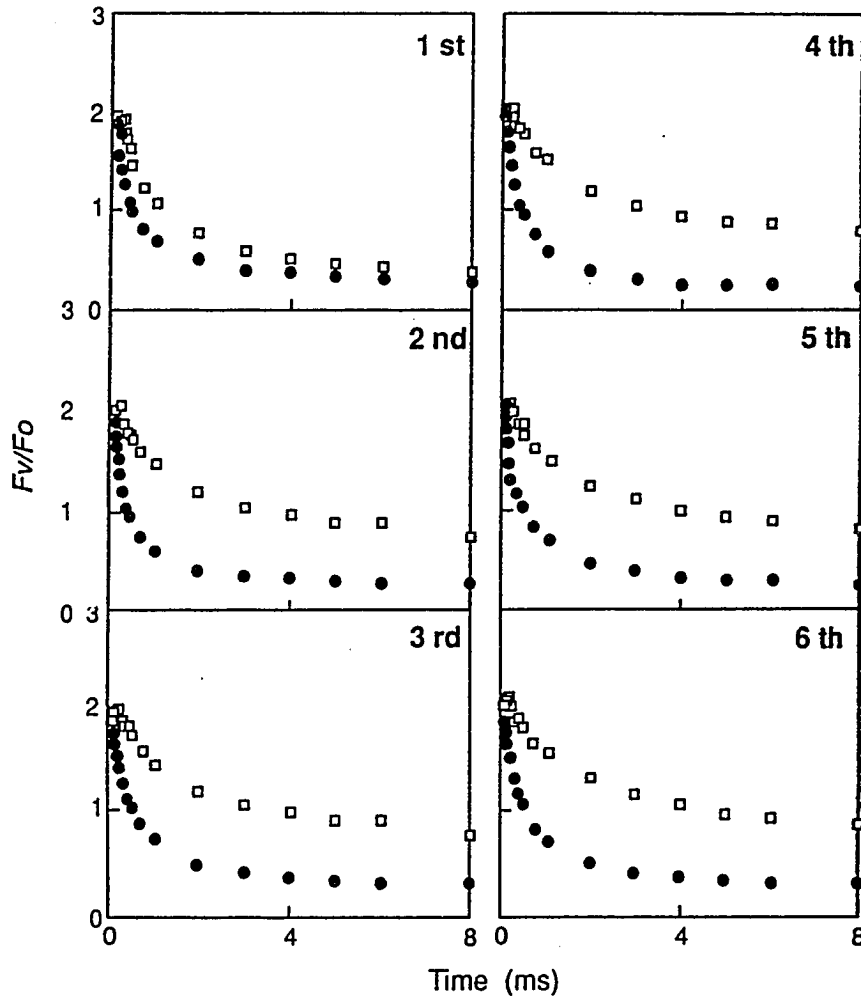


Fig. 3.1. Effect of formate addition on the Chl a fluorescence yield decay at pH 6.5 in spinach thylakoids. The number in each panel refers to the actinic flash number. Open squares, samples treated with 100 mM formate; closed circles, control.  $F_v$  refers to variable Chl a fluorescence yield, and  $F_o$  to minimum fluorescence yield in weak light. The time for dark-adaptation and formate-treatment was 15 min. The reaction medium contained 0.4 M sorbitol, 50 mM NaCl, 2 mM MgCl<sub>2</sub> and MES buffer for pH 6.5. The addition of 20 mM bicarbonate totally restored the  $F_v/F_o$  decay to the control level.

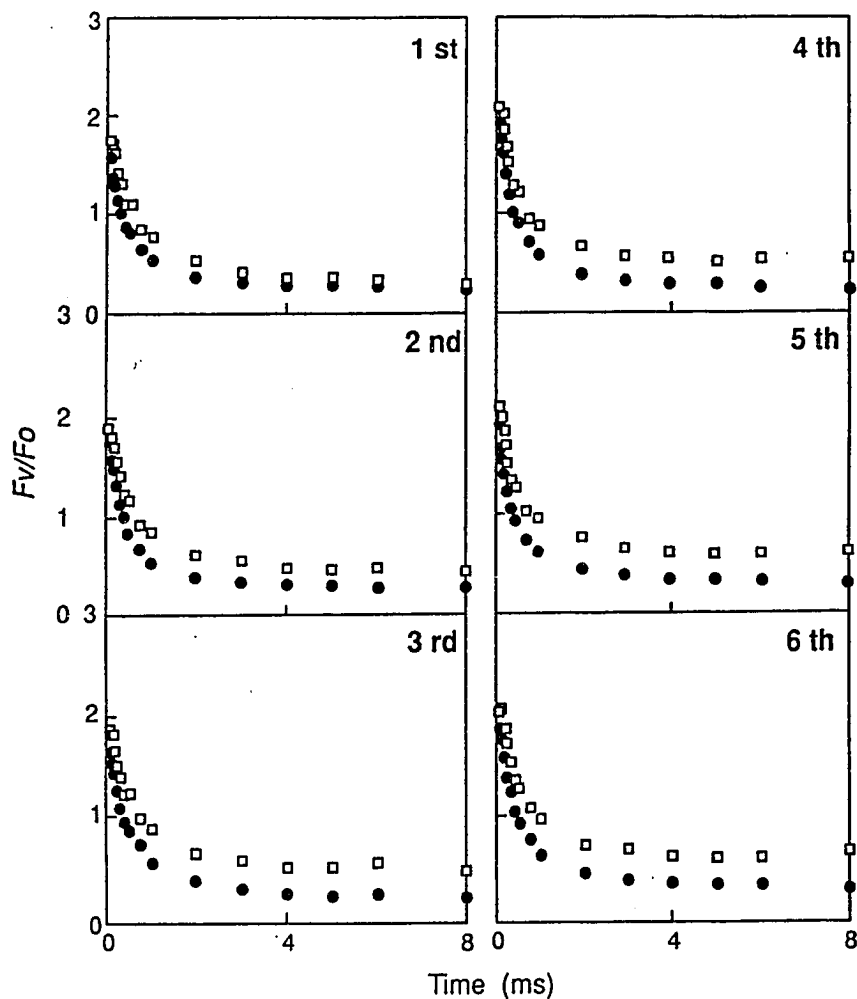


Fig. 3.2. Effect of formate addition on the Chl a fluorescence yield decay at pH 7.5 in spinach thylakoids. The number in each panel refers to the actinic flash number. Open squares, samples treated with 100 mM formate; closed circles, control.  $F_v$  refers to variable Chl a fluorescence yield, and  $F_o$  to minimum fluorescence yield in weak light. Other experimental conditions are the same as that in Fig.3.1. The addition of 20 mM bicarbonate totally restored the  $F_v/F_o$  decay to the control level.

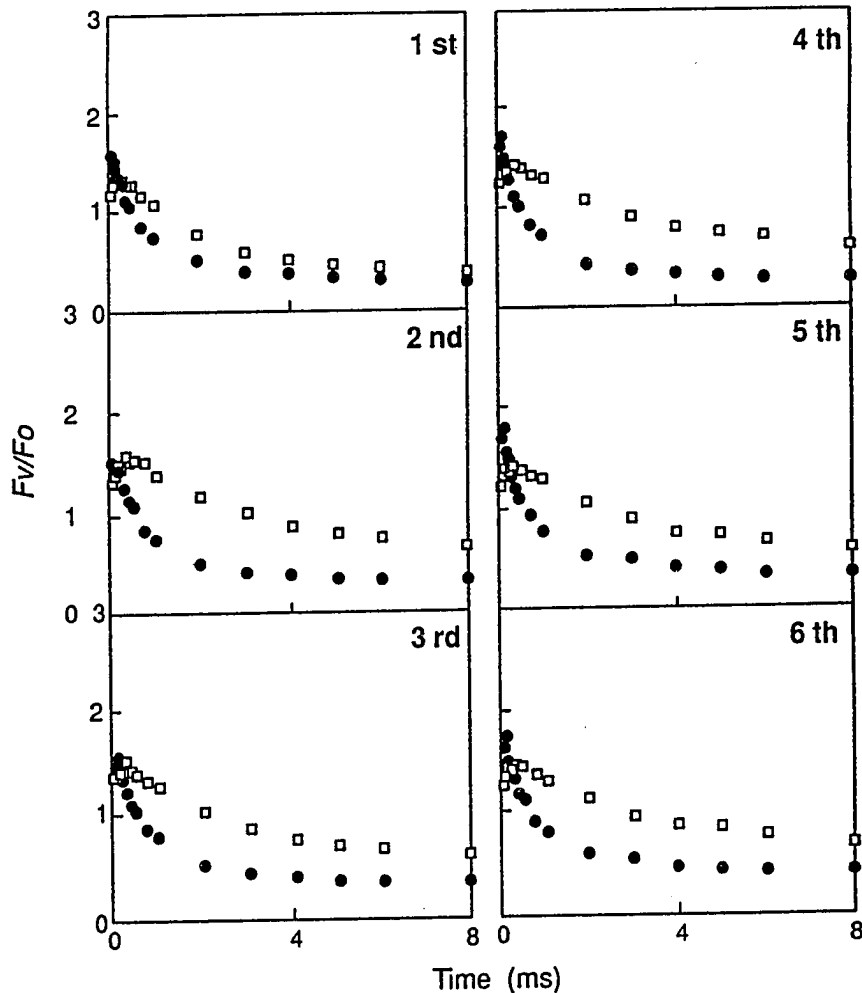


Fig. 3.3. Effect of formate addition on the Chl a fluorescence yield decay at pH 6.0 in spinach thylakoids. The number in each panel refers to the actinic flash number. Open squares, samples treated with 100 mM formate; closed circles, control.  $F_v$  refers to variable Chl a fluorescence yield, and  $F_o$  to minimum fluorescence yield in weak light. Other experimental conditions are the same as that in Fig. 3.1. The addition of 20 mM bicarbonate totally restored the  $F_v/F_o$  decay to the control level.

$Q_BH_2$ . The addition of 20 mM bicarbonate restored the variable Chl a fluorescence decay to the control level at the 3 pH's used demonstrating the competition between formate and bicarbonate.

The effect of formate was, however, different at the three pH's. After flash 2, the slowing down of fluorescence yield decay was much larger at 6.5 (Fig. 3.1) than at pH 7.5 (Fig. 3.2). This is in apparent contrast with the previous results of Eaton-Rye and Govindjee (1988a) who had used a long-term formate-treated thylakoids. We have not attempted here to resolve this difference, but, instead focussed on our simple system. In addition, another complication was observed at pH 6.0: a rising phase in the Chl a fluorescence yield at short time ( $< 500 \mu s$ ) after the flash (Fig. 3.3). This increase is related to the additional formate effect before  $Q_A$  and will be discussed in Chapter VIII.

If the differences of the variable Chl a fluorescence decay between formate-treated and control samples,  $F_v/F_{o(\text{formate})} - F_v/F_{o(\text{control})}$ , are plotted, a maximal increase is found after the second and subsequent flashes at different pH's (Fig. 3.4). The fact that two actinic flashes produce the largest inhibitory effect on the fluorescence yield decay is obvious at pH 6.0 (Fig. 3.4C). However, the effects after flashes 4 and 6 are also high, and within the errors, at both 6.0 and 6.5 (Figs. 3.4B and C). It is difficult to decipher these differences at pH 7.5 as the effects are rather small, but it seems that flash 2 does not produce the maximum effect and the effect saturates at higher flash numbers. This is reminiscent of flash number dependence of  $t_{50}$ , observed by

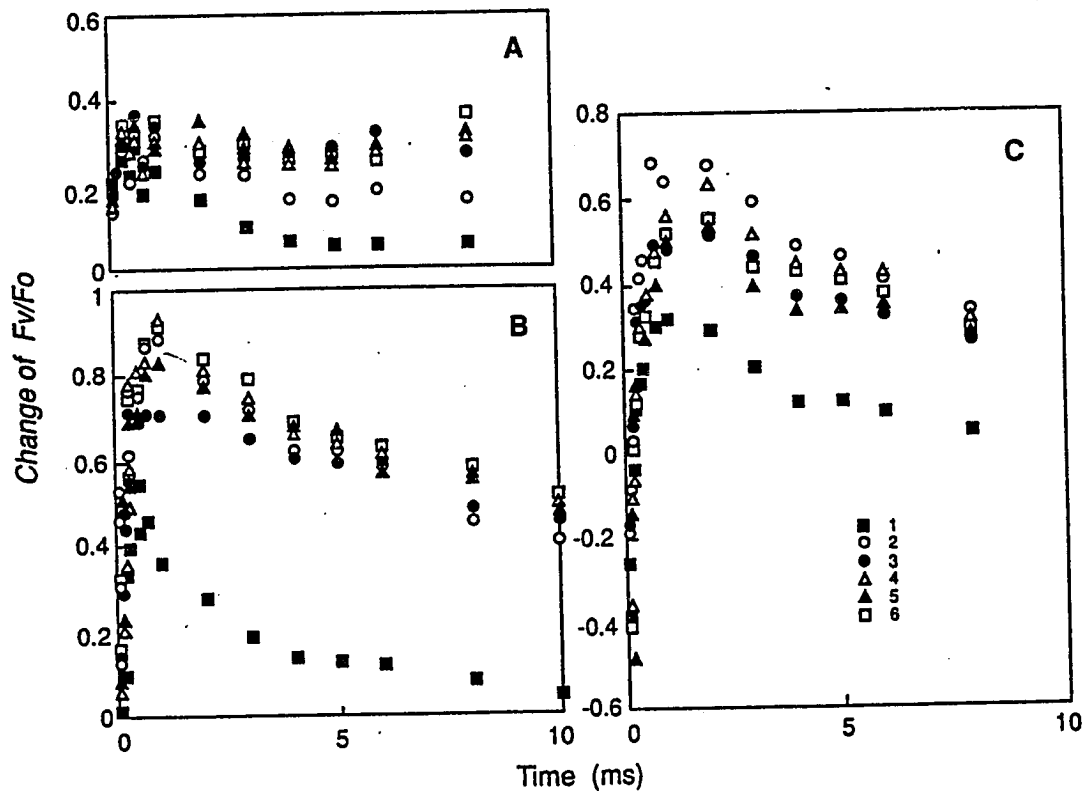


Fig. 3.4. Time course of formate-induced change in the yield of Chl a fluorescence in spinach thylakoids at 3 different pHs. A: at pH 7.5; B: at pH 6.5; and C: at pH 6.0. The symbols in panel C define the number of the actinic flash used. The data were calculated from Figs. 3.1 to 3.3 by subtracting the yield of the control from that of the formate treated sample.

Eaton-Rye and Govindjee (1988a,b). In any case, the results can be explained by assuming that formate binding limits the availability of protons for the formation of  $Q_BH_2$ . The  $H^+$  binding has a relatively weak effect on the kinetics and equilibrium of electron transfer after the first flash (H. Robinson and Crofts, A.R. personal communication), and, thus, our results on the absence of a significant effect by formate treatment after the first flash is consistent with this observation if protonation hypothesis is invoked for the formate effect. We also note a decrease in  $F_v/F_o$  at pH 6.0; this effect is due to an additional effect on the donor side of PS II and will be discussed in Chapter VIII.

The requirement of at least two flashes for the increased level of inhibitory action of formate was further analyzed by first converting Chl a fluorescence yields into  $[Q_A^-]$ . The  $[Q_A^-]$  decay involves multiple processes (see e.g. Crofts et al., 1984; Cao and Govindjee, 1990b; Etienne et al., 1990). Results of the  $[Q_A^-]$  decay can be quantified in terms of three major (fast, intermediate and slow) exponential components. Their amplitudes ( $A_1 - A_3$ ) and lifetimes ( $\tau_1 - \tau_3$ ) were obtained from the  $[Q_A^-]$  decays up to 1 s as summarized in Tables 3.1 and 3.2 for pH's 6.5 and 7.5 for flashes 1 - 5. The fast (subms) component reflects the average kinetics of direct reoxidation of  $Q_A^-$  by  $Q_B$  and by  $Q_B^-$  since no attempt was made in these experiments to start from all  $Q_B$  state. The intermediate component (ms) reflects the  $[Q_A^-]$  equilibrium, partially controlled by the movement of plastoquinone to PS II without bound  $Q_B$ , and the slow one (s) reflects the back-reaction between  $Q_B^-$  and different



TABLE 3.1. Amplitudes (A) and lifetimes ( $\tau$ ) of components of the  $Q_A^-$  decay after flashes 1-5, in control thylakoids at pH's 6.5 and 7.5. Chl  $a$  fluorescence yield decays were measured up to 1 s. Six  $\mu\text{M}$  DCMU was added to obtain  $F_{\text{max}}$  at  $t = 0$  and to set  $[Q_A^-]_{\text{max}}$  at 1. This analysis is based on one experiment only.

pH	flash number	$A_1$	$\tau_1$ ( $\mu\text{s}$ )	$A_2$	$\tau_2$ (ms)	$A_3$	$\tau_3$ (s)	$X^2$
6.5	1	0.49	410	0.10	5.7	0.15	2.4	0.44
	2	0.51	560	0.08	4.1	0.17	3.7	0.38
	3	0.45	600	0.10	2.5	0.16	3.1	0.74
	4	0.42	420	0.22	1.2	0.14	3.0	0.60
	5	0.40	330	0.23	1.3	0.17	3.4	0.50
7.5	1	0.32	120	0.38	0.53	0.23	1.0	0.69
	2	0.35	440	0.29	1.1	0.21	1.2	0.62
	3	0.32	370	0.30	0.89	0.21	1.4	0.31
	4	0.34	310	0.38	1.0	0.18	1.6	0.51
	5	0.37	300	0.28	0.93	0.22	1.3	0.51

TABLE 3.2. Amplitudes (A) and lifetimes ( $\tau$ ) of three components of the  $Q_A^-$  decay after flashes 1-5, in 100 mM formate-treated thylakoids at pH's 6.5 and 7.5. For other details, see TABLE 3.1. This analysis is based on one experiment only.

pH	flash number	$A_1$	$\tau_1$ ( $\mu\text{s}$ )	$A_2$	$\tau_2$ (ms)	$A_3$	$\tau_3$ (s)	$X^2$
6.5	1	0.38	1500	0.08	22	0.19	6.8	0.64
	2	0.20	1700	0.21	14	0.26	3.2	0.57
	3	0.23	1500	0.15	14	0.31	2.1	0.55
	4	0.22	1100	0.21	13	0.28	2.4	0.40
	5	0.23	1600	0.18	17	0.30	2.1	0.35
7.5	1	0.50	280	0.11	12	0.29	4.4	2.7
	2	0.43	750	0.06	16	0.32	3.4	0.66
	3	0.39	670	0.06	11	0.36	3.7	0.34
	4	0.45	610	0.04	12	0.36	3.7	0.59
	5	0.42	480	0.05	13	0.39	3.2	0.34

S states of the oxygen evolving complex, particularly  $S_2$ . A combination of both amplitudes of the intermediate and the slow components,  $A_2 + A_3$ , could be chosen to represent a quasi-steady-state  $[Q_A^-]$  due to  $[Q_A^-]$  equilibria.

A general picture at the 2 pH's used is as follows. In control thylakoids and after one flash, 32% - 49% of the  $[Q_A^-]$  decay is through the fast component ( $\tau_1$  ranging from 120 to 410  $\mu$ s), 25 - 61% through the intermediate and the slow components (Table 3.1). There is no definite flash number dependence observable in control thylakoids in agreement with the observations in earlier publications (see e.g. Eaton-Rye and Govindjee, 1988a,b).

After the second flash and at pH 6.5, the  $[Q_A^-]$  decay in the formate incubated thylakoids demonstrates (Table 3.1) (1) an increase in  $\tau_1$  from 560  $\mu$ s to 1700  $\mu$ s; and (2) a decrease of  $A_1$  from 0.51 to 0.20 and, thus, an increase in the ratio of  $A_1$  to  $(A_2 + A_3)$  from 2 to 0.4. These results indicate (a) decreases in the rate constants of the  $Q_A^-$  reoxidation by  $Q_B/Q_B^-$  and (b) shifts of the equilibrium  $Q_A^-Q_B \rightleftharpoons Q_AQ_B^-$  towards the left. This effect is sustained after second and subsequent flashes. At pH 7.5, however, there is no significant large difference in either  $\tau_1$  or the ratio of  $A_1$  to  $(A_2 + A_3)$ . In view of the preliminary nature of this analysis, further experiments and analysis are necessary to obtain quantitative results.

The above analysis suggests that formate causes an increase of the lifetime of  $Q_A^-$  reoxidation by  $Q_B^-$  and shifts of the equilibrium  $Q_A^-Q_B \rightleftharpoons Q_AQ_B^-$  towards the left after the second and subsequent

flashes at pH 6.5. Our analysis shows the requirement of at least two flashes for the full formate effect on both  $\tau_1$  and equilibrium  $[Q_A^-]$  and is consistent with the previously suggested role for bicarbonate in protonation since bicarbonate fully reversed all the effects.

To check if the effects of 100 mM formate, observed here, are due to surface potential changes, 100 mM of NaCl was added to spinach thylakoid suspensions instead of Na formate in experiments otherwise identical to those used in Fig. 3.2. No effect was observed on the decay of  $[Q_A^-]$  after any of the six actinic flashes (data not shown). Therefore, the effect observed on the addition of Na formate cannot be attributed to changes in the surface potential of thylakoids.

#### D. A Working Scheme for the Action of Formate at the Plastoquinone Reductase Site

Figure 3.5 shows a simplified working scheme that explains the formate effect (Figs. 3.1 to 3.4) on the two-electron gate in PS II.

When the plastoquinone pool is oxidized, the total (T) amount of the dark-adapted PS II RC's in the thylakoid membrane, to which formate (F) is added, is expected to be in one of the following states:  $Q_A$  (without  $Q_B$  bound),  $Q_A Q_B$  (with  $Q_B$  bound),  $FQ_A$  ( $Q_A$  with formate bound) and  $FQ_A Q_B$  ( $Q_A$  with both  $Q_B$  and formate bound). The formate-free and formate-bound RC's can be represented as:

$$\begin{aligned}
 [RC] &= [Q_A] + [Q_A Q_B] \\
 &= \{1 + K_c/[PQ]\} [Q_A Q_B] \qquad (3.1)
 \end{aligned}$$



$$\begin{aligned} \text{and } [\text{FRC}] &= [\text{FQ}_A] + [\text{FQ}_A\text{Q}_B] \\ &= \{1 + K_o/[\text{PQ}]\} [\text{FQ}_A\text{Q}_B] \end{aligned} \quad (3.2)$$

where,  $[\text{PQ}]$  is the *in vivo* PQ concentration.  $[\text{RC}]$  and  $[\text{FRC}]$  represent the concentration of formate-free and formate-bound PS II RC's respectively. The total amount of RC,  $[\text{RC}]_T$ , includes both  $[\text{RC}]$  and  $[\text{FRC}]$ . Equations (3.1) and (3.2) imply that the concentration of each form of RC (RC or FRC) can be directly determined by the concentration of the  $\text{Q}_B$  bound complexes ( $\text{Q}_A\text{Q}_B$  and  $\text{FQ}_A\text{Q}_B$ ),  $K_o$  and  $[\text{PQ}]$ . In our scheme, we have two branches of electron flow in the  $\text{Q}_A\text{-Fe-}\text{Q}_B$  complex: (1) without formate bound (front of the scheme) and (2) with formate bound (back of the scheme). Open arrows indicate reduction of  $\text{Q}_A$  following the first or second actinic flash. Solid arrows represent equilibria in dark reactions involving electron flow, the binding of quinone or formate and protonation.  $K_o$  is the dissociation constant for PQ at the  $\text{Q}_B$  binding site and is assumed to be independent of formate binding.  $K_F$  and  $K_F'$  are dissociation constants for formate at the PS II RC when  $\text{Q}_B$  is absent and when  $\text{Q}_B$  is bound, respectively.  $K_F' = [\text{FQ}_A\text{Q}_B]/[\text{F}][\text{Q}_A\text{Q}_B]$ ;  $K_F = [\text{FQ}_A]/[\text{F}][\text{Q}_A]$ . The estimation of kinetic parameters for formate binding at PS II RC's is based on the above scheme.

The following assumptions were made in the derivation of equations describing formate binding to PS II RC's:

(1)  $k_F$  and  $k_{-F}$  are defined as the on-rate and off-rate binding constants of formate at PS II RC's; their ratio defines the

dissociation constant of formate binding,  $K_f$ .  $k_f$  is a second-order constant, whereas  $k_{-f}$  is a first-order constant. We assume that the dissociation constant of formate at PS II RC's with vacant  $Q_B$  site and that with bound  $Q_B$  site are equal, i.e.,  $K_f = K_f'$ . This means that, unlike herbicides, the binding of formate does not compete with PQ. The two types of centers are separate and formate does not exchange rapidly between them. For the same reason,  $K_o$ , the dissociation constant of PQ or PQH<sub>2</sub> for the  $Q_B$  binding site, is assumed to remain unchanged in the formate binding process.

(2) Compared to the rates of the reduction of  $Q_A$ , the electron transfer from  $Q_A^-$  to  $Q_B$  or  $Q_B^-$ , the binding of  $Q_B$  at its binding site and the protonation of reduced  $Q_B$ , formate binding is assumed to be relatively slow. Therefore, the concentration of [FRC] is determined only by the formate binding process, and other reactions mentioned above can be assumed to be at their equilibrium poise. Furthermore, the rate of formate binding is very slow even when compared with the dark interval (1 second) between two actinic flashes, so that the fraction of formate bound centers does not change during the period between the last actinic flash and the assaying flash sequence.

After the first actinic flash, all of the PS II RC's have transferred one electron to form  $Q_B^-$  in most centers. We suggest that the protonation of  $Q_B^-$  is drastically reduced in the formate-bound PS II RC's (see bold cross in Fig. 3.5). Therefore, although the second photoreaction can take place in the formate bound PS II RC's and  $FQ_A^-Q_B^-$  can form, further reoxidation of  $Q_A^-$  will be

hampered after the second flash since protonation is needed for plastoquinol ( $Q_BH_2$ ) formation. This brings about the large increase of the Chl a fluorescence yield measured, for example, at 1 ms after the second actinic flash. We shall use the fluorescence yield at 1 ms after the second flash to calculate the fraction of the formate-bound PS II RC's in Chapter IV. The protonation steps during  $Q_BH_2$  formation in PS II have not yet been deciphered. From our present results we cannot decide whether the first or the second or both protonation steps are hindered in formate-bound RC's.

The above description fits well with the results at pH 6 and 6.5 (Fig. 3.4). However, results at pH 7.5 are difficult to understand because even in untreated thylakoids (Table 3.1) the lifetime of  $Q_A^-$  reoxidation is somewhat smaller at alkaline than at the acid pH. Perhaps, one can invoke other factors in explaining these results (see e.g., Eaton-Rye and Govindjee, 1988a).

#### D. Conclusion

In this chapter, we have provided a working scheme for formate binding at the electron acceptor side of PS II RC. I will use this scheme to derive equations, which describe the binding of formate to its binding site in  $Q_A-Fe-Q_B$  complex in Chapter IV. Furthermore, results presented here strongly support the protonation hypothesis for the bicarbonate-reversible formate effect at the  $Q_A-Fe-Q_B$  complex of PS II. Future experiments will help us to understand the relationship between the binding species and the protonation steps

leading to  $Q_bH_2$  formation, and to refine the scheme for the action of bicarbonate-reversible inhibitors.



**CHAPTER IV. KINETIC CHARACTERISTICS OF FORMATE/FORMIC ACID  
BINDING AT THE PLASTOQUINONE REDUCTASE SITE SUGGESTS THAT FORMIC  
ACID IS THE ACTIVE SPECIES**

A. Introduction

The requirement for CO<sub>2</sub> in the Hill reaction was originally thought to indicate an involvement of CO<sub>2</sub> in the O<sub>2</sub> evolution (Warburg and Krippahl, 1958, 1960; see Warburg, 1964). Good (1963) was the first to critically examine the effect of various anions on the bicarbonate dependence of the rate of the Hill reaction; he found that small monovalent anions increased the dependence of the Hill reaction rate on bicarbonate in chloroplasts. Particularly effective were formate and acetate, which suggested that the bicarbonate ion, not CO<sub>2</sub>, is the important species. Stemler and Govindjee (1973) took advantage of this suggestion to obtain reproducible large bicarbonate dependence of ferricyanide or 2,6-dichlorophenolindophenol reduction by treating isolated thylakoids with formate or acetate at low pH and high salt concentration in a CO<sub>2</sub>-free atmosphere. Depending upon the pH dependence of the ratio of bicarbonate to CO<sub>2</sub> at equilibrium, Blubaugh and Govindjee (1986) discovered that the Hill reaction rate is stimulated in direct proportion to the equilibrium bicarbonate concentration, but is independent of the equilibrium CO<sub>2</sub> concentration. It was, thus, suggested that bicarbonate is the binding species to the effector site.

In this chapter, kinetic characteristics of formate binding are studied at the plastoquinone reductase site. A pH dependence of

the on-rate constant and the initial binding rate of formate is obtained. This leads to a new insight into the binding species problem. Our data suggest that formic acid, not formate, may be the active species. Thus, [ $\mu\text{M}$ ], not [ $\text{mM}$ ], of the inhibitor may be effective at the plastoquinone reductase site.

Data described in this chapter is based on a recent paper of the author (Xu et al., 1991).

## B. Materials and Methods

The isolation of spinach thylakoids, the measurement of Chl a fluorescence and the calculation of  $[\text{Q}_\text{A}^-]$  were as described in Chapter II. The largest increase of  $[\text{Q}_\text{A}^-]$  was found at 1 ms after the actinic flash (see Chapter III). Therefore, the change of  $[\text{Q}_\text{A}^-]_{(\text{formate})} - [\text{Q}_\text{A}^-]_{(\text{control})}$  at 1 ms was chosen to study the kinetic characteristics of formate binding throughout our study. The dark-adaptation time for thylakoids was 15 minutes. The reaction medium contained 0.4 M sorbitol, 50 mM NaCl, 2 mM MgCl<sub>2</sub> and MES buffer at pH 6.5.

On the basis of the assumptions of the working scheme shown in Fig. 3.5 in Chapter III, we equate the formate bound reaction centers detected after the second flash with the fraction of formate bound reaction centers before the assaying flash sequence, so that  $[\text{FRC}] = [\text{FQ}_\text{A}^- \text{Q}_\text{B}^-]$ . Changes in the concentration of the formate bound PS II RC's are given by Equation (4.1) and monitored by the Chl a fluorescence yield after the second actinic flash:

$$\begin{aligned}
 d[\text{FRC}]/dt &= k_F[\text{F}][\text{RC}] - k_{-F}[\text{FRC}] \\
 &= k_F[\text{F}]([\text{RC}]_T - [\text{FRC}]) - k_{-F}[\text{FRC}]
 \end{aligned}
 \tag{4.1}$$

Under initial conditions, its normalized solution is

$$[\text{FRC}]/[\text{RC}]_T = k_F[\text{F}] (1 - \exp\{-(k_F[\text{F}] + k_{-F})t\}) / (k_F[\text{F}] + k_{-F})
 \tag{4.2}$$

The time course of formate binding in line with Equation (4.2) is obtained by plotting  $[\text{FRC}]/[\text{RC}]_T$  against time.  $[\text{FRC}]/[\text{RC}]_T$  will reach a constant level when the incubation time is long enough. Its first derivative is

$$d([\text{FRC}]/[\text{RC}]_T)/dt = k_F[\text{F}] \exp\{-(k_F[\text{F}] + k_{-F})t\}
 \tag{4.3}$$

The initial on-rate binding constant of formate,  $\{d([\text{FRC}]/[\text{RC}]_T)/dt\}_{t=0}$ , is equal to  $k_F[\text{F}]$  when  $t$  approaches 0 and is defined as  $C$ , which is dependent on the formate concentration in the initial condition and is directly measured from the initial slope of the time course. After plotting  $C$  against formate concentration,  $k_F$  is thereby determined, as defined.

The dissociation constant of formate,  $K_F$ , was calculated by using the formate concentration and the ratio between formate bound or unbound RC's. This ratio was determined from the constant level reached during the time course of formate binding. The off-rate binding constant,  $k_{-F}$ , was obtained from the ratio of  $k_F$  and  $K_F$ .

## C. Results and Discussion

### C.1. Determination of the rate constants for binding and unbinding, and the dissociation constant of formate at the plastoquinone reductase site

The time course of formate binding to spinach thylakoids at pH 6.5, as measured at different formate concentrations, is shown in Fig. 4.1. At pH 6.5, the initial rate of formate binding increased as the concentration of formate was raised. This result can be explained by the second-order binding process indicated in Equation (4.2). Furthermore, the higher plateau for  $[Q_A^-]$  at higher formate concentration also agrees with Equation (4.2). Thus, our experimental results are consistent with those for the binding scheme in Fig. 3.5.

In Fig. 4.2, the initial on-rate binding constant of formate,  $C$ , calculated from the slope of  $[Q_A^-]$  as a function of mixing time, and at different pH values, was plotted against formate concentration. The shape of the curves can be described by the Michaelis-Menten equation, implying a saturation effect. Although the reasons for this saturation effect are not discussed here, it may imply that it depends upon the binding equilibrium as well as the characteristics of the binding site.  $C$  increased with increasing formate concentration at all pH values (5.5-7.5) examined (Fig. 4.2; Equation (4.3)). The initial slope of  $C$ , reflecting the initial binding rate of formate when the formate concentration approaches zero, was also dependent upon the suspension pH. Its value was relatively larger at lower than at the higher pH's. Since the second-order on-rate constant for formate

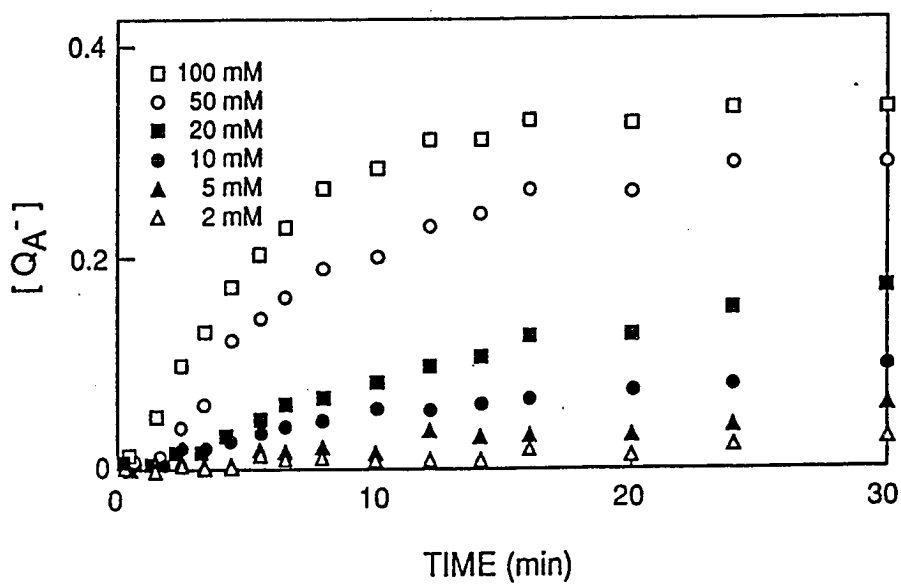


Fig. 4.1. Concentration and time dependence of formate/formic acid binding at pH 6.5, as measured by  $[Q_A^-]$  1 ms after the second actinic flash. Different symbols indicate the different concentrations of added formate (see key in the panel). The other experimental details were the same as in the legend of Fig. 3.1.

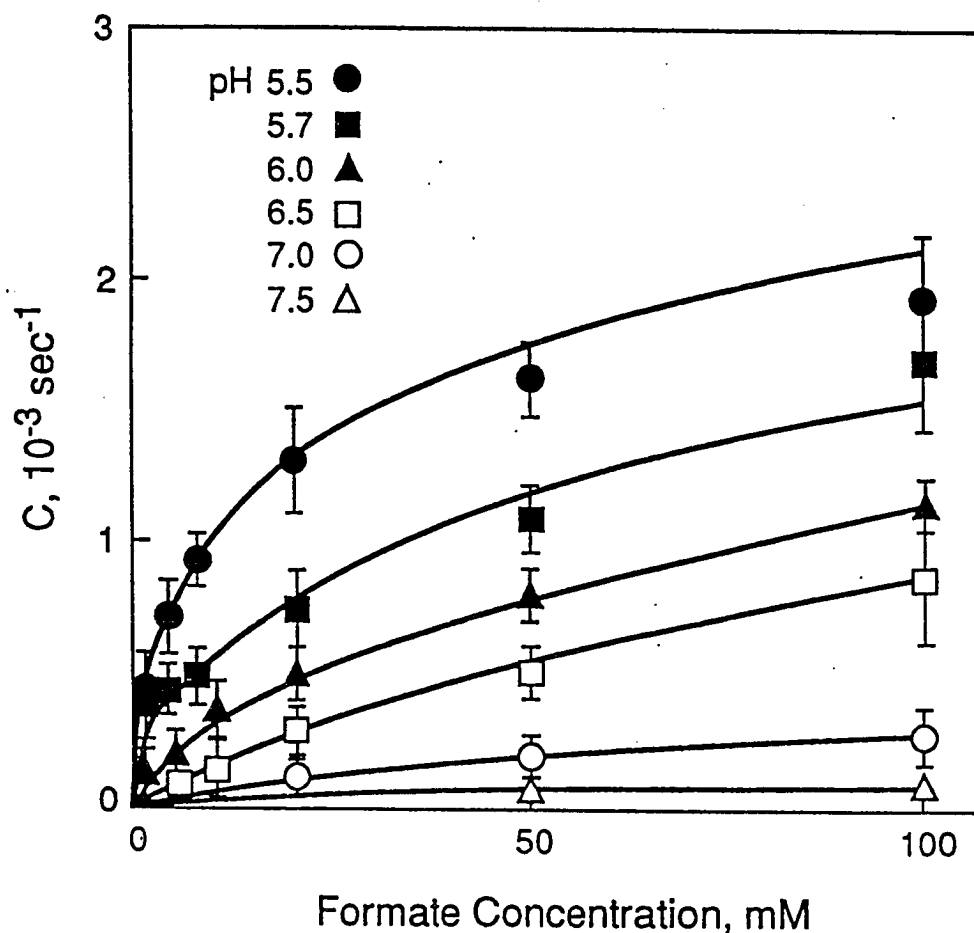


Fig. 4.2. Concentration dependence of the initial rate constant for formate/formic acid binding. The initial rate constant,  $C$ , was calculated from the slope of  $[Q_A^-]$  versus mixing time, for formate/formic acid binding on formate concentration in spinach thylakoids after the second actinic flash. Different symbols indicate the medium pH (see key in the figure). The other experimental conditions were the same as in the legend of Fig. 3.1. The number of experiments to obtain error bars was 4 to 6.

binding,  $k_F$ , is obtained from the initial slopes in Fig. 4.2, the pH dependence of the initial slope of C also demonstrates the pH dependence of  $k_F$ , the on-rate binding constant of formate.

The dissociation constant,  $K_F$ , was obtained under constant binding condition.  $k_{-F}$ , the first order rate constant for the release of formate from its binding site, was derived from the ratio between  $k_F$  and  $K_F$  in each case. The dissociation constant for formate was calculated to be 94 mM at pH 6.5. The rate constants for binding and unbinding as well as the dissociation constant of formate are listed in Table 4.1. The on-rate binding constant of formate,  $k_F$ , was highly pH dependent (top panel of Fig. 4.3): it is 18, 14, 5.6, 1.7 and 0.50  $10^{-2}\text{s}^{-1}\text{M}^{-1}$  at pH 5.5, 5.7, 6.0, 6.5, and 7.0, respectively (Table 4.1):  $k_F$  decreased with decreasing proton concentration. However, the off-rate constant,  $k_{-F}$ , is independent of pH.  $K_F$  also shows a pH dependence. It changes from 12 to 260 mM in the pH range of 5.5 to 7.5.

#### C.2. The binding species: formate or formic acid?

It has been tacitly assumed, thus far, that formate is the binding species that produces bicarbonate-reversible inhibition of electron flow between the  $Q_A$  and PQ pool. However, the pH dependence of the on-rate constant (top panel of Fig. 4.3) and of the initial binding rate (Fig. 4.2) of formate leads to a new insight into the binding species problem. In the medium, formate equilibrates with formic acid. The pK of formate is 3.75. In the 5.5 to 7.5 pH range, used in this study, the change of formic acid

TABLE 4.1. The on-rate ( $k_F$ ), the off-rate ( $k_{-F}$ ) binding constant, and the dissociation constant ( $K_F$ ) of the binding species (considered to be *formate* here) in spinach thylakoids.

pH	$k_F$		$k_{-F}$		$K_F$		n
	$10^{-2}S^{-1}M^{-1}$		$10^{-2}S^{-1}$		mM		
5.5	18	$\pm 6$	0.21	$\pm 0.04$	12	$\pm 4$	6
5.7	14	$\pm 5$	0.18	$\pm 0.05$	13	$\pm 5$	4
6.0	5.6	$\pm 3.0$	0.17	$\pm 0.03$	30	$\pm 16$	4
6.5	1.7	$\pm 0.93$	0.16	$\pm 0.03$	94	$\pm 51$	4
7.0	0.50	$\pm 0.25$	0.13	$\pm 0.01$	260	$\pm 130$	4

n = number of experiments;  $\pm$  indicates standard error.

TABLE 4.2. The on-rate ( $k_F$ ), the off-rate ( $k_{-F}$ ) binding constant, and the dissociation constant ( $K_F$ ) of the binding species (considered to be *formic acid* here) in spinach thylakoids.

pH	$k_F$		$k_{-F}$		$K_F$		n
	$S^{-1}M^{-1}$		$10^{-2}S^{-1}$		$\mu M$		
5.5	10	$\pm 3$	0.21	$\pm 0.04$	210	$\pm 60$	6
5.7	12	$\pm 4$	0.17	$\pm 0.05$	140	$\pm 50$	4
6.0	10	$\pm 6$	0.17	$\pm 0.03$	170	$\pm 100$	4
6.5	9.6	$\pm 5$	0.16	$\pm 0.03$	170	$\pm 90$	4
7.0	8.9	$\pm 4$	0.13	$\pm 0.01$	150	$\pm 70$	4

n = number of experiments;  $\pm$  indicates standard error.



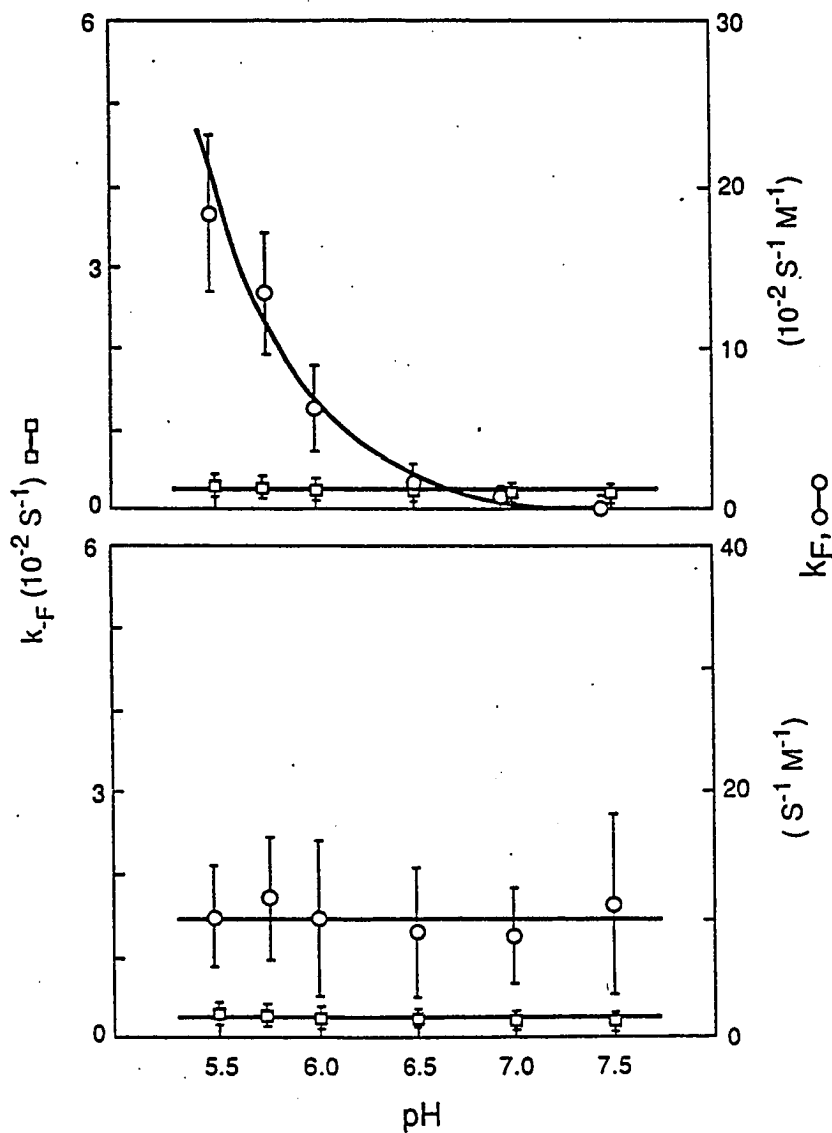


Fig. 4.3. pH dependence of the on-rate ( $k_F$ ) and the off-rate ( $k_{-F}$ ) binding constants when formate or formic acid is considered to be the binding species. Top: after the second actinic flash when formate is considered to be the binding species. Bottom: also after the second actinic flash, but when formic acid is considered to be the binding species. Number of experiments to obtain error bars was 4 to 6. Open circles:  $k_F$ ; open squares:  $k_{-F}$ .

concentration with the pH change is far greater than that of formate. At pH 6, 99.4% of the total amount of the two equilibrium species is formate, changing only to 99.94% at pH 7.0. It is obvious that the change in formate concentration is negligible when the medium pH changes from 5.5 to 7.5. In contrast, the change in formic acid concentration is highly dependent on the medium pH in the pH range of this study. Results (Fig. 4.2 and the top panel of Fig. 4.3), showing the pH dependence of the initial on-rate binding constant,  $C$ , and the second order rate constant,  $k_F$ , imply that formic acid, rather than formate, may be the binding species in PS II.

Since formic acid, not formate, appears to be the binding species, all of the data in Table 4.1 were recalculated using the concentration of formic acid. Using the pK value of formate (3.75) and the medium pH, the ratio between concentrations of formate and formic acid was derived. At pH 5.5, 6.0, 6.5 and 7.0, the concentration of formate is 56, 178, 563 and 1778 times the concentration of formic acid, respectively. The actual concentration of formic acid was calculated and replaced with that of formate in previous [F] in all calculations. New results listed in Table 4.2 are based upon the assumption that formic acid is the binding species. A remarkable result is observed (bottom panel of Fig. 4.3, also see Table 4.2): the on-rate constant,  $k_F$  (around  $10 \text{ s}^{-1}\text{M}^{-1}$ ) becomes pH independent in the pH range of 5.5 to 7.5. The off-rate constant of formate,  $k_{-F}$ , however, still remains pH independent as before. The dissociation constant,  $K_F$ , which was larger than 10 mM when formate

was thought to be the binding species, becomes 200  $\mu\text{M}$  and relatively independent of pH. It is satisfying that the concentration of formic acid required to inhibit  $Q_A$ -to- $Q_B$  reaction is in the micromolar range, not in the 10 millimolar range as would be the case if formate were the inhibitory species.

By taking advantage of the pH dependence of the equilibrium ratio of formate to formic acid to effectively hold one species constant while varying the other, we further probed the chemical nature of the active species of the inhibitor. Measurements of the initial on-rate binding constant,  $C$ , over a pH range from 5.5 to 7.5 indicated that the initial binding rate is proportional to the concentration of formic acid, but independent of formate concentration at constant formic acid concentration (Figs. 4.4 and 4.5). These results demonstrate rather convincingly that formic acid is the active species involved in the inhibitory process.

It has been suggested that bicarbonate and formate bind to  $\text{Fe}^{2+}$  or D1-R269 in PS II (Blubaugh and Govindjee, 1988a). If this is the case, formic acid would have to diffuse a certain distance (e.g., 10-20 Å) before reaching the binding site. It is therefore necessary to consider the influence of diffusion when analyzing the binding kinetics. First, the dependence of the initial binding rate constant,  $C$ , on formate concentration (Fig. 4.2) does not show a linear characteristic, as is expected for diffusion, but saturation. This is best seen from the set of straight lines obtained after the data in Fig. 4.2 were replotted as a double-reciprocal (Lineweaver-Burk) plot (Fig. 4.6). This implies that the effect of

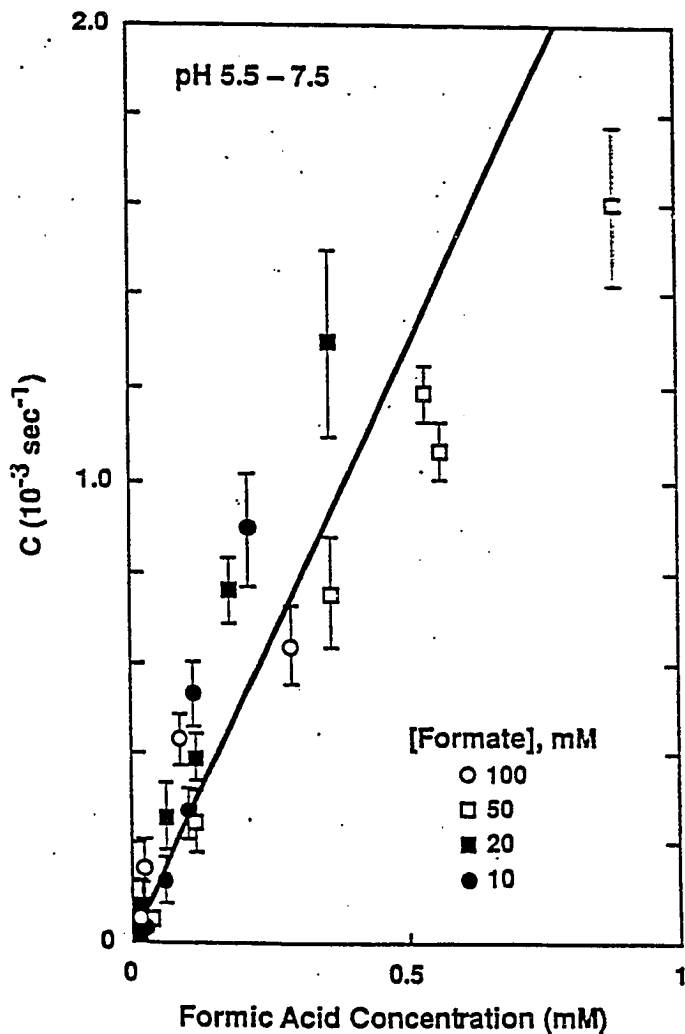


Fig. 4.4. Formic acid concentration dependence of the initial on-rate binding constant of formate/formic acid binding. The data were obtained from Fig. 4.2 at different suspension pH's and formate concentrations. Different symbols indicate the equilibrium formate concentration at several different medium pH. The drawn line was obtained by the least square method. One point at 0.9 mM formic acid (50 mM formate) was not included in the analysis.

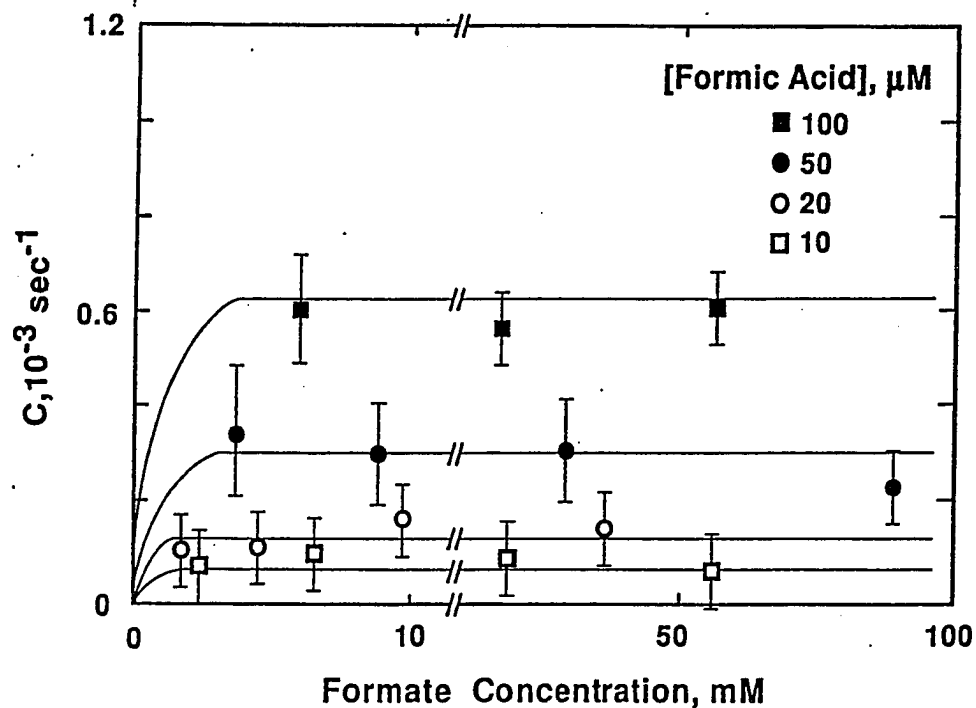


Fig. 4.5. Formate concentration dependence of the initial on-rate binding constant of formate/formic acid binding. The data were obtained from Fig. 4.2. Different symbols indicate four different equilibrium formic acid concentrations at several different medium pHs.

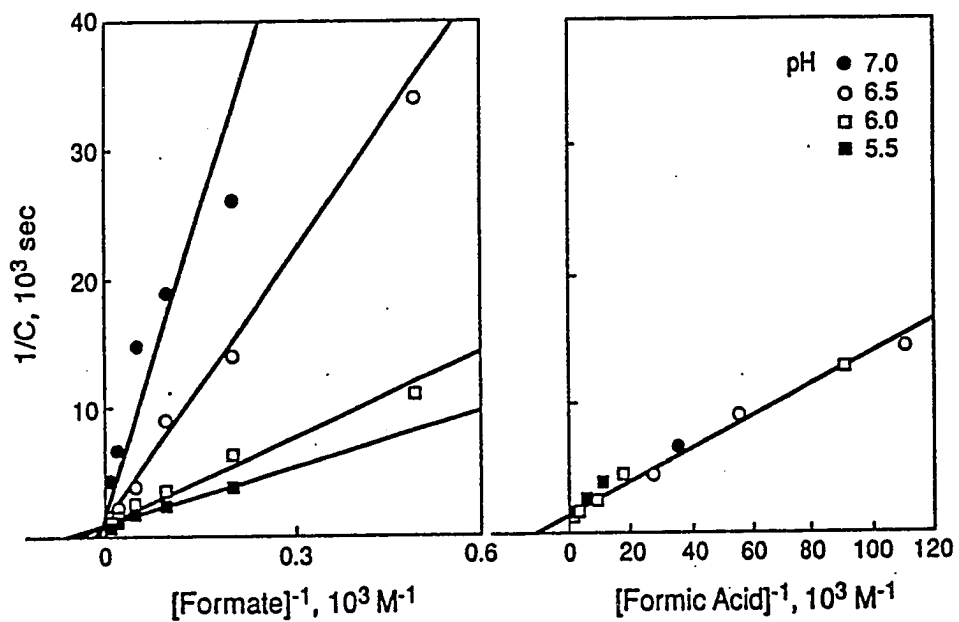


Fig. 4.6. Lineweaver-Burk plot for the initial binding constant when formate or formic acid is considered to be the binding species.  $C$ , initial binding constant; left: formate; and right: formic acid. The data were calculated from those in Fig. 4.2. Different symbols represent different pH values (see key in the right panel).

formate/formic acid follows the saturation characteristic of binding at a specific site on protein. Second, the time scale (minutes) of the formate/formic acid binding is much slower than the diffusion limited rate constant (in the order of  $10^5$  cm<sup>2</sup>/sec) calculated from typical diffusion coefficients for small organic molecules in water (Bruins, 1929). Therefore, we conclude that the binding dominates the time course of formic acid inhibition, and the effect of diffusion can be ignored in the analysis. For further discussion, see Chapter IX.

When formate was considered to be the binding species, a pH dependence was found for the double-reciprocal lines in the left panel of Fig. 4.6. Intercepts on the [concentration]<sup>-1</sup> line indicated that the Michaelis constant,  $K_m$ , related to the dissociation constant, is pH dependent.  $K_m$  is 16, 19, 56 and 100 mM when the pH is 5.5, 6, 6.5 and 7, respectively. The double-reciprocal line became pH independent when formic acid was taken as the binding species (right panel of Fig. 4.6).  $K_m$  is 91  $\mu$ M in this case. The  $K_m$  values fit  $K_f$  values in Table 4.1 and Table 4.2 within errors, as expected from the above conclusion that formic acid is the binding species. The intercepts on the 1/C axis indicated a maximal initial binding rate of about  $1.5 \cdot 10^{-3} \text{s}^{-1}$  for both formate and formic acid.

#### D. Conclusion

In this chapter, the apparent rate constants for binding and unbinding and the dissociation constant of formate were determined

in the pH range from 5.5 to 7.5. The rate of onset of inhibition following formate addition, reflecting the binding of formate/formic acid, was highly dependent on the pH of the suspension medium. Measurements on the initial binding rate, when one of the ( $\text{HCO}_2^-/\text{HCOOH}$ ) equilibrium species was kept constant, suggests that formic acid is the binding species that inhibits electron transfer at the  $Q_B$  binding site in PS II. The  $K_m$  of formic acid was shown to be about 90  $\mu\text{M}$ . This finding gives new insight into the binding niche of  $\text{CO}_2$ /bicarbonate; we need not consider only positively charged amino acids as binding components.



## CHAPTER V. DIFFERENTIAL EFFECTS ON $Q_A^-$ REOXIDATION AND EQUILIBRIA BY CHLOROACETIC ACIDS EXHIBIT THE IMPORTANT ROLE OF $CX_3$ GROUP

### A. Introduction

We have shown in Chapter IV that formic acid, rather than formate, is the species that reversibly inhibits reoxidation of  $Q_A^-$  by  $Q_B$  and affects  $[Q_A^-]$  equilibria. This has implications on the binding niche of bicarbonate-reversible inhibitors in the D1/D2 protein. In this chapter, we have extended our study to (1) acetate and its several chlorinated analogues: monochloroacetate, dichloroacetate and trichloroacetate, and (2) phenol. The  $pK_a$  values of acetate and chloroacetates are closer to that of formate ( $pK_a$ 's range from 4.73 to 0.70) than that of phenol ( $pK_a = 9.9$ ). Furthermore, formate, bicarbonate, acetate and chloroacetates all have an identical carboxyl group on one side, but different groups on the opposite side. Phenol has, in addition, a hydroxyl group similar to that of bicarbonate. Thus, this study is expected to provide further information on the relationship between the structure and the activity of the bicarbonate reversible (or irreversible) inhibitors, as well as the mechanism of action of plastoquinone reduction.

### B. Materials and Methods

The isolation of spinach thylakoids, the measurement of Chl a fluorescence and the calculation of  $[Q_A^-]$  were as described in Chapter II. The fitting of  $[Q_A^-]$  decay data into three (and sometimes four) exponential decays was carried out by the GLOBALS

UNLIMITED™ global analysis software.  $[Q_A^-]$  is given in relative units with 1 being  $[Q_A^-]_{\max}$  obtained in the presence of 6  $\mu\text{M}$  DCMU. Thus, the sum of the analyzed amplitudes (A's) need not add to 1 in our analysis. Thawed thylakoids were suspended in 0.4 M sorbitol, 50 mM NaCl, 2 mM  $\text{MgCl}_2$  and 1 nM gramicidin to a final Chl concentration of 10  $\mu\text{M}$ . Eighty  $\mu\text{M}$  quinhydrone was added to keep most of  $Q_B$  in the oxidized state before the measurements began. The pH of the suspension was adjusted by using 20 mM MES (at pH 6.0 and 6.5) or 20 mM HEPES (at pH 7.5).

To study the concentration dependence of the inhibition of  $Q_A^-$  reoxidation by the chemicals used, the increase in the concentration of  $Q_A^-$  in the PS II reaction centers is plotted as  $[Q_A^-]_{\text{treated}} - [Q_A^-]_{\text{control}}$ . The increase was estimated after 1 minute incubation of thylakoids with the chemical and at 5 ms after the actinic flashes.

Molecular geometries as well as the dipole moment of acetic acid and its chloride derivatives were calculated as described in Chapter II.

## C. Results

### C.1. Inhibition of the $Q_A^-$ reoxidation and effects on $Q_A^-$ equilibria by acetate and three chloroacetates.

#### C.1.a. Acetate

Figure 5.1 shows  $[Q_A^-]$  decays in control, 100 mM acetate ( $\text{pK}_a = 4.73$ ) treated and acetate plus 20 mM bicarbonate treated thylakoids at pH 7.5 (A1 - A4) and pH 6.0 (B1 - B4). These  $[Q_A^-]$  decay measurements, monitoring  $Q_A^-$  reoxidation and equilibria were

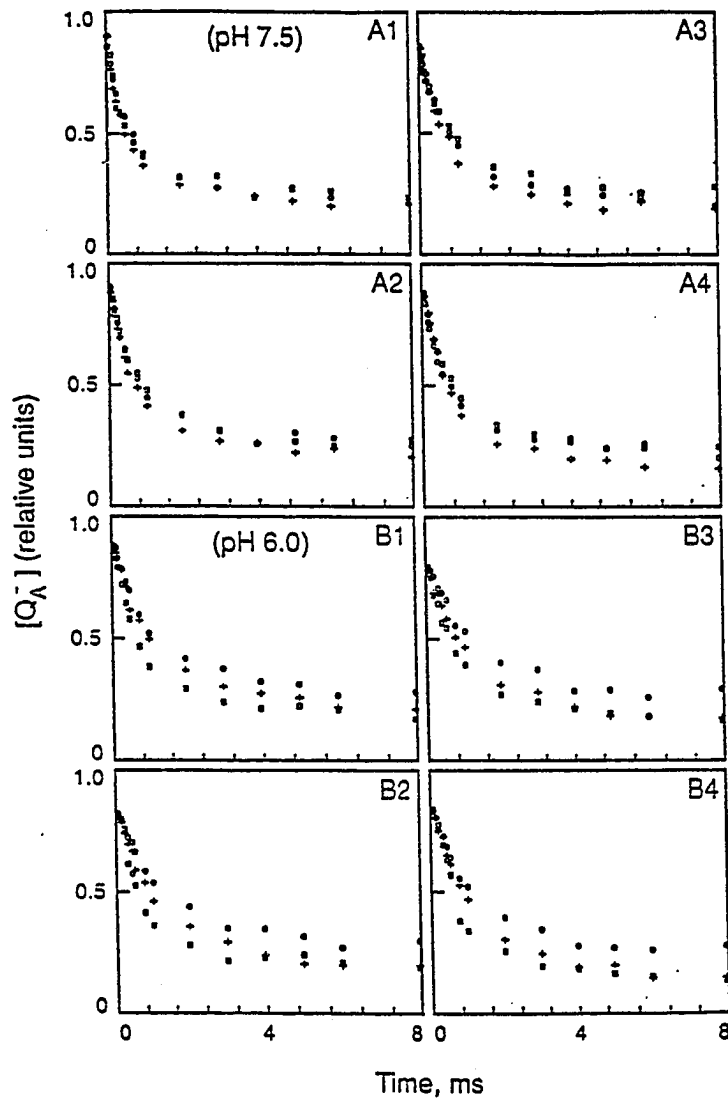


Fig. 5.1. Decay of  $[Q_A^-]$  after an actinic flash in control and acetate-treated ( $\pm$  bicarbonate) thylakoids at pH 7.5 and at pH 6.0. The number in each panel refers to the actinic flash number 1 - 4. Panels A: pH 7.5; Panels B: pH 6.0. The dark-adaptation time was 5 min. In the reaction medium, 0.4 M sorbitol, 50 mM NaCl, 2 mM  $MgCl_2$ , 1 nM gramicidin and 80  $\mu$ M quinhydrone were included. Open circles, 100 mM acetate-treated; pluses, control; open squares, acetate-treated spinach thylakoids to which 20 mM bicarbonate was added.

based on the decay of Chl a fluorescence yield after flash 1 (A1, B1), 2 (A2, B2), 3 (A3, B3) or 4 (A4, B4) (dark interval between flashes, 1 s). At pH 7.5, no significant inhibition of the  $Q_A^-$  reoxidation or an effect on  $Q_A^-$  equilibria is seen with acetate treatment, but, an effect on both  $Q_A^-$  reoxidation and equilibria is observed at pH 6.0. The increased effect at the lower pH is consistent with the conclusion that the acid, not the anion, is the active inhibitory species, as was found for the formic acid (Chapter IV).

The  $[Q_A^-]$  decay involves multiple processes (Crofts et al. 1984, Cao and Govindjee, 1990b; Etienne et al., 1990). Results were quantitated by describing the decay in terms of three major (fast, intermediate and slow) exponential components. Their amplitudes ( $A_1 - A_3$ ) and lifetimes ( $\tau_1 - \tau_3$ ) were derived from  $[Q_A^-]$  decays (up to 1 s) and summarized in Tables 5.1, 5.2, 5.3 and 5.4 for flashes 1 - 4. The fast (subms) component reflects the kinetics of direct reoxidation of  $Q_A^-$  by  $Q_B$  and/or  $Q_B^-$  (see e.g., Robinson and Crofts, 1983). The intermediate one (ms) is suggested to reflect the  $[Q_A^-]$  equilibrium, partially controlled by the movement of plastoquinone to PS II without bound  $Q_B$  (Crofts et al., 1984). The slow one (s) reflects the back-reaction between  $Q_B^-$  and different S states of the oxygen evolving complex, particularly  $S_2$ . The summation of amplitudes of the intermediate and the slow components,  $A_2 + A_3$ , represents a quasi-steady-state  $[Q_A^-]$  due to  $[Q_A^-]$  equilibria.  $(A_2 + A_3)/A_1$  is the ratio between the quasi-steady-state  $[Q_A^-]$  and

the  $[Q_A^-]$  that is oxidized by  $Q_B$  (or  $Q_B^-$ ). Data at pH 6 were chosen for analysis as they showed the largest inhibitory effect.

In control thylakoids (with 20 mM bicarbonate) and after one flash, 63% of the  $[Q_A^-]$  decay is through the fast component ( $\tau_1$ , 420  $\mu$ s), 15% through the intermediate ( $\tau_2$ , 3.3 ms) and 14% through the slow component ( $\tau_3$ , 1.8 s) (Table 5.1).  $(A_2 + A_3)/A_1$  is 0.46. No large changes were observed after flashes 2, 3 and 4 (Tables 5.2 - 5.4).

After flash one, the major effect of DCMU, the well-known PS II herbicide, is a drastic increase in  $A_3$  to 75% (Table 5.1) and concomitantly in  $(A_2 + A_3)/A_1$  to 11. This is accompanied by a drastic decrease in  $A_1$  to 8%. This shows almost complete inhibition of electron flow from  $Q_A^-$  to  $Q_B$ , since the latter is displaced by DCMU (Velthuys, 1981). Furthermore, in the 8% of centers, the electron flow was slowed to about 1.6 ms. The intermediate component is also very small (9%) and its lifetime was increased to about 140 ms; within the errors of measurements, no significant difference was obtained after flashes 2, 3 and 4 (Tables 5.2-5.4). Finally, DCMU did not alter  $\tau_3$  ( $1.8 \pm 0.3$  s). All of the above information can be used in evaluating the nature of effects by (chloro)acetates.

After the first flash, the incubation of thylakoids with 100 mM acetate causes an increase in  $\tau_1$  (from 420  $\mu$ s to 610  $\mu$ s) and a noticeable decrease in  $A_1$  (from 0.63 to 0.53). All other changes were within acceptable errors. The increase in  $\tau_1$  indicates an increase in the lifetime of the  $Q_A$  reoxidation by  $Q_B$ .  $(A_2 + A_3)/A_1$

TABLE 5.1. Amplitudes (A) and lifetimes ( $\tau$ ) of three components of the  $Q_A^-$  decay after flash 1, in control and (chloro)acetate-treated ( $\pm$  bicarbonate) spinach thylakoids at pH 6.0. Chl a fluorescence yield decays were measured up to 1 s. Concentration is 20 mM for bicarbonate or 100 mM for (chloro)acetates. Six  $\mu$ M DCMU was added to obtain  $F_{max}$  at  $t = 0$ .  $[Q_A^-]$  at  $F_{max}$  was arbitrarily set at 1.  $\tau_3 = 1.8 \pm 0.3$  s. Amplitudes were within  $\pm 0.05$ ,  $\tau_1$  within  $\pm 50$   $\mu$ s and  $\tau_2$  within  $\pm 2$  ms for control and acetate samples and within  $\pm 20$  ms for others (n = 2 - 4).

	$A_1$	$\tau_1$ ( $\mu$ s)	$A_2$	$\tau_2$ (ms)	$A_3$	$X^2$
1. control (with bicarbonate)	0.63	420	0.15	3.3	0.14	0.95
2. 1. + DCMU	0.08	1600	0.09	143	0.75	0.47
3. with acetate	0.53	610	0.21	9.0	0.16	0.68
4. 3. + bicarbonate	0.63	470	0.09	4.6	0.15	1.3
5. with monochloroacetate	0.47	710	0.27	70	0.21	1.2
6. 5. + bicarbonate	0.54	510	0.13	27	0.17	1.1
7. with dichloroacetate	0.41	970	0.08	65	0.44	0.37
8. 7. + bicarbonate	0.45	550	0.14	48	0.29	0.53
9. with trichloroacetate	0.16	640	0.10	99	0.42	0.34
10. 9. + bicarbonate	0.08	-*	0.14	-*	0.40	0.35

\* due to errors larger than 100  $\mu$ s and 20 ms for  $\tau_1$  and  $\tau_2$  in this sample,  $\tau_s$  were not determined.

TABLE 5.2. Amplitudes (A) and lifetimes ( $\tau$ ) of three components of the  $Q_A^-$  decay after flash 2, in control and (chloro)acetate-treated ( $\pm$  bicarbonate) spinach thylakoids at pH 6.0. Chl a fluorescence yield decays were measured up to 1 s. Concentration is 20 mM for bicarbonate or 100 mM for (chloro)acetates. Six  $\mu$ M DCMU was added to obtain  $F_{max}$  at  $t = 0$ .  $[Q_A^-]$  at  $F_{max}$  was arbitrarily set at 1.  $\tau_3 = 2.5 \pm 0.4$  s. Amplitudes were within  $\pm 0.05$ ,  $\tau_1$  within  $\pm 50$   $\mu$ s and  $\tau_2$  within  $\pm 2$  ms for control and acetate samples and within  $\pm 20$  ms for others (n = 2 - 4).

	$A_1$	$\tau_1$ ( $\mu$ s)	$A_2$	$\tau_2$ (ms)	$A_3$	$X^2$
1. control (with bicarbonate)	0.62	490	0.10	6.0	0.15	1.8
2. 1. + DCMU	0.09	1100	0.06	98	0.83	0.19
3. with acetate	0.51	610	0.17	12	0.19	0.81
4. 3. + bicarbonate	0.64	440	0.12	5.9	0.14	1.2
5. with monochloroacetate	0.50	920	0.18	53	0.20	0.67
6. 5. + bicarbonate	0.61	570	0.09	24	0.14	0.68
7. with dichloroacetate	0.31	920	0.16	46	0.49	0.36
8. 7. + bicarbonate	0.53	640	0.14	86	0.21	0.51
9. with trichloroacetate	0.09	1700	0.17	114	0.56	0.22
10. 9. + bicarbonate	0.18	1000	0.14	54	0.48	0.32

TABLE 5.3. Amplitudes (A) and lifetimes ( $\tau$ ) of three components of the  $Q_A^-$  decay after flash 3, in control and (chloro)acetate-treated ( $\pm$  bicarbonate) spinach thylakoids at pH 6.0. Chl a fluorescence yield decays were measured up to 1 s. Concentration is 20 mM for bicarbonate or 100 mM for (chloro)acetates. Six  $\mu$ M DCMU was added to obtain  $F_{\max}$  at  $t = 0$ .  $[Q_A^-]$  at  $F_{\max}$  was arbitrarily set at 1.  $\tau_3 = 2.3 \pm 0.5$  s. Amplitudes were within  $\pm 0.05$ ,  $\tau_1$  within  $\pm 50 \mu$ s and  $\tau_2$  within  $\pm 2$  ms for control and acetate samples and within  $\pm 20$  ms for others ( $n = 2 - 4$ ).

	$A_1$	$\tau_1$ ( $\mu$ s)	$A_2$	$\tau_2$ (ms)	$A_3$	$X^2$
1. control (with bicarbonate)	0.60	770	0.08	17	0.11	0.93
2. 1. + DCMU	0.09	1100	0.18	290	0.72	0.12
3. with acetate	0.50	850	0.13	14	0.17	0.80
4. 3. + bicarbonate	0.54	500	0.17	5	0.12	1.4
5. with monochloroacetate	0.43	920	0.22	73	0.19	0.42
6. 5. + bicarbonate	0.55	670	0.13	69	0.12	0.77
7. with dichloroacetate	0.30	920	0.14	29	0.49	0.33
8. 7. + bicarbonate	0.47	700	0.13	66	0.24	0.61
9. with trichloroacetate	0.09	990	0.14	72	0.61	0.20
10. 9. + bicarbonate	0.19	800	0.13	22	0.52	0.34

TABLE 5.4. Amplitudes (A) and lifetimes ( $\tau$ ) of three components of the  $Q_A^-$  decay after flash 4, in control and (chloro)acetate-treated ( $\pm$  bicarbonate) spinach thylakoids at pH 6.0. Chl a fluorescence yield decays were measured up to 1 s. Concentration is 20 mM for bicarbonate or 100 mM for (chloro)acetates. Six  $\mu$ M DCMU was added to obtain  $F_{\max}$  at  $t = 0$ .  $[Q_A^-]$  at  $F_{\max}$  was arbitrarily set at 1.  $\tau_3 = 1.9 \pm 0.3$  s. Amplitudes were within  $\pm 0.05$ ,  $\tau_1$  within  $\pm 50 \mu$ s and  $\tau_2$  within  $\pm 2$  ms for control and acetate samples and within  $\pm 20$  ms for others ( $n = 2 - 4$ ).

	$A_1$	$\tau_1$ ( $\mu$ s)	$A_2$	$\tau_2$ (ms)	$A_3$	$X^2$
1. control (with bicarbonate)	0.69	520	0.11	5.4	0.10	1.1
2. 1. + DCMU	0.08	960	0.10	17	0.80	0.22
3. with acetate	0.58	800	0.13	12	0.14	0.98
4. 3. + bicarbonate	0.66	410	0.15	5.0	0.09	1.1
5. with monochloroacetate	0.53	980	0.18	85	0.15	0.72
6. 5. + bicarbonate	0.64	490	0.11	11	0.12	0.64
7. with dichloroacetate	0.32	820	0.12	21	0.50	0.41
8. 7. + bicarbonate	0.53	520	0.11	20	0.25	0.56
9. with trichloroacetate	0.11	1300	0.14	64	0.63	0.37
10. 9. + bicarbonate	0.21	880	0.14	39	0.49	0.22

increases from 0.46 to 0.70, indicating that acetate also causes a shift of equilibrium  $Q_A^-Q_B^- \rightleftharpoons Q_AQ_B^-$  towards  $[Q_A^-]$ . The addition of 20 mM bicarbonate reverses the  $[Q_A^-]$  decay to its control level after flashes 1 - 4 (Fig. 5.1). The inhibition of  $Q_A^-$  oxidation and the effect on  $Q_A^-$  equilibria by acetate is much weaker than that by formate (cf. Fig. 5.1 with Fig. 3.1). Furthermore, the difference between the effect after flash 1 and flash 2 is not as obvious for acetate as it was for formate (Chapter III).

#### C.1.b. Monochloroacetate

Figure 5.2 shows  $[Q_A^-]$  decays in control, 100 mM monochloroacetate (MCA;  $pK_a = 2.81$ ) treated and MCA plus 20 mM bicarbonate treated thylakoids at pH 7.5 (A1 - A4) and pH 6.0 (B1 - B4) after flashes 1 - 4. No significant inhibition of the  $Q_A^-$  reoxidation or an effect on  $Q_A^-$  equilibria by MCA seems to be there at 7.5. However, a large effect appears to occur at pH 6.0 both in the reoxidation rate of  $Q_A^-$  as well as in  $Q_A^-$  equilibria reactions (cf. panels A and B). These effects, after all of the 4 flashes, are much larger than those in the presence of 100 mM acetate at pH 6.0 (cf. Fig. 5.1 with Fig. 5.2, panels B).

Analysis of the  $[Q_A^-]$  decays, after the first flash, displays that in the MCA incubated thylakoids (Table 5.1): (1)  $\tau_1$  increases from 420  $\mu$ s to 710  $\mu$ s; (2)  $\tau_2$  increases from about 3 ms to 70 ms; (3)  $A_1$  decreases from 63% to 47%; (4)  $A_3$  increases from 14% to 21%; and (5)  $(A_2 + A_3)/A_1$  increases from 0.46 to 1.0. The latter implies a shift of the equilibrium  $Q_A^-Q_B^- \rightleftharpoons Q_AQ_B^-$  towards  $[Q_A^-]$  by MCA. The



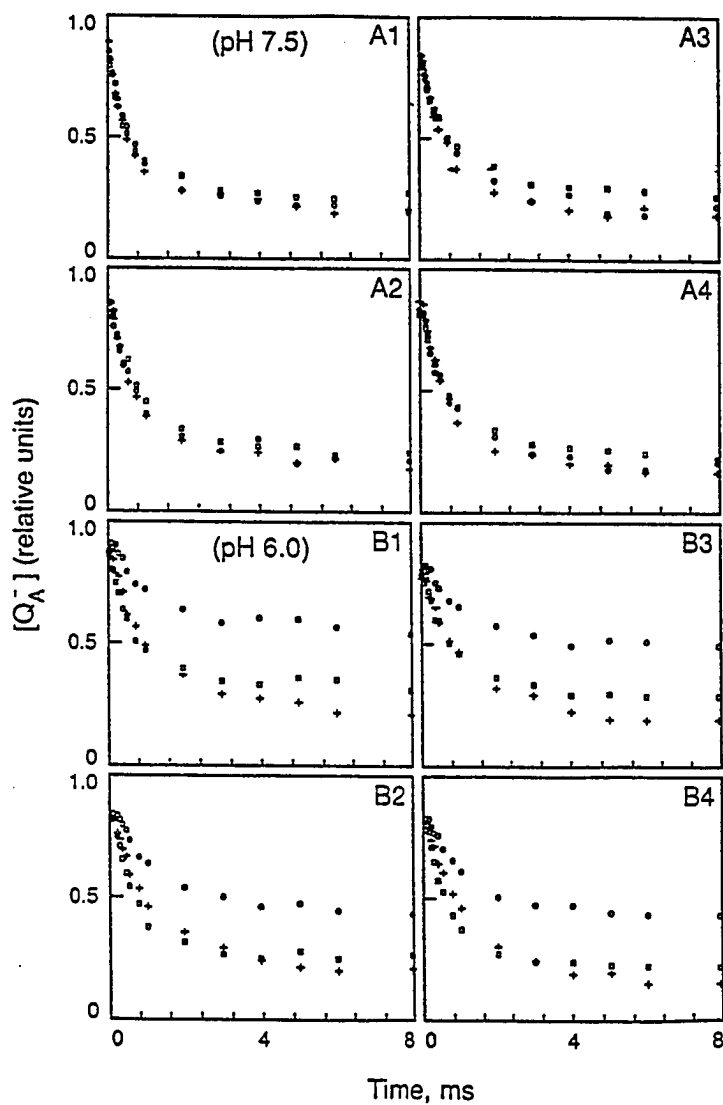


Fig. 5.2. Decay of  $[Q_A^-]$  after an actinic flash in control and monochloroacetate-treated ( $\pm$  bicarbonate) spinach thylakoids at pH 7.5 and at pH 6.0. The experimental condition was the same as in Fig. 5.1. Open circles, 100 mM monochloroacetate-treated; pluses, control; open squares, monochloroacetate-treated to which 20 mM bicarbonate was added.

increase of  $\tau_1$  shows that MCA induces an increase of the lifetime of the  $Q_A$  reoxidation by  $Q_B$ . After flashes 2, 3 and 4 (Tables 5.2-5.4), effects were essentially similar, but  $\tau_1$  was larger (920  $\mu$ s) than that after flash 1. The addition of 20 mM bicarbonate restored the  $[Q_A^-]$  decays to the control level (Fig. 5.2); however, the restoration of  $\tau_1$  and  $\tau_2$  was not complete (Tables 5.1-5.2). A comparison of results on MCA with acetate suggests that an enhancement of the inhibition of  $Q_A^-$  oxidation by  $Q_B$  (or  $Q_B^-$ ) and of equilibrium  $[Q_A^-]$  may have been caused by the chloride substitution in  $CH_3$ .

#### C.1.c. Dichloroacetate

$[Q_A^-]$  decays in control, 100 mM dichloroacetate (DCA;  $pK_d = 1.30$ ) treated and DCA plus 20 mM bicarbonate treated thylakoids are shown in Fig. 5.3 at pH 7.5 (A1 - A4) and pH 6.0 (B1 - B4) after actinic flash 1 (A1, B1), 2 (A2, B2), 3 (A3, B3) or 4 (A4, B4). At pH 6.0, DCA causes an observable inhibition of the  $Q_A^-$  reoxidation as well as an increased  $[Q_A^-]$  equilibrium. These effects are seen even at pH 7.5, and are larger than those induced by MCA treatment (cf. Fig. 5.2 with Fig. 5.3), indicating that further replacement of hydrogen in  $CH_2Cl$  by chloride enhances the inhibition of  $Q_A^-$  reoxidation and equilibration. A comparison of data in panels A with those in panels B shows that after all of the 4 flashes, not only the inhibition of  $[Q_A^-]$  decay, but also the equilibrium  $[Q_A^-]$  is larger at pH 6 than at pH 7.5. In contrast to data with acetate and MCA, the restoration of  $[Q_A^-]$  decay to the control by the addition of 20 mM sodium bicarbonate is only partial in the DCA-

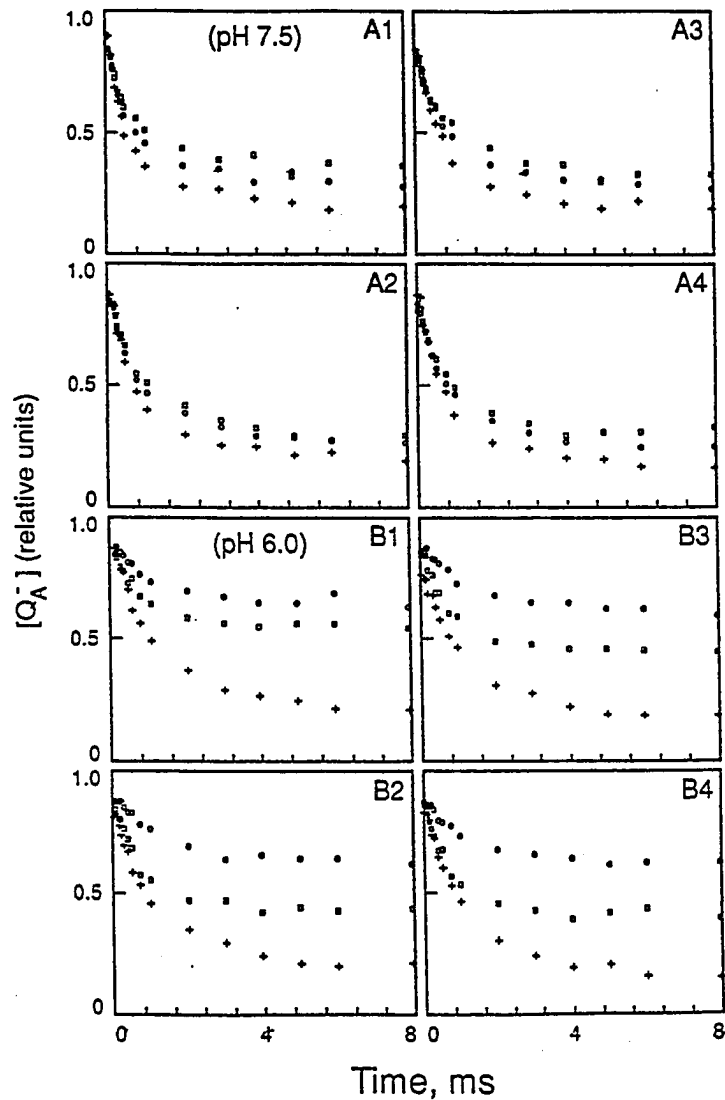


Fig. 5.3. Decay of  $[Q_A^-]$  after an actinic flash in control and dichloroacetate-treated (+ bicarbonate) spinach thylakoids at pH 7.5 and at pH 6.0. The experimental condition was the same as in Fig. 5.1. Open circles, 100 mM dichloroacetate-treated; pluses, control; open squares, dichloroacetate-treated to which 20 mM bicarbonate was added.

treated sample (Fig. 5.3). This is particularly true for the effects on  $Q_A^-$  equilibration. The replacement of a second hydrogen by another chloride in the acetate appears to enhance the inhibition of the  $Q_A^-$  reoxidation and equilibration. These effects must be due to its altered binding in the  $Q_A$ -Fe- $Q_B$  complex.

After the first flash, the  $[Q_A^-]$  decay in the DCA incubated thylakoids shows (Table 5.1) (1) an increase in  $\tau_1$  from 420  $\mu$ s to 970  $\mu$ s; (2) an increase of  $\tau_2$  from 3 ms to 65 ms; (3) a decrease of  $A_1$  from 63% to 41%; (4) an increase of  $A_3$  from 14% to 44%; and (5) an increase of  $(A_2 + A_3)/A_1$  from 0.46 to 1.3. The increase of  $(A_2 + A_3)/A_1$  shows that DCA induced a shift of the  $Q_A^-Q_B \leftrightarrow Q_AQ_B^-$  equilibrium towards  $[Q_A^-]$ . The increase of  $\tau_1$  shows that DCA also causes an increase of the lifetime of the  $Q_A$  reoxidation by  $Q_B$ . These results are intermediate between the control and 6  $\mu$ M DCMU-treated samples. After flashes 2, 3 and 4 (Tables 5.2-5.4), there was a further small but significant increase in  $A_3$  and decrease in  $A_1$  without significant change in  $\tau_3$  and  $\tau_1$ ;  $(A_2 + A_3)/A_1$  increased to 2.1. The decrease in  $A_1$  and increase in  $A_3$  slightly more after the second and subsequent actinic flashes than after the first one is partially reminiscent of results with the effects of formate on  $Q_A^-$  reoxidation (cf. Chapter III with those in Tables 5.1 - 5.4). Thus, in both cases, the protonation at the  $Q_B$ -binding site may have been affected after the addition of the inhibitors. However in the case of DCA, a drastic inhibition is observed already after the first flash at pH 6 (Fig. 3.B1) and a significant inhibition at pH 7.5 (Fig. 3.A1). DCA has been shown here to cause a significant

equilibrium shift of  $Q_A^-Q_B^- \leftrightarrow Q_AQ_B^-$  towards  $[Q_A^-]$  as well as an increase of the lifetime of the  $Q_A^-$  reoxidation by  $Q_B/Q_B^-$ . Partial restoration of  $[Q_A^-]$  decay by bicarbonate makes it a unique inhibitor.

#### C.1.d. Trichloroacetate

Figure 5.4 shows  $[Q_A^-]$  decays in control, 100 mM trichloroacetate (TCA;  $pK_d = 0.70$ ) treated and TCA plus 20 mM bicarbonate treated thylakoids at pH 7.5 (A1 - A4) and pH 6.0 (B1 - B4) after flashes 1 - 4. Both the inhibition of the  $Q_A^-$  reoxidation and the equilibrium  $[Q_A^-]$  appear to be greatly enhanced here compared to that with MCA or DCA, especially at pH 7.5. However, somewhat larger effects occur at lower pH (pH 6.0) than at the higher pH (pH 7.5). In contrast to other acetates, the addition of 20 mM sodium bicarbonate to 100 mM TCA-treated samples can hardly restore the  $[Q_A^-]$  decay to the control level (Fig. 5.4), displaying a bicarbonate irreversible inhibition similar to that with DCMU (data not shown).

Analysis of the  $[Q_A^-]$  decay, after the first flash and at pH 6, shows that in the TCA incubated thylakoids,  $\tau_1$  increases only to 640  $\mu$ s but  $\tau_2$  increases to 99 ms, and  $A_3$  increases to 42% (Table 5.1). However,  $A_1$  is greatly decreased to 16%.  $(A_2 + A_3)/A_1$  increases from 1.3 to 3.3 after flash one, indicating that TCA causes a significant shift of equilibrium  $Q_A^-Q_B^- \leftrightarrow Q_AQ_B^-$  towards  $Q_A^-$ . The large decrease in the amplitude of the fast component is partly due to a decrease in the  $F_{max}$  extrapolated to time zero. In this particular

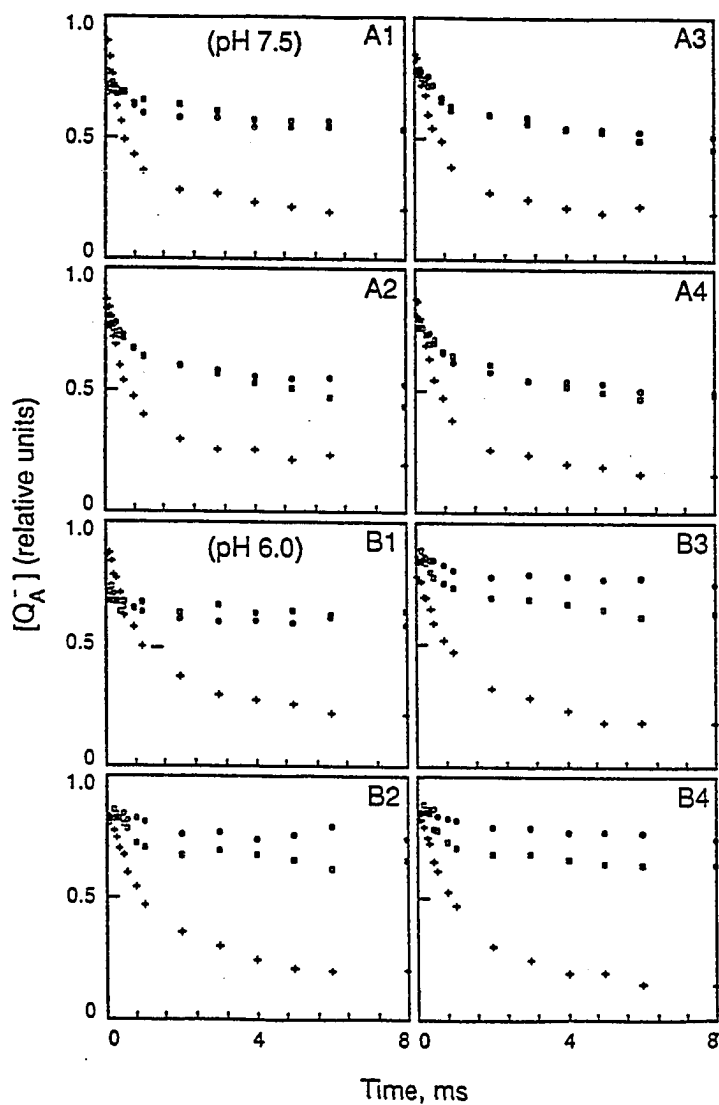


Fig. 5.4. Decay of  $[Q_A^-]$  after an actinic flash in control and trichloroacetate-treated (+ bicarbonate) spinach thylakoids at pH 7.5 and at pH 6.0. The experimental condition was the same as in Fig. 5.1. Open circles, 100 mM trichloroacetate-treated; pluses, control; open squares, trichloroacetate-treated to which 20 mM bicarbonate was added.

case, the four-component analysis by the GLOBALS program displayed a rising phase in the  $\mu\text{s}$  time range. This could be explained by an additional blockage by TCA on the electron donor side of PS II (for a discussion of the rising phase, see Kramer et al., 1990). It is consistent with the earlier suggestion of a donor side effect by high concentration (1M) of acetate (Saygin et al., 1986). This effect on  $F_{\text{max}}$ , and thus, on the electron donor side of PS II is, however, not obvious after the second and subsequent flashes (cf. panels B2 - B4 with B1 in Fig. 5.4). Furthermore, it is not reversed by bicarbonate.

After flashes 2, 3 and 4,  $A_3$  increases from 10-15% to 56-63%,  $A_1$  decreases from 60-70% to about 10% and  $\tau_1$  increases from 490-770  $\mu\text{s}$  to 1000-1700  $\mu\text{s}$  (Tables 5.2 - 5.4).  $(A_2 + A_3)/A_1$  increases further to a very large value of 8.1 (flash 2). Comparing these data with 6  $\mu\text{M}$  DCMU data, the  $Q_A^-$  reoxidation must be almost totally blocked in the presence of 100 mM TCA at pH 6.0 after the second and subsequent flashes (Fig. 5.4). In the presence of 6  $\mu\text{M}$  DCMU,  $(A_2 + A_3)/A_1$  is 10 - 11, only a bit higher than that with TCA (also see Fig. 5 in Appendix B). Results with TCA suggest that the third chloride substitution further enhances the inhibition of the reoxidation of  $Q_A^-$  by  $Q_B$ , shifts the apparent equilibrium towards high  $[Q_A^-]$ , and greatly decreases the reversibility by bicarbonate.

#### C.1.e. A comparison of the effect of chloroacetates: a hierarchy in the effects on the $Q_A Q_B$ reactions

In the presence of DCA and TCA, and at pH 6, the inhibitory effect on  $Q_A^-$  reoxidation by  $Q_B$  and on equilibrium  $[Q_A^-]$  is already

large after flash 1, but it is more after the second and subsequent flashes. This is particularly obvious for TCA. Figure 5.5 compares the decay of  $[Q_A^-]$  up to 30 ms after the first with that after the second flash in samples treated with 100 mM acetate, MCA, DCA or TCA. A hierarchy in the effects on the  $Q_A^-$  decay is obvious. Acetic acid has a very small difference between flash 1 and 2. DCA shows a higher equilibrium  $[Q_A^-]$  more after the second, than after the first flash. TCA, on the other hand, seems to inhibit  $Q_A^-$  reoxidation as well as increase equilibrium  $[Q_A^-]$  more after the second than after the first flash. MCA behaves differently and deserves a separate study (Chapter VI). After all flashes,  $A_3$  increases and  $A_1$  decreases when the number of the chloride moiety of chloroacetic acids increases (Tables 5.1 and 5.2). A sequential increase of  $(A_2 + A_3)/A_1$  is observed, and thus, a hierarchy in changes in the equilibrium  $[Q_A^-]$  and/or the inhibition of the  $Q_A^-$  reoxidation by  $Q_B$  occurs as follows: TCA > DCA > MCA > acetic acid. This order indicates a likely correlation between the chloride substitution and the inhibitory strength of (chloro)acetic acid.

#### C.1.f. Concentration dependence of chloroacetates

To quantitatively analyze the inhibition caused by (chloro)acetic acids on  $Q_A^-$  reoxidation, the increase of  $[Q_A^-]$  was measured at 1 and 5 ms after each flash. The values of  $[Q_A^-]_{\text{treated}} - [Q_A^-]_{\text{control}}$ , estimated at 5 ms after 1 - 4 flashes, are plotted against concentration of acetate, mono-, di- or tri-chloroacetate (Fig. 5.6). The  $[Q_A^-]_{\text{treated}} - [Q_A^-]_{\text{control}}$  values, measured



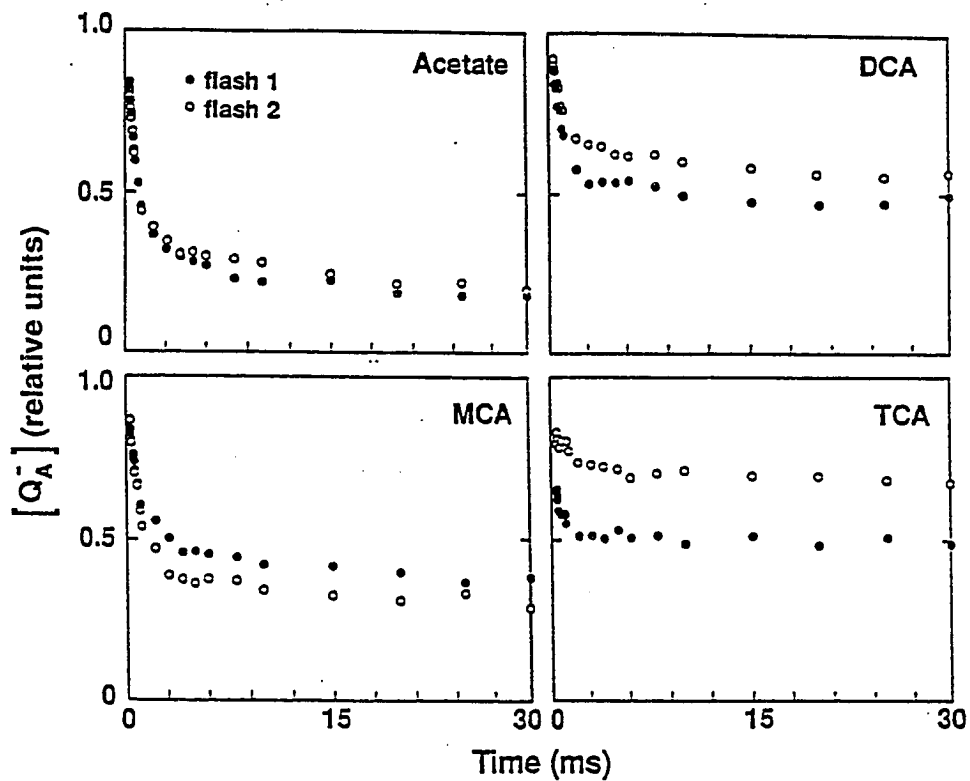


Fig. 5.5. A comparison of the  $[Q_A^-]$  decay after flash 1 with that after flash 2 in the presence of acetate, monochloroacetate (MCA), dichloroacetate (DCA) and trichloroacetate (TCA) at pH 6. Concentration of each chemical, 100 mM. Spinach thylakoids. For other details, see the legend of Fig. 5.1.

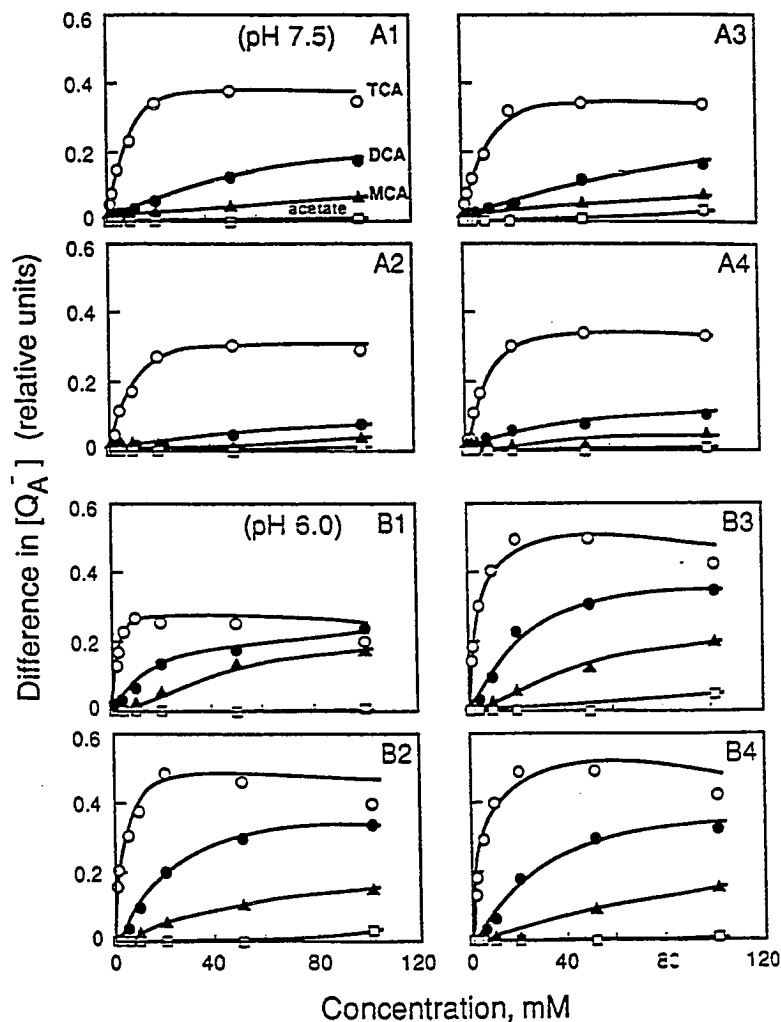


Fig. 5.6. Dependence of  $[Q_A^-]_{\text{treated}} - [Q_A^-]_{\text{control}}$  on acetate and chloroacetate concentrations at pH 6 and 7.5. The number in each panel refers to the actinic flash. Panels A: pH 7.5; Panels B: pH 6.0. The changes of  $[Q_A^-]$  were measured at 5 ms after the actinic flash. The mixing time of chemical with spinach thylakoids was 30 seconds. Open squares: acetate; closed triangles: monochloroacetate; closed circles: dichloroacetate, and open circles: trichloroacetate. For other details, see the legend of Fig. 5.1.

at 1 ms, display similar results (data not shown). The increase caused by TCA is the largest, and the one by acetate is the weakest at all concentrations used. The initial slope of increases in  $[Q_A^-]_{\text{treated}} - [Q_A^-]_{\text{control}}$ , as a function of inhibitor concentration, shows the same hierarchy as in equilibrium  $[Q_A^-]$  and/or the inhibition of the  $Q_A^-$  reoxidation: TCA > DCA > MCA > acetic acid. At pH 6, DCA and TCA cause larger increases in  $[Q_A^-]_{\text{treated}} - [Q_A^-]_{\text{control}}$  after the second and subsequent, than after the first flash. However, at pH 7.5, the effect is much larger after the first than after the second flash (Figs. 5.3, 5.4 and 5.6).

#### C.1.g. pH dependence

The pH dependence (pH 5.5 to 7.5 range) of the TCA-induced changes in  $[Q_A^-]$  was further studied in the lower concentration (0 - 10 mM) range.  $[Q_A^-]_{\text{treated}} - [Q_A^-]_{\text{control}}$ , estimated at 5 ms after flashes, is plotted against the concentration of TCA (Fig. 5.7). Lowering the pH of the suspension medium from 7.5 to 5.5 leads to an increase in the initial slope of changes in  $[Q_A^-]_{\text{treated}} - [Q_A^-]_{\text{control}}$  plotted as a function of TCA concentration. The flash number dependence of the inhibition is clear: a larger increase in  $[Q_A^-]_{\text{treated}} - [Q_A^-]_{\text{control}}$  can be seen after flashes 2 - 4 than after the first flash (Fig. 5.7). The  $[Q_A^-]$  decays in acetic acid-, MCA- and DCA- treated samples also show a stronger inhibition of the  $Q_A^-$  reoxidation at pH 5.5 than at pH 6.0 (data not shown). These results are consistent with our earlier conclusion that the acid, not the anion, maybe the active inhibitory species (Chapter IV).

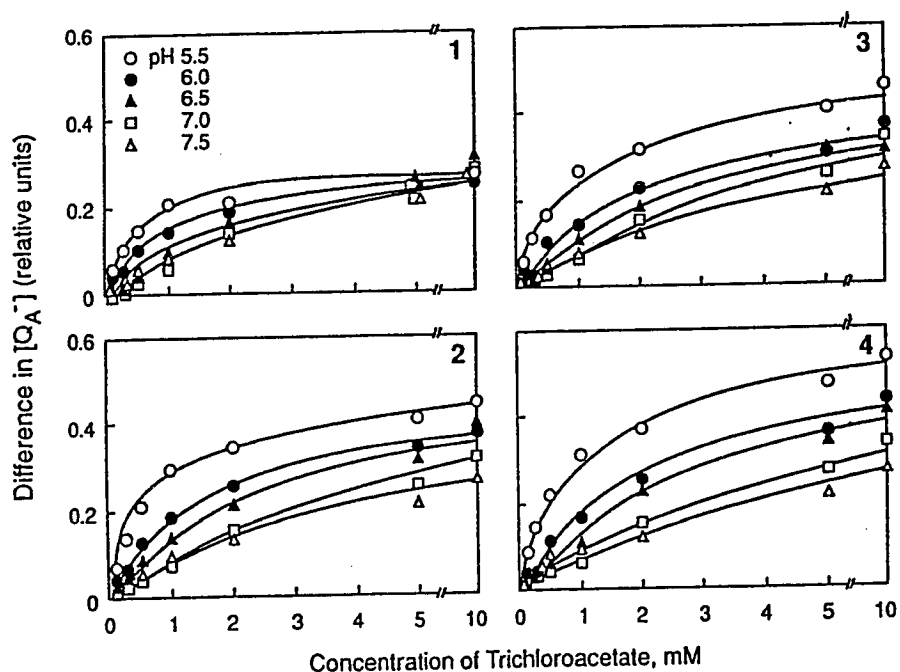


Fig. 5.7. Dependence of  $[Q_A^-]_{\text{treated}} - [Q_A^-]_{\text{control}}$  on the concentration of trichloroacetate at different pH's and after different actinic flashes. The number in each panel refers to the actinic flash. The changes of  $[Q_A^-]$  were measured at 5 ms after the actinic flash. The mixing time of chemicals with spinach thylakoids was 30 seconds. Open circles: pH 5.5; closed circles: pH 6.0; closed triangles: pH 6.5; open squares: pH 7.0 and open triangles: pH 7.5.

## C.2. The inhibition of the $Q_A^-$ reoxidation and effects on $Q_A^-$ equilibria by phenol

Phenol has a hydroxy group. In the reaction medium, it dissociates into a phenolic anion and proton. Its  $pK_d$  value is 9.9, higher than the pH range used in this study and the  $pK_d$  values of formate and (chloro)acetates. It may, thus, act differently than the inhibitors thus far used. Figure 5.8 shows  $[Q_A^-]$  decays in control, 1 mM phenol-treated and phenol plus 20 mM bicarbonate treated spinach thylakoids at pH 7.5 (A1 - A4) and pH 6.0 (B1 - B4) after flash 1 (A1, B1), 2 (A2, B2), 3 (A3, B3) or 4 (A4, B4). It appears that the incubation of thylakoids with phenol not only inhibits the  $Q_A^-$  reoxidation but also increases equilibrium  $[Q_A^-]$ . The phenol-induced inhibition of the  $Q_A^-$  reoxidation by  $Q_B$  and increases in equilibrium  $[Q_A^-]$  are also dependent on the suspension pH (cf. panels A with B in Fig. 5.8). In contrast to data with formate (Chapter III and IV) and (chloro)acetates (this chapter), phenol inhibits the  $Q_A^-$  reoxidation more at pH 7.5 than at pH 6.0. In changing the pH from 6.0 to 7.5, the change of phenolic anion concentration is far greater than that of phenol, the latter being negligible. At pH 6.0, 98% of the total amount of the two equilibrium species is phenol, changing to 92% at pH 7.5. In contrast, the concentration of phenolic anion increases 4 times (from 2% to 8%). These results imply that phenolic anion rather than phenol may be the active binding species in PS II. No significant bicarbonate recovery was observed (Fig. 5.8), indicating that bicarbonate cannot compete with phenolic anion.

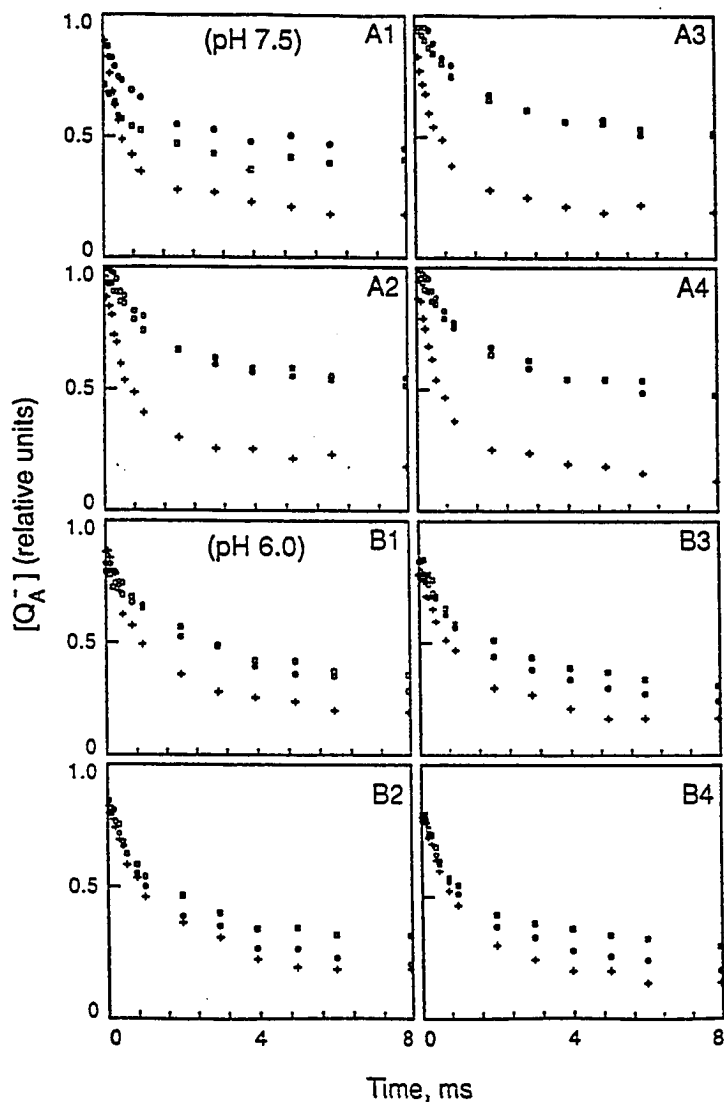


Fig. 5.8. Decay of  $[Q_A^-]$  after an actinic flash in control and phenol-treated (+ bicarbonate) thylakoids at pH 7.5 and 6.0. The number in each panel refers to the actinic flash numbers 1 - 4. Open circles, 1 mM phenol-treated; pluses, control; open squares, phenol-treated spinach thylakoids to which 20 mM bicarbonate was added. For other details, see the legend of Fig. 5.1 and Materials and Methods.

Either phenol is bound at a site different from the bicarbonate, or it is so tightly bound that bicarbonate cannot displace it.

$[Q_A^-]_{\text{treated}} - [Q_A^-]_{\text{control}}$ , measured at 5 ms after flashes 1 - 4, is plotted as a function of phenol concentration in Fig. 5.9. The increase of  $[Q_A^-]$  is proportional to the phenol concentration. The saturated level of  $[Q_A^-]_{\text{treated}} - [Q_A^-]_{\text{control}}$  could not be reached in the phenol concentration range ( $< 2\text{mM}$ ) used here. Unlike formate (Chapter IV), phenol does not show any flash number dependence of the inhibition either at pH 6 or 7.5. This suggests that phenol may directly inhibit the  $Q_A$ -to- $Q_B$  electron transfer as other PS II herbicides do.

#### D. Discussion

As already mentioned in Chapter I, Warburg and Krippahl (1960) observed that the Hill reaction with quinone or  $\text{Fe}(\text{CN})_6^{3-}$  as electron acceptor is dependent on bicarbonate. A low Hill reaction rate is found without bicarbonate, but the addition of bicarbonate results in an enhancement of this activity. Good (1963) examined the effect of various anions on the Hill reaction rate in higher plant chloroplasts and concluded that: (1) smaller monofunctional anions (formate, acetate) cause a bicarbonate-dependent inhibition of Hill reaction rates; (2) anions with hydroxyl close to the carboxyl (glycolate, salicylate, lactate) produce a bicarbonate-independent inhibition on Hill reaction rate; and (3) anions consisting mainly of large or polyfunctional ions (citrate, oxalate, malonate, maleate, arsenate, phosphate and pyrophosphate)

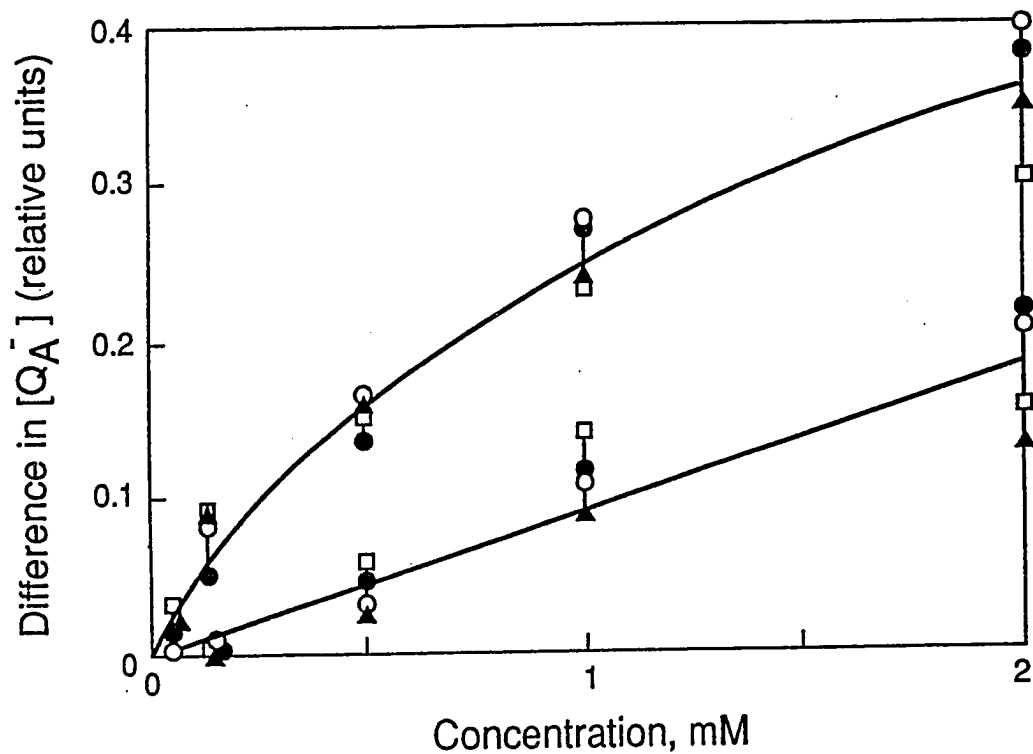


Fig. 5.9. Dependence of  $[Q_A^-]_{\text{treated}} - [Q_A^-]_{\text{control}}$  on the phenol concentration. The changes of  $[Q_A^-]$  were measured at 5 ms after the actinic flash. The mixing time of chemical with thylakoids was 30 seconds. The upper curve was measured at pH 7.5 and the lower at pH 6.0. Different symbols denote different flash numbers: open squares, first; closed triangles, second; closed circles, third and open circles, fourth. Other experimental conditions were the same as in Fig. 5.1.



do not affect the Hill reaction rate. In this Chapter, we have extended this list to phenol and chloroacetates, and studied their effects at the specific  $Q_AQ_B$  site.

Halogenated acetates have commonly been used as protein modifiers. At high concentrations (10% in the suspension medium), they neutralize the surface charge of the protein and nonspecifically denature the protein. Stemler (1985) showed that bromoacetate, a protein modifier, as well as a structural analogue of formate and bicarbonate, binds to the PS II reaction center. After a short time of the incubation of maize thylakoids, bromoacetate competed with bicarbonate in binding to PS II. After overnight incubation of maize thylakoids with a high concentration of bromoacetate, the binding of  $H^{14}CO_3^-$  to PS II was abolished. Results of the analysis of  $[Q_A^-]$  decay components, described in this chapter, suggest that (chloro)acetates selectively bind in the  $Q_A$ -Fe- $Q_B$  complex. At pH 6, DCA and TCA increase equilibrium  $[Q_A^-]$  and inhibit the  $Q_A^-$  reoxidation somewhat more after the second and subsequent flashes than after the first flash (Figs. 5.5 and 5.6). In comparison, formate shows a much more pronounced difference between the first and second flash data (Eaton-Rye and Govindjee, 1988a; Chapter III). In addition, DCA and TCA greatly inhibit electron flow from  $Q_A^-$  to  $Q_B$  as herbicides do (Figs. 5.3, 5.4 and 5.6). These results demonstrate that (chloro)acetates must hamper the formation of plastoquinol. Therefore, chloroacetates should be considered as inhibitors of the electron acceptor side of PS II;

their predominant site of action has been shown in this chapter to be in the  $Q_A$ -Fe- $Q_B$  region.

The COOH group, but not  $COO^-$ , contributes to the formate binding in the  $Q_A$ -Fe- $Q_B$  region (Chapter IV). Results on pH dependence of the effects of acetate ( $pK_d = 4.73$ ; Fig. 5.1), MCA ( $pK_d = 2.81$ ; Fig. 5.2), DCA ( $pK_d = 1.30$ ; Fig. 5.3) and TCA ( $pK_d = 0.70$ ; Fig. 5.7) are consistent with this prediction. The  $[Q_A^-]$  decay after actinic flashes is inhibited more at the lower than at the higher pH by acetate or chloroacetates. Acetic acid and chloroacetic acid have an identical carboxyl group. Their  $pK_d$  values are much lower than the medium pH in this study (from 5.5 to 7.5). When the medium pH is lowered from 7.5 to 6.0, the ionic portion in the total amount of the two equilibrium species decreases. It is lowered from 94.1% to 78.0% for acetate; however, it is lowered only slightly from 99.0% to 96.0% for MCA, from 99.8% to 99.1% for DCA and from 99.9% to 99.5% for TCA. On the contrary, changes in the acidic forms are from 5.9% to 22% for acetic acid, from 1% to 4% for MCA, from 0.2% to 0.9% for DCA and from 0.1% to 0.4% for TCA. Therefore, the change in the concentration of weak acid with the pH change is far greater than that of its ionic form. The prediction that  $-COOH$  is the candidate for binding/inhibiting in  $Q_A$ -Fe- $Q_B$  region is, thus, consistent with results in this chapter on (chloro)acetic acids.

A correlation between the number of chlorides replacing hydrogen and the binding affinity is made here for the first time. Equilibrium  $[Q_A^-]$  and inhibition of the  $Q_A^-$  reoxidation by  $Q_B$

increases with the increase of the number of the chloride moiety in the  $CX_3$  group (Figs. 5.1 - 5.4), implying that the active groups should include not only  $-COOH$  but also  $-CX_3$ . The most prominent features of chloride replacement on  $[Q_A^-]$  decay are the increase of the amplitude of the slow component and the decrease of that of the fast one (Figs. 5.1 - 5.4; Tables 5.1 - 5.4). The reversal of the inhibitor-induced effects by bicarbonate becomes difficult with the increase in the number of chlorides. This implies an increase in their binding strength and the inhibition of the  $Q_A^-$  reoxidation by  $Q_B$  and/or an enhancement of equilibrium  $[Q_A^-]$ . Unlike, formate/formic acid, TCA behaves more like the herbicides, but DCA is intermediate.

Since the sequential substitution of hydrogen by chloride in (chloro)acetic acid decreases the  $pK_d$  value from 4.7 to 0.7, one could first assume that the increase in the amount of anion is the major cause for the increase of the inhibitory effect. The substitution of hydrogen by chloride in  $CX_3$  causes little change in the percentage of anion in the total amount of two equilibrium species (anionic and acidic). At pH 7.5, dichloroacetate is 99.8% of the total amount and trichloroacetate is almost the same (99.9%). The percentage change of anion in the total amount would not explain the large increase in the inhibition (Figs. 5.3 and 5.4). Thus, the enhancement in the inhibition seems to have nothing to do with the change of the percentage amount of anion.

In order to understand the nature of the sequentially increased inhibition of  $Q_A^-$  reoxidation and/or enhancement of

equilibrium  $[Q_A^-]$  by (chloro)acetic acids, the initial slopes of the change of  $[Q_A^-]_{\text{treated}} - [Q_A^-]_{\text{control}}$  versus the anion concentration (obtained after flash 2 in Fig. 5.6) were plotted as a function of the  $pK_d$ 's of the inhibitors (solid squares in Fig. 5.10). The percentage of anions (closed circles) or acids (solid triangles) and the anion/acid ratio (open circles) were also plotted against the  $pK_d$  values (see abscissa). The initial slope of the  $[Q_A^-]$  change does not match either the changes in percentage of the anions or the acids. It is also not correlated with the acid/anion ratio. However, a very weak correlation is observed with the anion/acid ratio, the largest noncorrelation being for DCA (Fig. 5.10).

In Fig. 5.11, the initial slopes of  $[Q_A^-]_{\text{treated}} - [Q_A^-]_{\text{control}}$  (solid squares, obtained after flash 2 in Fig. 5.7) for trichloroacetic acid were plotted as a function of pH (5.5 - 7.5) and compared with the percentage of the anions (closed circles) or the acids (solid triangles), and the anion/acid ratio (open circles). In contrast to Fig. 5.10, an approximate correlation of the initial slope with the percentage of acid, or the acid/anion ratio is observed. However, the  $[Q_A^-]$  data do not match either the change in the percentage of the anion or the anion/acid ratio. Figure 5.11 suggests that the change of the inhibitory activity can be explained by the proportional change of acid in the case of single species, such as TCA. A similar conclusion was obtained separately for DCA, MCA and acetate (data not shown). This is consistent with our previous observation that the COOH not the  $COO^-$  is active group (Chapter IV). However, when different species

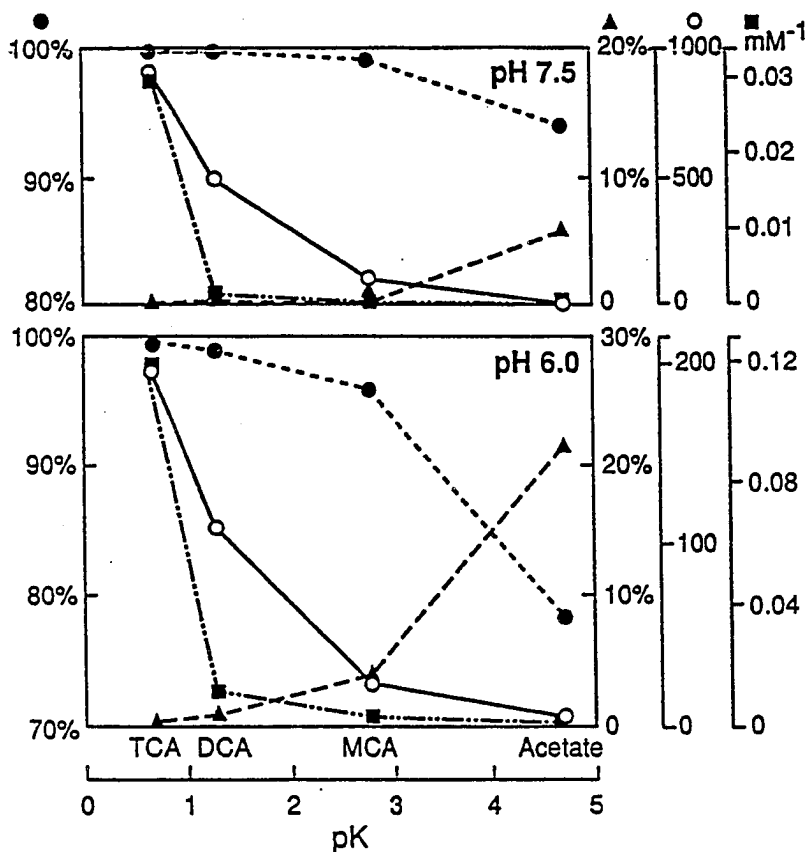


Fig. 5.10. A comparison of the change in  $[Q_A^-]$  with the change in the proportion of the ionic or the acidic form of the inhibitors. The abscissa shows the  $pK_a$  values of the acetate and chloroacetates, whereas the ordinate shows the following: closed circles, percentage of the ionic form of the chemical in medium; solid triangles, percentage of the protonated form of the chemical in medium; open circles, the ratio of the ionic to the acidic forms, and solid squares, the inhibition of the reoxidation of  $Q_A^-$  monitored as the initial slope of the change of  $[Q_A^-]$ ,  $[Q_A^-]_{\text{treated}} - [Q_A^-]_{\text{control}}$ , with respect to a change in the inhibitor concentration after the second flash (see Fig. 5.8). Note the different scales for the different data (see both the left and the right ordinates).

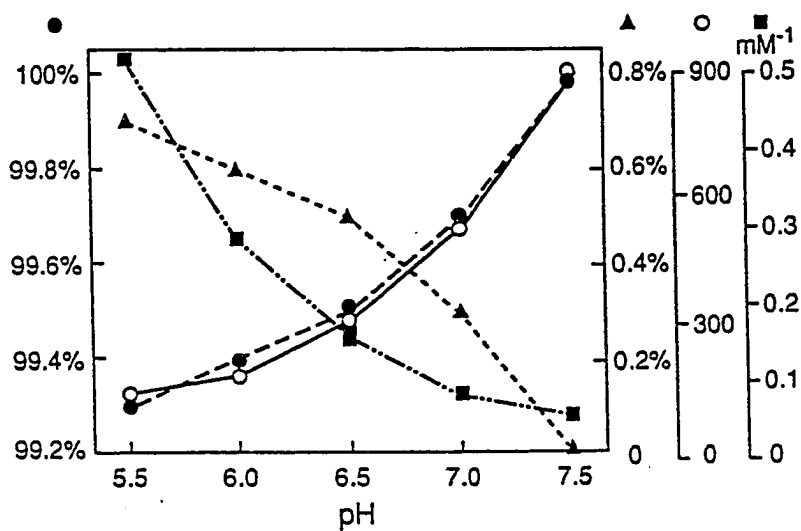


Fig. 5.11. A comparison of the pH dependence of the change of  $[Q_A^-]$  with the change in proportion of trichloroacetate or trichloroacetic acid and their ratio. Closed circles, percentage of the trichloroacetate in the medium; solid triangles, percentage of the trichloroacetic acid in the medium; open circles, the ratio between the ionic to the acidic forms; solid squares, initial slope of the change of  $[Q_A^-]$ ,  $[Q_A^-]_{\text{treated}} - [Q_A^-]_{\text{control}}$ , with respect to a change in the inhibitor concentration after the second actinic flash. Note the different scales for the different data (see both left and right ordinates).

of (chloro)acetates are compared (Fig. 5.10), no clear-cut correlation is observed between the ionic/acidic form and the inhibitory effect. Thus, additional factors must be considered.

With the above in mind, we calculated the molecular geometry and dipole moments of (chloro)acetic acids in an apolar environment (dielectric constant, 1.5) with the PCMODEL molecular modeling program (Table 5.5). The change in dipole moments does not correlate with the changes in  $[Q_A^-]$ , obtained with various inhibitors having different number of chloride substitutions in  $CX_3$ . However, it remains to be seen if the dipole moment of the head group, i.e., across the  $CX_3$  group would correlate with the changes in  $[Q_A^-]$ . The replacement of hydrogen by chloride leads to a large change in the geometry of  $CX_3$  but no change in the geometry of the COOH group (Fig. 5.12, Table 5.5). As the number of the chloride moiety increases, the angle between the major planes of the molecules increases, and there is an obvious increase in the size and shape of the  $CX_3$  group of the molecules, chloride being much larger than the hydrogen. Thus, the change of the geometry of chloroacetic acids shows a general correlation with the hierarchy of their inhibitory activities.

The log of the partition coefficient (P) of (chloro)acetic acids is also listed in Table 5.5 (Hansch and Leo, 1979). The values of log P increase when the number of the chloride moiety increases. An approximate correlation between the inhibitory effect and changes in partition coefficients of (chloro)acetic acids appears to exist. Such a correlation between the partition

Table 5.5. Dipole moments, the angles between two major planes, log of the partition coefficient and hydrophobic constant of (chloro)acetic acids. Dipole moments ( $\mu$ , Debye) in Column A and the angle (degree) between the two major planes of the molecule were calculated by using the MMX molecular mechanics (forcefield) calculation method with the PCMODEL molecular modeling program (in a solution of a dielectric constant of 1.5). Dipole moments in Column B, measured in benzene solution between 25° and 30°C, are from McClellan (1963). Log of partition coefficient (P), measured in diethyl ether/water system, is from Hansch (1969). Hydrophobic constant,  $\pi$ , is calculated as shown in Chapter II; acetic acid is taken as the parent molecule.

	Dipole Moment		Angle between two major planes (in degrees)	log P	$\pi$
	A ( $\mu$ )	B			
acetic acid	1.61	0.74	1.5	-0.33	0.00
MCA	3.25	2.3	1.5/27.0*	0.32	0.65
DCA	2.53	-	14.0/28.0*	1.33	1.66
TCA	2.12	1.10	53.0	1.54	1.87

\* values are listed for their two configurations.



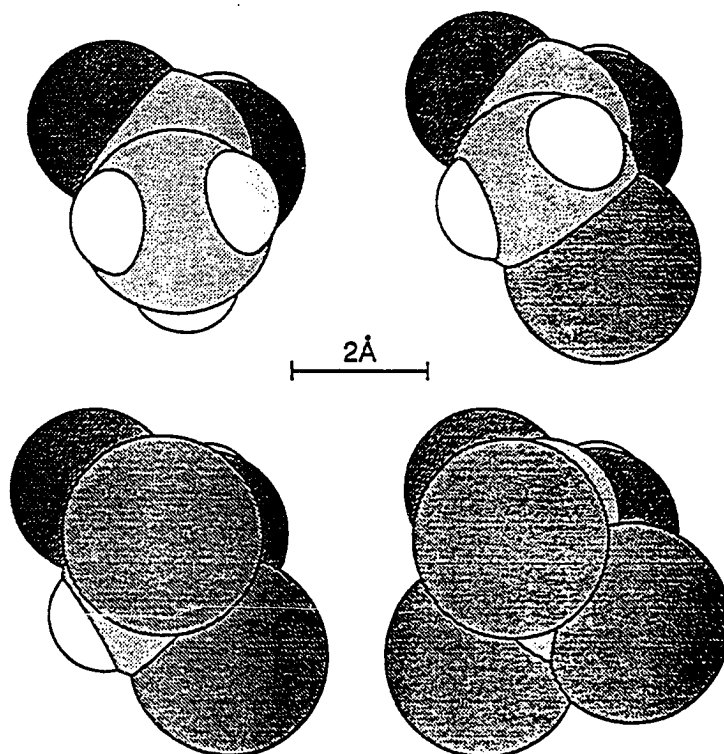


Fig. 5.12. Molecular geometry of acetic acid and chloroacetic acids in an apolar solvent. Dielectric constant, 1.5. Top left: acetic acid; top right: monochloroacetic acid; bottom left: dichloroacetic acid; and bottom right: trichloroacetic acid. Models were obtained by using the MMX molecular mechanics calculation method with the PCMODEL molecular modeling program.

coefficient of herbicides and their inhibitory effects has been discussed by Shipman (1980) and Oettmeier (1992).  $P$ , the octanol/water partition coefficient, is a measure of the free energy required for a molecule to shed its solvation shell of water molecules and enter into a lipid environment. Within each class of PS II herbicides, there usually is a linear relationship between  $\log P$  and the log of the reciprocal of the herbicide concentration ( $I_{50}$ ) at which electron transport from PS II is inhibited by 50%. We will use diethyl ether/water partition coefficient from Hansch and Leo (1979) in this thesis. The hydrophobic constant ( $\pi$ ) for (chloro)acetic acids was estimated (Table 5.5) from the partition coefficient, discussed above, from Eq. (2.3) (Hansch, 1969; Hansch and Leo, 1979). According to the definition,  $\pi$  for acetic acid ( $x = H$ ) is defined as zero. It is obvious that the hydrophobic constant ( $\pi$ ) increases when the number of the chloride moiety increases. The so-called "hydrophobic bond" is one of the main interactions available to protein for binding a chemical compound. (Chloro)acetic acid molecules with larger hydrophobic groups may provide more substantial binding affinity. An approximate correlation between the inhibitory effect and changes in geometry and hydrophobicity of acetic acid and chloroacetic acids, thus, appears to exist. (Chloro)acetic acids may bind on the electron acceptor side of the D1-D2 protein of PS II to show the effects observed in this Chapter.

## E. Conclusion

In this chapter, we have shown that a hierarchy exists in the inhibitory activity of the various chloroacetates on the  $Q_A^-$ -to- $Q_B$  electron transfer: trichloroacetic acid > dichloroacetic acid > monochloroacetic acid > acetic acid. On the other hand, the bicarbonate reversibility follows the reverse of the series. The correlated enhancement of the inhibition with the number of the chloride moiety implies that the active group also includes the  $CX_3$  head. The inhibitory activity appears to be related to the geometry of the  $CX_3$  head and the hydrophobicity of the (chloro)acetic acids that are suggested to bind in the  $Q_A$ -Fe- $Q_B$  niche on the D1-D2 protein of PS II. This provides new information about the property of the binding of weak acids in the  $Q_A$ -Fe- $Q_B$  complex of the D1/D2 protein of PS II. Incubation of thylakoids with (chloro)acetates results in a pH dependent inhibition of the  $Q_A^-$  oxidation by  $Q_B$  and/or change in equilibrium  $[Q_A^-]$ ; a larger effect at the lower pH supports the previous suggestion that an active group is COOH not  $COO^-$ . In contrast, pH dependence of the inhibition by phenol of the  $Q_A^-$  oxidation by  $Q_B$  suggests that phenolic ion is the binding species.

**CHAPTER VI. DIFFERENTIAL EFFECTS ON  $Q_A^-$  REOXIDATION AND EQUILIBRATION BY MONOHALOGENATED ACETATES AND THE BICARBONATE-REVERSIBLE APPARENT STABILIZATION OF  $Q_B^-$  BY MONOCHLOROACETATE**

A. Introduction

In Chapter III, we showed that bicarbonate-reversible inhibitors like formate act by inhibiting protonation at the  $Q_B$  site. In Chapters IV and V, we showed that (1) the acidic form, rather than the anionic form of single functional weak acids, is the acting/binding species in the bicarbonate reversible (or irreversible) inhibition of the  $Q_A^-$  oxidation by  $Q_B$  and/or increase in equilibrium  $[Q_A^-]$  and (2) mono-, di-, and tri-chloroacetic acids differentially inhibit the  $Q_A^-$  reoxidation and/or enhance the equilibrium  $[Q_A^-]$  in the order: TCA > DCA > MCA > acetate, and that their activity may be correlated with their geometrical property and hydrophobicity. The aim of the experiments in this chapter is to further investigate the importance of the halogen moiety in the mechanism of inhibition of  $Q_A^-$  reoxidation and equilibration by using monobromo-, monochloro- and monofluoroacetates.

B. Materials and Methods

The preparation of the spinach thylakoids, the measurement and analysis of the  $[Q_A^-]$  decay and the calculation of the molecular geometry, the dipole moment and the hydrophobic constant were as described in Chapter II. The hydrophobic constants ( $\pi$ ) for acetic acid and monohalogenated acetic acids were estimated by using Eq. (2.3). The  $\pi$  for acetic acid ( $x = H$ ) is defined as zero.

## C. Results and Discussion

### C.1. Halogenated acetic acids differentially affect the $Q_A^-$ -to- $Q_B$ electron flow and equilibration

Figure 6.1 shows  $[Q_A^-]$  decays in control, MFA (monofluoroacetate), MCA (monochloroacetate) and MBA (monofluoroacetate) treated thylakoids at pH 7.5 (left panels) and 6.0 (right panels) after actinic flash 1 (upper panels) or 2 (lower panels) (dark interval between flashes, 1 s). The dark incubation time was 10 minutes. At pH 6.0, the addition of 100 mM monohalogenated acetates apparently cause both increases in the lifetime of the  $Q_A^-$  reoxidation by  $Q_B/Q_B^-$  and shifts of the equilibrium  $Q_A^-Q_B \rightleftharpoons Q_AQ_B^-$  towards  $[Q_A^-]$ . This is more obvious after flash 1 than after flash 2 (also see Chapter V). These effects were marginal at pH 7.5. This observation on pH dependence is consistent with our earlier conclusion that the acid, not the anion, is the active species for the inhibition of the  $Q_A^-$  oxidation and/or increase in equilibrium  $[Q_A^-]$  (Chapters IV and V).

What is new here is that MFA, MCA ( $pK_d = 2.80$ ) and MBA ( $pK_d = 2.86$ ) inhibit the  $Q_A^-$  oxidation in different degrees. The hierarchy of inhibition, most clearly observed at pH 6 and after flash 1, is  $MBA > MCA > MFA$ . The  $[Q_A^-]$  decay is mostly restored to its control level after the addition of bicarbonate in the case of MCA (Fig. 5.2). Similar reversibility experiments for MBA and MFA are, however, not available. The time dependence of  $[Q_A^-]$  decay after an actinic flash (see e.g., Robinson and Crofts, 1983; Etienne et al., 1990) is described by three major (fast, intermediate and slow, also see description in Chapter V) exponential decay processes.

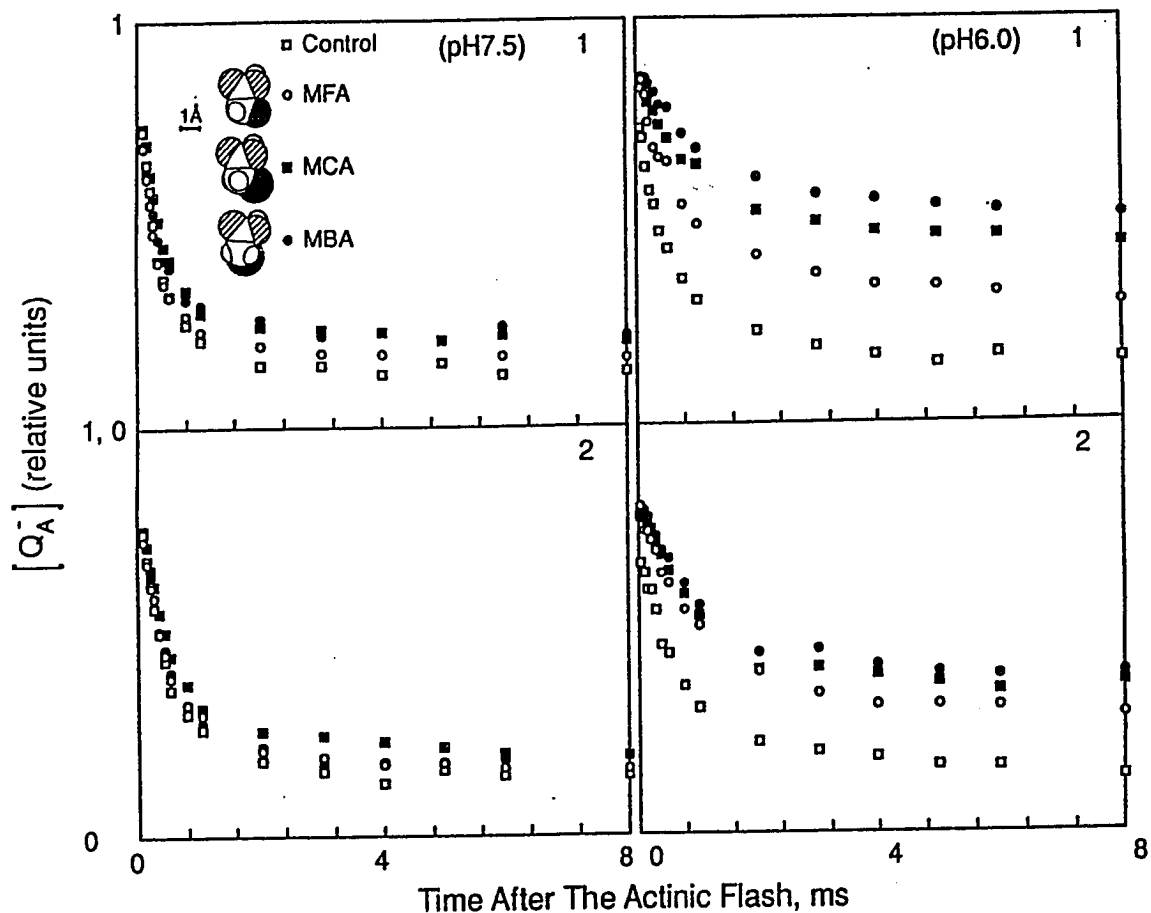


Fig. 6.1.  $[Q_A^-]$  decays in monohalogenated acetate-treated thylakoids. Decay of  $[Q_A^-]$  was calculated from Chl *a* fluorescence yield after actinic flash 1 (upper) or 2 (lower) in the control and monohalogenated acetate treated spinach thylakoids at pH 6.0 (right) and at pH 7.5 (Left). The dark-adaptation time was 10 min. In the reaction medium, 0.4 M sorbitol, 50 mM NaCl, 2 mM MgCl<sub>2</sub>, 40 μM hydroquinone, 40 μM benzoquinone and 1 nM gramicidin were included. Open circles, control; open squares, control; solid circles, control; solid squares. Inset: molecular geometry of monohalogenated acetic acids in apolar solvent (dielectric constant, 1.5).

After flashes 1 - 4 and at pH 6.0 (Table 6.1), both  $\tau_1$ , the lifetime of  $Q_A^-$  oxidation by  $Q_B/Q_B^-$  and  $\tau_2$ , the lifetime related to  $[Q_A^-]$  equilibrium show the hierarchy: MBA > MCA > MFA. Furthermore,  $A_1$ , the amplitude of the fast component reflecting the contribution of the  $Q_A^-$  oxidation by  $Q_B/Q_B^-$ , decreases, whereas  $A_3$ , the amplitude of the slowest component ( $\tau_3$ ,  $2.5 \pm 0.4$  s) reflecting the contribution of the back-reaction between  $Q_B^-$  and  $S_2$  state (see e.g., Etienne et al., 1990), increases with MFA, MCA and MBA present.

The inhibitory hierarchy among the various monohalogenated acetates can be explained by differences in their geometry (inset in Fig. 6.1). The size of the halogen shows a general correlation with the inhibitory activity: bromide is the largest in size and MBA causes the largest inhibition. Another correlation is with the hydrophobic constant ( $\pi$ ): MBA (0.97), MCA (0.65) and MFA (0.06) (Hansch and Leo, 1979). The partition coefficients and hydrophobic constants increase with the  $CX_3$  size and the inhibitory strength of halogenated acetic acids. MBA with largest hydrophobicity provides the strongest inhibition.

#### C.2. MCA induces apparent stabilization of $Q_B^-$

The flash number dependence of  $[Q_A^-]$  is shown in Figures 6.2 and 6.3. Fig. 6.2 shows the complete data, whereas Fig. 6.3 shows the data measured at 300 and 400  $\mu$ s after flashes in control thylakoids (dark adapted with hydroquinone and benzoquinone). A binary oscillation with peaks at even flashes (2, 4 and 6) is

TABLE 6.1. Amplitudes (A) and lifetimes ( $\tau$ ) of three components of the  $[Q_A^-]$  decay, in control and halogenated acetate-treated spinach thylakoids at pH 6.0. Amplitudes were within  $\pm 0.05$ .  $\tau_1$  within  $\pm 50$   $\mu$ s and  $\tau_2$  within  $\pm 2$  ms for control samples and 10 - 20 ms for others.  $\tau_3$  (for all samples) was  $2.5 \pm 0.4$  s.

Flash number		A <sub>1</sub>	$\tau_1$ ( $\mu$ s)	A <sub>2</sub>	$\tau_2$ (ms)	A <sub>3</sub>	X <sup>2</sup>
1	control	0.55	510	0.13	5.0	0.11	0.79
	+ MFA	0.50	760	0.22	20	0.16	0.44
	+ MCA	0.39	1200	0.29	87	0.17	0.40
	+ MBA	0.34	1700	0.34	104	0.18	0.44
2	control	0.46	540	0.15	4.7	0.12	0.88
	+ MFA	0.48	1100	0.17	26	0.16	0.59
	+ MCA	0.44	950	0.17	32	0.21	0.57
	+ MBA	0.42	1100	0.16	50	0.23	0.47
3	control	0.41	620	0.15	3.9	0.09	0.70
	+ MFA	0.47	1100	0.16	35	0.13	0.72
	+ MCA	0.34	1200	0.18	44	0.23	0.42
	+ MBA	0.32	1700	0.22	78	0.21	0.50
4	control	0.51	630	0.14	4.5	0.07	0.87
	+ MFA	0.49	990	0.19	27	0.14	0.67
	+ MCA	0.46	1100	0.17	75	0.17	0.69
	+ MBA	0.40	1100	0.18	52	0.21	0.50



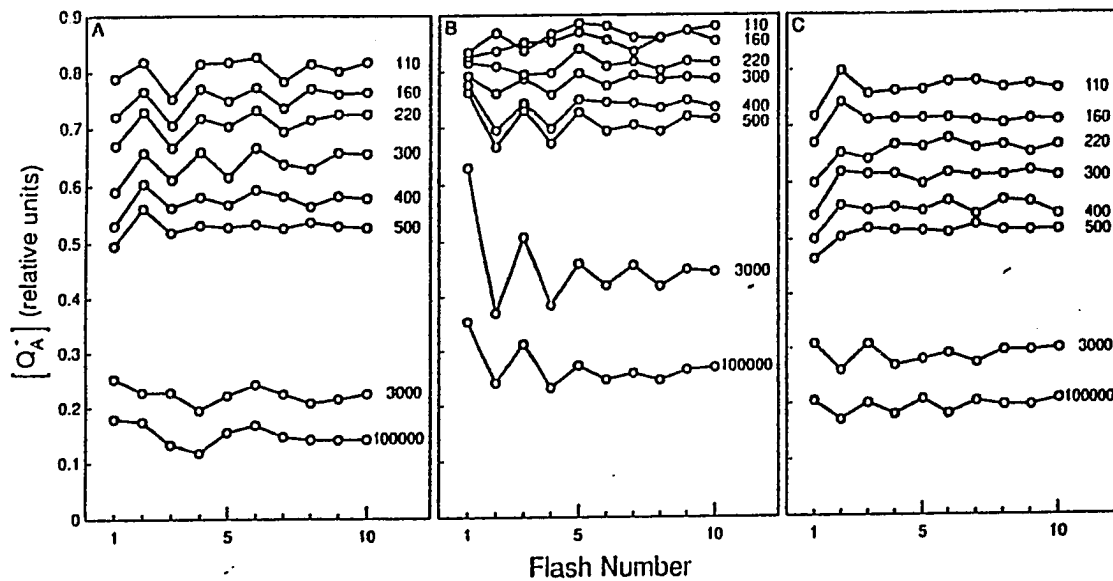


Fig. 6.2. Flash number dependence of  $[Q_A^-]$  from 110  $\mu\text{s}$  to 100 ms after actinic flashes in control, MCA treated (+ bicarbonate) thylakoids at pH 6.0. Panel A: control; Panel B: 100 mM MCA; and Panel C: MCA plus 20 mM bicarbonate. The dark-adaptation time was 5 min. In the reaction medium, 0.4 M sorbitol, 50 mM NaCl, 2 mM  $\text{MgCl}_2$ , 40  $\mu\text{M}$  hydroquinone, 40  $\mu\text{M}$  benzoquinone and 1 nM gramicidin were included.

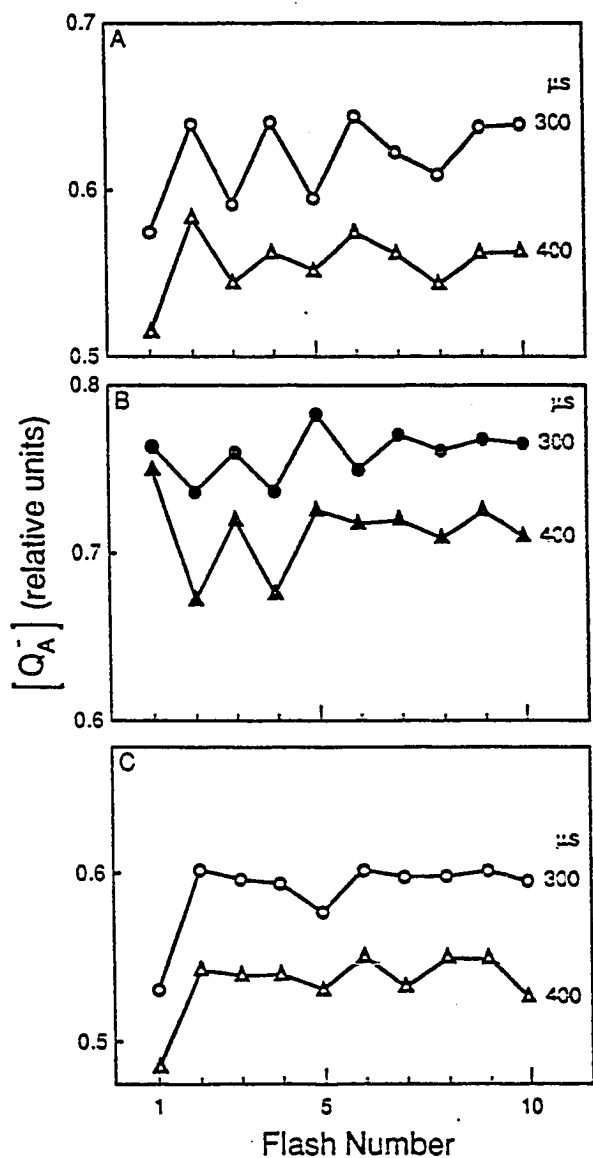


Fig. 6.3. Flash number dependence of  $[Q_A^-]$  at 300 and 400  $\mu$ s after actinic flashes in control and MCA treated ( $\pm$  bicarbonate) thylakoids at pH 6.0. Panel A: control; Panel B: 100 mM MCA treated; and Panel C: MCA plus 20 mM bicarbonate. The dark-adaptation time was 10 min. In the reaction medium, 0.4 M sorbitol, 50 mM NaCl, 2 mM  $MgCl_2$ , 40  $\mu$ M hydroquinone, 40  $\mu$ M benzoquinone and 1 nM gramicidin were included.

obvious in the 100 - 400  $\mu$ s range. This binary pattern is due to the oxidation rate of  $Q_A^-$  by  $Q_B$  after odd flashes to be faster than that by  $Q_B^-$  after even numbered flashes (Bowes and Crofts, 1980; Robinson and Crofts, 1983). Interestingly, we observed here that this binary oscillation of  $[Q_A^-]$  is reversed by MCA, higher  $[Q_A^-]$  being observed between 220  $\mu$ s and 100 ms after odd than even flashes (Fig. 6.2B). This rephasing of the binary oscillation is seen very clearly after 400 - 500  $\mu$ s after the flash (Fig. 6.2.B). Furthermore, the largest difference between  $[Q_A^-]$  after flashes 1 and 2 is seen at 3 ms. It is three times larger than that measured at 300  $\mu$ s.

The above results suggest that MCA produces an apparent stabilization of  $Q_B^-$ . We may consider two non-mutually exclusive possibilities: (1) the ratio of  $Q_B$  to  $Q_B^-$  in darkness, prior to actinic flashes, decreases; this ratio is normally high (7/3) in dark-adapted thylakoids (see e.g. Wollman, 1978); (2) MCA causes a change in the equilibrium of  $Q_A^-Q_B \rightleftharpoons Q_AQ_B^-$  reaction such that the apparent  $[Q_B^-]$  is increased. In Section C.1. of this chapter, we have indeed shown that MCA inhibits the  $Q_A^-$ -to- $Q_B$  electron flow and shifts the equilibrium  $Q_A^-Q_B \rightleftharpoons Q_AQ_B^-$  towards the left. If this equilibrium shift were the only major effect produced by MCA, we find it difficult to understand the dramatic reversal of the binary oscillation observed at 3 ms, and the absence of this phenomenon with TCA (data not shown) that is also known to shift the equilibrium towards  $[Q_A^-]$ . Thus, we suggest that a combination of a change in the ratio of  $Q_B$  to  $Q_B^-$  and a change in equilibrium of  $Q_A^-Q_B \rightleftharpoons Q_AQ_B^-$

reaction is responsible for the unusual effects of MCA. What is of interest to this thesis is that the addition of 20 mM bicarbonate abolishes, to some extent, the MCA effect (Fig. 6.2C, Fig. 6.3C). We do not know the reason why there is an irreversible component in this phenomenon. The rephasing of the first and second flashes is obvious.

The normal binary oscillation was also reversed by MBA (data not shown). However, the effect of MBA is smaller than that of MCA and was, thus, not investigated further.

#### D. Conclusion

We have established here that monohalogenated acetic acids inhibit not only the reoxidation of  $Q_A^-$  but also increase the equilibrium  $[Q_A^-]$  at the plastoquinone reductase site in PS II with the hierarchy of effectiveness to follow the order: MBA > MCA > MFA. This order seems to be related to their size and to their hydrophobicity, but not to their dipole moments (3.11, 3.14 and 3.25 for MBA, MFA and MCA respectively) since they are all within a narrow range.

A novel observation in this chapter is the rephasing of the binary oscillation in  $[Q_A^-]$  as a function of flash number from a maxima after even flashes to odd flashes. This suggests an apparent stabilization of  $Q_B^-$ . The mechanism of such an effect is not yet obvious, but one could speculate on the possibility of repulsion of the negative charge on  $Q_B^-$  by the negatively polarized asymmetric chlorine atom of MCA, followed by its movement towards a positively

charged niche and consequent stabilization. A MCA-induced change in equilibrium in the  $Q_A^-Q_B \leftrightarrow Q_AQ_B^-$  can explain the data between 110  $\mu$ s - 300  $\mu$ s after the flash. However, an increase in the equilibrium  $[Q_A^-]$  cannot explain the persistence of the binary oscillation of  $[Q_A^-]$  up to 10 flashes in the 300  $\mu$ s to 100 ms range. The most likely interpretation of our data is that MCA changes the ratio of  $Q_B^-$  to  $Q_B$  in dark. We leave open the question of whether  $Q_B^-$  is stabilized or not for future experiments. Oxamic acid (aminooxoacetic acid,  $NH_2COCO_2H$ ), which has a similar molecular weight as MCA but a lower dipole moment of 2.84, shows a 50% lower ratio of  $[Q_A^-]$ , measured 1 ms after flash 1 over 2 than that observed after MCA (data not shown). This suggests the possibility that the dipole moment in a certain geometry of these acid derivatives may also modulate the inhibitory effect on  $Q_A^-$  oxidation.

**CHAPTER VII. PRELIMINARY EXPERIMENTS ON THE EFFECTS ON  $Q_A^-$   
REOXIDATION AND EQUILIBRATION BY TRIMETHYL ACETATE, PROPIONIC  
ACID AND AZIDE**

A. Introduction

In Chapters IV, V and VI, it was shown that  $CX_3$  in halogenated acetic acids plays important roles in the reactions at the  $Q_A-Fe-Q_B$  complex. Halogen substitution for hydrogens in  $CX_3$  enhances the inhibition of  $Q_A^-$  reoxidation, alters the equilibrium between  $Q_A^-Q_B$  and  $Q_AQ_B^-$ , and/or provides apparent stabilization of  $Q_B^-$  probably due to changes in geometry, hydrophobicity and electrostatic property. In this chapter, the effect of change in geometrical size of  $CX_3$  by replacement of hydrogens with methyl groups has been examined. The effects of propionic acid and trimethylacetic acid on  $[Q_A^-]$  decay are monitored by measuring the decay of Chl a fluorescence yield after a single flash. The effect of several small weak acids (e.g., azide) are also discussed.

B. Materials and Methods

The isolation of spinach thylakoids and the measurement of Chl a fluorescence were as described in Chapter II. Freshly thawed thylakoids were suspended in a medium containing 0.4 M sorbitol, 50 mM NaCl, 2 mM  $MgCl_2$ , 40  $\mu M$  hydroquinone, 40  $\mu M$  benzoquinone and 1 nM gramicidin, with a final [Chl] of 10  $\mu M$ . The pH of the suspension was adjusted by using 20 mM MES (at pH 6.0) and 20 mM HEPES (at pH 7.5).

Propionic acid, trimethylacetic acid, ethyl and methyl formate, nitrite, azide, cyanate and thiocyanate were purchased from Sigma.

### C. Results and Discussion

In both trimethylacetate and propionate, hydrogens in  $CX_3$  group of acetic acid are replaced by methyl. However, there are two more methyl groups in  $CX_3$  of trimethylacetic acids than that of propionic acid. Decays of the normalized Chl a fluorescence yield measured in the control (solid squares), (100 mM) trimethylacetate-treated (closed circles) and (100 mM) propionate-treated (open circles) thylakoids at pH 6.0 after flash 1 or 2 are shown in Fig. 7.1. Trimethylacetate caused a distinct slowing down in the Chl a fluorescence decay after both actinic flash 1 and 2, as shown previously for some other small weak organic acids (see chapter V and VI). Propionic acid also caused a slowing down of the yield of Chl a fluorescence, but it was of much smaller magnitude. The distinct effects of formate after flash 1 or 2 (Chapter III) are, however, not observed here. Due to the preliminary nature of the work presented in this thesis, I have not transferred Chl a fluorescence yield into  $[Q_A^-]$ , but the observed slowing of Chl a fluorescence yield decay indicates a possible blockage of the  $Q_A^-$  reoxidation as well as a shift in the equilibrium of  $Q_A^-Q_B \leftrightarrow Q_AQ_B^-$  towards the left. The effects caused by either propionate or trimethylacetate are pH dependent, being much stronger at pH 6.0 than at pH 7.5 (data not shown). As before, this could be explained

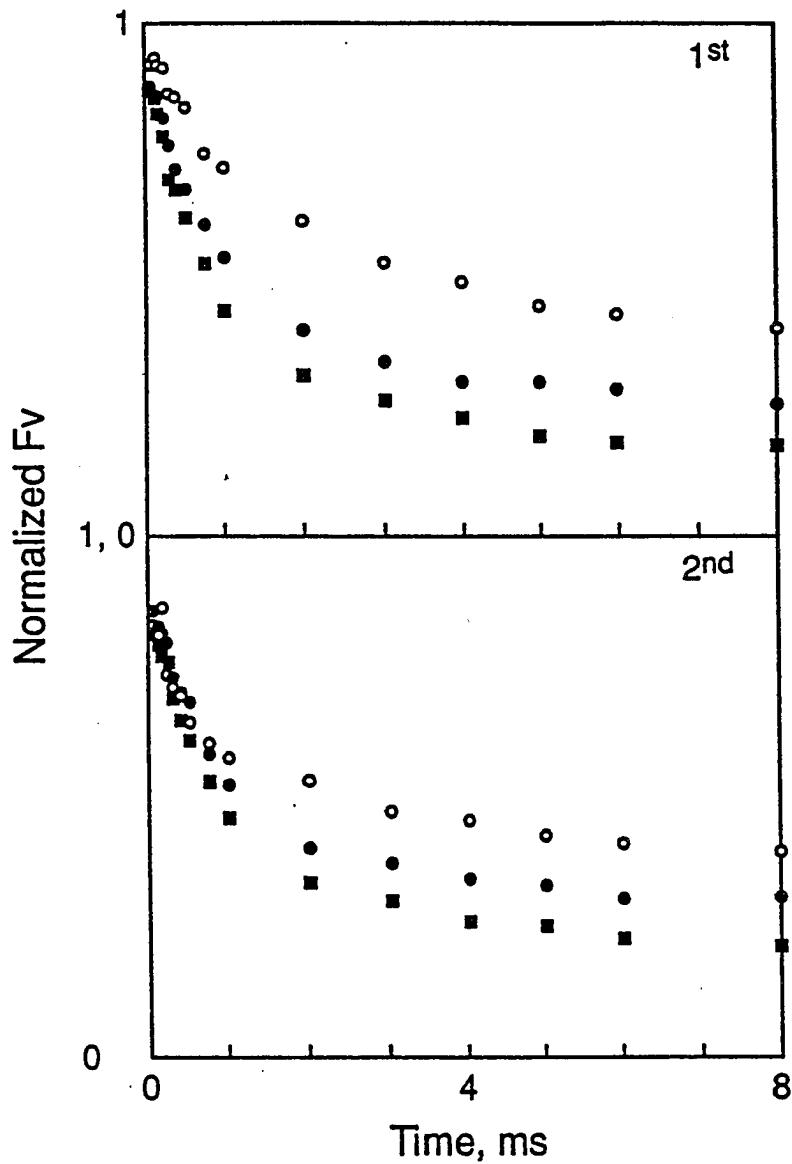


Fig. 7.1. Decay of  $[Q_A^-]$  after flash 1 or 2 in control, trimethylacetate-treated and propionic acid treated thylakoids at pH 6.0. The dark-adaptation time was 5 min. The reaction medium contained 0.4 M sorbitol, 50 mM NaCl, 2 mM MgCl<sub>2</sub>, 40  $\mu$ M hydroquinone, 40  $\mu$ M benzoquinone and 1 nM gramicidin. Solid squares, control spinach thylakoids; Open circles, 100 mM trimethylacetate-treated; closed circles, 100 mM propionate-treated samples.



by the suggestion that the acidic form is the active species for the alteration of reaction at the  $Q_A$ -Fe- $Q_B$  complex. Since trimethylacetate causes a large slowing of Chl a fluorescence yield decay after flash 1, it must act as dichloroacetic acid or trichloroacetic acid, but not as formate.

As noted above, the effects by propionic acid are weaker than that by trimethylacetic acid (Fig. 7.1), suggesting that the effects on the reaction in the  $Q_A$ -Fe- $Q_B$  complex are enhanced when two hydrogens in  $CX_2$  of propionic acid are further replaced with methyl groups in trimethylacetic acid.

To explore further the structural requirement for the inhibitor binding niche, methyl formate was used. Here, a methyl is linked to  $COO^-$  side of formate to form methyl formate. No effect of 100 mM methyl formate was found on Chl a fluorescence yield decay curves. On the other hand, 100 mM ethyl formate slowed Chl a fluorescence yield decay curves (data not shown). However, this effect was weaker than by trimethylacetate at the same concentration. We don't yet understand the significance of these preliminary observations.

Weak acids such as nitrite, cyanate, formate, thiocyanate, acetate, azide and to a lesser extent, bicarbonate, were shown to stimulate the protonation in the L-E212N mutant of *Rhodobacter sphaeroides*, which suffers a total block in the normal protonation necessary for the double reduction of  $Q_B$  (Takahashi and Wraight, 1991). In PS II, however, formate has been suggested to inhibit the protonation to reduced  $Q_B$  and bicarbonate to facilitate this

protonation (see Chapter III). Furthermore, nitrite and azide were shown by Cao and Govindjee (1990b) to function in cyanobacterial PS II in the same manner as formate does. Thus, the reaction center of photosynthetic bacteria and of PS II are affected differently by these weak acid anions, as already alluded to in Chapter I.

In view of the above, I investigated the effects of some of the above-mentioned weak acids. I confirmed that nitrite (100 mM) behaved like formate as was already known (Eaton-Rye et al., 1986; Cao and Govindjee, 1990b). In addition, I found (1) that the effect on the equilibrium  $[Q_A^-]$  was pH dependent, being stronger at pH 6.0 than at pH 7.5; and (2) the largest inhibition occurs after the second and subsequent flashes (data not shown). Therefore, we can now be certain that nitrite acts in the same manner as formate. The effects are of comparable magnitude.

Azide (100 mM), on the other hand, had two effects on the Chl a fluorescence yield decay curves after actinic flashes: (1) the maximum fluorescence yield was greatly decreased and (2) the fluorescence yield decay rate was greatly slowed down (Fig. 7.2). These features are quite different than that shown by formate and indicate that azide has additional effects on PS II. An interesting and new observation was that if formate was added prior to the addition of azide, the above mentioned decrease of maximum fluorescence was abolished (see Fig. 7.2). This implies that azide and formate may compete for the same binding site. If formate is bound, azide cannot bind. The reverse was also true as the addition of formate after azide addition caused no further change.

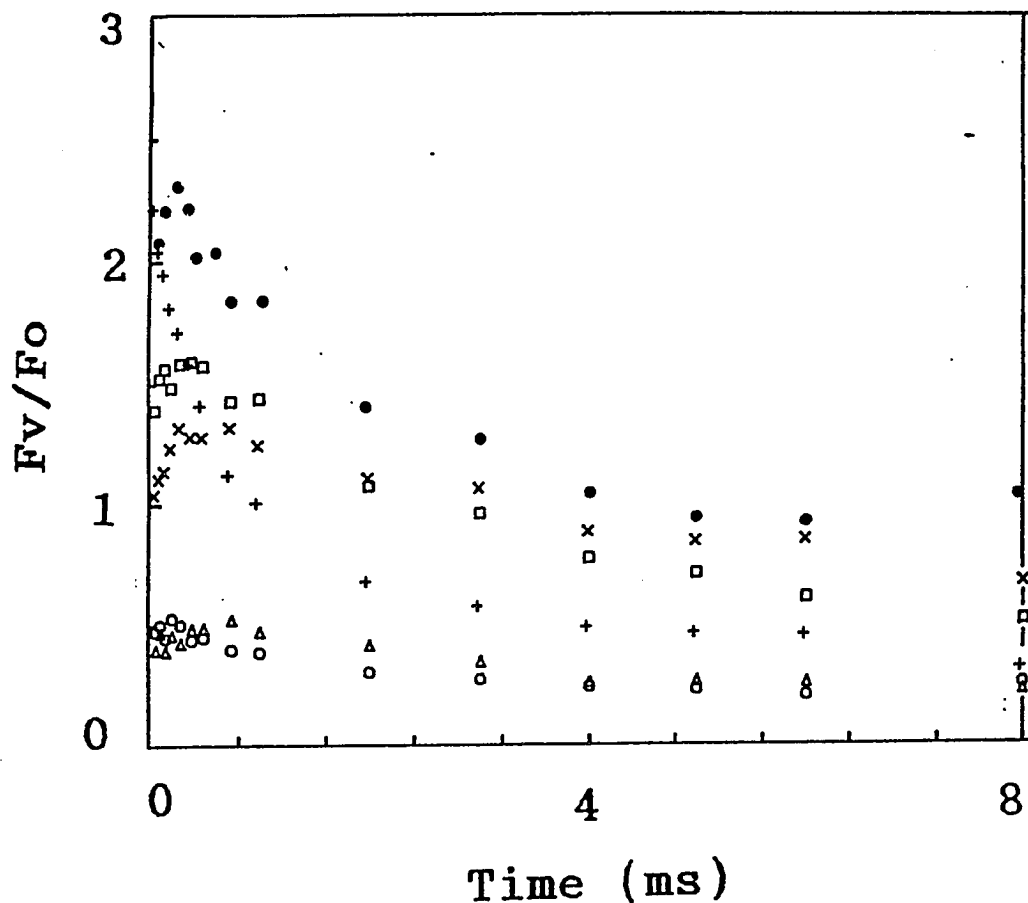


Fig. 7.2. Effects of formate and azide on the decay of variable Chl a fluorescence yield, measured at pH 6.0 and after the first actinic flash. +, control spinach thylakoids; x, 100 mM formate treated; open squares, 100 mM azide added 1 min after the addition of 100 mM formate; o, 100 mM azide; open triangles, 100 mM formate added 1 min after the addition of 100 mM azide; closed circles, values of 100 mM azide treated sample normalized by multiplication with a factor of 4.5.

Cyanate (10 mM) and thiocyanate (10 mM) did not show any effect on the Chl a fluorescence decay after flashes 1 - 4 at both pH 7.5 and 5.5. No conclusion could be made due to the preliminary nature of my experiments. They are mentioned here only for the sake of completeness, but they could be the starting point for another detailed study comparing the bacterial reaction centers and PS II.

#### D. Conclusion

The geometrical requirement for the derivatives of acetic acids was extended in this chapter. We used propionic acid and trimethylacetic acid where hydrogens are replaced by methyl groups in the CX<sub>3</sub> of acetic acid. Trimethylacetic acid, that had 2 more CH<sub>3</sub> groups than propionic acid, slowed to a greater degree the [Q<sub>A</sub><sup>-</sup>] decay, monitored by the Chl a fluorescence yield decay. This effect may be related to differences in their hydrophobicity. Preliminary experiments with several small weak organic acids hint at further possible differences with bacterial reaction centers and imply that azide and formate may bind to a common site on PS II.

## CHAPTER VIII. PRELIMINARY RESULTS ON AN ADDITIONAL EFFECT OF FORMATE/FORMIC ACID PRIOR TO $Q_A$ IN PS II

### A. Introduction

In addition to the site of action of bicarbonate on the electron acceptor side of PS II, another site on the electron donor side of PS II has been proposed (see e.g., Stemler, 1982). This effect could be on the  $O_2$  evolution step itself, between Mn and the electron carrier Z, or between Z and the reaction center chlorophyll a P680 (see Fig. 1.1). Jursinic and Dennenberg (1990) have observed a small but significant (i.e., beyond the error limits) slowing down of the kinetics of  $O_2$  evolution upon formate addition to photosynthetic systems. Jursinic et al. (1976), using a repetitive flash technique, were unable to demonstrate any bicarbonate/formate effect between Mn and Z. This, however, could not demonstrate if there was any effect or not on individual steps dependent upon the redox states of the "S" state of the oxygen evolution complex. Furthermore, using again a repetitive flash technique, Jursinic et al. (1976) could not demonstrate any bicarbonate/formate effect between Z and P680. Govindjee et al. (1989) extended this observation to individual Z to P680 reactions dependent upon the redox states of the "S" state and concluded that there was no bicarbonate/formate effect on any of the Z to P680 steps.

Mende and Wiessner (1985) discovered that  $CO_2$ -depletion caused different effects in the green alga *Chlamydomonas stellata* depending upon

the time of CO<sub>2</sub> depletion. After prolonged depletion (>15 min), CO<sub>2</sub> depletion mainly blocked the electron flow beyond Q<sub>A</sub>; however, in the short-term range of depletion (< 15 min), a blockage on the electron donor side of PS II was observed. El-Shintinawy and Govindjee (1990) succeeded in reproducing this observation in spinach leaf discs. They used a formate infiltration method for CO<sub>2</sub> depletion, needing only 10 seconds for the short-term treatment. Decreases in chlorophyll a fluorescence yield during fluorescence induction after the short-term formate infiltration of spinach leaf discs led El-Shintinawy and Govindjee to suggest that an inhibition of electron donor side of PS II indeed occurs. However, almost identical observations were made when hydroxylamine, instead of water, was an electron donor leading to the suggestion that this effect was between "Z" and Q<sub>A</sub>. In collaboration with El-Shintinawy, I have made a similar conclusion in *Chlamydomonas reinhardtii* cells (El-Shintinawy et al., 1990). This is discussed in this chapter. In addition, I have also discussed here my preliminary observations of a donor side effect on spinach thylakoids at low pH.

## B. Materials and Methods

The growth conditions for *Chlamydomonas reinhardtii* cells, the thylakoid isolation, the formate treatment of cells, the (mild) heating of cells, the measurement of oxygen evolution rates, the Chl a fluorescence transient measurements and the kinetics of decay of Q<sub>A</sub><sup>-</sup> to Q<sub>A</sub> were done as described in Chapter II. For electron flow measurements, 1 mM 2,5-dimethyl-p-benzoquinone (DMQ) was used as an

artificial electron acceptor and 1 mM ferricyanide was used to keep DMQ in the oxidized state. DBMIB, 2,5-dibromo-6-isopropyl-p-benzoquinone (0.5  $\mu\text{M}$ ), was used as an inhibitor of electron flow between photosystems II and I (Trebst et al., 1970).

## C. Results and Discussion

### C.1. Experiments with *Chlamydomonas reinhardtii*

The existence of a bicarbonate-reversible formate effect on the electron flow from  $Q_A$  to  $Q_B^{(-)}$  was confirmed in the green eukaryotic alga *C. reinhardtii* (see El-Shintinawy et al., 1990). A long term (hours) formate treatment did slow the rate of oxidation of  $Q_A^-$ , measured by variable Chl a fluorescence decay after an actinic flash. Addition of 2 mM  $\text{HCO}_3^-$  to the formate treated samples fully reversed all of these effects. The formate/bicarbonate effects on the electron flow from  $Q_A^-$  to  $Q_B^{(-)}$  were accompanied by effects on the dimethylquinone/ferricyanide Hill reaction: a fourfold stimulation was observed upon the addition of 20 mM  $\text{HCO}_3^-$  (pH adjusted, 6.5) to formate-treated samples. Since this stimulation was observed in the presence of DBMIB, which inhibits intersystem electron flow, it is unrelated to  $\text{CO}_2$  fixation in intact systems. Thus, it is due to formate/bicarbonate effect on PS II reactions in intact cells of *C. reinhardtii* cells.

In order to establish the donor side effect of formate, a short-term treatment (5 minutes) was applied to *Chlamydomonas* cells in dilute tris-acetate phosphate medium (see Chapter II). The

short-term formate treatment brought about a dramatic quenching in the Chl a fluorescence transient, suggesting a blockage on the electron donor side of PS II. Furthermore, addition of 10 mM bicarbonate restored the Chl a fluorescence transient to the control level. To locate the site of this inhibition, heated (45°C, 3min) and hydroxylamine-treated *C. reinhardtii* cells were used. (Mild heating blocks O<sub>2</sub> evolution and hydroxylamine is an artificial electron donor to PS II.) Cells were incubated for 5 minutes in a medium containing 25 mM formate or formate plus bicarbonate in the presence of 10 mM hydroxylamine at pH 7.3. Figure 8.1 (trace 1) shows a Chl a fluorescence transient of *C. reinhardtii* cells incubated for 5 minutes in the diluted culture medium without the addition of formate or bicarbonate. Trace 2 shows the quenching of the fluorescence in 5 min formate-treated cells that had been pretreated with heat and 10 mM hydroxylamine. Trace 3 shows the restoration by 10 mM HCO<sub>3</sub><sup>-</sup> of the fluorescence of these cells. This result suggests that the site of inhibition by short-term formate treatment (and its reversibility by bicarbonate addition) occurs after the site of electron donation by hydroxylamine, i.e., between "Z" (or "D") and Q<sub>A</sub>. It is not yet possible to decipher if this effect is between Z and P680, at the reaction center itself, or between pheophytin and Q<sub>A</sub>. Further research is needed to unravel this additional formate/bicarbonate effect on PS II.



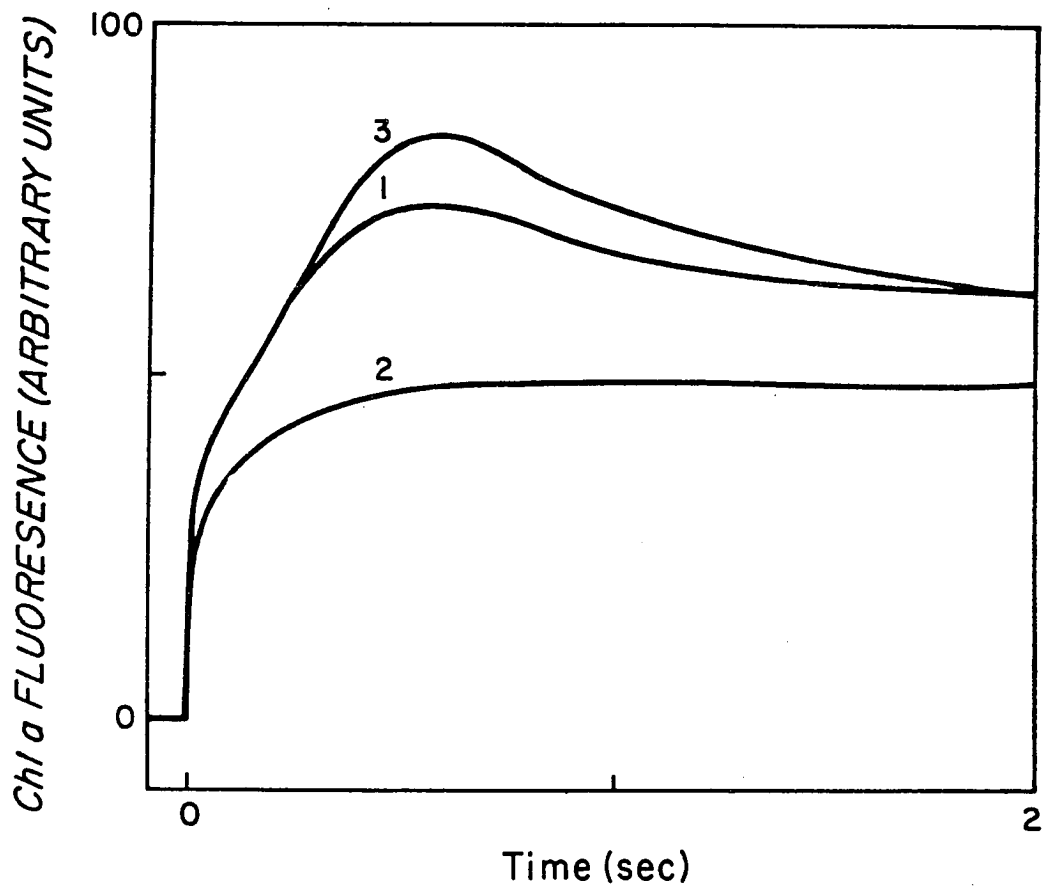


Fig. 8.1. Chl a fluorescence transient in mild-heat and hydroxylamine-treated *C. reinhardtii* cells. The  $F_0$  value was 15 on the scale on the ordinate. Trace 1: control; Trace 2: short-term formate-treated (25 mM for 5 minutes); Trace 3: restored with bicarbonate (2.5 mM). (After El-Shintinawy, F., Xu, C. and Govindjee, 1990.)

## C.2. Experiments with spinach thylakoids

As noted in Chapter III, formate treatment of thylakoids sometimes shows a reduction in  $F_{\max}$  especially at the lower pH's (5.5-6.0) (see Fig. 8.2). This is followed by a fluorescence rise due to equilibration of  $ZP680^+ \leftrightarrow Z^+P680$  reaction, where  $P680^+$  is a quencher of Chl a fluorescence (see Butler, 1972; Kramer et al., 1990). These results are best explained by suggesting that formate, in addition to its effects on the electron acceptor side of PS II, also blocks electron flow between Z and P680. We will now look at the data on formate binding.

The time course of formate binding in spinach thylakoids was followed by monitoring Chl a fluorescence 1 ms after the second flash, as a function of the mixing time, after the injection of a formate solution at different pH's (for details, see Chapter IV). The change in the concentration of  $Q_A^-$ ,  $[Q_A^-]_{(formate)} - [Q_A^-]_{(control)}$ , reflects the fraction of PS II in which formate is bound. The increases in  $[Q_A^-]_{(formate)} - [Q_A^-]_{(control)}$  are due to the formate binding leading to the acceptor side effects on PS II. The pH dependence of time course of  $[Q_A^-]_{(formate)} - [Q_A^-]_{(control)}$  is shown in Fig. 8.3 for flash 1 (upper panel) or 2 (lower panel). The initial rate of formate binding increased as the pH was decreased as discussed in Chapter IV. At acidic pHs (e.g., pH 6) and at shorter times after mixing ( $\leq 3$  minutes), a decrease in the Chl a fluorescence yield was observed. This had led to a lowered calculated  $[Q_A^-]$ . It is more obvious when the fluorescence is measured after the second flash than after the first (Fig. 8.3). The decrease is interpreted as an

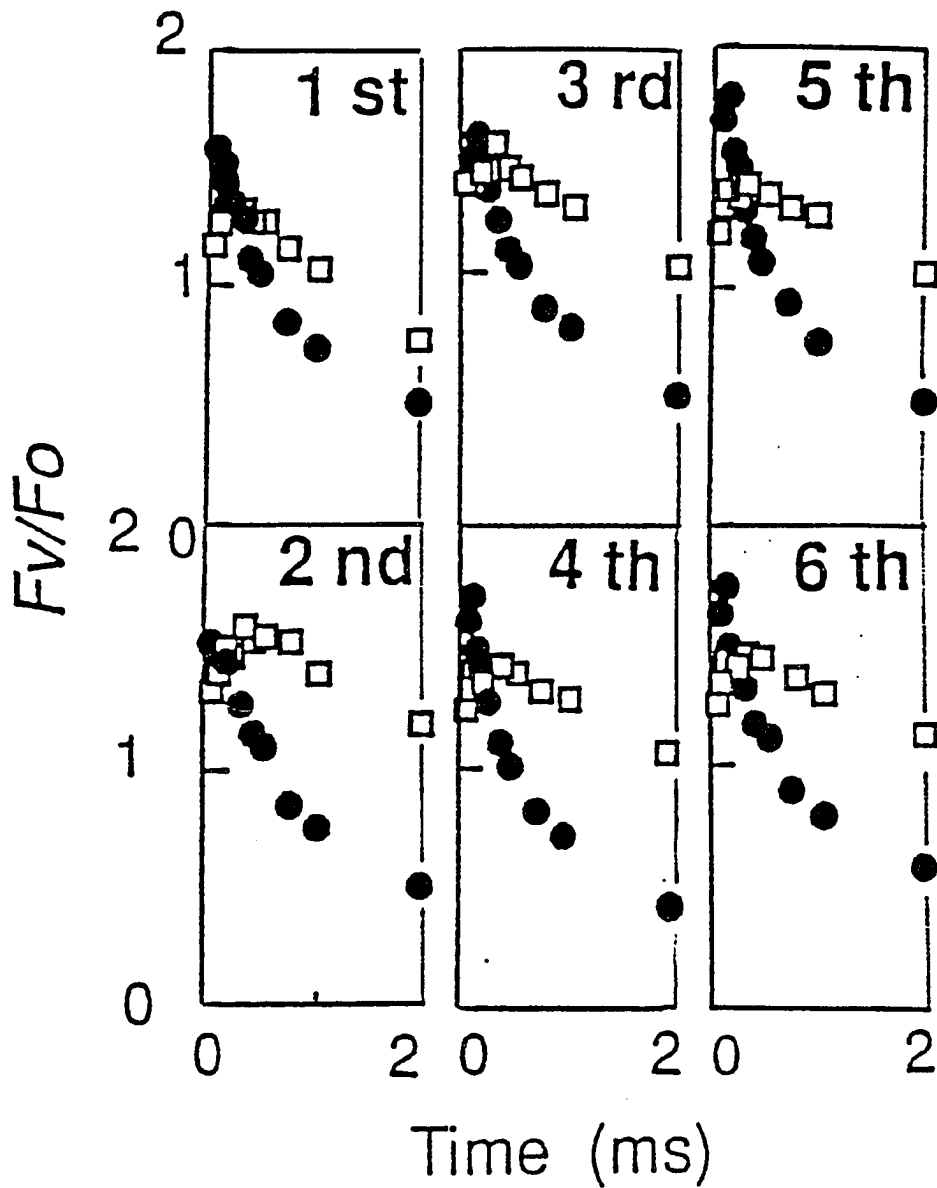


Fig. 8.2. Effect of formate addition on the Chl a fluorescence yield decay up to 2 ms at pH 6.0 in spinach thylakoids. The number in each panel refers to the actinic flash number. Open squares, samples treated with 100 mM formate; closed circles, control.  $F_v$  refers to variable Chl a fluorescence yield, and  $F_o$  to minimum fluorescence yield in weak light. Other experimental conditions are the same as that in Fig. 3.1.

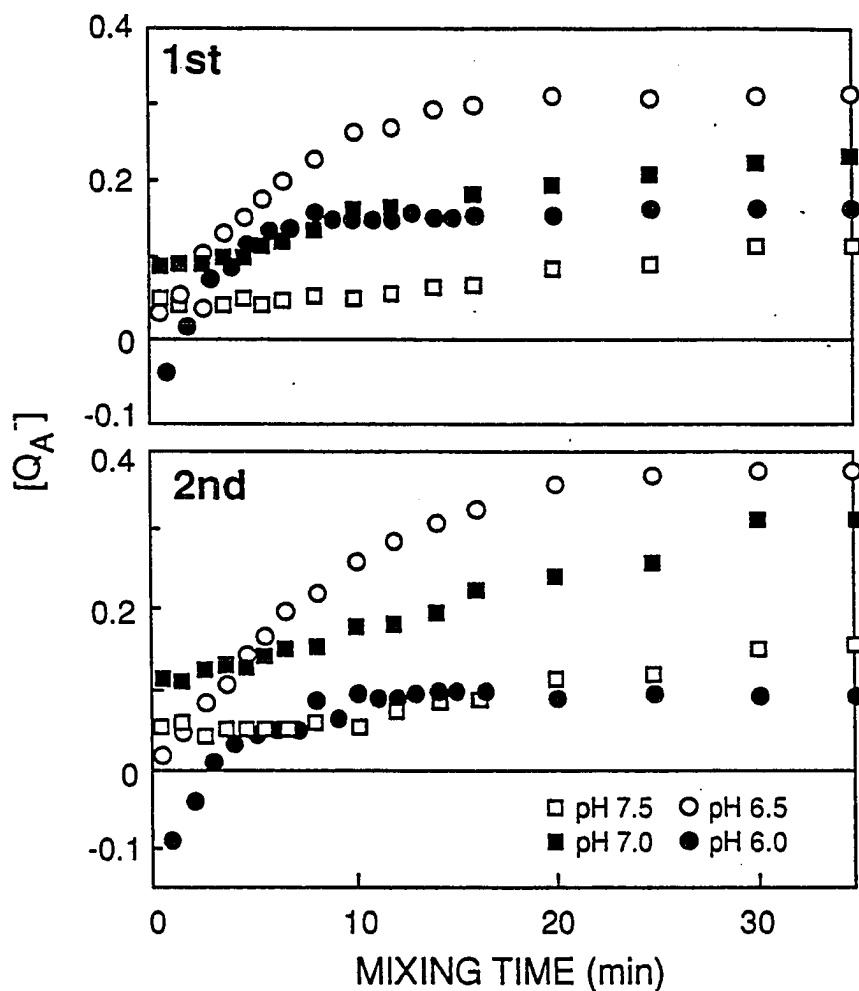


Fig. 8.3. Time dependence of formate/formic acid binding at different pH, as measured by Chl a fluorescence yield 1 ms after flashes 1 and 2.  $[Q_A^-]$  was calculated from this yield without any consideration for any quencher of fluorescence other than  $Q_A^-$ . Different symbols indicate different pH (see key in the panel). Other experimental details were as in Fig. 3.1.

additional secondary effect of formate/formic acid on the electron flow pathway before  $Q_A$  and is consistent with the results in Figs. 8.1 and 8.2. The lower fluorescence yield (from which  $[Q_A^-]$  was calculated) may be due to an increased amount of P680<sup>+</sup>, or Pheo<sup>-</sup>, which acts as a fluorescence quencher (Butler 1972).

Formate was in equilibrium with formic acid; the latter is a weak acid which could move across the thylakoid membrane to induce internal acidification in the thylakoid lumen. Therefore, we tested if internal acidification was responsible for the effect observed above. First, the effect was not due to change of the pH of the medium as it did not change after the addition of 100 mM formate. Second, nigericin, which is known to abolish the pH gradient across the thylakoid membrane (Junge and Jackson, 1982), did not significantly influence the time course of formate binding after the first and second flashes at both pH 6.0 and 6.5 (data not shown). Thus, it is highly unlikely that the internal acidification in the lumen is the reason for the decreased fluorescence upon formate treatment at pH 6.0.

#### D. Conclusion

Our preliminary observations have confirmed the existence of a formate/bicarbonate effect before  $Q_A$  in both algal cells and in spinach thylakoids. Results on chlorophyll a fluorescence induction after the short-term formate-treated *C. reinhardtii* cells showed an bicarbonate-reversible inhibitory site of formate effect prior to  $Q_A$  (Fig. 8.1). This inhibitory effect is also shown within a short

incubation time in spinach thylakoids treated with 100 mM formate at a low pH (pH 6.0 or lower) (Figs. 8.2 and 8.3). It is already known that high (1 M) concentration of acetate irreversibly inhibits the donor side of PS II (Saygin et al., 1986; Bock et al., 1988). Further research is needed to pinpoint the site and mechanism of the formate/bicarbonate effect prior to  $Q_A$ .

## CHAPTER IX. SUMMARY AND GENERAL DISCUSSION

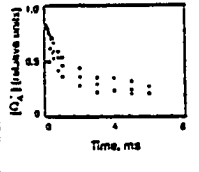
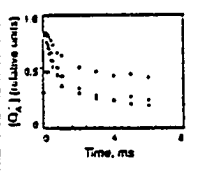
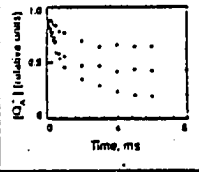
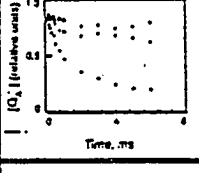
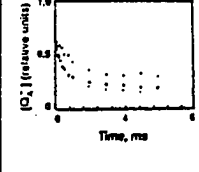
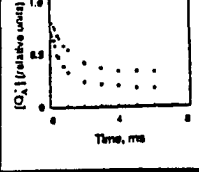
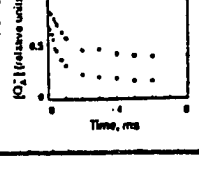
When I began work on this thesis, it was known that: (1) treating thylakoids with monovalent anions (formate, nitrite or acetate) causes a bicarbonate-reversible inhibition of electron transport supported by a Hill oxidant; (2) the major site of the formate/bicarbonate effect is the quinone-acceptor complex of PS II, particularly the  $Q_A^-$ -to- $Q_B^{(-)}$  reaction; and (3) the possible binding sites of bicarbonate/formate are the non-heme iron. Recently, certain positive amino acid residues in the D1 and D2 proteins have been implicated in bicarbonate binding (see Chapter I; Blubaugh and Govindjee, 1988a; Govindjee, 1991). The objective of this thesis has already been presented in Chapter I. Certain key results in the preceding chapters will now be summarized. Then the concepts previously developed will be discussed and an attempt will be made to incorporate the available information into a coherent explanation for the binding/action of weak organic acids in the  $Q_A$ -Fe- $Q_B$  niche of the D1/D2 protein of the PS II reaction center.

### A. Hierarchy of Inhibitory Effects: Correlation with Hydrophobicity

Some of the interesting results of this thesis are summarized in Table 9.1. A number of single functional weak organic acids (monochloroacetic acid (MCA), dichloroacetic acid (DCA), trichloroacetic acid (TCA), monobromoacetic acid (MBA),

Table. 9.1. A summary of major results in this thesis.  $[Q_A^-]$  decays were taken at pH 6.5 for formic acid and at pH 6.0 for others. Two  $\tau_1$  values for MCA-treated sample were obtained from two sets of experimental data, the one in parenthesis belongs to the set with MFA and MBA, and the other to the set with DCA and TCA. The  $\tau_1$  and  $(A_2 + A_3)/A_1$  for the control spinach thylakoid were 420  $\mu$ s and 0.59, respectively. Log P is from Hansch and Leo (1979). See text for details.



Name	Structure	$[O_2^-]$ decay after flash 2	$\tau_1$ ( $\mu s$ )	$\frac{(A_2 + A_3)}{A_1}$	Bicarbonate Reversibility	log P
acetic acid	<chem>CC(=O)O</chem>		610	0.92	+++	-0.33
MCA	<chem>CClC(=O)O</chem>		920 (770)	1.8 (1.3)	+++	0.32
DCA	<chem>CCl(C)C(=O)O</chem>		920	3.2	++	1.33
TCA	<chem>CCl(C)C(=O)O</chem>		1700	24	+	1.54
formic acid	<chem>C=O(O)</chem>		1100	1.7	+++	-0.40
MFA	<chem>FC(=O)O</chem>		650	0.78	+++	-0.27
MBA	<chem>Brc1ccccc1C(=O)O</chem>		860	1.4	++	0.64

monofluoroacetic acid (MFA), propionic acid, trimethylacetic acid and oxamic acid) cause (1) an increase of the lifetime ( $\tau_1$ ) of the  $Q_A^-$  reoxidation by  $Q_B/Q_B^-$ , and (2) a shift of the  $Q_A^-Q_B \rightleftharpoons Q_AQ_B^-$  equilibrium towards  $[Q_A^-]$ , as monitored by the ratio of the amplitudes of the slow to the fast components,  $(A_2 + A_3)/A_1$ , of the  $[Q_A^-]$  decay (Table 9.1). In addition, the concentration of acetates needed to give the same effect on changes in  $[Q_A^-]$  for TCA, DCA and MCA are estimated (from Fig. 5.6 for flash 2 at pH 6) to have the ratio of 1 : 5 : 25. An obvious hierarchy of these effects followed the order: (1) TCA ( $pK_d = 0.7$ ) > DCA ( $pK_d = 1.3$ ) > MCA ( $pK_d = 2.8$ ) > acetic acid ( $pK_d = 4.7$ ); (2) MBA ( $pK_d = 2.9$ ) > MCA ( $pK_d = 2.8$ ) > MFA for both  $Q_A^-$  reoxidation and  $Q_A^-$  equilibration. Furthermore, in the case of the first set, the bicarbonate reversibility followed the inverse order: acetic acid  $\geq$  MCA > DCA  $\gg$  TCA. A correlation of these activities with the molecular geometry was presented in Chapters V and VI. Since the hydrophobic constant (or log P) of TCA, DCA, MCA and acetate are 1.87 (1.54), 1.66 (1.33), 0.65 (0.32) and 0 (-0.33), an excellent, although approximate, correlation is observed between it and the inhibitory effects of the (chloro)acetates at the  $Q_AQ_B$  complex. Furthermore, the hydrophobic constants (or log P) of MBA, MCA and MFA are 0.97 (0.64), 0.65 (0.32) and 0.06 (-0.27); this also correlates with their effects at the  $Q_AQ_B$  complex. No obvious correlation, however, exists with dipole moments since they are 2.12, 2.53, 3.25 and 1.61 for TCA,

DCA, MCA and acetate, respectively. Similar noncorrelation of dipole moments ( $\mu$ ) with the inhibitory effects of MBA ( $\mu = 3.11$ ), MCA ( $\mu = 3.25$ ) and MFA ( $\mu = 3.14$ ) is observed. However, it remains to be seen if a correlation exists between the dipole moment of the head group. (Data with other series were too preliminary to be included in the above discussion.)

## B. Protonation and Active Inhibitory Species

Experiments in this thesis show that the largest bicarbonate-reversible increase of the lifetime of the  $Q_A^-$  reoxidation by  $Q_B/Q_B^-$  and shift of the  $Q_A^-Q_B \leftrightarrow Q_AQ_B^-$  equilibrium towards  $[Q_A^-]$  occur after the second and subsequent flashes in formate/formic acid treated thylakoids (see Table 3.2). These data suggest that a bicarbonate-reversible inhibition of the protonation reaction occurs near the  $Q_B^-$  binding site. Formate binding near the  $Q_B$  site is proposed to restrict proton binding for the formation of plastoquinol,  $Q_BH_2$  (for details, see Chapter III). Bicarbonate reverses this implying its involvement in normal protonation near the  $Q_B$  binding site.

The reaction center protein may stabilize  $Q_B^-$  in a hydrophobic environment without the need for direct protonation of the semiquinone anion (Wraight, 1979; Crofts et al., 1984); this protonation may occur on a neighboring amino acid. Shipman (1980) discussed three non-mutually exclusive means for this stabilization process: (1) uptake of  $H^+$  on a protein binding site near  $Q_B^-$ ; (2) the generation of a strong static electric field across the binding site near  $Q_B$ ; and (3) the relaxation of the protein conformation

when  $Q_B$  is reduced. The function of bicarbonate may be to somehow aid in the processes that lead to protonation of  $Q_B^-$ ; some of the bicarbonate-reversible inhibitors may function by displacing bicarbonate.

A ubiquitous pH dependence of the increase of the lifetime of the  $Q_A^-$  oxidation by  $Q_B/Q_B^-$  and the shift of the  $Q_A^-Q_B \rightleftharpoons Q_AQ_B^-$  equilibrium towards  $Q_A^-$  was observed following the addition of formate, acetate, (chloro)acetates and (methyl)acetates, the inhibition being larger as the pH is lowered. These data suggested that the acidic not the anionic form is the active inhibitory species. Furthermore, measurements on the initial binding rate of formate or formic acid, when one of them is fixed, also suggested that formic acid is the active binding species (Chapter IV). Thus, extending this argument to other small weak acid inhibitor may mean that in all cases it is the acidic form that is active. However, the pH dependence of the inhibition by weak acids can also be explained by two other alternative explanations. The first explanation considers that at low pH, as compared to high pH, neutralization of negative surface charges facilitates the entry of formate ions, and thus, does not support the formic acid being the active species. The second explanation is that at low pH, as compared to high pH, more  $CO_2$  is released and thus one may be measuring this event rather than the formate binding. We show below that these are not valid explanations here.

In all cases it has been shown that at neutral pH the thylakoid carries net negative charges on its surface (Barber,

1982). The negative charge is almost certainly derived from carboxyl groups associated with glutamic and aspartic acid residues. When the pH of the suspension medium is lowered, the thylakoid membrane becomes electroneutral at about 4.3. The D1 interhelical D-E loop is on the stroma side, part of which must constitute the pathway for the entry of herbicides and weak acids since  $Q_b$  is located here (Trebst, 1986). This region has six negatively charged residues (D1-E226, D1-E229, D1-E231, D1-E242, D1-E243 and D1-E244) and two positively charged residues (D1-R257 and D1-R225) (Fig. 9.1). The extra negatively charged residues may produce a electrostatically repulsive force to anions (formate, nitrite, or acetate) and thus make them difficult to diffuse into the  $Q_b$  binding niche at neutral pH. When the pH of the suspension medium is lowered (from 7.5 to 5.5 in this study), the negatively charged residues are protonated. Thus, anions may therefore be suggested to be free to diffuse to its binding sites at the lower pH. However, we do not consider this explanation acceptable because of the following. All thylakoids used in our studies were dark incubated with 120 mM  $Na^+$  and 5 mM  $Mg^{2+}$  for 5-10 minutes.  $Mg^{2+}$  is the predominant counterion to compensate the negative charges (Barber, 1982). There is considerable experimental evidence that 5 mM  $Mg^{2+}$  is sufficient to diminish the thylakoid membrane potential from 64 mV initially to 8 mV when equilibrium is reached at pH 7.0 (Barber, 1982). Therefore, the surface charges were almost neutralized in our experiments.

# D1

# D2

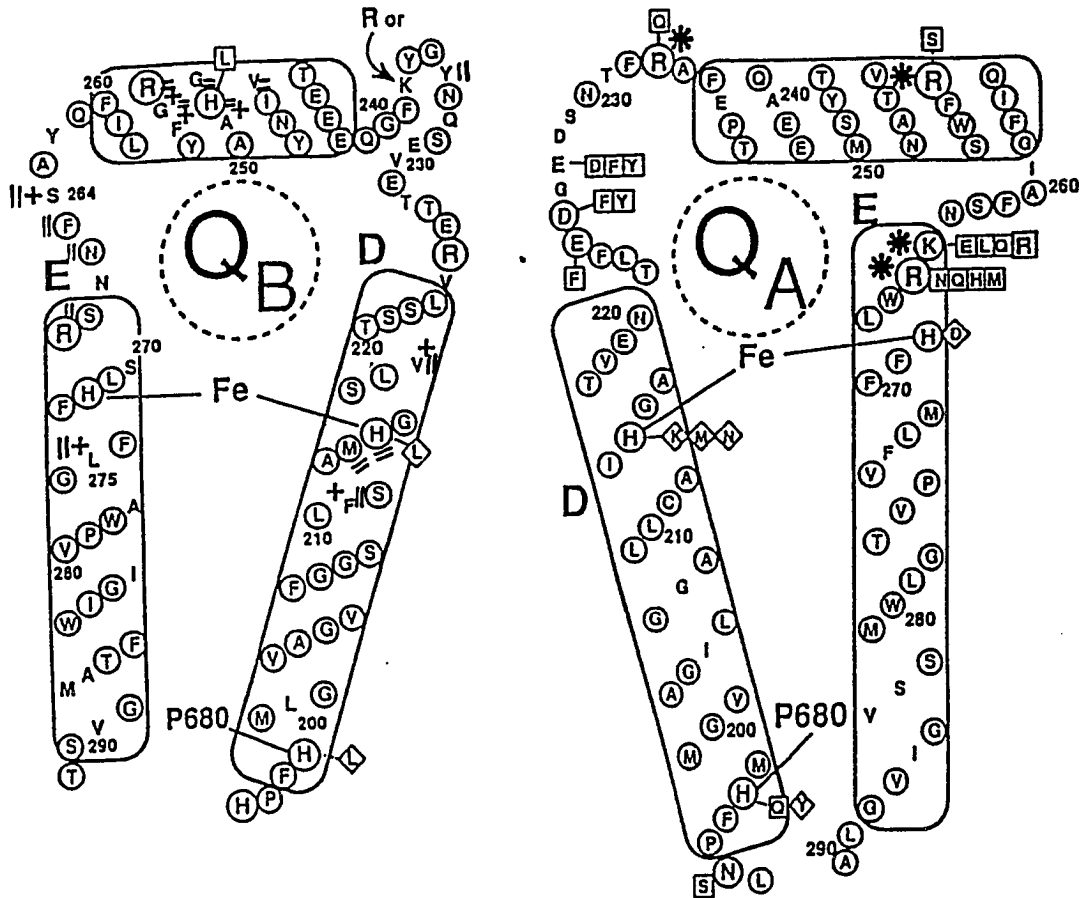


Fig. 9.1. A schematic diagram of a possible folding model of the D-E loop, D and E  $\alpha$ -helices of the D1 and D2 polypeptides of *Synechocystis sp.* PCC 6803. (For original references and diagram, see the review by Govindjee and Van Rensen, 1992.) + refers to herbicide-resistant mutants; amino acids in boxes next to amino acids in the sequence refer to mutations published in the literature; double lines indicate the residues suggested by Trebst to be in contact within the  $Q_B$  binding niche; and \* indicates the available mutations shown to be related to the bicarbonate effect.

Our conclusion that formic acid is the active species (Chapter IV) is not complicated by diffusion arguments. The initial binding rate constant should be closely related to the diffusion rate at low concentration, when diffusion dominates the binding process. A linear relationship is expected. However, such a linear relationship was not observed between the initial binding rate constant and the formate concentration (Fig. 4.2). On the contrary, a Lineweaver-Burk plot (Fig. 4.7) for the formate/formic acid binding displayed a saturation kinetics characteristic of binding at a specific site of the protein. Moreover, at a fixed formate concentration, the initial rate constant was independent of the pH ranging from 5.5 to 7.5 (Fig. 4.4), clearly indicating that the time course of the binding studied had nothing to do with the pH change. Therefore, the surface charge hypothesis is not feasible.

In the second alternative explanation for the observed pH dependence of the inhibition by weak acids, it is suggested that the change in the initial rate of  $[Q_A^-]$  reflects the dissociation of bicarbonate not the binding of formate since formate is a competitive anion of bicarbonate binding. The  $pK_a$  value of bicarbonate is 6.4. In the studied pH range of 5.5 to 7.5, there are large changes in the concentration of bicarbonate. Therefore, it may very well be possible that the change in the initial rate of  $[Q_A^-]$  is due to the dissociation of bicarbonate, although the measurements and the calculation lead to the conclusion that formic acid is the binding species. The following discussion demonstrates that this explanation is also incorrect.

The pH dependence (pH 5.5-7.4) of the inhibition of the  $Q_A^-$  oxidation was also observed in spinach thylakoids previously bubbled with  $N_2$  in the presence or absence of NO (Diner and Petrouleas, 1990). At pH 5.5 and without NO or any other inhibitor, it takes more than 2.5 hours for bicarbonate to completely dissociate from its binding site. At pH 7.4, incubation longer than 3 hours produces only a small amount of bicarbonate dissociated (less than 20% of that at pH 5.5). These changes are not a measurement of  $CO_2$  release but bicarbonate dissociation, because it was shown previously that the equilibration between carbonic species in aqueous solution is easy to complete within 1 minute (Cooper et al., 1968).

Two observations contradict the possibility that the dissociation of bicarbonate is measured in the presence of weak acids and NO. The addition of NO (Diner and Petrouleas, 1990) and formate (Chapter IV) greatly accelerates the initial rate of the inhibition of  $Q_A^-$  reoxidation and increase of equilibrium [ $Q_A^-$ ]. The saturated level is reached within 5 minutes rather than several hours at pH 5.5. The initial rate of change in [ $Q_A^-$ ] is much faster (> one order) than the initial dissociation rate of bicarbonate calculated in ordinary circumstance (Diner and Petrouleas, 1990). Moreover, the measurement of the inhibition of  $Q_A^-$  oxidation and increase of equilibrium [ $Q_A^-$ ] following the addition of NO or formate started after 10 minutes of dark incubation. By this time, the carbonic species could be considered to be in a quasi-equilibrium state. Owing to the quasi-equilibrium and the slowly



changing rate of bicarbonate dissociation, an equilibrium constant of bicarbonate dissociation is used to describe the change in  $[Q_A^-]$  under initial conditions. The initial rate mainly reflects the binding of chemicals added, not the dissociation of bicarbonate.

### C. General Discussion: Binding Niche

The observation that weak acid, not anion, is the inhibitory species (see section B) raises additional questions regarding the nature of the binding niche of bicarbonate as well as bicarbonate-reversible inhibitors.

As previously indicated, weak acids must bind in the  $Q_A$ -Fe- $Q_B$  complex in the D1/D2 protein (see Figures 9.1 and 9.2). A group of herbicides also act on this reducing side of PS II. These herbicides include amides, benzimidazoles, biscarbamates, carbamates, hydroxy-benzonitriles, nitrophenols, phenyl ureas, pyridazinones, S-triazines, triazinones, uracil and ureas (Shipman, 1980; Oettmeier, 1992). They all have a hydrophobic component. The primary function of the hydrophobic components is to increase the lipid solubility and to improve contact ability of the herbicides with the hydrophobic surface of the binding site. Weak acids share this common feature of herbicides. In Section A (this Chapter), we have already emphasized the correlation between the hydrophobic constant of weak acids and their inhibitory activities on the  $Q_A Q_B$  complex. A knowledge of the mechanism of binding of PS II herbicides can aid us in understanding the weak acid/bicarbonate effects on PS II.

```

1 (M-numbering)      21                               41                               61
L   ALLSFER-KYRVRGGTLIGGDL-FDFWV--GFIYFVGGFFGVSAIFFLF
M   ADYQTIYTOIQARGPHITVSGEWGDNDRVGKPFYSYWL--GKI-GDAQI--GFIYLGASGTAAFAFGS
D1  MTAILERRESESLWGRF-CNWITSTENRLYI-GWFGVLMIFLLTATSVFIIAFIA
D2  MTIAVGKFTKD-EKDLFDSMDDLRRDRFVFGWSGLLLEFCAYFALGGWFTGTF

      81                               101
L   LGVSLIGYAASQGPTWDP-----FAISINPPDLKYGL-GAAP-----LLEGGFWQAITVCA
M   TAILIILFNMAAEVHFDPLOFFRQFFWLGLYPPKAQYGM-GIPP-----LHGGGWWLMAGLPM
D1  APPVDIDGI-REPVSGS-LLYGNNIISGAIIPTSAIGLHFYPIWEA-ASVDEWLYNGGPYELIVLHF
D2  ATSWYTHGLASSYLEGCNFLTAAVSTP----ANSLAHSLLLLWGPEAQGDFTRWCQLGGLWAFVALHG

121                               141                               161                               181
L   LGAFISWMLREVEISRKLGIGWHVPLAFCVPIFMFCVLOVFRELLLLGSWGHAFPYGILSHLDWVNNFG
M   TLSLGSWWIRVYSRARALGLGTHIAWNFAAAIFFVLCIGCIHETLVGVSWSEGVPPGIIWPHIDWLTAFES
D1  LLGVACYMGFEWELSFRLGMRPWIAVAYSAPVAATAVFLIYPIGQGSFSDGMPLGISGTFNFMIVEQ
D2  AFALIGFMLRQFELARSVQLRPYNAIAFSGPIAVFVSVFLIYELGQSGWFFAPSEGVAAIFRFILFEQ

      201                               221                               241
L   YOYLNWHYMPGMSSVSFLFVNAMALGLHGLLILSVANPGDG-----DKVKTAEH-----EN
M   IRYGNFYYCPAGFSIGFAYGCGLLFAAHGATILAVARFGGDREIEQITDRGTAVER-----AA
D1  AEH-NILMHPEHMLGVAGVFGGSLFSAMHGSLVTSSLIRETTENESA--NEGYRFGQEEETYNIVAAH
D2  GFH-NWTLNPEHMMGVAGVLGAALLCAIHCATVENTLF-EDGDGANT--FRAFNPTQAEETYSMVTAN
      sp.p.                               Fe

      261                               281                               301
L   OYFRD--VVGYS-IGALSIRLGLFLASNIFLTGAFGTIASGPFWTRGWPEWGWWLDIPFWS*
M   LFWRW--TIGFN-ATIESVFRGWFFSLMVMVSASVGILLTGTFTV-DNWYLWCVKHGAAPDYPALPA
D1  GYFGRLIFQYASFNNSRSLFFFLAAWPVVGIWFTALGISTMAFNLNGFNFN-OSVVDSQGRVINTWAD
D2  RFWSQ-IFGVA-FSNKRWLEFFLMLFPVTGLWMSALGVVGLALNLRAYDFVSQEIRAAEDPEFETFYT
      q                               Fe

      321
M   TPDPASLPGAPK*
D1  IINRANLGMEVMHE--RNAHNPLDLAAIEAPSTNG*
D2  KNILLNEGIRAWMAAQQPHEN-LIFPEEVLPRGNAL*

```

Fig. 9.2. Sequence alignment of the L and M subunits from *Rh. viridis* and the D1 and D2 proteins from spinach chloroplast (from Michel and Deisenhofer, 1987). Residues binding to the special reaction center pair (sp.p) and to the non-heme iron (Fe), and residues forming the major part of the quinone-binding sites (q) are indicated. The location of the transmembrane helix in *Rh. viridis* is shown by bars above the L subunit sequence. Numbers refer to the M subunit from *Rh. viridis*.

The forces involved in the binding of herbicide and plastoquinone in the  $Q_A$ -Fe- $Q_B$  complex may involve covalent binding, hydrogen bonding, London-van der Waal's interaction and electrostatic interaction (see e.g. Crofts et al., 1987). Shipman (1980) had suggested that the primary electrostatic interaction is between the dipole moment of the herbicide and the localized electric field on the protein. A common feature of these herbicides is a polar component represented by its dipole moment. The dipole moments for PS II herbicides range from 2.7 - 5.5 (Shipman, 1980). As noted earlier, the dipole moments of MCA, DCA, TCA, MBA and MFA range from 2.12 to 3.25. Thus, the forces involved in the binding of weak acids may be similar to that of herbicides. However, as noted in section A, we did not observe any correlation between dipole moments and the inhibitory activity of the chemicals used.

Positive residues such as arginine are the appropriate candidates to form the cation end of the salt bridge (Blubaugh and Govindjee, 1988a) if the anion bicarbonate is considered to be the active stimulatory species. However, for the inhibitory substances, if weak acids, not anions, are active species, as suggested in this thesis, they may hydrogen bond to the overlapping binding sites of herbicides or at other places, including the positively charged amino acids. The crystallographic structure of human lactoferrin, the only other (bi)carbonate-Fe protein, reveals that the oxygens of carbonate are H-bonded to neighboring amino acid residues (including arginine) in addition to a bidentate ligand to  $Fe^{3+}$

(Anderson et al., 1989), proving that a H-bond is possible for the binding of bicarbonate/weak acid.

The presumed PS II residues involved in herbicide hydrogen bond formation could include the hydroxyl group of D1-S264, the backbone amide nitrogen of D1-F265, and the backbone amide oxygen of D1-A263 (Tietjen et al., 1991). The drastic influence of formate on the binding of herbicide to D1 and vice versa (Khanna et al., 1981; Van Rensen and Vermaas, 1981), as well as the excessive sensitivity of D1-S264A of *Chlamydomonas reinhardtii* (Govindjee et al., 1991b) and D1-S264A of *Synechocystis sp.* PCC 6714 (Govindjee et al., 1990) herbicide resistant mutants to the formate/bicarbonate effect, suggest that bicarbonate/weak acid could make H-bond to D1-S264.

However, herbicide resistant mutant D1-L275F of *C. reinhardtii* (Govindjee et al., 1991b) is insensitive to the formate/bicarbonate effect. This suggests that this mutation changes drastically the binding of formate/bicarbonate. Since Chl a fluorescence decay kinetics of D1-L275F is as normal as that of the wild type (Govindjee, personal communication), it is considered likely that formate binding has been hampered in this mutant. It may also mean that L275F mutant can function without bicarbonate!

D1-G256D, D1-F255Y, D1-V219I of *C. reinhardtii* and D1-F211S of *Synechocystis sp.* PCC 6714 (Govindjee et al., 1990) herbicide resistant mutants are almost as sensitive to the formate/bicarbonate effect

as the wild type, implying that they retain a sensitive binding site for bicarbonate/weak acids.

Some binding sites of weak acids are on the D2 protein since D2-K264X and D2-R265X (Diner et al., 1991) as well as D2-R251S and D2-R233Q of *Synechocystis* 6803 (Cao et al., 1991) show enhanced sensitivity to bicarbonate/formate effect. The similarity between these mutants breaks down since there is a remarkable difference between the D2-K264X/D2-R265X and the D2-R233Q/D2-R251S sets. The D2-K264X/D2-R265X mutants have the  $Q_A^-Q_B \leftrightarrow Q_AQ_B^-$  equilibrium drastically towards  $Q_A^-Q_B$  without formate/NO treatment, and they require >10X more bicarbonate than the wild type for recovery to normal conditions. D2-K264X and D2-R265X appear to be close to the non-heme iron, shown in the putative model in Figure 9.3 (A). It is possible that D2-K264 and D2-R265 may be involved in bicarbonate binding in a major way. On the other hand, D2-R251S and D2-R233Q, but not D2-R139H (Govindjee and J. Cao, personal communication), are ten times more sensitive than the wild type to formate. Thus, D2-R233 and D2-R251 may be involved in stabilization of bicarbonate binding (Cao et al., 1991). The diagram of Fig. 9.3(A) suggests that D2-R251 and even D2-R233 may be in the neighborhood.

Direct interaction of some exogenous ligand of formate/bicarbonate with the non-heme iron in the  $Q_A-Fe-Q_B$  complex is supported by EPR (Vermaas and Rutherford, 1984; Petrouleas and Diner, 1990; Bowden et al., 1991) and Mossbauer studies (Diner and Petrouleas, 1987a; Semin et al., 1990). The modulation of these signals by bicarbonate/formate was interpreted as implying that

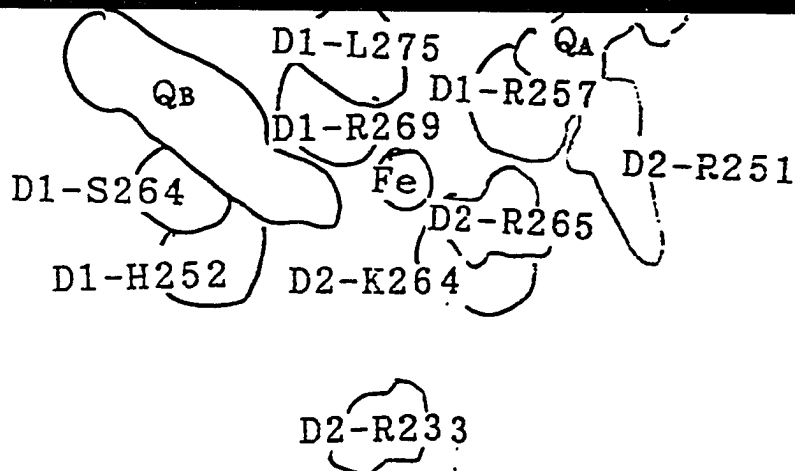
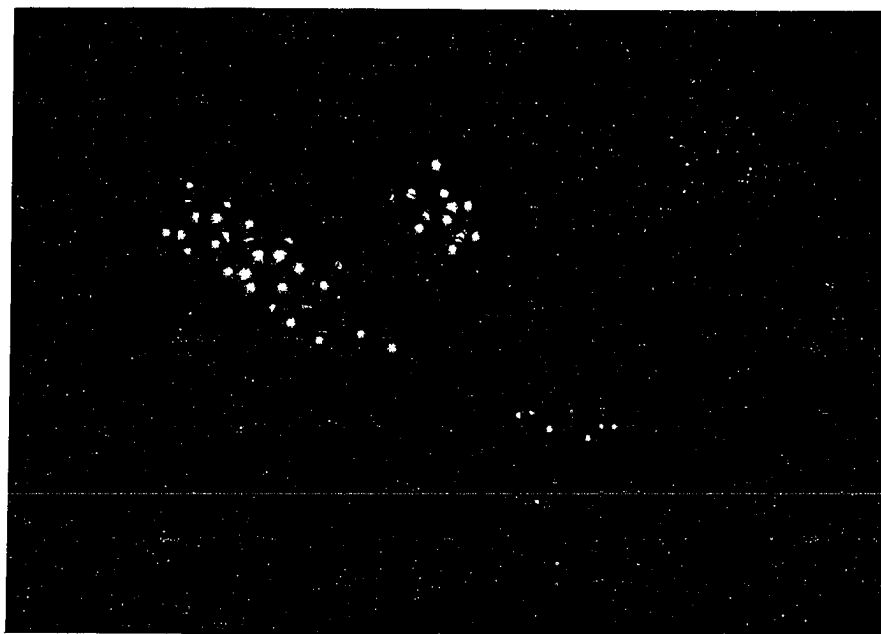


Fig. 9.3 (A). A schematic diagram of a portion of the D1 and D2 polypeptides of PS II in the  $Q_A$ -Fe- $Q_B$  region. The figure is courtesy of C. Gibas and Govindjee; it is based on the PS II model of H.H. Robinson, C. Yerkes, and A.R. Crofts (unpublished). This model used the amino acid sequence of the D1 polypeptide from *Anacystis nidulans* and the D2 polypeptide from spinach and the reaction center coordinates of *Rhodospseudomonas viridis*. In this diagram, certain key amino acids are highlighted that are either involved in herbicide resistance (D1-S264, D1-L275), the bicarbonate effect (D2-R251, D2-R265, D2-K264, D2-R233, D1-R257 and D1-R269) or suggested to be involved in protonation (D1-H252). See text for references.

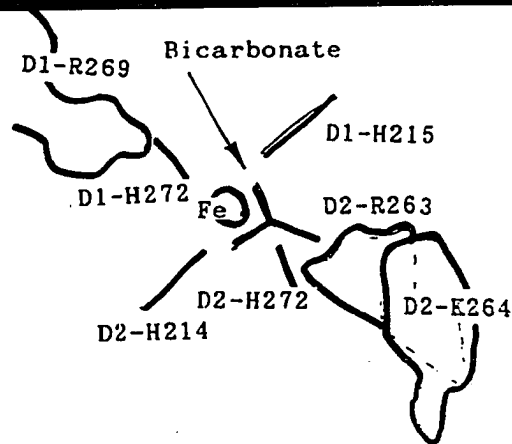
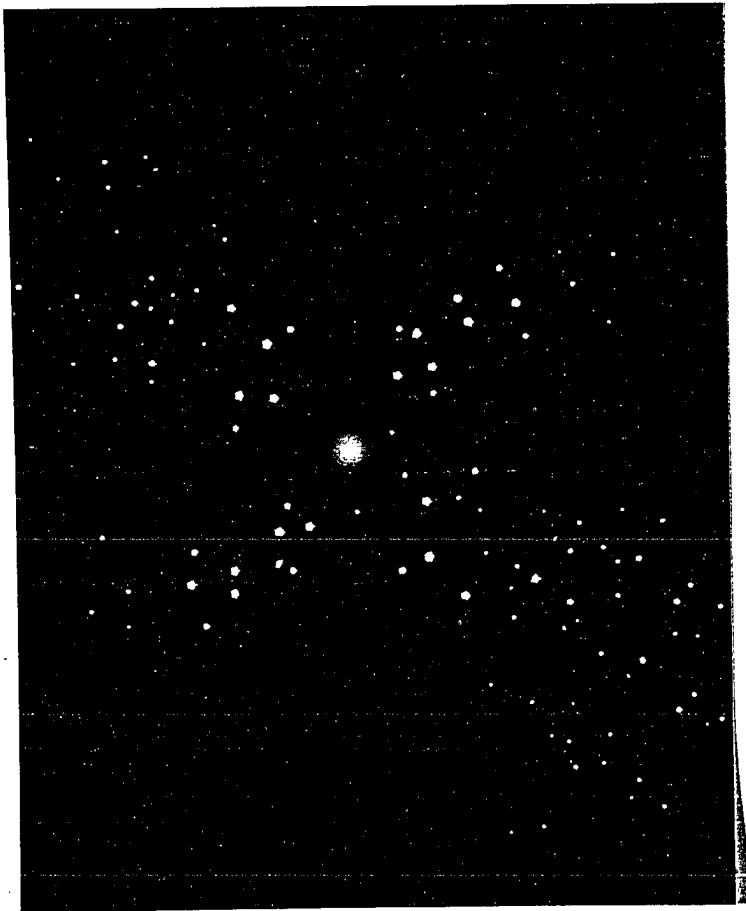


Fig. 9.3 (B). Another view of Fig. 9.3 (A) showing all the four histidines (D1-H272, D1-H215, D2-H214 and D2-H272) involved in binding to the non-heme iron. Also shown is a possible site for bicarbonate (green) binding. For other details, see Fig. 9.3 (A). Courtesy of C. Gibas and Govindjee.

they could form the fifth, possibly the sixth ligand of the iron. Fig. 9.3(B) shows a possible location for bicarbonate (C. Gibas and Govindjee, personal communication).

The role of the non-heme iron (high-spin ferrous,  $S=2$ ,  $Fe^{2+}$ ) in the  $Q_A$ -Fe- $Q_B$  complex is not yet understood. Observations suggest that the non-heme iron can influence the redox equilibrium between  $Q_A$  and  $Q_B$  and oxidation of non-heme iron leads to a conformational change of the  $Q_A$ -Fe- $Q_B$  complex: (1) the non-heme iron could be oxidized by ferricyanide and it can rapidly oxidize  $Q_A^-$  (Bowes and Crofts, 1980); and (2) oxidation of the non-heme iron markedly alters the binding affinity of herbicides (Diner and Petrouleas, 1987a). The semiquinone EPR signals of both  $Q_A$  and  $Q_B$  are dramatically distorted by the magnetic interactions with the iron (Vermaas and Rutherford, 1984; Petrouleas and Diner, 1990; Bowden et al., 1991). The competitive interaction with the iron between NO and formate/bicarbonate leads to the suggestion that formate ligands to a NO-nonoccupied site on the iron or outside the first coordination sphere of the iron. It is equally possible that weak acids, used in this thesis, may also interact with non-heme iron, but this remains to be tested.

The bicarbonate effect is specific for the PS II reaction center and has not been observed in photosynthetic bacteria (see Chapter I and a review by Govindjee, 1991). TCA does not produce any inhibition of  $Q_A^-$  oxidation in purple photosynthetic bacteria (X.Wang, personal communication) although a dramatic inhibition of  $Q_A^-$ -to- $Q_B$  electron flow was found in PS II system (Chapter V). The



explanation for these differences may involve differences in the amino acid sequence and the molecular structure of PS II versus bacterial reaction center (Fig. 9.2). In purple bacteria, a glutamic acid (M-E234) residue is suggested to provide two ligands to the non-heme iron (Deisenhofer et al., 1985; Michel and Deisenhofer, 1988). However, this glutamate is not conserved in D2. Instead, it had been suggested that bicarbonate acts as a ligand to the iron in PS II (Michel and Deisenhofer, 1988). Wang et al. (1992) replaced M-E234 with glutamine, glycine and valine by site-directed mutagenesis in *Rhodobacter sphaeroides*. All mutants showed normal electron transfer behavior and the absence of a formate/bicarbonate effect. Thus, M-E234 is not even important for  $Q_A$  to  $Q_B$  reaction. The absence of a formate-bicarbonate effect in Wang's M-E234X mutants implies that this glutamate is of no consequence in taking over the function of bicarbonate.

There may be other primary structural differences in the  $Q_A$ -Fe- $Q_B$  complex between D1/D2 protein of PS II and L/M subunits of purple bacteria to explain the absence of formate/bicarbonate effect in bacterial system. There are 14 amino acid residues in the D-E loop of D1 that are not found in the L subunit and 7 residues in the D-E loop of D2 that are not found in the M subunit (Fig. 9.2). We do not yet know if these extra residues may be associated with the bicarbonate/formate effect. Furthermore, the difference in the bicarbonate effect between PS II and bacterial reaction center may lie in differences in amino acid residues in D1/D2 protein and

in the corresponding residues in L/M subunits. A search is now in progress in the laboratories of Govindjee and B. Diner.

The protonatable amino acid residues in the *Rhodobacter sphaeroides* reaction center were proposed to constitute two chains for proton transport to  $Q_B^{2-}$  (Feher et al., 1989). Specifically, L-E212 and L-D213 were shown to be strongly implicated in the proton transport to the  $Q_B$  site (Paddock et al., 1989; Takahashi and Wraight, 1990, 1991, 1992). The protonation role of weak acids (azide, formate, bicarbonate, etc.) becomes obvious when these proton transport chains are blocked by mutation (Takahashi and Wraight, 1991). Crofts et al. (1987) proposed that D1-H252 and D1-R225 to be involved in proton transport in PS II. Bicarbonate was assigned an important role in the protonation of reduced  $Q_B$  (Eaton-Rye and Govindjee, 1988; Blubaugh and Govindjee, 1988a). It is possible that bicarbonate acts in PS II as an analogue to the carboxyl acid residues of proton conduction pathways in photosynthetic bacteria. Bicarbonate may work cooperatively with as yet unknown proton conduction pathway in PS II.

#### D. Final Remarks

Although a great deal of evidence now supports the concept that bicarbonate plays an important role in proton transport in PS II in vivo, it has been argued that endogenous bound bicarbonate is not a requirement for electron flow in PS II when all anion binding sites are considered empty of most anions. This suggestion was given because of the inability of Stemler (1989) and Jursinic and

Stemler (1992) to observe CO<sub>2</sub> release in such thylakoids that still retain high rates of electron flow. There is, of course, the possibility that in their thylakoids, that had been depleted of all easily-depletable bicarbonate and other anions, CO<sub>2</sub> released from the tightly bound sites, when formate is added to such preparations, may have just filled the multitude of available empty sites. Furthermore, the high oxygen evolution rates observed by Jursinic and Stemler (1992) appears contradictory with those of Chl a fluorescence measurements by Diner and Petrouleas (1990). In the latter case, a large increase of variable Chl a fluorescence was observed in thylakoids that were depleted of CO<sub>2</sub> without the addition of anions. Ireland et al. (1987) have also observed a block beyond Q<sub>A</sub> in leaves when CO<sub>2</sub> levels are reduced without the use of inhibitors. Flash number dependence of the [Q<sub>A</sub><sup>-</sup>] decay is very helpful in studying the role of bicarbonate effect on the protonation of reduced Q<sub>B</sub>. Thus, it is essential to simultaneously measure Chl a fluorescence parameters under conditions of Jursinic and Stemler (1992).

On the other hand, the conclusion that the bound bicarbonate is not a strict requirement for PS II reaction per se under certain experimental conditions is certainly feasible because one of the suggested function of bicarbonate is the transport of protons. Thus, thylakoids, under certain specific conditions, can transfer protons without intervention of bicarbonate, similar to reactions in photosynthetic bacteria. This is, of course, highly probable when there are plenty of protons around. However, if true, its

mechanism remains to be studied and understood. It is incumbent upon researchers to test the conclusion that there is indeed no CO<sub>2</sub> bound when monovalent ions are low or absent. The conclusion of Jursinic and Stemler (1992) that under their experimental conditions, all anion binding sites are empty is difficult for me to imagine. However, at present, it is neither possible to exclude, nor to establish the necessity of bicarbonate as an obligate cofactor in the Q<sub>B</sub> reduction.

In this thesis, I have presented data which makes, among others, three important points:

(1) Several bicarbonate-reversible inhibitors, that act on the electron acceptor side of PS II, show large inhibition of Q<sub>A</sub><sup>-</sup> reoxidation and an increase of equilibrium [Q<sub>A</sub><sup>-</sup>] after second and subsequent, but not first, actinic flash; this has been interpreted to mean that bicarbonate functions to aid in protonation necessary for the stabilization of Q<sub>B</sub><sup>-</sup>.

(2) The active species of several bicarbonate-reversible inhibitors is COOH, not COO<sup>-</sup> group; this suggests that the search for the binding niche should be expanded beyond the positively charged amino acids.

(3) The binding niche of Q<sub>A</sub>-Fe-Q<sub>B</sub> pocket in the D1/D2 protein of PS II when probed with halogenated acetates shows a hierarchy in their ability to inhibit Q<sub>A</sub><sup>-</sup> oxidation and to increase equilibrium [Q<sub>A</sub><sup>-</sup>]. This follows the order: TCA > DCA > MCA > acetic acid, or MBA > MCA > MFA. On the other hand, bicarbonate reversibility follows the reverse order. A relationship exists between these effects, the

nature of the CX<sub>3</sub> group, the geometry of the inhibitors, and the hydrophobicity of the inhibitors.

Future progress in the understanding of the molecular basis of the "bicarbonate effect" in PS II is expected when a joint effort involving molecular biology, biochemistry, biophysics and plant physiology is mounted.

## REFERENCES

- Allen, J.P., Feher, G., Yeates, T.O., Komiya, H. and Rees, D.C. (1988) Structure of the reaction center from *Rhodobacter sphaeroides* R-26: protein-cofactor (quinones and Fe<sup>2+</sup>) interaction. Proc. Nat. Acad. Sci. USA, 85, 8487-8491.
- Andersson, B.F., Baker, H.M., Morris, G.E., Rice, D.W. and Baker, E.N. (1989) Structure of human transferrin: Crystallographic structure analysis and refinement at 2.8 Å. J. Mol. Biol., 209, 711-734.
- Anonymous (1990) PCMODEL: Molecular Modeling Software for the IBM PC/XT/AT and PS2 Apple Macintosh Series. Serena Software, Box3076, Bloomington, IN47402-3076.
- Ausländer, P. and Junge, W. (1974) The electric generator in the photosynthesis of green plants II. Kinetic correlation between protolytic reactions and redox reactions. Biochim. Biophys. Acta, 357, 285-298.
- Barber, J. (1982) Influence of surface charges on thylakoid structure and function. Annu. Rev. Plant Physiol., 33, 261-295.
- Barber, J. (1987) Photosynthetic reaction centers: a common link. Trends Biochem. Sci., 12, 321-326.
- Beechem, J.M., Gratton, E., Ameloot, M., Knutson, J.R. and Brand, L. (1991) The GLOBAL analysis of fluorescence intensity and anisotropy decay data: second generation theory and programs. In: Lakowicz, J.R. (ed.), Topics in Fluorescence Spectroscopy, Vol. II, Principle. pp. 241-305, Plenum Press, New York.
- Beijer, C. and Rutherford, A.W.C. (1987) The iron-quinone acceptor complex in *Rhodospirillum rubrum* chromatophores studied by EPR. Biochim. Biophys. Acta, 899, 169-178.
- Blubaugh, D. and Govindjee (1986) Bicarbonate, not CO<sub>2</sub>, is the species required for the stimulation of photosystem II electron transport. Biochim. Biophys. Acta, 848, 147-151.
- Blubaugh, D. and Govindjee (1988a) The molecular mechanism of the bicarbonate effect at the plastoquinone reductase site of photosynthesis. Photosyn. Res., 19, 85-128.
- Blubaugh, D. and Govindjee (1988b) Sites of inhibition by disulfiram in thylakoids membranes. Plant Physiol., 88, 1021-1025.
- Bock, C.H., Gerken, S., Stehlik, D. and Witt, H.T. (1988) Time resolved EPR on Photosystem II particles after irreversible

and reversible inhibition of water cleavage with high concentrations of acetate. FEBS Lett. 227, 141-146.

- Bowden, S.J., Hallahan, B.J., Ruffle, S.V., Evans, M.C.W. and Nugent, J.H.A. (1991) Preparation and characterisation of photosystem two core particles with and without bound bicarbonate. Biochim. Biophys. Acta, 1060, 89-96.
- Bowes, J. and Crofts, A.R. (1980) Binary oscillation in the rate of reoxidation of the primary acceptor of Photosystem II. Biochim. Biophys. Acta, 590, 373-384.
- Bruins, H.R. (1929) Coefficients of Diffusion in Liquids. In: Washburn, E.W. (ed.), International Critical Tables of Numerical Data. Physics, Chemistry and Technology, Vol.5, pp. 63-76, McGraw Hill, New York.
- Butler, W.L. (1972) On the primary nature of fluorescence yield changes associated with photosynthesis. Proc. Natl. Acad. Sci. U.S.A., 69, 3420-3422.
- Cao, J. and Govindjee (1988) Bicarbonate effect on electron transport in a cyanobacterium *Synechocystis* PCC 6803. Photosynth. Res., 19, 277-285.
- Cao, J. and Govindjee (1990a) Anion effects on the electron acceptor side of Photosystem II in a transformable cyanobacterium *Synechocystis* 6803. In: Baltscheffsky, M. (ed.), Current Research in Photosynthesis. Vol.I, pp. 515-518, Kluwer Academic Publishers, Dordrecht.
- Cao, J. and Govindjee (1990b) Chlorophyll *a* fluorescence transient as an indicator of active and inactive photosystem II in thylakoid membrane. Biochim. Biophys. Acta, 1015, 180-188.
- Cao, J., Vermaas, W.F.J. and Govindjee (1991) Arginine residues in the D2 polypeptide may stabilize bicarbonate binding in photosystem II of *Synechocystis* sp. PCC 6803. Biochim. Biophys. Acta, 1059, 171-180.
- Cooper, T.G., Tchen, T.T., Wood, H.G. and Benedict, C.R. (1968) The carboxylation of phosphoenolpyruvate and pyruvate: I. The active species of "CO<sub>2</sub>" utilized by phosphoenolpyruvate carboxykinase, carboxytransphosphotylase, and pyruvate. J. Biol. Chem., 243, 3857-3863.
- Crofts, A.R. and Wraight, C.A. (1983) The electrochemical domain of photosynthesis. Biochim. Biophys. Acta, 726, 149-185.
- Crofts, A.R., Robinson, H.H. and Snozzi, M. (1984) Reactions of quinone at catalytic sites: a diffusional role in H<sup>+</sup>-transfer. In:

- Sybesma, C. (ed.), *Advances in Photosynthesis Res. Vol.1*, pp. 461-468. M. Nijhoff/W. Junk, The Hague.
- Crofts, A.R., Robinson, H.H., Andrews, K., Van Doren, S. and Berry, E.D. (1987) Catalytic site for reduction and oxidation of quinones. In: Papa, S., Chance, B. and Ernster, L., (eds.), *Cytochrome Systems*, pp. 617-624. Plenum press, New York.
- Deisenhofer, J. and Michel, H. (1989) The photosynthetic reaction center from the purple bacterium *Rhodospseudomonas viridis*. *EMBO J.*, 8, 2149-2169.
- Deisenhofer, J., Epp, O., Miki, K., Huber, R. and Michel, H. (1985) Structure of the protein subunits in the photosynthetic center of *Rhodospseudomonas viridis* at 3 Å resolution. *Nature (London)*, 318, 618-624.
- Delsome, R. (1971) New results about chlorophyll fluorescence *in vivo*. In: Forti, G., Avron, M. and Melandri, A. (eds.), 2nd Int. Congr. Photosynthesis Res., pp. 187-195. Dr. W. Junk Publishers, The Hague.
- Diner, B.A. and Petrouleas, V. (1987a) Light-induced oxidation of the acceptor-side Fe(II) of photosystem II by exogenous quinones acting through the Q<sub>B</sub> binding site II. Blockage by inhibitors and their effects on the Fe(III) EPR spectra. *Biochim. Biophys. Acta*, 893, 138-148.
- Diner, B.A. and Petrouleas, V. (1987b) Q<sub>400</sub>, the non-heme iron of the Photosystem II iron-quinone complex. A spectroscopic probe of quinone and inhibitor binding to the reaction center. *Biochim. Biophys. Acta* 895, 107-125.
- Diner, B.A. and Petrouleas, V. (1990) Formation by NO of nitrosyl adducts of redox components of the Photosystem II reaction center. II. Evidence that HCO<sub>3</sub><sup>-</sup>/CO<sub>2</sub> binds to the acceptor side non-heme iron. *Biochim. Biophys. Acta* 1015, 141-149.
- Diner, B.A. and Wollmann, F.A. (1980) Isolation of highly active Photosystem II particles from *Chlamydomonas reinhardtii*. *Eur. J. Biochem.*, 10, 521-526.
- Diner, B.A., Schenck, C.C. and de Vitry, C. (1984) Effects of inhibitors, redox state, and isoprenoid chain length on the affinity of ubiquinone for the secondary acceptor binding site in the reaction centers of photosynthetic bacteria. *Biochim. Biophys. Acta*, 766, 9-20.
- Diner, B., Petrouleas, V. and Wendolski, J.J. (1991) The iron-quinone electron-acceptor complex of Photosystem II. *Physiol. Plant.* 81, 423-436.



- Eaton-Rye, J.J. and Govindjee. (1988a) Electron transfer through the quinone acceptor complex of Photosystem II in bicarbonate-depleted spinach thylakoid membranes as a function of actinic flash number and frequency. *Biochim. Biophys. Acta*, 935, 237-247.
- Eaton-Rye, J.J. and Govindjee. (1988b) Electron transfer through the quinone acceptor complex of Photosystem II after one or two actinic flashes in bicarbonate-depleted spinach thylakoid membranes. *Biochim. Biophys. Acta*, 935, 248-257.
- Eaton-Rye, J.J., Blubaugh, D. and Govindjee. (1986) Action of bicarbonate on photosynthetic electron transport in the presence or absence of inhibitory anions. In: Papageorgiou, G., Barber, J. and Papa, S. (eds.), *Ion Interactions in Energy Transfer Biomembranes* pp. 263-278. Plenum Press, New York.
- El-Shintinawy, F. and Govindjee (1990) Bicarbonate effects in leaf discs from spinach. *Photosyn. Res.*, 24, 189-200.
- El-Shintinawy, F., Xu, C. and Govindjee (1990) A dual bicarbonate-reversible formate effect in *Chlamydomonas* cells. *J. Plant Physiol.*, 136, 421-428.
- Etienne, A-L, Ducruet, J.M., Ajilani, G. and Vernotte, C. (1990) Comparative studies on electron transfer in Photosystem II of herbicide-resistant mutants from different organisms. *Biochim. Biophys. Acta*, 1015, 435-440.
- Farinneau, J. and Mathis, P. (1983) Effects of bicarbonate on electron transfer between plastoquinones in Photosystem II. In: Inoue, Y., Crofts, A.R., Govindjee, Murata, N., Renger, G. and Satoh, S., (eds.), *The Oxygen Evolving System of Photosynthesis*, pp. 317-325, Academic Press, Tokyo.
- Feher, G., Allen, J.P., Okamura, M.Y. and Rees, D.C. (1989) Structure and function of bacterial photosynthetic reaction centers. *Nature(London)*, 339, 111-116.
- Good, N.E. (1963) Carbon dioxide and the Hill reaction. *Plant Physiol.*, 38, 298-304.
- Gorman, D.S. and Levine, R.P. (1965) Cytochrome f and plastocyanin: their sequence in the photosynthetic electron transport chain of *Chlamydomonas reinhardtii*. *Proc. Natl. Acad. Sci. USA*, 54, 1665-1669.
- Govindjee (1991) A unique role of carbon dioxide in Photosystem II. In: Abrol, Y.P., Wattal, P.N., Gnanam, A., Govindjee, Ort, D.R. and Teramura, A.H., (eds.), *Impact of Global Climatic Changes on Photosynthesis and Plant Productivity*, pp. 349-370. Oxford and

IBH Pub., New Delhi.

- Govindjee and Eaton-Rye, J.J. (1986) Electron transfer through Photosystem II acceptors: interactions with anions. *Photosyn. Res.*, 10, 365-379.
- Govindjee and Van Rensen, J.J.S. (1978) Bicarbonate effect on the electron flow in isolated broken chloroplasts. *Biochim. Biophys. Acta*, 505, 183-213.
- Govindjee and Van Rensen, J.J.S. (1992) Photosystem II reaction center and bicarbonate. In: Norris, J. and Deisenhofer, J. (eds.), *Reaction Centers, Vol. II*, in press, Academic Press, Orlando.
- Govindjee, Pulles, M.P.J., Govindjee, R., Van Gorkom, H.J. and Duysens, L.N.M. (1976) Inhibition of the reoxidation of the secondary electron acceptor of Photosystem II by bicarbonate depletion. *Biochim. Biophys. Acta*, 449, 602-605.
- Govindjee, Robinson, H.H., Crofts, A.R. and Van Rensen, J.J.S. (1989) Bicarbonate does not influence electron transport to the reaction center: chlorophyll *a* fluorescence rise in microsecond. *Naturwissenschaften*, 76, 719-721.
- Govindjee, Vernotte, C., Peteri, B., Astier, C. and Etienne, A.L. (1990) Differential sensitivity of bicarbonate-reversible formate effects on herbicide-resistant mutants of *Synechocystis* 6714. *FEBS Lett.*, 267, 273-276.
- Govindjee, Weger, H.G., Turpin, D.H., van Rensen, J.J.S., de Vos, O.J. and Snel, J.F.H. (1991a) Formate releases carbon dioxide/bicarbonate from thylakoid membranes. *Naturwissenschaften*, 78, 168-170.
- Govindjee, Schwarz, B., Rochaix, J-D. and Strasser, R. (1991b) The herbicide-resistant D1 mutant L275F of *Chlamydomonas reinhardtii* fails to show the bicarbonate-reversible formate effects on chlorophyll *a* fluorescence transients. *Photosyn. Res.*, 27, 199-208.
- Hallahan, B.J., Ruffle, S.V., Bowden, S.J. and Nugent, J.H.A. (1991) Identification and characterisation of EPR signals involving  $Q_B$  semiquinone in plant Photosystem II. *Biochim. Biophys. Acta*, 1059, 181-188.
- Hansch, C. (1969) Theoretical consideration of the structure-activity relationship in photosynthesis inhibitors. In: Metzner, H. (ed.), *Progress in Photosynthesis Research, Vol. III*, pp. 1685-1692, Metzner, Tubingen.

- Hansch, C. and Leo, A. (1979) Substituent Constants for Correlation Analysis in Chemistry and Biology. See pp. 174-176, John Wiley & Sons, New York.
- Ireland, C.R., Baker, N.R. and Long, S.P. (1987) Evidence for a physiological role of CO<sub>2</sub> in the regulation of photosynthetic electron transport in leaves. *Biochim. Biophys. Acta.* 893, 434-443.
- Joliot, A. and Joliot, P. (1964) Étude cinétique de la réaction photochimique libérant d'oxygène au cours de la photosynthèse. *C. R. Acad. Sci. Paris* 258, 4622-4625.
- Junge, W. and Jackson, J.B. (1982) The development of electrochemical potential gradients across photosynthetic membranes. In: Govindjee, (ed.), *Photosynthesis Vol.1*, pp. 589-646, Academic press, New York.
- Jursinic, P.A. and Dennenberg, R.J. (1990) Oxygen release time in leaf discs and thylakoids of peas. *Biochim. Biophys. Acta*, 1020, 195-206.
- Jursinic, P.A. and Govindjee (1977) Temperature dependence of delayed light emission in the 6-340 microsecond range after a single flash in chloroplasts. *Photochem. Photobiol.* 26, 617-628.
- Jursinic, P.A. and Stemler, A. (1992) High rates of Photosystem II electron flow occur in maize thylakoids when the high-affinity binding site for bicarbonate is empty of all monovalent anions or has bicarbonate bound. *Biochim. Biophys. Acta*, 1098, 359-367.
- Jursinic, P., Warden, J. and Govindjee (1976) A major site of bicarbonate effect in system II reaction: evidence from EPR signal II<sub>vf</sub>, fast fluorescence yield changes and delayed light emission. *Biochim. Biophys. Acta*, 440, 322-330.
- Khanna, R., Wagner, R., Junge, W. and Govindjee (1980) Effects of CO<sub>2</sub>-depletion on proton uptake and release in thylakoid membranes. *FEBS Lett.* 121, 222-224.
- Khanna, R., Pfister, K., Keresztes, A., Van Rensen, J.J.S. and Govindjee (1981) Evidence for a close spatial location of the binding sites for CO<sub>2</sub> and for Photosystem II inhibitors. *Biochim. Biophys. Acta*, 634, 105-116.
- Klimov, V.V. and Krasnovskii, A.A. (1981) Pheophytin as the primary electron acceptor in Photosystem II reaction centers. *Photosynthetica*, 15, 592-609.
- Kramer, D., Robinson, H. and Crofts, A.R. (1990) A portable multi-flash kinetic fluorimeter for measurement of donor and acceptor

reaction of Photosystem 2 in leaves of intact plants under field conditions. *Photosyn. Res.* 26, 181-193.

- Mathis, P. and Paillet, G. (1981) Primary processes of photosynthesis. In: Hatch, M.D. and Boardman, N.K. (eds.) *The Biochemistry of Plant: Vol.8, Photosynthesis*, pp. 97-161, Academic Press, Sydney.
- McClellan, A.L. (ed.) (1963) *Tables of Experimental Dipole Moment*. pp. 52-65. Freeman, W.H. & Co. S. Francisco.
- Mende, D. and Wiessner, W. (1985) Bicarbonate *in vivo* requirement of Photosystem II in the green alga *Chlamydomonas stellata*. *J. Plant Physiol.* 118, 259-266.
- Michel, H., and Deisenhofer, J. (1987) The structural organization of photosynthetic reaction centers, *Progress in Photosynthesis Research*, 1, 353-362.
- Michel, H., and Deisenhofer, J. (1988) Relevance of the photosynthetic reaction center from purple bacteria to the structure of Photosystem II. *Biochemistry*, 27, 1-7.
- Michel, H., Epp, O. and Deisenhofer, J. (1986) Pigment-protein interactions in the photosynthetic reaction centre from *Rps. viridis*. *EMBO J.*, 5, 2445-2451.
- Nugent, J.H.A., Corrie, A.R., Demetriou, C. Evans, M.C.W., and Lockett, C.J. (1988) Bicarbonate binding and the properties of Photosystem II electron acceptors. *FEBS Lett.*, 235, 71-75.
- Oettmeir, W. (1992) Herbicides of Photosystem II. *Topics in Photosynthesis*, 11, in press.
- Paddock, M.L., Williams, J.C., Rongey, S.H., Abresch, E.C., Feher, G. and Okamura, M.Y. (1987) Characterization of three herbicide-resistant mutants of *Rhodospseudomonas sphaeroides* 2.4.1: structure-function relationship. In: Biggins, J. (ed.), *Progress in Photosynthesis Research, Vol III*: pp. 811-814, Martinus/Nijhoff Publishers, Dordrecht.
- Petrouleas, V. and Diner, B.A. (1986) Identification of Q400, a high-potential electron acceptor of Photosystem II, with the iron of the quinone-iron acceptor complex. *Biochim. Biophys. Acta*, 849, 264-275.
- Petrouleas, V. and Diner, B.A. (1990) Formation by NO of nitrosyl adducts of redox components of the Photosystem II reaction center. I. NO binds to the acceptor-side non-heme iron. *Biochim. Biophys. Acta* 1015, 131-140.

- Porra, R.J., Thompson, W.A. and Kriedemann, P.E. (1989) Determination of accurate extinction coefficients and simultaneous equations for assaying chlorophylls a and b extracted with four different solvents: verification of the concentration of chlorophyll standards by atomic absorption spectroscopy. *Biochim. Biophys. Acta* 975, 384-394.
- Rich, P.R. and Moss, D.A. (1987) The reactions of quinones in higher plant photosynthesis. In: Barber, J. (ed.), *The Light Reaction*, pp. 421-445, Elsevier, Amsterdam.
- Robinson, H.H. and Crofts, A.R. (1983) Kinetics of the oxidation-reduction reactions of the Photosystem II quinone acceptor complex, and the pathway for deactivation. *FEBS Lett.*, 153, 221-226.
- Robinson, H.H. and Crofts, A.R. (1984) Kinetics of proton uptake and the oxidation-reduction reactions of the quinone acceptor complex of PS II from pea chloroplasts. In: Sybesma, C. (ed.), *Advances in Photosynthesis Research*, Vol. I, pp. 477-481, Nijhoff/Dr. W. Junk., The Hague.
- Saygin, O., Gerken, S., Meyer, B. and Witt, H.T. (1986) Total recovery of O<sub>2</sub> evolution and nanosecond reduction kinetics of chlorophyll-a<sub>II</sub><sup>+</sup>(P-680<sup>+</sup>) after inhibition of water cleavage with acetate. *Photosyn. Res.*, 9, 71-78.
- Semin, B.A., Loviagina, E.R., Aleksandrov, A.Y., Kaurov, Yu.N. and Novakova, A.A. (1990) Effects of formate on Mossbauer parameters of the non-heme iron of PS II particles of cyanobacteria. *FEBS Lett.*, 270, 184-186.
- Shim, H., Cao, J., Govindjee and Debrunner, P.G. (1990) Purification of highly active oxygen-evolving photosystem II from *Chlamydomonas reinhardtii*. *Photosyn. Res.* 26, 223-228.
- Shipman, L.L. (1980) Theoretical study of the binding site and mode of action for Photosystem II herbicides. *J. Theor. Biol.*, 90, 123-148.
- Shopes, R.J., Blubaugh, D.J., Wraight, C.A. and Govindjee (1989) Absence of a bicarbonate-depletion effect in electron transfer between quinones in chromatophores and reaction centers of *Rhodobacter sphaeroides*. *Biochim. Biophys. Acta*, 974, 114-118.
- Siggel, U., Khanna, R., Renger, G. and Govindjee (1977) Investigation of the absorption changes of the plastoquinone system in broken chloroplasts. *Biochim. Biophys. Acta*, 462, 196-207.
- Snel, J.F.H. and J.J.S. van Rensen (1983) Kinetics of the

reactivation of the Hill reaction in CO<sub>2</sub>-depleted chloroplasts by addition of bicarbonate in the absence and in the presence of herbicide. *Physiol. Plant.* 57, 422-427.

- Stemler A. (1982) The functional role of bicarbonate in photosynthetic light reaction II. In: Govindjee, (ed.), *Photosynthesis Vol.II*, pp. 513-538, Academic Press, New York.
- Stemler A. (1985) Carbonic anhydrase: molecular insights applied to photosystem II research in thylakoid membrane. In: Lucas, W.J. and Berry, J.A. (eds.), *Inorganic Carbon Uptake by Aquatic Photosynthetic Organism*, pp. 377-387. American Society of Plant Physiologists, Rockville, MD.
- Stemler A. (1989) Absence of a formate-induced release of bicarbonate from Photosystem II. *Plant Physiol.*, 77, 974-977.
- Stemler, A. and Govindjee (1973) Bicarbonate ion as a crucial factor in photosynthetic oxygen evolution. *Plant Physiol.*, 52, 119-123.
- Takahashi, E. and Wraight, C.A. (1990) A crucial role for Asp in the proton transfer pathway to the secondary quinone of the reaction centers from *Rhodobacter sphaeroides*. *Biochim. Biophys. Acta*, 1020, 107-111.
- Takahashi, E. and Wraight, C.A. (1991) Small weak acids stimulate proton transfer events in site-directed mutants of the two ionizable residues, Glu<sup>L212</sup> and Asp<sup>L213</sup>, in the Q<sub>B</sub>-binding site of *Rhodobacter sphaeroides*. *FEBS Lett.* 283, 140-144.
- Takahashi, E. and Wraight, C.A. (1992) Proton electron transfer in the acceptor quinone complex of *Rhodobacter sphaeroides* reaction centers: characterization of site-directed mutants of the two ionizable residues, Glu<sup>212</sup> and Asp<sub>13</sub>, in the Q<sub>B</sub> binding site. *Biochemistry*, 31, 855-866.
- Tietjen, K.G., Kluth, J.F., Andree, R., Haug, M., Lindig, M., Muller, K.H., Wroblowsky, H.J. and Trebst, A. (1991) The herbicide binding niche of photosystem II - a model. *Pestic. Sci.* 31, 65-72.
- Trebst, A. (1986) The topology of the plastoquinone and herbicide binding peptides of Photosystem II in the thylakoid membrane. *Z. Naturforsch.* 41C, 240-245.
- Trebst, A., Harth, E. and Draber, W. (1970) On a new inhibitor of photosynthetic electron transport in isolated chloroplasts. *Z. Naturforsch.* 25, 1157-1159.
- Van Rensen, J.J.S. (1982) Molecular mechanism of herbicide action

- near Photosystem II. *Physiol. Plant.* 54, 515-521.
- Van Rensen, J.J.S. (1992) The role of bicarbonate on the activity of Photosystem II. In: Abrol, Y., Mohanty, P. and Govindjee, (eds.), *Photosynthesis and Plant Productivity*, in press, Oxford University Press/IBH, New Delhi.
- Van Rensen, J.J.S. and Vermaas, W.F.J. (1981) Action of bicarbonate and Photosystem II inhibiting herbicides on electron transport in pea grana and in the thylakoids of a blue-green alga. *Physiol. Plant.* 51, 106-110.
- Van Rensen, J.J.S., Tonk, W.J.M. and de Bruijn, S.M. (1988) Involvement of bicarbonate in the protonation of the secondary quinone electron acceptor of Photosystem II via the non-haem iron of the quinone-iron acceptor complex. *FEBS Lett.* 226, 347-351.
- Velthuys, B.R. (1981) Electron transport dependent competition between plastoquinone and inhibitors for binding to Photosystem II. *FEBS Lett.* 126, 277-281.
- Velthuys, B.R. (1982) The function of plastoquinone in electron transfer. In: Trumpower, B.L. (ed.), *Function of Quinone in Energy-conserving Systems*, pp. 401-408, Academic Press, New York.
- Velthuys, B.R. and Ames, J. (1974) Charge accumulation at the reducing side of system II of photosynthesis. *Biochim. Biophys. Acta* 333, 85-94.
- Vermaas W.F.J. and Govindjee (1981) The acceptor side of Photosynthesis. *Photochem. Photobiol.* 34, 775-793.
- Vermaas, W.F.J. and Ikeuchi, M. (1991) Photosystem II. In: Bogorad, L. and Vasil, I.K. (eds.), *The Photosynthetic Apparatus: Molecular Biology and Operation*, pp. 25-111, Academic Press, San Diego.
- Vermaas, W.F.J. and Rutherford, A.W.C. (1984) EPR measurements on the effects of bicarbonate and atrazine resistant on the acceptor side of Photosystem II. *FEBS Lett.* 175, 243-247.
- Vermaas W.F.J., Van Rensen, J.J.S. and Govindjee (1982) The interaction between bicarbonate and the herbicide ioxynil in the thylakoid membrane and the effects of amino acid modification on bicarbonate action. *Biochim. Biophys. Acta.* 681, 242-247.
- Wang, X., Cao, J., Maroti, P., Stilz, H.U., Finkle, U., Lauterwasser, C., Zinth, W., Oesterhelt, D., Govindjee and Wraight C.A. (1992) Is bicarbonate in Photosystem II the equivalent of the glutamate ligand to the iron atom in

- bacterial reaction centers? *Biochim. Biophys. Acta.* 1100, 1-8.
- Warburg, O. (1964) Prefactory chapter. *Ann. Rev. Biochem.* 33, 1-18.
- Warburg, O. and Krippahl, G.Z. (1958) Hill-Reaktionen. *Z. Naturforsch.* 13B, 509-514.
- Warburg, O. and Krippahl, G.Z. (1960) Notwendigkeit der Kohlensäure für die chinon und ferricyanid reaktionen in grünen grana. *Z. Naturforsch.* 15B, 367-369.
- Wasielewski, M.R., Johnson, D.G., Seibert, M. and Govindjee (1989a) Determination of the primary charge separation rate in isolated photosystem II reaction centers with 500-fs time resolution. *Proc. Nat. Acad. Sci. USA*, 86, 524-528.
- Wasielewski, M.R., Johnson, D.G., Govindjee, Preston, C. and Seibert, M. (1989b) Determination of the primary charge separation rate in Photosystem II reaction centers at 15K. *Photosyn. Res.* 22, 89-100.
- Wollman, F.A. (1978) Determination and modification of the redox state of the secondary acceptor of Photosystem II in the dark. *Biochim. Biophys. Acta*, 503, 263-273.
- Wraight, C.A. (1979) Electron acceptors of bacterial photosynthetic reaction centers. *Biochim. Biophys. Acta*, 548, 309-327.
- Wraight, C.A. (1981) Oxidation-reduction physical chemistry of the acceptor quinone complex in bacterial photosynthetic reaction centers: evidence for a new model of herbicide activity. *Isr. J. Chem.*, 21, 348-354.
- Wraight, C.A. (1982) The involvement of stable semiquinone in the two-electron gates of plant and bacterial photosystems. In: Trumppower, B.L. (ed.), *Function of Quinone in Energy-conserving Systems*, pp. 181-211, Academic Press, New York.
- Xu, C., Taoka, S., Crofts, A.R. and Govindjee (1991) Kinetic characteristics of formate/formic acid binding at the plastoquinone reductase site in spinach thylakoids. *Biochim. Biophys. Acta*, 1098, 32-40.
- Zimmermann, J.-L and Rutherford, A.W. (1986) Photoreductant-induced oxidation of Fe<sup>2+</sup> in the electron acceptor complex of Photosystem II. *Biochim. Biophys. Acta*, 851, 416-423.



# Characteristics of Five New Photoautotrophic Suspension Cultures Including Two *Amaranthus* Species and a Cotton Strain Growing on Ambient CO<sub>2</sub> Levels<sup>1</sup>

Received for publication April 15, 1988 and in revised form July 25, 1988

CHUNHE XU, L. C. BLAIR, S. M. D. ROGERS, GOVINDJEE, AND J. M. WIDHOLM\*

Departments of Physiology and Biophysics and Plant Biology (C.X., G.) and Agronomy (L.C.B., S.M.D.R., J.M.W.) University of Illinois, Urbana, Illinois 61801

## ABSTRACT

Suspension cultures of cotton (*Gossypium hirsutum*), *Amaranthus cruentus*, *A. powellii*, *Datura innoxia*, and a *Nicotiana tabacum*-*N. glauca* fusion hybrid were adapted to grow photoautotrophically under continuous light. The cotton strain grew with an atmosphere of ambient CO<sub>2</sub> (about 0.06 to 0.07% in the culture room) while the other strains required elevated CO<sub>2</sub> levels (5%). Photoautotrophy was indicated by the requirement for CO<sub>2</sub> and for light for growth. The strains grew with doubling times near 14 days and had from 50 to 600 micrograms of chlorophyll per gram of fresh weight. The cells grew in small to moderate sized clumps with cell sizes from 40 to 70 micrometers (diameter). Like most photoautotrophic cultures described so far the ribulose 1,5-bisphosphate carboxylase (RuBPCase) activity levels were well below those of mature leaves. The phosphoenolpyruvate carboxylase levels were not elevated in the *C.* *Amaranthus* species. The cells showed high dark respiration rates and had lower net CO<sub>2</sub> fixation under high O<sub>2</sub> conditions. Dark CO<sub>2</sub> fixation rates ranged from near 10 to 30% of that in light. Fluorescence emission spectra measurements show that the cell antenna pigment systems of the four strains examined are similar to that of chloroplasts of green plants. The cotton strain which was capable of growth under ambient CO<sub>2</sub> conditions showed the unique properties of a high RuBPCase activation level in ambient CO<sub>2</sub> and a stable ability to show net CO<sub>2</sub> fixation in 21% O<sub>2</sub> conditions.

lower RuBPCase<sup>2</sup> activity which often leads to RuBPCase to PEPCase activity ratios near one. These differing characteristics are not really surprising since photoautotrophic cultured cells are growing and dividing unlike a mature leaf. Thus, the cultured cells should be compared to developing leaves which do have high respiration rates and a lower ratio of RuBPCase to PEPCase activity (1, 14). Probably because of these characteristics all photoautotrophic cultures described thus far require elevated CO<sub>2</sub> levels, usually 1 to 5%, for growth and have CO<sub>2</sub> compensation concentrations higher than that of mature leaves (reviewed in 11, 20).

To date, no species with the C<sub>3</sub> photosynthesis pathway has been grown photoautotrophically. Photoheterotrophic, green cultures of the C<sub>3</sub> species, *Gisekia pharnaceoides* (25), *Portulaca oleracea* (12, 13) and *Frodichia gracilis* (15) have been initiated and used in photosynthesis studies, but these cultures were grown with 2 to 2.5% sucrose in the culture medium.

Photoautotrophic cultures can be used for many purposes including the selection of mutants resistant to photosynthetic herbicides, for screening for herbicidal activity, and for herbicide mechanism of action studies. The photoautotrophic cultures may be valuable for producing desired compounds if chloroplasts are involved in the biosynthesis. Studies of chloroplast development and breakdown can be readily studied during the reversible transition to and from photoautotrophy as controlled by the culture medium and conditions. The large numbers of cells and the readily controllable conditions may permit the selection of mutants with alterations in different photosynthetic components. Suspension cultures always provide materials well adapted to labeling studies and rapid medium manipulation and easy extraction.

In this report we describe the initiation and characterization of five new photoautotrophic cultures including two from *C.* species and one which grows on ambient CO<sub>2</sub> levels.

## MATERIALS AND METHODS

**Origin of Suspension Cultures.** The photoautotrophic cotton (*Gossypium hirsutum* cv Stoneville 823) culture designated COT-P was initiated as described previously (4). The photoautotrophic cultures of *Datura innoxia* (denoted DAT-P) and a *Nicotiana tabacum*-*Nicotiana glauca* fusion hybrid (denoted NTG-P) were derived from the heterotrophic line of *D. innoxia* initiated by Ranch and Giles (22) and the fusion hybrid T3g1C (9).

The first higher plant tissue culture described as being photoautotrophic, i.e. growing with CO<sub>2</sub> and light as the sole carbon and energy source, respectively, was that of Bergmann (3) who grew *Nicotiana tabacum* suspension cultures. Since that time only about ten different species have been grown photoautotrophically in liquid medium (reviewed by Horn and Widholm [11], Newmann and Bender [20]). That agar or agarose not be present in the medium for strict photoautotrophy was demonstrated by McHale (16) who showed that these substances either could be used themselves or contained impurities to support callus growth in CO<sub>2</sub>-free air with no sugar added.

In general, the photoautotrophic cultures described thus far have much higher dark respiration rates than mature levels and

<sup>1</sup> Supported by funds from the McKnight Interdisciplinary Photosynthesis Research Program, the SOHIO/UI Center of Excellence in Crop Molecular Genetics and Genetic Engineering, and the Illinois Agricultural Experiment Station.

<sup>2</sup> Abbreviations: RuBPCase, ribulose 1,5-bisphosphate carboxylase; MS, Murashige and Skoog (18) basal medium; NAA, naphthaleneacetic acid; PEP, phosphoenolpyruvate; PEPCase, phosphoenolpyruvate carboxylase; RuBP, ribulose 1,5-bisphosphate.

The mixotrophic and photoautotrophic cultures showed light sensitivity since sudden increases in light intensity killed the cells especially during the transition from mixotrophic to photoautotrophic conditions. The flasks with photoautotrophic medium had rubber stoppers which caused less shading than the inverted paper cups of the mixotrophic flasks. This decreased shading led to an increase in incident light of 6 to 7 times as determined by light measurements. Self shading, where the cells in a dense culture reduce the effective irradiance per cell by shading each other, might also be important as indicated by experiments where small inoculation densities resulted in no growth, unless additional shading was imposed. In addition, we found that the COT-PA culture would not grow if the usual inverted paper cup which is normally placed over the top of the culture flask was replaced by a small transparent cap. Despite repeated attempts to adapt the COT-PA cells to unshaded conditions, they would not survive unless a carbon source such as soluble starch was also present.

**Photoautotrophic Growth.** The five newly initiated suspension cultures studied here (COT-PA, APO-P, ACR-P, DAT-P, NTG-P) had been growing for at least 18 months with 6 week subculture intervals. The COT-PA cells were grown under ambient CO<sub>2</sub> conditions in the culture room (about 600–700  $\mu\text{L CO}_2 \text{ l}^{-1}$ ) but the other strains required higher CO<sub>2</sub> levels (5% used normally). The cells were grown in medium lacking sucrose with minimal levels of organic compounds (0.95 mg/L of a vitamin mixture, 1 mg/L NAA, 0.2 mg/L kinetin, 1.2 g/L Hepes, 0.73 mg/L picloram, and 29.2 mg/L EDTA). Even if all of these organic compounds are metabolized by the cells this should not be sufficient to maintain continuous growth. The growth of four of the new strains and that of COT-P (4) which was used as a control, showed that decreasing the usual CO<sub>2</sub> levels decreased growth greatly and that light was absolutely required for growth (Table I). This evidence indicates that these suspensions are indeed photoautotrophic *i.e.* utilize light energy to fix CO<sub>2</sub> for growth.

The growth rates calculated from a series of growth studies give doubling times near 14 d. The COT-P and APO-P cells did have doubling times near 8 d in experiments shown in Table I where a lower than normal quantity of cells was used as inoculum. The cells generally grew in variable sized clumps, usually with fewer than 30 loosely packed cells, with the mean cell size being in the range from 40 to 70  $\mu\text{m}$  in diameter (Fig. 1). The cells have numerous chloroplasts and no clearly different features which would distinguish each cell type at least at the light microscopic level. Figure 1 shows COT-PA, COT-P, APO-P, and DAT-P cells as representative examples.

**Photosynthetic Characteristics.** The five newly developed cultures were studied during two successive culture cycles of either 4 or 6 weeks while growth and the parameters listed below were

Table I. Requirements for CO<sub>2</sub> and Light for Growth of Photoautotrophic Cultures during a 28 d Incubation

Cell Strain	Initial Fresh Weight	Net FW increase		
		Normal <sup>a</sup>	Low CO <sub>2</sub> <sup>b</sup>	Dark <sup>c</sup>
COT-PA	0.16	2.2	0.80	0
COT-P	0.22	2.3	0.88	0
APO-P	0.26	4.4	0	0
DAT-P	0.63	3.0	0.77	0
NTG-P	1.1	3.8	0.50	0

<sup>a</sup> 5% CO<sub>2</sub> blown through flasks except for COT-PA where flask was grown under ambient CO<sub>2</sub> condition with inverted waxed paper cup over the flask top. <sup>b</sup> All grown under ambient CO<sub>2</sub> condition with inverted waxed paper cup sealed with Parafilm over the flask top. <sup>c</sup> All grown under the 'normal' conditions in flasks wrapped in aluminum foil to exclude light.

measured at 2 week intervals. Only representative data from one culture cycle is presented to save space. Data was also collected for the previously characterized COT-P strain (4) as a control for comparative purposes.

The five new strains contained the following levels of Chl listed as the ranges found in different growth experiments and at different times during the culture cycle in  $\mu\text{g Chl g}^{-1}$  fresh weight: COT-PA, 218 to 607; APO-P, 114 to 294; ACR-P, 148 to 231; DAT-P, 101 to 226; and NTG-P, 47 to 237. The level measured in COT-P used as a control, varied from 263 to 639  $\mu\text{g Chl g}^{-1}$  fresh weight which is similar to the values reported previously for this strain (4). These Chl levels are similar to most of the values reported for other photoautotrophic cell lines (reviewed in 11 and 20). The exceptions would be two different soybean strains which now contain near 2000  $\mu\text{g Chl g}^{-1}$  fresh weight (23, 24). These soybean strains gradually increased in Chl content so the strains described here may do likewise.

When CO<sub>2</sub> exchange was measured with an IR gas analyzer under culture medium conditions, all strains showed high dark respiration at time zero and after 4 weeks of growth (Table II). The values ranged from 8.8 to 98.0  $\mu\text{mol CO}_2 \text{ mg}^{-1} \text{ Chl h}^{-1}$ . These values are similar to those generally found with photoautotrophic cultures including COT-P (4), but are higher than that usually found in mature leaves. For example, Kisaki *et al.* (14) showed that the dark respiration rates of mature leaves of greenhouse grown tobacco (*Nicotiana tabacum*) were 8  $\mu\text{mol CO}_2 \text{ mg}^{-1} \text{ Chl h}^{-1}$  or less. Forrester *et al.* (7) reported dark respiration rates for mature soybean leaves from growth chamber plants of no more than 14  $\mu\text{mol CO}_2 \text{ g}^{-1}$  fresh weight  $\text{h}^{-1}$  which would be near 5  $\mu\text{mol CO}_2 \text{ mg}^{-1} \text{ Chl h}^{-1}$  assuming about 3 mg Chl  $\text{g}^{-1}$  fresh weight.

Net CO<sub>2</sub> fixation of from 2.4 to 28.5  $\mu\text{mol CO}_2 \text{ mg}^{-1} \text{ Chl h}^{-1}$  was measured in all strains in light in a 350  $\mu\text{L CO}_2$  and 2% O<sub>2</sub> atmosphere. The CO<sub>2</sub> fixation rate in light decreased greatly in an atmosphere of 21% O<sub>2</sub> and in many cases was negative. Only the COT-PA cells showed net fixation in 21% O<sub>2</sub> at both times shown and this also occurred with these cells at other measurement times as well. Previously the COT-P cells did not show net CO<sub>2</sub> fixation at either 2% or 21% oxygen conditions with the low CO<sub>2</sub> concentration used (4) while soybean cells did show net fixation at most times even with 21% O<sub>2</sub> (23).

The decrease in net CO<sub>2</sub> fixation found with increasing O<sub>2</sub> levels is usually considered to be due to the oxygenase activity of the C<sub>3</sub> fixation enzyme, RuBPcase-oxygenase. The increased oxygen would compete with CO<sub>2</sub> and directly cause less CO<sub>2</sub> fixation and, in addition, stimulate photorespiration through production of phosphoglycolate (21). Photorespiration, in turn, releases CO<sub>2</sub> which would additionally decrease the net CO<sub>2</sub> fixed. Studies with photoautotrophic tobacco cells have shown that increased O<sub>2</sub> concentrations decrease net photosynthesis and growth and that increased CO<sub>2</sub> levels can reverse the inhibition of photosynthesis but not of growth (17). These results are consistent with our data and indicate that photorespiration is occurring in these cells.

When fixation of <sup>14</sup>CO<sub>2</sub> was measured under both dark and light conditions under the culture medium pH of 4.5 (Table III), the dark fixation varied from 1.3 to 13.9  $\mu\text{mol CO}_2 \text{ mg}^{-1} \text{ Chl h}^{-1}$  and light fixation was from 9.0 to 47.8  $\mu\text{mol CO}_2 \text{ mg}^{-1} \text{ Chl h}^{-1}$ . In general, the dark fixation was less than 24% that in light except for the NTG-P strain, where the dark values are from 28 to 33% of the light values. The COT-P values determined here are similar to those of Blair *et al.* (4) when a 5 min incubation time was used.

The RuBPcase activity was low in all strains with the initial activity (that measured before *in vitro* activation with CO<sub>2</sub> and MG<sup>2+</sup>) being from about 6 to 64  $\mu\text{mol CO}_2 \text{ mg}^{-1} \text{ Chl h}^{-1}$  (Table IV). Mature spinach leaves grown in a growth chamber have

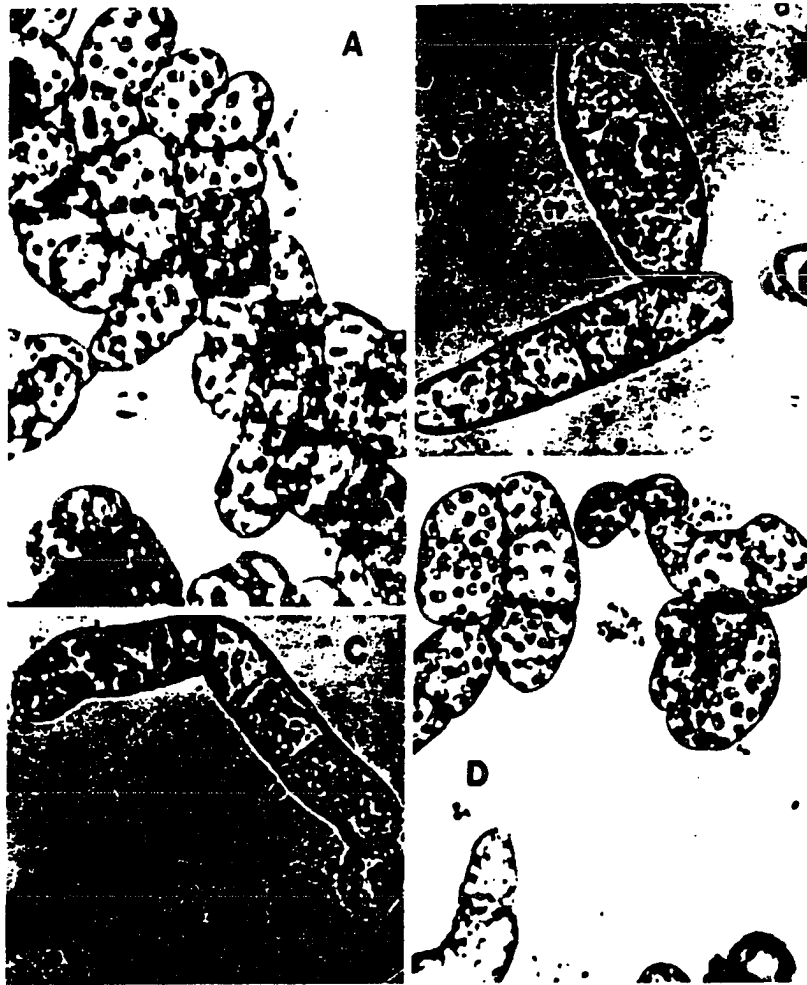


FIG. 1. Phase contrast microscope pictures of A. COT-PA cells 6 weeks after transfer; B. COT-P cells 6 weeks after transfer; C. DAT-P cells 4 weeks after transfer; D. APO-P cells 6 weeks after transfer. The size bar represents  $10^3 \mu\text{m}$ .

total RuBPcase activity of about  $500 \mu\text{mol CO}_2 \text{ mg}^{-1} \text{ Chl h}^{-1}$  with about 86% activation (*i.e.* the initial activity is about 86% of the total). The activation levels in the photoautotrophic cultures described here ranges from 16 to 64%, which is similar to other reports where low activation levels were noted in photoautotrophic cultures.

The PEPcase levels of the photoautotrophic strains ranged from low levels near  $10 \mu\text{mol CO}_2 \text{ mg}^{-1} \text{ Chl h}^{-1}$  for COT-PA, COT-P, and APO-P to near 20 for ACR-P, to 40 for DAT-P and near 80 for NTG-P. These values can be compared to levels near  $80 \mu\text{mol mg}^{-1} \text{ Chl h}^{-1}$  for growth chamber grown spinach leaves and the COT-P cells measured previously (4). The reason for the low PEPcase activity measured in COT-P cells in the present studies is not known. It is possible that the cells might have changed since the previous assays were run (4). This conclusion is supported by recent data obtained with the COT-PA cells and a coupled enzyme assay which gave PEPcase activity levels near  $20 \mu\text{mol CO}_2 \text{ mg}^{-1} \text{ Chl h}^{-1}$  (C Roeske, JM Widholm, unpublished data).

The fluorescence emission spectra of the photoautotrophic cells (SB-P, DAT-P, COT-P, and COT-PA) obtained at room temperature showed a peak at 685 nm (Fig. 2) which has been suggested to originate in the antenna Chl *a* molecules of PSII

(19). At 77 K the fluorescence emission spectra showed three bands near 685 (F685), 695 (F695), and 740 (F740) nm. Both the F685 and F695 nm bands originate in the antenna Chl *a* molecules of PSII, F685 in the so-called CP-43 complex, and F695 in the so-called CP-47, the antenna that feeds energy to the reaction center II complex. F740, that is composed of at least two subbands, originates in the antenna Chl *a* of PSI. The 77 K spectra, shown here, are similar to those found in green algae (8) and chloroplasts of higher plants (6). Our results with the photoautotrophic cells suggest that their antenna systems are similar to those of other green plants. Minor differences in the ratio of F685-F695 of different cell lines may be due to slightly different experimental conditions and/or slightly different ratios of antenna systems within them.

## CONCLUSIONS

The five new photoautotrophic suspension cultures described here have the usual characteristics of photoautotrophic cultures: high dark respiration, low RuBPcase activity, low RuBPcase activation levels, and low Chl levels which would all cause these cultures to have net photosynthesis rates which are relatively low in comparison to mature leaves. The reason for some of these

Table II. Net CO<sub>2</sub> Exchange Rates of Photoautotrophic Suspension Cultures Measured by IR Gas Analysis at Time Zero and After 28 d of Growth

Cell Strain	Time after Transfer	CO <sub>2</sub> Exchange		
		Dark 2% O <sub>2</sub>	Light 2% O <sub>2</sub>	Light 21% O <sub>2</sub>
	<i>d</i>	μmol CO <sub>2</sub> mg <sup>-1</sup> Chl h <sup>-1</sup>		
COT-PA	0	-37.3	+16.6	+1.53
	28	-35.6	+20.4	+4.08
COT-P	0	-16.3	+9.8	0
	28	-48.5	+17.5	-6.62
APO-P	0	-8.8	+7.7	+4.41
	28	-39.9	+7.7	-6.13
ACR-P	0	-16.6	+2.43	0
	28	-33.6	+10.1	+4.02
DAT-P	0	-56.0	+28.5	ND <sup>a</sup>
	28	-78.8	+25.8	+10.1
NTG-P	0	-21.6	+10.0	+2.37
	28	-50.0	+7.8	-6.88

<sup>a</sup> Not determined.

Table III. <sup>14</sup>CO<sub>2</sub> Fixation by Photoautotrophic Suspension Cultures Measured at Time Zero and after 28 d of Growth

Cell Strain	Time after Transfer	<sup>14</sup> CO <sub>2</sub> Fixation		
		Dark 2% O <sub>2</sub>	Light 2% O <sub>2</sub>	Rate dark / Rate light × 100
	<i>d</i>	μmol mg <sup>-1</sup> Chl h <sup>-1</sup>		%
COT-PA	0	3.87	16.1	24
	28	3.90	19.4	20
COT-P	0	4.1	27.9	15
	28	9.1	37.9	24
APO-P	0	1.76	9.0	20
	28	6.1	28.0	22
ACR-P	0	1.29	13.5	10
	28	3.88	38.1	10
DAT-P	0	1.69	27.9	6
	28	5.4	47.8	11
NTG-P	0	8.8	31.6	28
	28	13.9	41.7	33

Table IV. PEPcase and RuBPcase Activities in Photoautotrophic Suspension Cultures at Time Zero and After 28 d of Growth

Cell Strain	Time after Transfer	Enzyme Activity			RuBPcase activation (initial / total) × 100
		PEPcase	RuBPcase (initial)	RuBPcase (total)	
	<i>d</i>	μmol mg <sup>-1</sup> Chl h <sup>-1</sup>			%
COT-PA	0	11.8	36.2	56.4	64
	28	14.3	29.4	51.9	57
COT-P	0	8.4	28.7	49.6	58
	28	9.7	14.3	65.0	22
APO-P	0	12.4	8.7	20.8	42
	28	13.1	33.1	78.9	42
ACR-P	0	20.1	16.7	41.1	41
	28	22.1	50.0	98.9	51
DAT-P	0	37.9	6.2	35.6	17
	28	41.3	25.2	94.1	27
NTG-P	0	78.3	6.4	40.2	16
	28	87.6	64.2	214	30

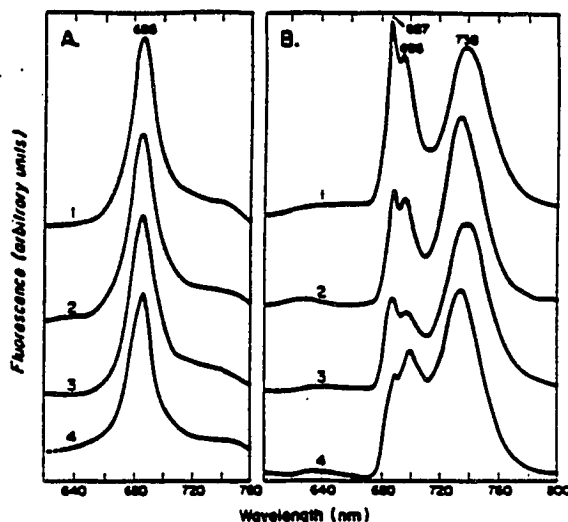


FIG. 2. Fluorescence emission spectra from SB-P (1), DAT-P (2), COT-P (3), and COT-PA (4) cells measured at room temperature (A) and at 77 K (B).

differences may be the continuous cell division in the cell cultures relative to that of the mature leaves (23).

The photoautotrophic cultures initiated from the C<sub>3</sub> species APO-P and ACR-P were not appreciably different from the other photoautotrophic strains from C<sub>3</sub> species. In particular, the PEPcase activities were not higher than the other species studied here, as they would be in the whole plants. No <sup>14</sup>CO<sub>2</sub> fixation product analysis studies were done, however, to determine the CO<sub>2</sub> fixation efficiency of the RuBPcase versus the PEPcase activities *in vivo*. Previous studies usually show that the <sup>14</sup>CO<sub>2</sub> is fixed into the products expected for the proportion of RuBPcase and PEPcase measured *in vitro*.

The unique COT-PA strain which grows on ambient CO<sub>2</sub> levels (about 600–700 μL/L in the culture room) does not have any clearly different characteristics as measured in these studies except for the reproducible ability to show net CO<sub>2</sub> fixation in 21% O<sub>2</sub> (Table II) and a relatively high stable RuBPcase activation level (about 60% as shown in Table IV).

While it is clear that the carbon fixation enzyme makeup of these cells is different from that of mature leaves it appears that the PSII antenna pigment composition is similar to that of leaves of green plants.

These five strains are continuing to grow with repeated sub-culturing for a period of at least 1 year after completion of these studies, so they appear to be capable of continuous growth under these conditions. During this period we have been able to remove the HEPES and all of the vitamins except thiamine from the culture medium and have found that the Chl levels of the COT-P, COT-PA, DAT-P, and NTG-P had remained constant while the APO-P and ACR-P levels had increased to 1700 and 875 μg Chl g<sup>-1</sup> fresh weight, respectively (C Goldstein, JM Widholm, unpublished data).

Further studies are needed to determine if different culture conditions might affect the PEPcase levels of the C<sub>3</sub> species cultures and to determine why the COT-PA and not the other cultures can grow on ambient CO<sub>2</sub> levels.

*Acknowledgments*—We wish to thank Clady Goldstein for some cell samples, and W. L. Ogren for discussion and for facilities for the enzyme assays.

## LITERATURE CITED

1. AOYAGI K, JA BASHAM 1986 Appearance and accumulation of C<sub>2</sub> carbon pathway enzymes in developing wheat leaves. *Plant Physiol* 80: 334-340
2. ARNON DI 1949 Copper enzymes in isolated chloroplasts. Polyphenoloxidase in *Beta vulgaris*. *Plant Physiol* 24: 1-10
3. BERGMANN L 1967 Growth of green suspension cultures of *Nicotiana tabacum* var. "Samson" with CO<sub>2</sub> as carbon source. *Planta* 74: 243-249
4. BLAIR LC, CJ CHASTAIN, JM WIDHOLM 1988 Isolation and characterization of a cotton (*Gossypium hirsutum* L.) photoautotrophic cell suspension culture. *Plant Cell Rep* 7: 266-269
5. BLUBAUGH D 1987 The mechanism of bicarbonate activation of plastoquinone reduction in photosystem II of photosynthesis. PhD thesis, University of Illinois at Urbana-Champaign, Urbana
6. BRIANTAS JM, C VERNOTTE, GH KRAUSE, E WEIS 1986 Chlorophyll *a* fluorescence of higher plant chloroplasts and leaves. In Govindjee, J Amer. DC Fork, eds. *Light Emission by Plants and Bacteria*. Academic Press, Orlando, pp 539-586
7. FORRESTER ML, G KROTKOV, CD NELSON 1966 Effect of oxygen on photosynthesis, photorespiration and respiration in detached leaves. I. Soybean. *Plant Physiol* 41: 422-427
8. GOVINDJEE, K SATOH 1986 Fluorescence properties of chlorophyll *b* and chlorophyll *c* containing algae. In Govindjee, J Amer. DC Fork, eds. *Light Emission by Plants and Bacteria*. Academic Press, Orlando, pp 497-538
9. HORN ME, T KAMEYA, JE BROTHERTON, JM WIDHOLM 1983 The use of amino acid analog resistance and plant regeneration ability to select somatic hybrids between *Nicotiana tabacum* and *N. glauca*. *Mol Gen Genet* 192: 235-240
10. HORN ME, JH SHERRARD, JM WIDHOLM 1983 Photoautotrophic growth of soybean cells in suspension culture. *Plant Physiol* 72: 426-429
11. HORN ME, JM WIDHOLM 1984 Aspects of photosynthetic plant tissue culture. In GB Collins, J Perolina, eds. *Applications of Genetic Engineering to Crop Improvement*. Martinus Nijhoff Dr. W. Junk, Boston, pp 113-161
12. KENNEDY RA 1976 Photorespiration in C<sub>2</sub> and C<sub>3</sub> plant tissue cultures: significance of Kranz anatomy to low photorespiration in C<sub>2</sub> plants. *Plant Physiol* 58: 573-575
13. KENNEDY RA, JE BARNER, WM LASTICH 1977 Photosynthesis in C<sub>2</sub> plant tissue cultures: significance of Kranz anatomy to C<sub>2</sub> acid metabolism in C<sub>2</sub> plants. *Plant Physiol* 59: 600-603
14. KIKAZI T, S HIRABAYASHI, N YANO 1973 Effect of the age of tobacco leaves on photosynthesis and photorespiration. *Plant Cell Physiol* 14: 505-514
15. LASTICH WM, HP KORTCHAK 1972 Chloroplast structure and function in tissue cultures of a C<sub>2</sub> plant. *Plant Physiol* 49: 1021-1023
16. MCHALE NA 1985 Conditions for strict autotrophic culture of tobacco callus. *Plant Physiol* 77: 240-242
17. MCHALE NA, I ZELITCH, RB PETERSON 1987 Effect of CO<sub>2</sub> and O<sub>2</sub> on photosynthesis and growth of autotrophic tobacco callus. *Plant Physiol* 84: 1055-1058
18. MURASHIGE T, F SKOOG 1962 A revised medium for rapid growth and bioassays with tobacco tissue cultures. *Physiol Plant* 15: 473-497
19. MURATA N, K SATOH 1986 Absorption and fluorescence emission by intact cells, chloroplasts, and chlorophyll-protein complexes. In Govindjee, J Amer. DC Fork, eds. *Light Emission by Plants and Bacteria*. Academic Press, Orlando, pp 137-160
20. NEUMANN KEH, L BINDER 1987 Photosynthesis in cell and tissue culture systems. In CE Green, DA Somers, WP Hackert, DD Buehler, eds. *Plant Tissue and Cell Culture*. Alan R. Liss, New York, pp 151-165
21. OGBURN WL 1984 Photorespiration: pathways, regulation, and modification. *Ann Rev Plant Physiol* 35: 415-442
22. RANCHO JP, XL GELB 1980 Factors affecting growth and aggregate dissociation in batch suspension cultures of *Desmodium illinoense* (Miller). *Ann Bot* 46: 667-683
23. ROGERS SMD, WL OGBURN, JM WIDHOLM 1987 Photosynthetic characteristics of a photoautotrophic cell suspension culture of soybean. *Plant Physiol* 84: 1451-1456
24. ROGERS SMD, JM WIDHOLM 1988 Comparison of photosynthetic characteristics of two photoautotrophic cell suspension cultures of soybean. *Plant Sci* 56: 69-74
25. SEDIH S, A GNANAM 1983 Photosynthesis in cell suspension culture of a C<sub>2</sub> plant, *Giantia phanerocoides* L. *Plant Cell Physiol* 24: 1033-1041

Regular paper

## Fluorescence characteristics of photoautotrophic soybean cells

C. Xu,<sup>1</sup> S. M. D. Rogers,<sup>2</sup> C. Goldstein,<sup>2</sup> J. M. Widholm<sup>2</sup> & Govindjee<sup>1,3</sup>

<sup>1</sup>Departments of Physiology and Biophysics and <sup>3</sup>Plant Biology and <sup>2</sup>Department of Agronomy, University of Illinois at Urbana-Champaign, IL 61801, USA

Received 3 June 1988; accepted in revised form 10 October 1988

**Key words:** higher plant photosynthesis, chlorophyll *a* fluorescence, plastoquinone pool, photoautotrophic soybean cell, diuron, atrazine, primary (quinone) electron acceptor,  $Q_B/Q_B^-$ , (soybean, spinach)

### Abstract

We report here the first measurements on chlorophyll (Chl) *a* fluorescence characteristics of photoautotrophic soybean cells (cell lines SB-P and SBI-P). The cell fluorescence is free from severe distortion problems encountered in higher plant leaves. Chl *a* fluorescence spectra at 77 K show, after correction for the spectral sensitivity of the photomultiplier and the emission monochromator, peaks at 688, 696 and 745 nm, representing antenna systems of photosystem II-CP43 and CP47, and photosystem I, respectively. Calculations, based on the complementary area over the Chl *a* fluorescence induction curve, indicated a ratio of 6 of the mobile plastoquinone (including  $Q_B$ ) to the primary stable electron acceptor, the bound plastoquinone  $Q_A$ . A ratio of one between the secondary stable electron acceptor, bound plastoquinone  $Q_B$ , and its reduced form  $Q_B^-$  was obtained by using a double flash technique. Owing to this ratio, the flash number dependence of the Chl *a* fluorescence showed a distinct period of four, implying a close relationship to the 'S' state of the oxygen evolution mechanism. Analysis of the  $Q_A^-$  reoxidation kinetics showed (1) the halftime of each of the major decay components ( $\sim 300 \mu\text{s}$  fast and  $\sim 30 \text{ms}$  slow) increases with the increase of diuron and atrazine concentrations; and (2) the amplitudes of the fast and the slow components change in a complementary fashion, the fast component disappearing at high concentrations of the inhibitors. This implies that the inhibitors used are able to totally displace  $Q_B$ . In intact soybean cells, the relative amplitude of the 30 ms to  $300 \mu\text{s}$  component is higher (40:60) than that in spinach chloroplasts (30:70), implying a larger contribution of the centers with unbound  $Q_B$ . SB-P and SBI-P soybean cells display a slightly different sensitivity of  $Q_A^-$  decay to inhibitors.

**Abbreviations:** CA-complementary area over fluorescence induction curve, Chl-chlorophyll, diuron: DCMU - 3-(3,4-dichlorophenyl)-1,1-dimethylurea,  $F_m$ -maximum chlorophyll *a* fluorescence,  $F_0$ -minimum chlorophyll *a* fluorescence,  $F_v = F_t - F_0$ , where  $F_v$  = variable chlorophyll *a* fluorescence, and  $F_t$  = chlorophyll *a* fluorescence at time *t*. PS II-photosystem II,  $Q_A$ -primary (plastoquinone) electron acceptor of PS II,  $Q_B$ -secondary (plastoquinone) electron acceptor of PS II,  $t_{50}$ -the time at which the concentration of reduced  $Q_A$  is 50% of that at its maximum value

### Introduction

For several decades, Chlorophyll *a* (Chl *a*) fluorescence has been used as an intrinsic indicator of the photosynthetic reactions of isolated chloro-

plasts of green plants. Since Chl *a* fluorescence is in competition with photochemical reactions and other processes in chloroplasts, it has been widely used to monitor variations in photosynthetic activity (see, e.g., Duysens 1986).

Light-induced charge separation initiates the transport of reducing equivalents from the reaction center of photosystem II (PS II) to the plastoquinone (PQ) pool via a specially organized complex of two bound plastoquinones,  $Q_A$  and  $Q_B$ .  $Q_A$  is a one electron acceptor and is tightly bound, whereas  $Q_B$  is a two electron acceptor, and is loosely bound in the  $Q_B$  and  $Q_B^{2-}$  forms (Crofts and Wraight 1983). The Chl *a* fluorescence yield depends upon the redox state of  $Q_A$ , being high when the concentration of  $Q_A^-$  is high (Duysens and Sweers 1963). The size of the PQ pool can be measured by using Chl *a* fluorescence induction, i.e., fluorescence as a function of time of illumination. The area above the fluorescence induction curve (complementary area, CA) is proportional to the number of electrons accumulated in the light by the electron acceptor side of PS II and, therefore, is equivalent to the amount of PQ which has been reduced (Malkin and Kok 1966, Velthuys and Amesz 1974). Thus the measurements of CA, before and after the electron flow inhibition, have allowed estimates of the ratio of PQ pool size to  $Q_A$ . One can also measure, with a weak flash, the changes in the variable Chl *a* fluorescence yield correlated with the concentration of  $Q_A^-$  after a strong saturating flash. From such measurements it is feasible to estimate the kinetics and equilibrium parameters for the reaction of  $Q_A^-$  with  $Q_B$  or  $Q_B^{2-}$  when one or two electrons have accumulated from the reaction center of PS II, and then for the reactions of plastoquinone (PQ) and plastoquinol ( $PQH_2$ ) at the  $Q_B$  binding site (see, e.g., Robinson and Crofts 1983, 1987, Taoka et al. 1983).

Up to now, most efforts have been put into the development of the methodology for Chl *a* fluorescence measurements with isolated chloroplasts from higher plants. Efforts are being made to use fluorescence in the study of photosynthetic phenomena in intact leaves (see Walker 1981, Sivak and Walker 1983, Walker et al. 1983, 1985). For example, state transition, energy transfer during the development of the photosynthetic apparatus, and the effects of physiological and environmental factors have been studied in intact leaves through Chl *a* fluorescence measurements (see, e.g., reviews by Briantais et al. 1986, Renger and Schreiber 1986). However, since intact leaves have higher absorbance and exhibit stronger scattering of

incident light than isolated chloroplasts, their emission spectra are highly distorted due to reabsorption of fluorescence. In addition, kinetics of fluorescence are also distorted due to the light attenuation (Malkin et al. 1981); fluorescence kinetics from the interior cells are slower due to the lower light intensities, and, one measures, therefore, an average kinetics. The complexity of using intact leaves and the lack of direct biochemical data to compare with the results of fluorescence measurements make the interpretation of fluorescence in intact leaves less definitive than in isolated chloroplasts. Furthermore, the relationship of Chl *a* fluorescence to the mechanism by which plastoquinone acceptors work in intact leaves is still unresolved.

Recently, higher plant tissue culture techniques have been increasingly used for research in the areas of plant physiology, genetics and development. Now, rapidly growing photoautotrophic suspension cultures have become available for use in photosynthesis research using intact higher plant cells (Rogers et al. 1987, Xu et al. 1988). Thus Chl *a* fluorescence measurements can be used to study photosynthetic phenomena in higher plants by using suspensions of small cell clumps. Such cells are better suited for Chl *a* fluorescence measurements *in vivo* for higher plants because they can be used in dilute samples and, thus, will be relatively free of distortions encountered in leaf samples. Furthermore, it will be possible to compare their data with those from cyanobacteria, and lower plants such as red and green algae (Fork and Mohanty 1986, Govindjee and Satoh 1986).

In this paper, we present the first systematic Chl *a* fluorescence measurements of photoautotrophic soybean cells. We show that soybean cells possess a similar antenna system as that in chloroplasts of other higher plants. Furthermore, the ratio of the plastoquinone pool (including  $Q_B$ ) to  $Q_A$  is 6 and the ratio between  $Q_B$  and  $Q_B^{2-}$  after dark adaptation is one. Analyses of the kinetics of  $Q_A^-$  reoxidation suggests that the  $Q_B$  binding sites can be totally occupied by the electron transport inhibitors used. The detailed fluorescence study of soybean cells, presented here, suggests that it may be of use for the general application of fluorescence in plant physiology.

## Materials and methods

The intact soybean (*Glycine max* Merr.) cell lines SB-P (*Corsoy*) and SBI-P (PI-437 833) were established by Horn et al. (1983) and Rogers and Widholm (1988), respectively. The cells were cultured in a  $\text{KN}^0$  medium (Rogers et al. 1987), which contained in addition to inorganic salts (Murashige and Skoog 1962), Thiamine-HCl, kinetin and naphthalene acetic acid as the sole organic components (see Rogers and Widholm 1988). The cells were photoautotrophically cultured for 14 days at 28°C in a 5%  $\text{CO}_2$  atmosphere under continuous light of 300  $\mu\text{mol photon m}^{-2} \text{s}^{-1}$ , and were shaken at 130 rpm on a gyratory shaker. The pH of the  $\text{KN}^0$  medium before cell growth was about 5.2 (or 7.0 with 5 mM Hepes buffer), but within 48 h the medium pH dropped to around 4.2, and then rose to 5.0 after 14 days (Horn et al. 1983).

After growth for three weeks under the illumination of a metal-halide lamp for 16 hours every day, the mature soybean (*Corsoy*) leaves were collected from the green house for fluorescence measurement.

The isolation of spinach (*Spinacia oleracea*) chloroplasts were performed as previously described by Eaton-Rye and Govindjee (1988).

Chlorophyll was extracted in 80% acetone (v/v) and its concentration was determined spectrophotometrically using the method of Arnon (1949). The cells were diluted in  $\text{KN}^0$  medium to give a chlorophyll concentration of about 10  $\mu\text{g/ml}$  in the double flash fluorescence experiment, and about 40  $\mu\text{g/ml}$  in the fluorescence transient experiment.

Chlorophyll *a* fluorescence spectra and fluorescence transient measurements were made using a laboratory-built spectrofluorometer. The exciting light was provided by a Kodak 4200 projector with the light filtered by two Corning blue filters (CS 4-71, and CS 5-56). Fluorescence emission was detected, with a slitwidth of 3.3 nm, by a S-20 photomultiplier (EMI 9558B) through a Bausch and Lomb monochromator, protected from the exciting light by a red Corning filter (CS 2-61). Signals were stored and analyzed by Biomation 805 waveform recorder and a LSI-11 computer (see Blubaugh 1987). Other details are in the legend of Fig. 1.

Chlorophyll *a* fluorescence kinetics after single flashes of light were measured by an instrument

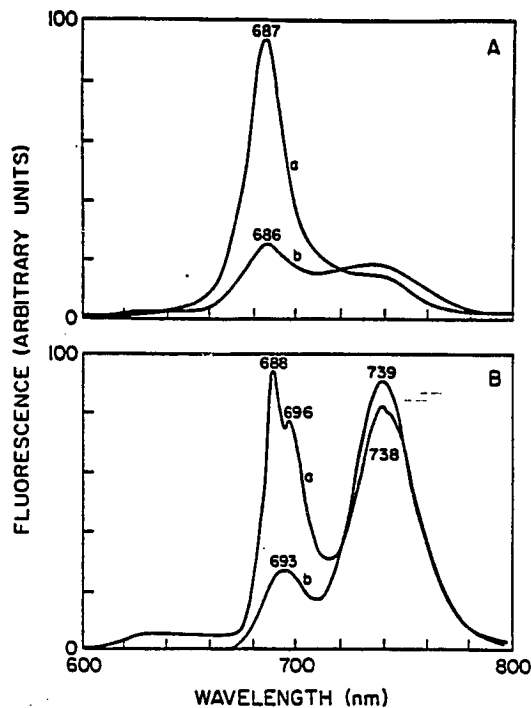


Fig. 1. Fluorescence emission spectra (from 600 to 800 nm) of SB-P cells (subfig. a) and soybean leaves (subfig. b) at (A) room temperature and (B) 77 K. Monochromator, Bausch and Lomb (focal length, 500 nm,  $f/5$ , grating size, 100  $\times$  100 mm, blazed at 750 nm, linear dispersion, 3.3 nm/mm); photomultiplier, S-20, EMI 9558B. Spectra were normalized at 724 nm. Spectra presented here, are not corrected for the spectral response of the monochromator and the photomultiplier. Wavelengths shown on the graph are for the peaks of emission.

described by Eaton-Rye (1987). Fresh soybean cell suspensions were diluted in a dark reaction vessel and dark-adapted at room temperature for 10 min. A flow cuvette was filled from this vat. Because the size of cells is larger than that of thylakoid membrane fragments, the gas pressure in the flow system had to be changed from that used for thylakoids (see Eaton-Rye 1987). The illumination volume of the sample was 0.6 ml. At the end of each measurement, the cuvette was emptied by reversing the pressure. Using a weak measuring flash, the level of Chl *a* fluorescence yield of the soybean cells was measured at 685 nm (10 nm bandwidth) by a EMI 9558A photomultiplier tube. An FX-124 flash lamp (EG and G, 2.5  $\mu\text{s}$  duration at half-maximal peak height) was used as the saturating flash, where the measuring flash (2.5  $\mu\text{s}$  duration, CS 4-96 filter) was provided by the 1539A Stroboslave (General



Radio) flash system. After a series of saturating flashes, the measuring flash could be fired at variable times under computer control. For further details, see Eaton-Rye (1987) and Eaton-Rye and Govindjee (1988).

The concentration of reduced  $Q_A$  was estimated from the above Chl *a* fluorescence data by using the following equation (Joliot and Joliot 1964; see Mathis and Paillotin 1981):

$$\frac{F(t) - F_0}{F_{\max} - F_0} = \frac{(1 - p)q}{1 - pq} \quad (1)$$

where  $F(t)$  is the Chl *a* fluorescence yield at time  $t$ ,  $F_0$  is the fluorescence yield when all  $Q_A$  is in the oxidized state,  $F_{\max}$  is the maximum fluorescence yield when all  $Q_A$  is in the reduced state,  $p$  is the connection parameter or the probability of the intersystem energy transfer and  $q$  is the fraction of the closed reaction centers (i.e.,  $q = 1$ , when  $Q_A^-$  is maximum). Here  $p$  was taken as 0.5 (Joliot and Joliot 1964) for calculations in our paper. Therefore,  $q$  can be represented by the following formula:

$$q = \frac{F(t) - F_0}{(F_{\max} - F_0) - 0.5[F_{\max} - F(t)]} \quad (2)$$

Apparent halftimes of  $[Q_A^-]$  decay, labeled as  $t_{50}$ , are times at which  $[Q_A^-]$  is 50% of maximum  $[Q_A^-]$  (at  $t = 0$ ), whereas all other  $t_i$ s, given together with their amplitudes, are obtained from plots of  $\log$  of  $[Q_A^-]$  as a function of time after evaluation into a fast and a slow component.

## Results and discussion

### Fluorescence spectra

Fluorescence spectroscopy is a powerful means to analyze the components of light harvesting systems as well as the energy transfer between them in higher plants and algae (see, e.g., Briantais et al. 1986, Fork and Mohanty 1986, Govindjee and Satoh 1986). In order to minimize the influence of scattering and reabsorption of fluorescence in clumps of soybean cells, the cell suspension was filtered with cheese cloth to remove all the larger clumps. Figure 1 displays the fluorescence emission spectra of SB-P soybean cells at room temperature (A) and 77 K (B). At room temperature, reabsorp-

tion of fluorescence at 687 nm is dramatically reduced here (curve a) as compared to the soybean leaf (curve b). This is evident from the relatively high ratio (5.5) of fluorescence at 687 nm to that at 740 nm in cell suspensions in comparison to a low ratio (1.7) in leaves. At 77 K, the ratio of fluorescence at 688 nm to that at 740 nm changed from a value of 1.0 in the cell suspension to 0.3 in leaves. Furthermore, the separation of the emission bands at 688 and 696 nm was obliterated in the leaves at the 3.3 nm slitwidths used here. The 688 nm band is reabsorbed more than the 696 nm band. A single band at 693 nm was observed.

The fluorescence emission spectra, shown in Fig. 1, have not been corrected for the spectral sensitivity of the photomultiplier and the monochromator. This fluorescence emission spectrum of the SB-P cells obtained at room temperature has, however, the usual peak at 687 nm (F686), because the instrumental spectral response is almost flat in this region. F686 is universally found in all oxygenic photosynthetic samples (Murata and Satoh 1986); and, it has been suggested to originate in the antenna Chl *a* molecules of PS II. At the lower temperature (77 K), the uncorrected fluorescence emission spectrum of the SB-P cells showed three bands near 688 (F686), 696 (F695) and 739 (F740) nm. Corrections for the instrumental spectral response gave almost the same locations for these three peaks: at 688, 698 and 745 nm. Both F686 and F695 bands originate in the antenna Chl *a* molecules of PS II, the former in the so-called CP-43 (Chl *a*-protein complex of 43 kilodalton mass), and the latter in the so-called CP-47 (Chl *a*-protein complex of 47 kilodalton mass), the antenna complexes that feed energy to the reaction center II complex (Murata and Satoh 1986; for a review on pigment-protein complexes, see Green 1988). It is now generally agreed that F740 at 77 K belongs to photosystem I (PS I) complexes. The emission spectrum obtained for soybean cells is very similar to that found in chloroplasts from higher plants (Govindjee and Yang 1966). In green algae, the F740 band has two maxima at 717 and 725 nm (Cho and Govindjee 1970); soybean cells also show a double band (see Fig. 1B), but the bands are shifted to higher wavelengths, as expected for higher plants. This complex long-wavelength band is at still shorter wavelengths (712–720 nm) in cyanobacteria and red algae (Fork

and Mohanty 1986). The above result with the photoautotrophic soybean cells suggests that its antenna system is similar, as expected, to those of chloroplasts from other higher plants. Similar results have now been found by the authors in other photoautotrophic cell lines from intact tobacco, *Datura* and cotton cells (see Xu et al. 1988).

#### Fluorescence induction

The characteristics of PS II and of the plastoquinone electron acceptors have been studied in higher plants and algae by monitoring Chl *a* fluorescence induction curves (see, e.g., Govindjee and Papageorgiou 1971, Papageorgiou 1975). The initial ('origine') fluorescence (O level) is thought to be emitted from the antenna Chl *a* molecules prior to

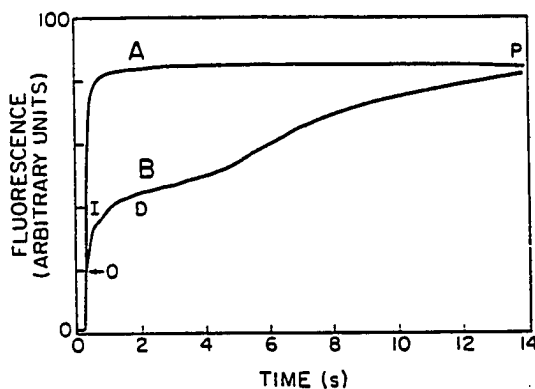


Fig. 2. Chlorophyll *a* fluorescence induction curves of SB-P cells in the presence (A) or absence (B) of 1  $\mu$ M DCMU. 'O' level is the initial level, and 'P' level is the maximal fluorescence level. At 'P' level all  $Q_A$  is reduced and at 'O' level all  $Q_A$  is in the oxidized form. (For I and D, see text.)

Table 1. The ratio between the Chl *a* fluorescence at  $F_{max}$  and  $F_0$  levels, the complementary area, derived from the Chl *a* fluorescence induction curve of the SB-P soybean cells with or without DCMU in Fig. 1, and the approximate half-time for the  $F_0$  to  $F_{max}$  rise

	$\frac{F_{max}}{F_0}$	Complementary area (relative units)	Approximate half-time for $F_0$ to $F_{max}$ rise, ms
-DCMU	5.1	49.3	390
+DCMU (1 $\mu$ M)	4.8	3.8	13

photochemistry and is, thus, independent of photochemical reaction. The true quantum yield of  $F_0$  (fluorescence at the 'O' level) can be measured when the first plastoquinone electron acceptor of PS II,  $Q_A$ , is fully oxidized before the onset of illumination (see, e.g., Govindjee and Papageorgiou 1971, Govindjee and Satoh 1986). The fluorescence rise, following the 'O' level, is generally considered to reflect the reduction of  $Q_A$ . Therefore the rapid transient at 685 nm depends mainly on the rate of the reduction of  $Q_A$  by PS II and the redox state of the PQ pool. At the end of the rapid transient (OIDP, where 'I' stands for an intermediate peak, D, a plateau and P, a peak), the fluorescence intensity reaches the maximum ( $F_{max}$ ). Figure 2 (curve B) shows the Chl *a* fluorescence induction curve of SB-P soybean cells which had been dark-adapted for five minutes before the measurement. The ratio between the fluorescence of the 'P' ( $F_{max}$ ) and the 'O' level ( $F_0$ ) is 4.4, which is quite close to the value reported in spinach chloroplasts and some algal cells (see, e.g., Yamagishi et al. 1978, Briantais et al. 1986). In some experiments with soybean cells, we were able to even reach a value of 5.0 for the ratio of 'P' to the 'O' level (Table 1). At the light intensity used, the approximate half time for the O-P rise is about 390 ms in the absence of any herbicide and 13 ms in the presence of 1  $\mu$ M diuron (DCMU, 3-(3,4)-dichloro-1,1-dimethyl urea; curve A; see Table 1). Diuron accelerates the Chl *a* fluorescence rise by occupying the  $Q_B$  binding site and, thus, preventing the reoxidation of  $Q_A^-$  (see, e.g., Velthuys 1981).

The complementary area above the fluorescence transient curve is proportional to the number of electrons accumulated on the electron acceptor side of PS II (Malkin and Kok 1966, Velthuys and Amesz 1974). In the absence of any inhibitor, it is proportional to the number of electron equivalents on the plastoquinone (PQ) pool,  $Q_A$  and  $Q_B$ , which have been reduced during illumination. However, in the presence of saturating concentration of diuron, the area is solely proportional to the number of electron equivalents on  $Q_A$ . In our experiment, the ratio of the complementary area without and with 1  $\mu$ M diuron is about 13. Since PQ accumulates two electrons to be reduced to plastoquinol, this shows that the ratio of the plastoquinone pool (including  $Q_B$ ) to  $Q_A$  is 6 in SB-P soybean cells. This value is of the same order of magnitude as reported

for isolated spinach chloroplasts (Malkin and Kok 1966, Robinson and Crofts 1983).

As noted earlier, the pH of the growth medium (pH 7.0) decreased rapidly to near 4.2 and gradually rose to near 5.0 by day 14 after inoculation. In order to correlate the photosystem II activity of the cell with the medium pH, the Chl *a* fluorescence transient was measured in different pH media. The cell suspensions were incubated in different pHs for, at least, 10 minutes before measurement. Varying the pH from 4.0 to 8.0 led to no significant changes in the kinetic characteristic of the fluorescence induction curve and in the intensities of fluorescence levels at 'O' and at 'P' (data not shown). The insensitivity of fluorescence of soybean cells to the medium pH may indicate that the chloroplast pH remains unchanged, since strong effects of pH have been reported on the 'P' level fluorescence of the oxygen evolving PS II enriched preparations (see Hodges and Barber 1986).

#### *Decay of Chl a fluorescence yield or $[Q_A^-]$ after light flash 1 or 2*

Using a double flash technique for Chl *a* fluorescence measurement, the kinetics of  $Q_A^-$  oxidation by  $Q_B$  and  $Q_B^-$  have been measured and the equilibrium binding constant for plastoquinone at  $Q_B$  site has been estimated in chloroplasts (see, e.g., Robinson and Crofts 1983, Taoka et al. 1983). Figure 3 shows the decay of chlorophyll *a* fluorescence yield measured by this technique in soybean cells and the effect of 1  $\mu$ M DCMU (diuron) on it; 10  $\mu$ M atrazine had a similar influence. A fluorescence rise component (in 250  $\mu$ s range) is explained to be due to a slow re-reduction of P-680<sup>+</sup> on the donor side of PS II, as already suggested for isolated chloroplasts (Robinson and Crofts 1987). The quencher P680<sup>+</sup> is reduced to P680 by the electron donor Z (see Butler 1973, for the idea that P680<sup>+</sup> is a quencher of Chl *a* fluorescence and Jursinic and Govindjee 1977, for the electron donation by Z in the  $\mu$ s range). The Chl *a* fluorescence decay in the micro- to millisecond range represents electron flow from the reduced  $Q_A$ ,  $Q_A^-$ , to  $Q_B$ ; diuron, however, blocks the decay by competing with plastoquinone and plastoquinol for the  $Q_B$  binding side (Velthuys 1981).

In isolated chloroplasts, the decay of  $Q_A^-$  to  $Q_A$  is

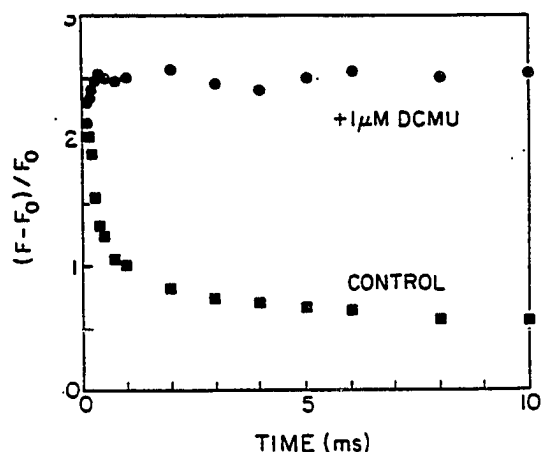


Fig. 3. The effect of electron transport inhibitor (DCMU) on the decay of Chl *a* fluorescence yield after the first actinic flash in SB-P cells. ■ and ● were without or with 1  $\mu$ M DCMU. *F* is for fluorescence yield at time *t* after the flash and *F*<sub>0</sub> is the fluorescence yield before the actinic flash, i.e., when  $[Q_A]$  is maximum.

faster after the first flash than after the second flash, because the electron transfer from  $Q_A^-$  to  $Q_B$  is faster than to  $Q_B^-$  and there is a preponderance of  $Q_B$  in dark adapted chloroplasts (see, e.g., Wollman 1978, Robinson and Crofts, 1983). In intact soybean cells, the time course of Chl *a* fluorescence emission after the first or the second flash was virtually identical, implying a ratio of one between  $Q_B$  and  $Q_B^-$  in dark-adapted cells (Fig. 4A). This is consistent with the result in spinach leaves, obtained by the thermoluminescence method (Rutherford et al. 1984). After the first flash, the initial 50%  $Q_B$  is reduced to 50%  $Q_B^-$  form and the initial 50%  $Q_B^-$  becomes 50%  $Q_B^{2-}$ , which then exchanges with the plastoquinone (PQ) pool to become 50%  $Q_B$ . Thus, the ratio of  $Q_B$  to  $Q_B^-$  is maintained as one, and the kinetics of Chl *a* fluorescence decay after the second flash is the same as after the first flash. A replot of Chl *a* fluorescence change on a log scale, as a function of time, shows two decaying components, a fast and a slow one (see Fig. 4B): both components have about the same kinetics and are of about the same magnitude after flash 1 and 2. This confirms the conclusion made above that  $[Q_B] = [Q_B^-]$  in dark-adapted cells.

Using equations (1) and (2), Chl *a* fluorescence yield was converted into the relative concentration of reduced  $Q_A$ . In SB-P and SBI-P soybean cells,

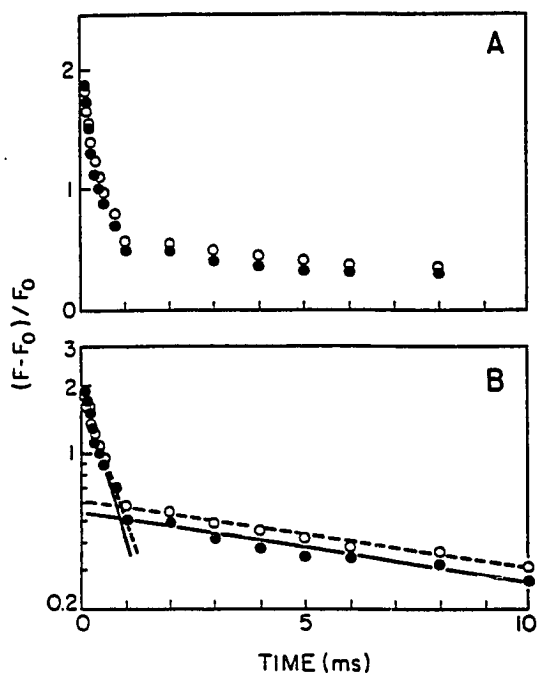


Fig. 4. (A) Decay of variable Chl *a* fluorescence  $[(F - F_0)/F_0]$  after first ( $\bullet$ ) and second ( $\circ$ ) actinic flashes, spaced 1 second apart, in SB-P cells. (B) same data, plotted on a semilogarithmic scale.  $F_0$  is the fluorescence yield taken with the measuring light when  $Q_A$  is oxidized and  $F(F(t))$  in equations (1) and (2) is the fluorescence yield after the actinic flash. From these data, a fast and a slow component can be separated. The amplitudes and the half-times of these components can be obtained from the intersections of the best-fit lines with the ordinate.

the  $F_{max}$  is often lower than that in isolated spinach thylakoid fragments. As mentioned under Methods, the value of  $p$ , the connection parameter, was taken as 0.5. Figure 5A shows the relative concentration of reduced  $Q_A$ ,  $[Q_A^-]/[Q_{total}]$  (equivalent to  $q$  in equations 1 and 2) as a function of time, whereas Fig. 5B shows a log plot of  $[Q_A^-]/[Q_{total}]$  as a function of time. Two distinct components (fast and slow) were clearly observed in this semi-logarithmic plot. In Fig. 5B, line 1 mainly represents the decay of the slow component, line 2 displays effects of both the fast and the slow components. By subtracting line 1 from line 2, line 3, indicating the decay of the fast component, is obtained. Both the amplitude and the half times of decay for each component can be extracted from this plot.

Figure 6 shows the plot for  $t_{50}$ , the time at which

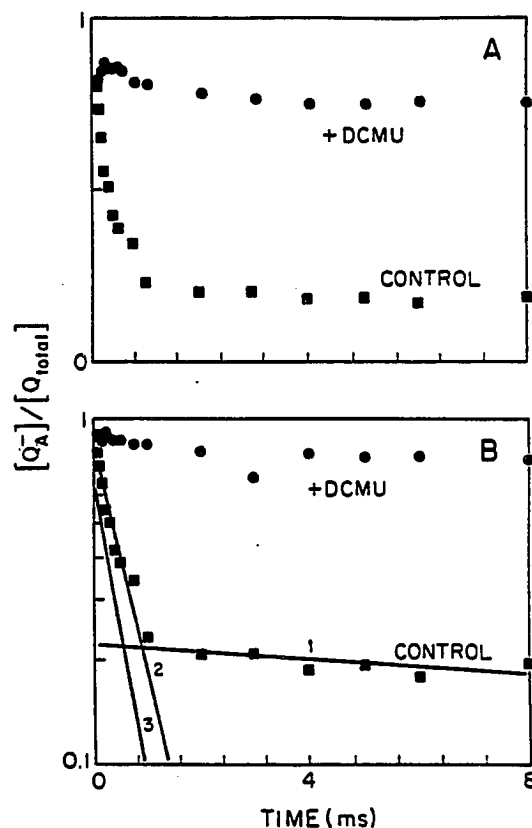


Fig. 5. (A) normal and (B) semi-logarithmic plots of the decay of  $q (= [Q_A^-]/[Q_{total}])$  after a single actinic flash from Chl *a* fluorescence decays in SB-P cells.  $\blacksquare$ , obtained in the absence of DCMU, while,  $\bullet$  was in the presence of  $0.8 \mu\text{M}$  DCMU. For details of curves 1, 2 and 3, see text.

$[Q_A^-]$  is 50% of that at time zero, against the concentrations of diuron (DCMU) and atrazine in soybean cells. Since the inhibitory effect of diuron is stronger than that of atrazine at the same concentration, the curve in Fig. 6A shows a shift to the lower side of the concentration range. Thus the midpoint of the  $t_{50}$  value in the presence of atrazine is at a much higher concentration than that in the presence of diuron.

Both the amplitudes and the half-times of the slow and the fast components of  $[Q_A^-]$  decay were obtained as shown in Fig. 5(B). From the semi-logarithmic plot, two different exponential decaying components are separated, the two best fit straight lines drawn, the half-times of the decaying components calculated and the amplitudes of the

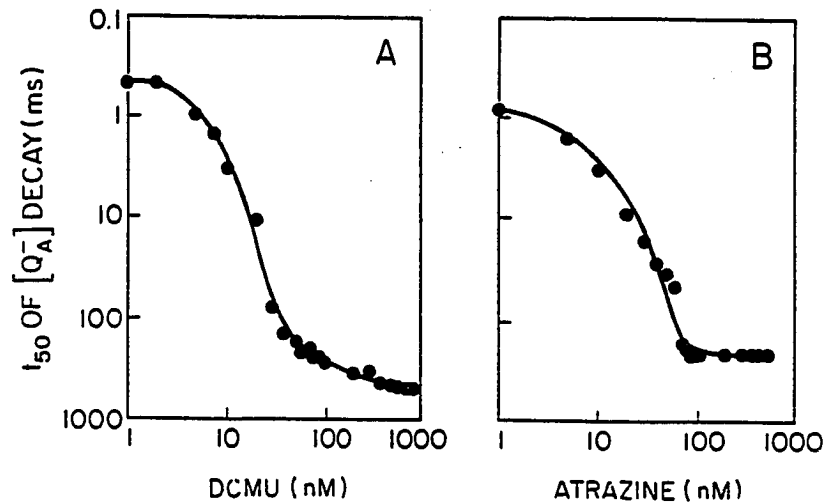


Fig. 6. Plots of  $t_{50}$ , i.e., time at which  $[Q_A^-]$  is 50% of that at  $F_{max}$ , versus concentration of (A) DCMU and (B) atrazine in SB-P cells.

different components obtained from the intersections of the two decay components on the ordinate. The amplitudes of both the fast and the slow decay components of  $[Q_A^-]$  as a function of [DCMU] and [atrazine] are plotted, respectively, in the left or right panels of Fig. 7. Results obtained with the cells (curves A–D) can be compared with those on isolated chloroplasts (curves E and F). The oxidation of  $Q_A^-$ , after one flash, is biphasic and it has been suggested (see Robinson and Crofts 1983) that the amplitude of the fast component is related to centers that have  $Q_B$  bound before the actinic flash, whereas, the slow component represents a second order process involving the binding of  $Q_B$  from the PQ pool. Electron transport inhibitors such as DCMU or atrazine induce an enhancement of Chl *a* fluorescence since they displace  $Q_B$  from its binding site and shift the equilibrium of the reaction  $Q_A^- + Q_B \rightleftharpoons Q_B^- + Q_A$  to the left (Velthuys 1981). We expect that an increase in the concentration of these inhibitors would decrease the amount of  $Q_B$  bound, and thus the amplitude of the fast component is expected to decrease. Indeed, we found the amplitude to decrease from a value of 70% to near zero (see Fig. 7). If the above expectation is correct, the results of Fig. 7 would imply that diuron and atrazine can totally displace  $Q_B$ . It appears from the data on halftimes of the decay of fast (Fig. 8) and slow (Fig. 9) components that high concentrations of inhibitors cause a slowing down

of both the components. We interpret these results to mean that the electron flow inhibitors induce the decrease of  $Q_B$  binding as well as the decrease of the exchange of PQ pool at the  $Q_B$  binding site.

A further comparison between the intact soybean cells and spinach chloroplasts was made from the data listed in Table 2. The halftime of the fast component is approximately 300  $\mu$ s and that of the slow component is approximately 30 ms. In spinach chloroplasts, the percent of the amplitude of the slow component usually is near 30. This value is almost the same as reported elsewhere (Eaton-Rye and Govindjee 1988). In intact soybean cells, the percent of the amplitude of the slow component, however, reaches 40, implying that the contribution of the centers with unbound  $Q_B$  is larger in these cells than in the spinach chloroplasts. As for the physiological meaning, it deserves further study. Although inhibitors increase the halftimes of both components, atrazine is less effective than diuron in the same concentration range. 0.5  $\mu$ M DCMU is much more effective at increasing the halftime of both components in spinach chloroplasts than in SB-P and SBI-P cells, but atrazine does not show a significant difference between each system. Data in Table 2 also show differences in the responses to the electron transport inhibitors between these two soybean cell lines. At a certain concentration (0.5  $\mu$ M DCMU or 5  $\mu$ M atrazine), each inhibitor produces a larger increase in the

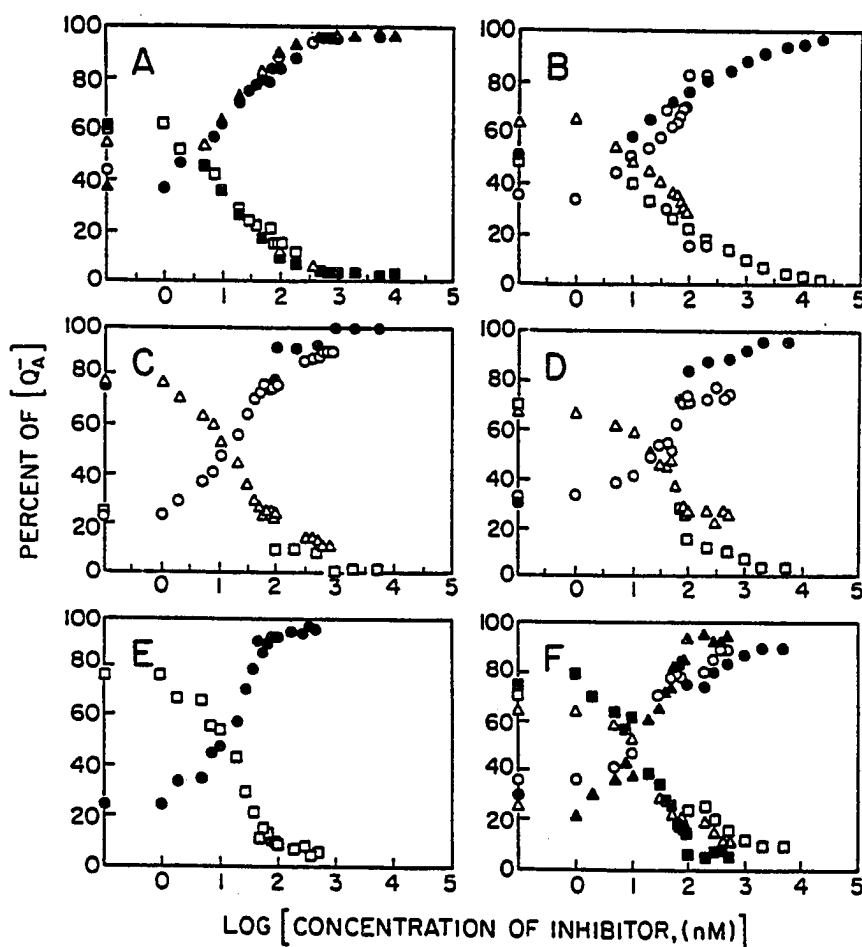


Fig. 7. The inhibitor concentration dependence of the amplitude of the fast and slow  $[Q_A^-]$  decay components in SB-P (A, B) and SBI-P (C, D) cells, and in spinach chloroplasts (E, F). Left panels: DCMU; right panels: atrazine. Symbols at the ordinate are control values. Different symbols represent different experiments. ●, ○ and ▲ represent data for the slow component, and ■, □ and △ for the fast component.

half-times of both the components of  $Q_A^-$  decay in SB-P cells than in SBI-P cells. Thus, this method may be successfully used in selecting herbicide resistance and other mutation among the various cell lines.

#### *Oscillations in flash dependence of Chl a fluorescence*

Delsome (1971) discovered a period-of-four oscillation in Chl *a* fluorescence emission in the green alga *Chlorella* and spinach chloroplasts, with maxi-

ma at flash 1, 5 and 9, and minima at flash 3, 7 and 11. By comparing the fluorescence yield with the sum of the concentrations of  $S_2$  and  $S_3$  states, calculated from oxygen evolution in spinach chloroplasts, he ascribed this oscillation to the cycling of these states associated with the water oxidation process. The reduction of  $Z^+$  ( $Z$  being the electron donor to  $P680^+$ ) by different S-states proceeds at different rates and different equilibria are involved (Babcock et al. 1976). In turn, this affects the re-reduction rate of  $P680^+$  by  $Z$  after an actinic flash and the associated equilibria between these two species (Robinson and Crofts 1987). The resulting

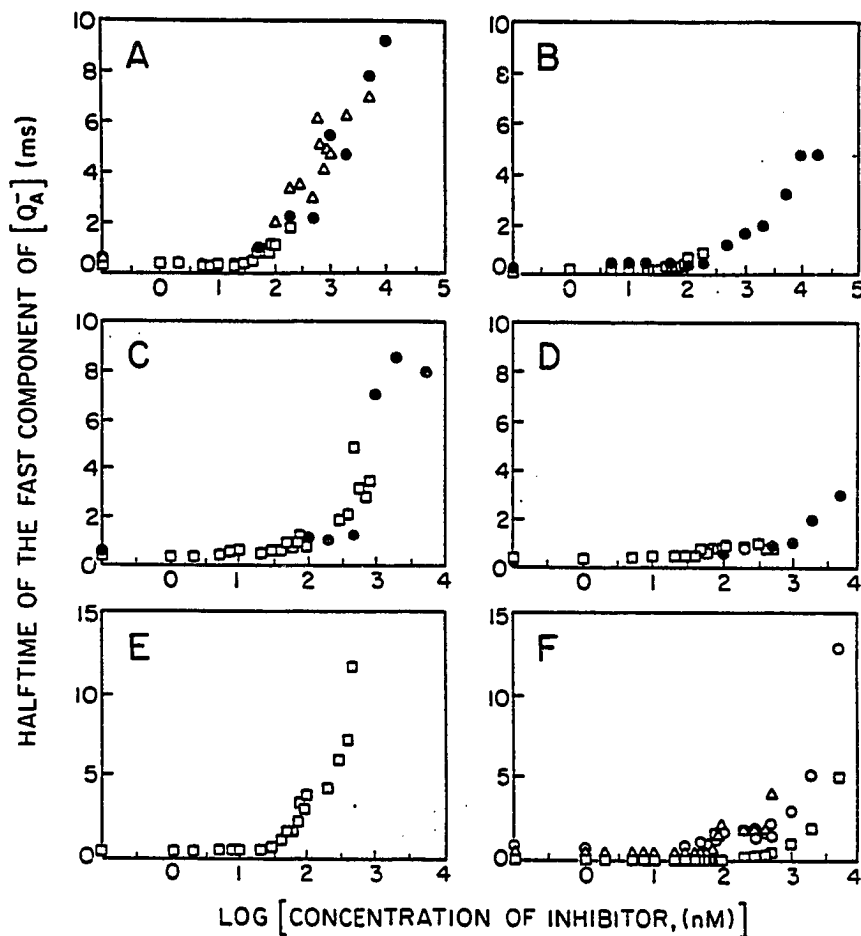


Fig. 8. The inhibitor concentration dependence of the half time of the fast  $[Q_A^-]$  decay component in SB-P cells (A, B), SBI-P cells (C, D) and spinach chloroplasts (E, F) obtained in the presence of DCMU (left panels) and atrazine (right panels). Symbols at the ordinate are control values. Different symbols represent different normalized experiments.

changes in the  $P680^+$  population produce the period-of-four oscillation (see Sonneveld et al. 1979). Maxima are at flashes 1 and 5 because electron donation to  $P680^+$  is fastest and most efficient when the system starts in the  $S_1$  state (see, e.g., Witt et al. 1986). Superimposed upon this oscillation, and seen at  $70 \mu s$  after the actinic flash, is a binary oscillation arising from the differential rates of  $Q_A^-$  oxidation by either  $Q_B$  after an odd number or  $Q_B^-$  after an even number of flashes (Robinson and Crofts 1983).

Since in intact soybean cells, the ratio of  $Q_B$  to  $Q_B^-$  is one (see Fig. 4), the influence of the binary oscillation is absent; therefore, the period-of-four

oscillation pattern predominates (Fig. 10A). This is most clearly observed in fluorescence  $70 \mu s$  after the flash. With increasing time ( $> 500 \mu s$ ) after the flash (Fig. 10A) and after the addition of DCMU ( $0.8 \mu M$ ) (Fig. 10B), this oscillation disappears and a drastically altered flash pattern is observed. At increasing times ( $> 500 \mu s$ ) after the flash, the influence of the donation of electrons by S-states is over; thus, a clear oscillation cannot be distinguished. Since the inhibitors, such as DCMU, inhibit PS II photoreaction by competing with the plastoquinone at the secondary quinone electron acceptor ( $Q_B$ ) site, the oscillation is abolished as the system is blocked in the  $S_2 Q_A^-$  state, and is indepen-

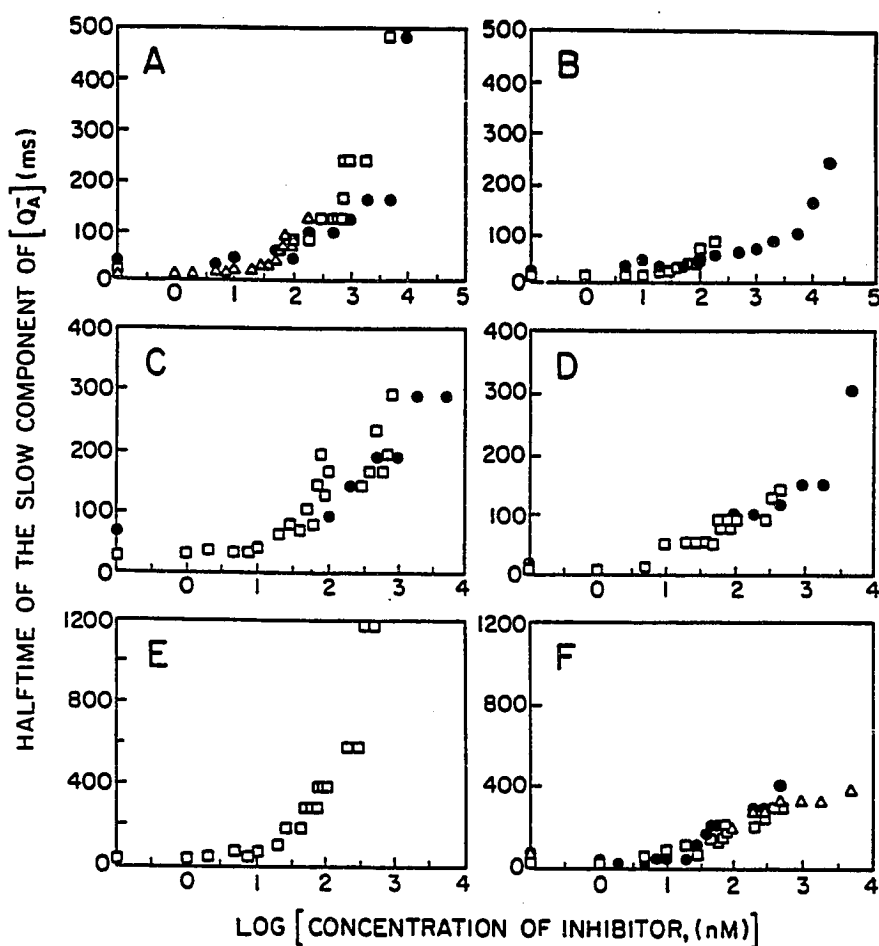


Fig. 9. The inhibitor concentration dependence of the half time of the slow  $[Q_A^-]$  decay components in SB-P cells (A, B), SBI-P (C, D) and in spinach chloroplasts (E, F). Left panels: DCMU; right panels: atrazine. Symbols at the ordinate are control values. Different symbols represent different normalized experiments.

Table 2. The amplitude ( $\alpha$ ) and the half-time ( $\tau$ ) of the fast (f) and slow (s)  $Q_A^-$  decay components, after the first flash, in SB-P and SBI-P cells (pH 5.5) and in spinach chloroplasts (pH 7.8)\*

	SB-P cells				SBI-P cells				Spinach chloroplasts			
	$\alpha_f$ %	$\alpha_s$ %	$\tau_f$	$\tau_s$	$\alpha_f$ %	$\alpha_s$ %	$\tau_f$	$\tau_s$	$\alpha_f$ %	$\alpha_s$ %	$\tau_f$	$\tau_s$
Control	60 ± 10	40 ± 10	297 ± 24 $\mu$ s	34 ± 9 ms	59 ± 2	41 ± 2	286 ± 10 $\mu$ s	23 ± 4 ms	73 ± 3	27 ± 3	368 ± 55 $\mu$ s	33 ± 5 ms
+ 0.5 $\mu$ M DCMU	6 ± 4	94 ± 4	2 ± 1 ms	199 ± 29 ms	5 ± 1	95 ± 1	2 ± 1 ms	108 ± 9 ms	5	95	12 ms	1200 ms
+ 5 $\mu$ M Atrazine	14 ± 8	86 ± 8	5 ± 3 ms	195 ± 32 ms	5	95	3 ms	96 ms	8 ± 1	92 ± 1	3 ± 1 ms	264 ± 74 ms

\* All values presented here should be rounded to the nearest whole number.



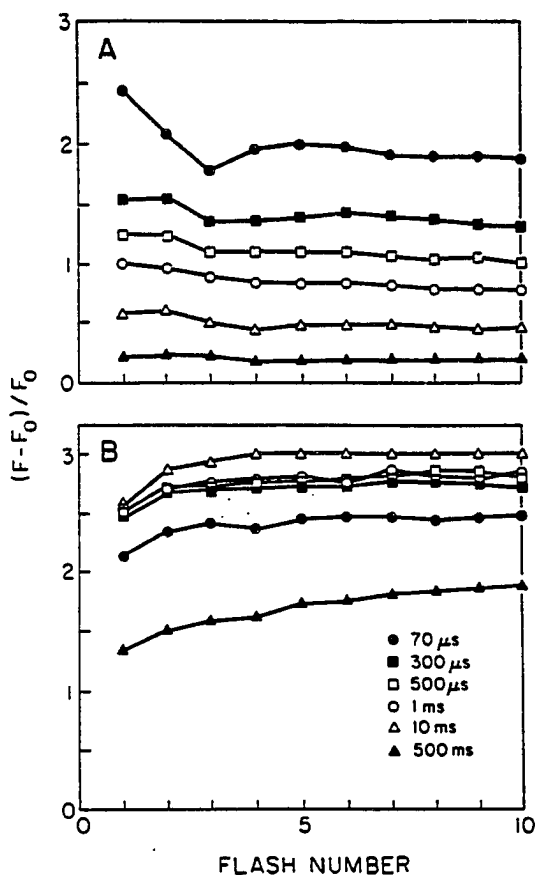


Fig. 10. Chlorophyll *a* fluorescence,  $(F - F_0)/F_0$ , measured at different times after an actinic flash as a function of flash number. The times indicated inside B are when the measuring flash was fired. A and B represent results with control and with  $0.8 \mu\text{M}$  DCMU treated SB-P cells.

dent of the flash number. In soybean cells, the Chl *a* fluorescence intensity at  $70 \mu\text{s}$  after the first flash is higher than that after the second flash. This is different from that in isolated spinach chloroplasts, indicating a somewhat higher percentage of  $Q_B^-$  existing in the intact soybean cells than in the isolated chloroplasts. We have already indicated on the basis of almost similar decay of  $Q_A^-$  after flash 1 and 2, that  $Q_B:Q_B^-$  ratio is 1.0 in soybean cells as opposed to 0.7:0.3 in isolated spinach chloroplasts (Wollman 1978). At early times ( $70 \mu\text{s}$ ), the decrease of the reoxidation rate of  $Q_A^-$  enhances the fluorescence intensity after the first flash. It appears that the minimum is after the third flash from  $70 \mu\text{s}$  to  $500 \mu\text{s}$  after the actinic flash, and after 1 ms, this

minimum shifts to flash 4. Detailed analysis of this data requires further study.

### Concluding remarks

During the past decade, interest has been growing in the practical application of Chl *a* fluorescence measurements as a rapid, sensitive, and nondestructive method for the determination of photosynthetic activity in higher plants. But in the practical use of Chl *a* fluorescence, many real problems have hampered the growth of this study (Briantais et al. 1986, Renger and Schreiber 1986). A photoautotrophic higher plant cell suspension is an easily manipulated system, not only for studying physiological and biochemical aspects of photosynthesis but also for studying the primary process of photosynthesis. Such cell lines have only been recently established (Rogers et al. 1987, Xu et al. 1988). Since problems such as reabsorption of fluorescence can be much more easily minimized in cells than in leaves (see Fig. 1), these cells can be used as reliable models for investigations on higher plant leaves.

We have shown here measurements on the fluorescence spectra of soybean cells (cell lines SB-P and SBI-P) at room temperature and 77 K; we found that these intact higher plant cells have identical antenna system as that of chloroplasts from other higher plants. Here, the long wavelength fluorescence band occurs at approximately 740 nm ( $F_{740}$ ). However, this band is shifted to about 725 nm in green algae and to still shorter wavelengths (e.g., 712–718 nm) in red and blue-green algae (Govindjee and Satoh 1986, Fork and Mohanty 1986). From the fluorescence induction curves, a ratio of the PQ pool (including  $Q_B$ ) to  $Q_A$  was calculated to be 6 (Fig. 2; Table 1). By using the double flash technique of Chl *a* fluorescence measurement, the decay kinetics after the first flash was found to be identical to that after the second flash, suggesting that the ratio of  $Q_B$  to  $Q_B^-$  is 1 (Fig. 4). The flash-dependence pattern also confirms this relation, indicating a higher relative concentration of bound  $Q_B^-$  in physiological conditions than in isolated thylakoids (Fig. 10).

Using equations (1) and (2), the concentration of  $Q_A^-$  was evaluated and then its decay. The decay of  $Q_A^-$  can be divided into two components (generally

represented in the  $\mu$ s and the ms time range, Fig. 5). The half times of these components in soybean cells were found to be similar to those in spinach chloroplasts in the range of 300  $\mu$ s or 30 ms. The relative proportion of the fast and slow component was approximately 60 to 40 in cells as opposed to 70 to 30 in chloroplasts, but the reason for these differences need to be studied further.

It is well known that the mechanism of diuron and atrazine action is to displace  $Q_B$  at its binding site. We show here that they not only influence the fast decay components of  $Q_A^-$  reoxidation but also the slow components. This implies that they affect not only the electron flow from  $Q_A^-$  to  $Q_B$ , but also the exchange between  $Q_B$  and the PQ pool (Table 2). Since the fast component, that is believed to be due to the bound  $Q_B$ , was totally replaced by the slow component upon inhibitor treatment (Fig. 7), we suggest that the inhibitors can fully replace  $Q_B$  at the  $Q_B$  binding site.

In this paper we have found that the two different lines of soybean cells display rather different sensitivities to the inhibitors. Although inhibitors used (DCMU and atrazine) replace  $Q_B$  at its binding site, the increases of the halftime of both components are not the same in different cell lines (Table 2). Thus, this method can be used as a means to screen inhibitor resistance cell lines.

Since the physiological condition of the intact (soybean) cells is different from that of the isolated (spinach) thylakoids, the diffusion of inhibitors across the membrane is expected to be different. In the plots showing the inhibitor concentration dependence of  $t_{50}$  of  $Q_A^-$  in intact cells (Fig. 6), the range covering the change in decay time over inhibitor concentration is broader than that obtained from chloroplasts (data not shown). The concentration of electron transfer inhibitors (such as DCMU and atrazine) needed to give the same effect is higher for cells than that observed for isolated chloroplasts (data not shown) simply because the data are plotted in terms of the concentration of the inhibitors in the outside medium, and that their actual concentration in the chloroplast *in vivo* may be smaller than that in isolated chloroplasts. Such problems deserve further study.

## Acknowledgements

We are grateful to Drs J. J. Eaton-Rye and D. J. Blubaugh for their help. This work was supported by the funds from the McKnight Interdisciplinary Photosynthesis Research Program.

## References

- Arnon D I (1949) Copper enzyme in isolated chloroplasts. Polyphenoloxidase in *Beta vulgaris*. *Plant Physiol* 24: 1-15
- Babcock G T, Blankenship R E and Sauer K (1976) Reaction kinetics for positive charge accumulation on the water side of chloroplast Photosystem II. *FEBS Lett* 61: 286-289
- Blubaugh D J (1987) The mechanism of bicarbonate activation of plastoquinone reduction in Photosystem II of photosynthesis. PhD Thesis, Biology, University of Illinois at Urbana-Champaign
- Briantais J, Vernotte C, Krause G H and Weis E (1986) Chlorophyll *a* fluorescence of higher plants: chloroplasts and leaves. In Govindjee, Ames J and Fork D C (eds) *Light Emission by Plants and Bacteria*, pp 539-583. Orlando: Academic Press
- Butler W L (1972) Primary photochemistry of Photosystem II of photosynthesis. *Accnts Chem Res* 6: 177-184
- Crofts A R and Wraight C A (1983) The electrochemical domain of photosynthesis. *Biochim Biophys Acta* 726: 149-185
- Delosme R (1971) New results about chlorophyll fluorescence 'in vivo'. In Forti G, Avron M and Melandri A (eds) *2nd Int Congr Photosynthesis Res*, pp 187-195. The Hague: Dr W Junk Publishers
- Duysens L N M (1986) Introduction to (bacterio) chlorophyll emission: a historical perspective. In Govindjee, Ames J and Ford D C (eds) *Light Emission by Plants and Bacteria*, pp 4-28. Orlando: Academic Press
- Duysens L N M and Sweers H E (1963) Mechanism of two photochemical reactions in algae as studied by means of fluorescence. In Japanese Society of Plant Physiologists (eds) *Studies of Microalgae and Photosynthetic Bacteria*, pp 353-372. Tokyo: University of Tokyo Press
- Eaton-Rye J J (1987) Bicarbonate reversible anionic inhibition of the quinone reductase in Photosystem II. PhD Thesis, Biology, University of Illinois at Urbana-Champaign
- Eaton-Rye J J and Govindjee (1988) Electron transfer through the quinone acceptor complex of Photosystem II in bicarbonate depleted spinach thylakoid membranes as a function of actinic flash number and frequency. *Biochim Biophys Acta*, 935: 237-247
- Fork D C and Mohanty P (1986) Fluorescence and other characteristics of bluegreen algae (cyanobacteria), red algae, and cryptomonads. In Govindjee, Ames J and Fork D C (eds) *Light Emission by Plants and Bacteria*, pp 451-496. Orlando: Academic Press

- Govindjee and Papageorgiou G C (1971) Chlorophyll fluorescence and photosynthesis: fluorescence transient. In Giese A C (ed) *Photophysiology* 6: 1-46. New York: Academic Press
- Govindjee and Satoh K (1986) Fluorescence properties of chlorophyll *b* and chlorophyll *c*-containing algae. In Govindjee, Amesz J and Fork D C (eds) *Light Emission by Plants and Bacteria*, pp 497-538. Orlando: Academic Press
- Green B (1988) The chlorophyll-protein complexes of higher plant photosynthetic membranes or just what green band is that? *Photosynthesis Research* 15: 3-32
- Hodges M and Barber J (1986) Analysis of chlorophyll fluorescence induction kinetics exhibited by DCMU-inhibited thylakoids and the origin of alpha and beta centers. *Biochim Biophys Acta* 828: 239-246
- Horn M E, Sherrard J H and Widholm J M (1983) Photoautotrophic growth of soybean cells in suspension culture. *Plant Physiol* 72: 426-429
- Joliot A and Joliot P (1964) Étude cinétique de la réaction photochimique libérant l'oxygène au cours de la photosynthèse. *CR Acad Sc Paris* 258: 4622-4625
- Jursinic P and Govindjee (1977) The rise in chlorophyll *a* fluorescence yield and decay in delayed light emission in tris-washed chloroplasts in the 6-100  $\mu$ s time range after an excitation flash. *Biochim Biophys Acta* 461: 253-267
- Malkin S and Kok B (1966) Fluorescence induction studies in isolated chloroplasts. I. Number of components involved in the reaction and quantum yield. *Biochim Biophys Acta* 126: 413-432
- Malkin S, Armond P A, Mooney H A and Fork D C (1981) Photosystem II photosynthetic unit sizes from fluorescence induction in leaves. *Plant Physiol* 67: 570-579
- Mathis P and Paillotin G (1981) Primary processes of photosynthesis. In Hatch M D and Boardman N K, eds. *The Biochemistry of Plants: Photosynthesis*, Vol 8: pp 97-161. Sidney: Academic Press
- Murashige T and Skoog F (1962) A revised medium for rapid growth and bioassays with tobacco tissue cultures. *Physiol Plant* 15: 473-497
- Murata N and Satoh K (1986) Absorption and fluorescence emission by intact cells, chloroplasts, and chlorophyll-protein complexes. In Govindjee, Amesz J and Fork D C (eds) *Light Emission by Plants and Bacteria*, pp 137-159. Orlando: Academic Press
- Papageorgiou G C (1975) Chlorophyll fluorescence: an intrinsic probe of photosynthesis. In Govindjee (ed) *Bioenergetics of Photosynthesis*, pp 319-371. New York: Academic Press
- Renger G and Schreiber U (1986) Practical applications of fluorometric methods to algae and higher plant research. In Govindjee, Amesz J and Fork D C (eds) *Light Emission by Plants and Bacteria*, pp 587-619. Orlando: Academic Press
- Robinson H H and Crofts A R (1983) Kinetics of the changes in oxidation-reduction reactions of the Photosystem II quinone acceptor complex, and the pathway for deactivation. *FEBS Lett* 153: 221-226
- Robinson H H and Crofts A R (1987) Kinetics of the changes in oxidation-reduction states of the acceptors and donors of Photosystem II in pea thylakoids measured by flash fluorescence. In Biggins J (ed) *Proceedings of the 7th International Congress of Photosynthesis*, Vol 2: pp 429-432. Dordrecht: Martinus Nijhoff Publishers
- Rogers S M D and Widholm J M (1986) Photosynthetic characteristics of photoautotrophic cell suspensions of soybean. *Plant Physiol* 80: S-46
- Rogers S M D and Widholm J M (1988) Comparison of photosynthetic characteristics of two photoautotrophic cell suspension cultures of soybean. *Plant Science* 56: 69-74
- Rogers S M D, Ogren W L and Widholm J M (1987) Photosynthetic characteristics of a photoautotrophic cell suspension culture of soybean. *Plant Physiol* 84: 1451-1456
- Rutherford A W, Govindjee and Inoue Y (1984) Charge accumulation and photochemistry in leaves studied by thermoluminescence and delayed light emission. *Proc Natl Acad Sci USA* 81: 1107-1111
- Sivak M N and Walker D A (1983) Some effects of CO<sub>2</sub> concentration and decreased O<sub>2</sub> concentration on induction of fluorescence in leaves. *Proc Roy Soc London B* 217: 377-392
- Sivak M N, Ditz K, Heber U and Walker D A (1985) The relationship between light scattering and chlorophyll *a* fluorescence during oscillations in photosynthetic carbon assimilation. *Arch Biochem Biophys* 237: 513-519
- Sonneveld A, Rademaker H and Duysens L N M (1979) Chlorophyll *a* fluorescence as a monitor of nanosecond reduction of the photooxidized primary donor P-680<sup>+</sup> of Photosystem II. *Biochim Biophys Acta* 548: 536-551
- Taoka S, Robinson H H and Crofts A R (1983) Kinetics of the reaction of the two-electron gate of Photosystem II: studies of the competition between plastoquinone and inhibitors. In Inoue Y, Crofts A R, Govindjee, Murata N, Renger G and Satoh K (eds) *The Oxygen Evolving System of Plant Photosynthesis*, pp 369-381. Tokyo: Academic Press
- Velthuys B R (1981) Electron-dependent competition between plastoquinone and inhibitors for binding to Photosystem II. *FEBS Lett* 126: 277-281
- Velthuys B R and Amesz J (1974) Charge accumulation at the reducing side of system II of photosynthesis. *Biochim Biophys Acta* 333: 85-94
- Walker D A (1981) Secondary kinetics of spinach leaves in relation to the onset of photosynthetic carbon assimilation. *Planta* 153: 273-278
- Walker D A, Sivak M N, Prinsley R T and Cheesbrough J K (1983) Simultaneous measurement of oscillations in oxygen evolution and chlorophyll *a* fluorescence in leaf pieces. *Plant Physiol* 73: 532-549
- Witt H T, Schlodder E, Brettel K and Saygin O (1986) Reaction sequences from light absorption to the cleavage of water in photosynthesis—routes, rates and intermediates. *Photosynth Res* 10: 453-471
- Wollman F A (1978) Determination and modification of the redox state of the secondary acceptor of Photosystem II in the dark. *Biochim Biophys Acta* 503: 263-273
- Xu C, Blair L C, Rogers S M D, Govindjee and Widholm J M (1988) Characteristics of five new photoautotrophic suspension cultures including two *Amaranthus* species and a Cotton strain growing on ambient CO<sub>2</sub> levels. *Plant Physiol*, in press
- Yamagishi A, Satoh K and Katoh S (1978) Fluorescence induction in chloroplasts isolated from the green alga *Bryopsis maxima* III. A fluorescence transient indicating proton gradient across the thylakoid membrane. *Plant and Cell Physiol* 19: 17-25

# Chlorophyll *a* Fluorescence Measurements of Isolated Spinach Thylakoids Obtained by Using Single-Laser-Based Flow Cytometry<sup>1</sup>

Chunhe Xu, Julie Auger, and Govindjee

Departments of Physiology and Biophysics and Plant Biology (C.X., G.) and Cell Science Center, Biotechnology Center (J.A.), University of Illinois at Urbana-Champaign, Urbana Illinois 61801

Received for publication May 30, 1989; accepted October 20, 1989

Flow cytometry data of spinach thylakoid membrane preparations indicate the presence of a homogeneous thylakoid population. Fluorescence data from a flow cytometer and comparison with data from two other fluorometers show that chlorophyll *a* fluorescence detected with a flow cytometer has the character of maximum fluorescence ( $F_{max}$ ), not of the constant component ( $F_0$ ). This conclusion is important since  $F_0$  measures fluorescence that is affected mostly by changes in excitation energy transfer and  $F_{max}-F_0$  (the variable fluorescence) by changes in photochemistry. This was demonstrated by: 1) The light intensity as well as diffusion rate dependence of the quenching effect of various quinones (p-benzoquinone, phenyl-benzoquinone, and 2,5-dibromo-3-methyl-6-isopropyl-p-benzoquinone, DBMIB) on fluorescence yield; quenching for the same concentration of these quinones was lower at the

higher than at the lower light intensities. 2) Temperature dependence of the fluorescence yield; increasing the temperature from 20 to 70°C did not show an increase in fluorescence yield using a flow cytometer in contrast to measurements with weak excitation light, but similar to those obtained for  $F_{max}$ . 3) Addition of an inhibitor diuron up to 100  $\mu$ M did not change the fluorescence intensity. A comparison of quenching of fluorescence by various quinones obtained by flow cytometry with those by other fluorometers suggests that the high intensity used in the cytometry produces unique results: the rate of reduction of quinones is much larger than the rate of equilibration with the bulk quinones.

**Key terms:** Constant fluorescence  $F_0$ , maximum fluorescence  $F_{max}$ , photosynthesis, quenching of fluorescence, quinones, diuron, ferricyanide (spinach)

Laser-activated flow cytometry has become an important experimental tool in various areas of animal cell physiology and microbiology. Important advantages of this technique are the capacity for rapid identification, quantification, and resolution of discrete subpopulations in heterogeneous cell samples on the basis of expression of cell surface marker or internal metabolic capabilities (9,23,26,31). Although chlorophyll (Chl) *a* fluorescence and light-scattering signals from higher plant and algal cells can be easily detected by this sophisticated technique, reports on the application of flow cytometry to marine biology and plant biology, particularly photosynthesis, are scarce (3).

In order for the readers to appreciate the significance of Chl *a* fluorescence in photosynthesis research, a brief background is provided (see the diagram). Photo-

synthesis is driven by two photosystems, I and II, leading to the oxidation of  $H_2O$  to molecular  $O_2$ , to the reduction of a pyridine nucleotide, and to the production of ATP (7). Chlorophyll *a* fluorescence is particu-

<sup>1</sup>This work was supported by funds from the McKnight Interdisciplinary Photosynthesis Research Program, and in part by Biomedical Shared Instrument Grant #S10 RR02277 from National Institute of Health, which provided a flow cytometer/cell sorter to the Cell Science Laboratory, Biotechnology Center, University of Illinois.

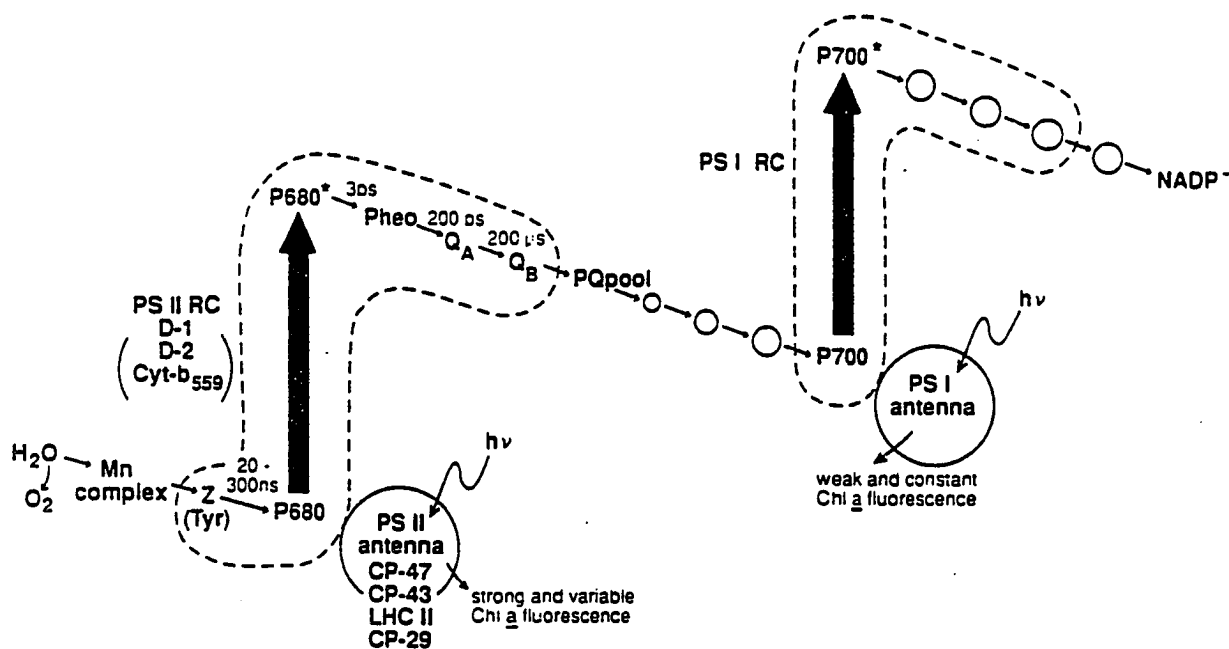


Diagram 1. A diagram showing the primary photochemical reactions and electron flow pathway in photosynthesis. Dashed lines encircle the components of the two multiprotein reaction center complexes, located in the thylakoid membrane. Electron flow is initiated when photons ( $h\nu$ ) excite the reaction center chlorophyll  $a$  P680 (in photosystem II, PS II) and P700 (in PS I) and/or when excitons from the antenna pigments reach these centers. P680\* and P700\* indicate the first singlet excited states of P680 and P700. The first reaction of P680\* is the conversion of excitonic energy into chemical energy (charge separation). This involves the formation of the cation P680\* and the anion pheophytin<sup>-</sup> (Pheo<sup>-</sup>) within 3 ps. The P680\* recovers its lost electron from Z (tyrosine-160 of the D<sub>1</sub> polypeptide of PS II). The positive charge on Z is then transferred to a Mn-complex located on the luminal portions of the D<sub>1</sub> and D<sub>2</sub> polypeptides of PS II. The Pheo<sup>-</sup> delivers the extra electron to a bound plastoquinone electron

acceptor Q<sub>A</sub>. The reduced Q<sub>A</sub> transfers its electron to another plastoquinone electron acceptor Q<sub>B</sub>, strongly bound only in its semiquinone form Q<sub>B</sub><sup>-</sup>. After two turnovers of the reaction center P680, Q<sub>B</sub>H<sub>2</sub> exchanges with the plastoquinone (PQ) pool. After four turnovers of the reaction center P680, the Mn complex accumulates four positive charges and oxidizes H<sub>2</sub>O to molecular O<sub>2</sub> and releases 4 H<sup>+</sup>s. Plastoquinol formed in PS II reduces oxidized P700 (P700<sup>+</sup>), formed in PS I RC (reaction center), via several intermediates. The names and details of only PS II (not PS I) intermediates are included here since most of chlorophyll  $a$  (Chl  $a$ ) fluorescence at room temperature originates in PS II. Furthermore, under normal conditions, only Chl  $a$  fluorescence of PS II varies with changes in photochemistry. CP-47, CP-43, LHC-II, and CP-29 stand for pigment-protein antenna complexes of PS II. The role of cytochrome *b559* (Cyt *b559*) is unknown.

larly sensitive to the functioning of photosystem II (PSII). In PS II, the water-plastoquinone oxido-reductase, light absorption leads to charge separation at the reaction center within 3 ps: the reaction center Chl  $a$  P680 is oxidized and the reaction center pheophytin (Pheo) is reduced (12). This is followed by electron flow from the reduced pheo to a tightly bound plastoquinone Q<sub>A</sub> within 200 ps, and then from reduced Q<sub>A</sub> to a loosely bound plastoquinone Q<sub>B</sub> within 200  $\mu$ s. The oxidized P680 is reduced by a manganese complex viz Z (a tyrosine residue). After two turnovers of the reaction center, Q<sub>B</sub> is double reduced and forms a plastoquinol molecule, and after four turnovers of the reaction center, H<sub>2</sub>O is oxidized to molecular O<sub>2</sub> (12). The PS II is located on the thylakoid membrane and is composed of a reaction center protein complex (D1/D2/cytochrome *b559* complex), several pigment-protein complexes that serve as antenna complexes (LHC-II, CP-29, CP-43, and CP-47), and non-pigmented protein complexes that are involved in electron flow. Most of the chlorophyll  $a$

fluorescence at room temperature originates in the antenna complexes of PS II, primarily in CP-43 and CP-47 (11,25). Chlorophyll  $a$  fluorescence is high when Q<sub>A</sub> in the reaction center is in the reduced state and low when Q<sub>A</sub> is in the oxidized state (8). When present, P680\* and Pheo<sup>-</sup> may act as quenchers of Chl  $a$  fluorescence. This Chl  $a$  fluorescence emission is in competition with many other processes in chloroplasts (7,8,11). It is expected that many analytical and separation techniques (e.g., selection of herbicide-resistant strains) may be useful in photosynthesis research based upon the analysis of Chl  $a$  fluorescence by flow cytometry.

Ashcroft et al. (3) reported the first flow cytometric measurements in intact chloroplasts and thylakoid membrane preparations from spinach and maize. Intact chloroplast preparations could be subdivided into at least two subgroups based on their light scatter and fluorescence characteristics. Ashcroft et al. (3) concluded that single-laser-based flow cytometry mea-

sures the constant component of Chl *a* fluorescence,  $F_0$ . This is, obviously, possible in a flowing system if the time of exposure is short (20). But, there was no evidence for this conclusion; furthermore, the observed dependence of Chl *a* fluorescence on the concentration of ferricyanide, an electron acceptor, questions the conclusion about the  $F_0$  nature of fluorescence. A thorough study and a clear explanation for flow cytometry Chl *a* fluorescence data are necessary before this technique can be applied for measurements on photosynthetic samples on a wider scale.  $F_0$  is a measure of the minimum Chl *a* fluorescence level when photochemical reaction rate is maximum and reaction centers of PS II are assumed to be open (see, e.g., ref. 11).

The relative quantum yield of Chl *a* fluorescence ( $\phi_f$ ), in the absence of a barrier to exciton migration, is best expressed (29) by the following equation:

$$\phi_f = k_f / (k_f + k_r + k_n + k[Q]) \quad (1)$$

where  $k_f$ ,  $k_r$ , and  $k_n$  are the rate constants for fluorescence, excitation energy transfer, and heat loss, and  $k[Q]$  is the term representing the quenching process by intrinsic or extrinsic quencher. When only intrinsic quencher exists, this term is written as  $k[Q_A]$ . In the absence of electron flow inhibitors and in weak light, all  $Q_A$  exists in the oxidized form. Thus  $k[Q_A]$  becomes maximum and a minimum fluorescence quantum yield level,  $F_0$ , is reached. This fluorescence level is affected mostly by changes in excitation energy transfer.

At high light intensities, when all  $Q_A$  molecules are  $Q_A^-$ ,  $k[Q_A]$  approaches zero and  $\phi_f$  approaches a maximum value ( $F_{max}$ ). Furthermore, addition of electron transport inhibitors, which inhibit beyond  $Q_A$ , moves the equilibrium to favor the formation of  $Q_A^-$ . Then  $k[Q_A]$  decreases and the quantum yield of Chl *a* fluorescence ( $F$ ) increases. In the presence of a saturating concentration of an inhibitor diuron, the maximum fluorescence quantum yield,  $F_{max}$ , is reached; here also,  $k[Q]$  in equation (1) approaches zero. The variable fluorescence, i.e., the difference between  $F$  (or  $F_{max}$ ) and  $F_0$ , is affected mostly by changes in photochemistry.

Since fluorescence intensity is one of the major parameters measured by a flow cytometer, it is necessary to reexamine the question of whether the instrument measures  $F_0$  in photosynthetic samples. We show in this paper that the Chl *a* fluorescence being monitored by the single-laser-based flow cytometer is the maximum fluorescence when the PS II reaction centers are locked in the  $Q_A^-$  state. In addition, comparison of measurements on the quenching of Chl *a* fluorescence by various quinones (p-benzoquinone, phenyl-benzoquinone, and 2,5-dibromo-3-methyl-6-isopropyl-benzoquinone, DBMIB) with those obtained by Karukstis et al. (15–17), using conventional methods, suggests that flow cytometry gives different and unique results due to the high intensity used; it is suggested here that this is due to higher rate of reduction of quinones than equilibration with the bulk quinones.

## MATERIALS AND METHODS

Spinach (*Spinacia oleracea*) thylakoids were prepared as previously described by Eaton-Rye and Govindjee (10). Thylakoids were stored in liquid nitrogen and thawed immediately prior to experiments. Chlorophyll *a* concentrations were determined according to ref. 2. The chlorophyll concentration for fluorescence measurements was about 20  $\mu$ M in flow cytometry, 10  $\mu$ M in the double flash fluorescence instrument (which measures the decay of  $Q_A^-$  to  $Q_A$ ), and 40  $\mu$ M in the fluorescence transient experiments (which measure  $F_0$  and  $F_{max}$ ).

A Coulter EPICS™ 751 single-laser-based flow cytometer was used in this work. This system is composed of the EPICS™ V Multiparameter Sensor and the MDADS (Multiparameter Data Acquisition and Display System). The sensor unit consists of hardware associated with sample flow, laser excitation, and fluorescence detection of the single-subpopulation suspensions. The single-laser excitation was achieved with a 5 W argon ion laser (Coherent, Palo Alto, CA) tuned to 488 nm with power output at 100 mW. Right-angle fluorescence, passed through a red cutoff Corning glass CS 2-58, was collected by an RCA 4526 photomultiplier tube. Forward and 90° light-scattering signals were collected by a photodiode and a Hamamatsu 72271-01 photomultiplier, respectively. Fluorescence pulse signals from each particle were integrated and processed through either a linear amplifier (IRFL) or a logarithmic amplifier (LIRFL) and then passed to the computer for digitization, display and storage. The relevant 256 channel frequency distribution histogram spans a three decade log scale when the log amplifier is used. Alignment and calibration were achieved by using fluorescent microspheres. The light intensity of the laser beam was calculated to be  $4 \times 10^7$  W m<sup>-2</sup> with a Coherent radiometer. The number of absorbed photons in the sample was about  $10^6$  and the light was polarized. The flow rate for the sample was 10 m/s.

The Chl *a* fluorescence of the sample was also measured, after a weak xenon flash, by a conventional double-flash fluorometer (10). Chl *a* fluorescence transients, i.e., changes in Chl *a* fluorescence from  $F_0$  to the  $F_{max}$  in continuous light, were measured by using a laboratory-built spectrofluorometer (5). The exciting light was provided by a Kodak 4200 projector with the light filtered by two Corning blue filters (CS 4-71 and CS 5-56). Fluorescence emission was detected by a S-20 photomultiplier (EMI 9558B) through a Bausch and Lomb monochromator and a Corning red filter CS 2-61. The light intensity of the exciting light, measured with a YSI-Kettering Model 65 Radiometer (Yellow Springs, Ohio), was  $2 \times 10^2$  W m<sup>-2</sup>.

## RESULTS

### Scattering and Fluorescence Measurements

Figure 1 displays the typical flow cytometry data obtained from measurements of spinach thylakoids.

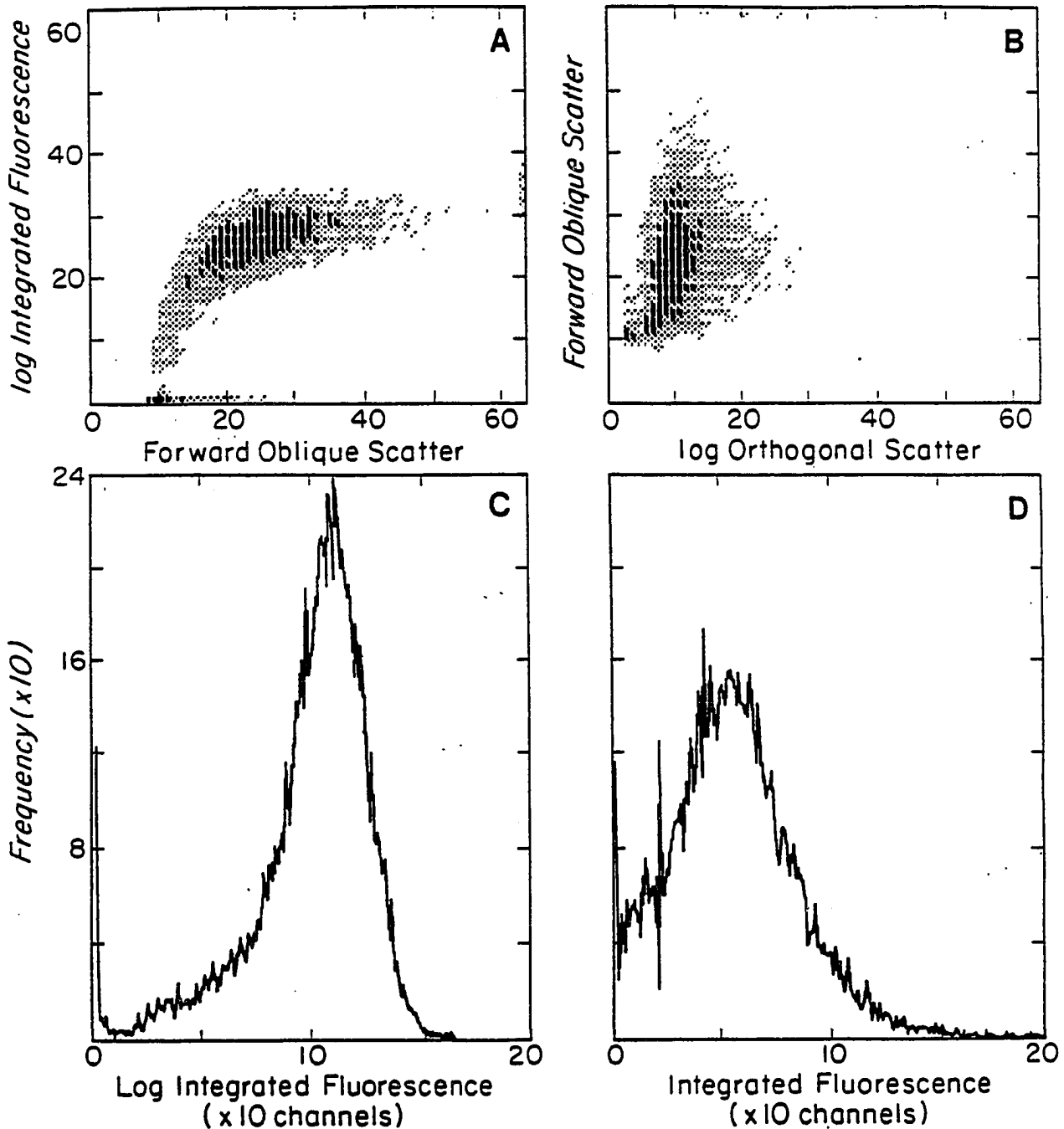


FIG. 1. Two-dimensional contour frequency distributions (histograms) for spinach thylakoids. Panel A: Logarithmic integrated Chl  $\alpha$  fluorescence as a function of forward oblique scatter (related to the size of the object). Panel B: Forward oblique scatter as a function of logarithmic orthogonal scatter (related to internal structure of the

object). Panels C and D: Subpopulation frequency as a function of logarithmic integrated fluorescence and integrated fluorescence, respectively. Histograms show only one major population for spinach thylakoid membrane preparations.

Data were plotted as two-dimensional frequency distributions (histograms). Panel A shows logarithmic integrated fluorescence as a function of forward oblique

scatter. Forward scatter measurements are somewhat related to the size and the refractive index of the organelle. Panel B shows the forward oblique scatter as

function of logarithmic orthogonal scatter. Orthogonal scatter is related to the internal structure of the organelle. Panels C and D display the population frequency data as functions of logarithmic integrated fluorescence and integrated fluorescence, respectively. Only one major population was shown on these histograms for spinach thylakoid membrane preparations. These data are consistent with those of Ashcroft et al. (3).

Fluorescence is linearly related to the concentration of the chromophore in fluorescence measurements (22). In the flow cytometer, the same level of fluorescence yield was maintained when the thylakoid concentration, in terms of Chl *a* concentration (5 to 500  $\mu\text{g/ml}$ ), was changed. This was as expected since by design the flow cytometry measurements indicate the fluorescence signal emitted by each particle, and the final fluorescence histogram represents a distribution plot from all the particles analyzed. Thus, this value is independent of thylakoid concentration within limits, as observed.

**Source of fluorescence.** The argon ion laser, used in flow cytometry experiments as the exciting source, was tuned to 488 nm. To ensure that there was no interference of scattered laser light, a 475 nm-long wavelength pass filter and a 530 nm short wavelength pass filter were placed in the front of the photomultiplier. If there was any excitation light scattered off the thylakoid suspension into the photomultiplier, a signal was expected. Since no signal was detected, this implied that scattering of the laser beam from the sample would not contribute to our measurements. Experiments were performed to determine whether the source of measured fluorescence was indeed Chl *a*. First, a partially bleached chloroplast suspension was prepared for comparison. In thylakoids in which 75–80% of the chlorophyll was extracted by 80% acetone, the fluorescence signal was one fourth of that of the control, showing a qualitative relationship between the chlorophyll content and the fluorescence signal. This indicates that the measured fluorescence signal in flow cytometry is chlorophyll fluorescence. Second, a red filter (Corning CS 2-58) was placed in front of the photomultiplier to cut off all the spectral signals shorter than 640 nm. Chlorophyll *a* fluorescence *in vivo* peaks at 685 nm (see, e.g., ref. 11,25). The observed signal with and without CS 2-58 was of the same amplitude, showing consistency with it being Chl *a* fluorescence. In all further experiments, the CS 2-58 filter was used.

**Effects of heat treatment.** Heat treatment influences the initial fluorescence  $F_i$  and the maximum fluorescence  $F_{\text{max}}$  of Chl *a* differently (28). Lavorel (20) had earlier discovered the heat-induced rise in initial Chl *a* fluorescence with a fluorometer. This heat-induced fluorescence increase was explained to reflect changes at the pigment level. Schreiber and Armond (28), who had also used a conventional fluorometer, showed that increasing the incubating temperature from 25 to 55°C (time, 5 min) produced a threefold in-

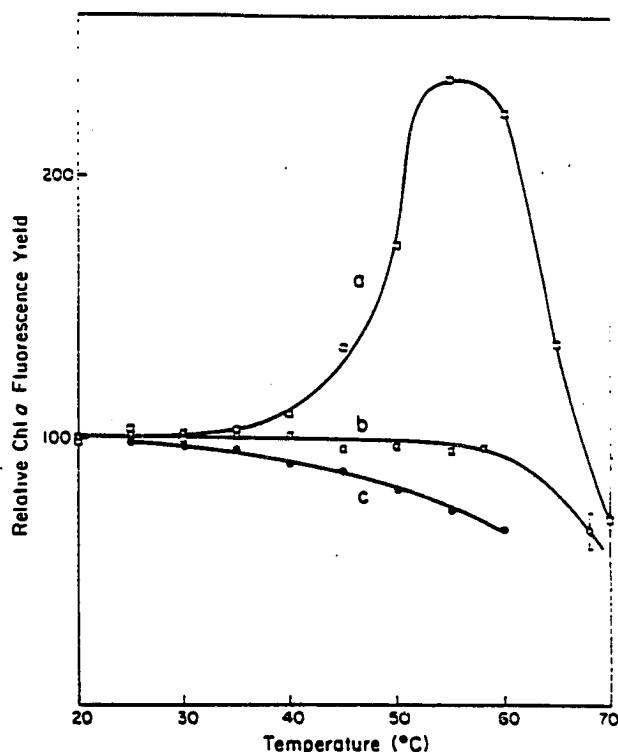


FIG. 2. Temperature dependence of Chl *a* fluorescence of spinach thylakoids. Curve a: Measured at low light intensity (sampling 1% of the centers) for initial Chl *a* fluorescence ( $F_i$ ) by a double-flash fluorometer. Curve b: Measured by Coulter EPICS™ 751 single-laser-based flow cytometer. Curve c: Measured by Schreiber and Armond (28) for  $F_{\text{max}}$ , excited at 480 nm. All fluorescence data have been normalized to 100 at 20°C. Flow cytometer data are similar to those of  $F_{\text{max}}$ , not  $F_i$ .

crease in the initial Chl *a* fluorescence yield ( $F_i$ ). Above 60°C, fluorescence decreased below the level seen at room temperature. The increase in fluorescence was explained (28) by a block of excitation energy migration in the pathway from the antenna pigments to the PS II reaction centers, i.e., a decrease in  $k_t$  in equation (1). This block was suggested to be related to a heat-induced structural change of pigments and thylakoid organization. On the other hand, a decrease in fluorescence was explained by Sane et al. (27) to be due to a change from the fluorescent *state I* to a weakly fluorescent *state II*. Recently, J. Cao and Govindjee (6) have suggested that most of the heat-induced fluorescence rise is not at the true  $F_0$  level but at a fluorescence level above  $F_0$ , perhaps at the so-called "T" level, the intermediate level of Chl *a* fluorescence ( $F_T$ ) (11). The increase of fluorescence found at 55°C was suggested to be due to an increase in the concentration of "inactive" PS II centers where reoxidation of  $Q_A^-$  is slowed. In contrast to results on  $F_i$ , heat treatment caused only a decrease in fluorescence intensity on  $F_{\text{max}}$  (28) (see trace c in Fig. 2). When we measured Chl *a* fluores-



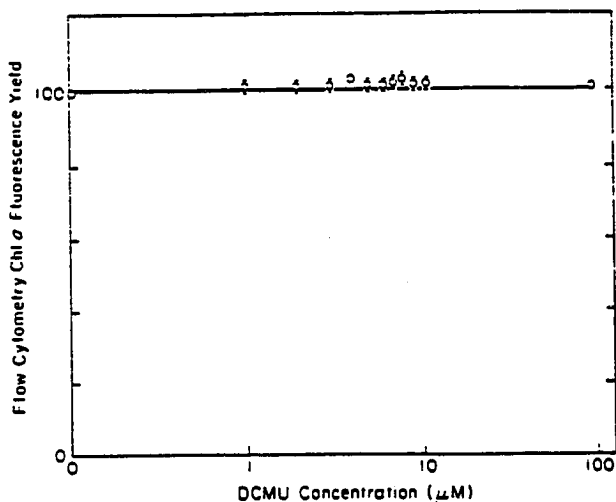


FIG. 3. Chl *a* fluorescence intensity of spinach thylakoids, measured by flow cytometry, as a function of DCMU concentration. Cytometry Chl *a* fluorescence data show that it is independent of DCMU concentration up to 100  $\mu\text{M}$ .

cence yield in heat-incubated chloroplasts by using single-laser-based flow cytometry, the fluorescence remained unchanged until 60°C and then decreased (trace b in Fig. 2). However, when the initial Chl *a* fluorescence ( $F_0$ ) of heat-treated chloroplasts was measured by weak light in the double-flash instrument, the rise was found in the 40 to 55°C range (trace a in Fig. 2). The temperature dependence of the flow cytometry result (trace b) is totally different from that for the initial fluorescence (trace a), but similar to that for  $F_{\text{max}}$  (trace c). Thus, the flow-cytometer-induced Chl *a* fluorescence is consistent with it being  $F_{\text{max}}$ . The quantitative difference between our observed results (trace b) and that of Schreiber and Armond (trace c) may be due to differences in samples used as well as to differences in light intensity, the latter being much higher for trace b.

**Effect of diuron concentration.** DCMU (3-(3,4)-dichlorophenyl-1,1, dimethyl urea), or diuron, inhibits photosynthetic electron transport by occupying the binding site of  $Q_B$ . Since  $Q_B$  is the secondary quinone electron acceptor of PS II, the reoxidation of  $Q_A^-$  is prevented (33). If the measuring light is very weak, the addition of herbicide should not influence the fluorescence yield at true  $F_0$ . Similarly, in bright actinic light, when fluorescence reaches  $F_{\text{max}}$  due to the blockage in reoxidation of  $Q_A^-$ , the addition of herbicide should not influence the fluorescence yield either (see equation 1; cf. ref. 8). However, at weak to moderate light intensities an increase of [DCMU] from 1 to 10  $\mu\text{M}$  should lead to a severalfold increase in Chl *a* fluorescence intensity. Since in our flow cytometric Chl *a* fluorescence experiment, the light intensity is not weak and since the addition of 1 to 100  $\mu\text{M}$  DCMU induced no change in Chl *a* fluorescence (Fig. 3), the single-laser-based

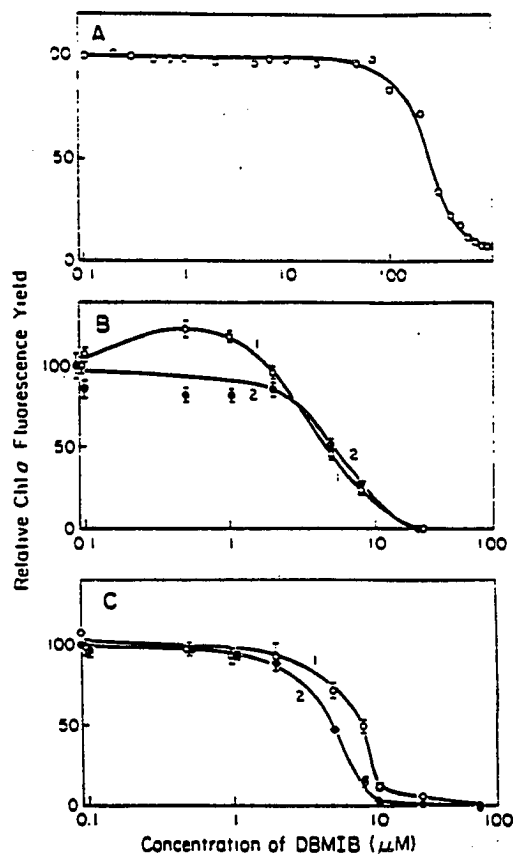


FIG. 4. DBMIB titration graphs of Chl *a* fluorescence intensity under different conditions for spinach thylakoids. The curve in panel A was measured with flow cytometer (light intensity  $4 \times 10^7 \text{ W m}^{-2}$ ). Curves 1 in panel B (initial Chl *a* fluorescence, close to  $F_0$ ) and in panel C (Chl *a* fluorescence measured at 17 sec, close to  $F_{\text{max}}$ ) were measured with  $2 \times 10^2 \text{ W m}^{-2}$  light intensity; and curves 2 were measured with  $12 \text{ W m}^{-2}$ . Note the difference in the abscissa scale between panel A and the other two.

flow cytometer must measure  $F_{\text{max}}$ , not a fluorescence level elicited by weak-to-moderate light.

#### Quenching by Extrinsic Quenchers

Fluorescence quenching is a general property of oxidized quinones (1). In the present study, three different fluorescence quenchers, 2,5-dibromo-3-methyl-6-isopropyl-p-benzoquinone (DBMIB), p-benzoquinone, and phenyl-benzoquinone, were selected to further characterize the properties of Chl *a* fluorescence measured by flow cytometry. DBMIB is an inhibitor that usually acts at the cytochrome  $b_6/f$  complex in a photosynthetic electron pathway (32). The oxidized form of DBMIB is more effective in fluorescence quenching than that of the other two quinones. A DBMIB titration graph obtained from flow cytometry Chl *a* fluorescence measurements is shown in Figure 4A; this can be compared with Kitajima and Butler's data (14) on  $F_0$  and  $F_{\text{max}}$  obtained by conventional fluorometry. Although

DBMIB displayed quenching in our flow cytometry measurements, the quenching effect of the same concentration of DBMIB was weaker than or absent relative to that observed by Kitajima and Butler for  $F_0$  and  $F_{max}$ . DBMIB concentrations for 50% quenching of Chl  $\alpha$  fluorescence are  $2 \times 10^{-4}$  M for flow cytometry (this paper),  $2 \times 10^{-3}$  for  $F_0$ , and  $1.1 \times 10^{-3}$  M for  $F_{max}$  (14). The DBMIB concentration at 50% quenching differs between the two types of experiments by more than one order of magnitude. We repeated these experiment with a double-flash fluorometer (10); our results (data not shown) were similar to that obtained in ref. 14. One possible explanation for the apparently contradictory data is the extremely high incident intensity ( $4 \times 10^7$  W m $^{-2}$ ) of the laser beam, which is five orders of magnitude stronger than that of the lamp used in the conventional fluorometer ( $2 \times 10^2$  W m $^{-2}$ ). In strong light, the photoreduction rate of DBMIB must be much larger than the rate of equilibration between the few reduced molecules of DBMIB and the large number of oxidized DBMIB molecules in the medium. Thus the effective amount of oxidized DBMIB in the vicinity of Chl  $\alpha$  molecules becomes less in the laser beam of the cytometry instrument than in the conventional fluorometers. The decrease in the amount of DBMIB, however, must be a local effect within the thylakoid since plenty of DBMIB is present in the suspension medium. The decrease in the effective amount of localized oxidized form of quinone analogues in bright light induces the shift of its titration graph. Experiments on Chl  $\alpha$  fluorescence transient were done to test the light-intensity dependence idea. By measuring Chl  $\alpha$  fluorescence transient, the initial fluorescence, ( $F_i$ , Fig. 4B), and the Chl  $\alpha$  fluorescence at 17 s after the commencement of illumination,  $F_{17s}$ , close to  $F_{max}$  (Fig. 4C), were obtained. DBMIB titration graphs were plotted at two different light intensities (traces 1 at  $2 \times 10^2$  W m $^{-2}$  and 2 at  $12$  W m $^{-2}$ , respectively). By decreasing the intensity of illuminating light, a shift of the DBMIB titration graph towards the low concentration side was found for  $F_{17s}$  (Fig. 4C). In contrast, the titration graph for  $F_i$  did not show any light-intensity-dependent shift (Fig. 4B). This indicates that the light-intensity dependence of the quinone quenching is related to the property of  $F_{max}$ , not  $F_i$ . This supports our conclusion that the fluorescence we measure with cytometry is likely to have  $F_{max}$  character, but not that of initial fluorescence. Although the explanation of the difference in the fluorescence intensity between the samples excited by high and low intensity (curves 1 and 2 in Fig. 4B) requires further study, it may be due to a greater reduction rate of  $Q_A$  to  $Q_A^-$  in curve 1.

Figure 5 displays the p-benzoquinone titration graphs of the Chl  $\alpha$  fluorescence measured by flow cytometry (panel A), by another fluorometer for fluorescence close to  $F_0$  (panel B), and for  $F_{17s}$  (panel C) respectively. Similar titration graphs are displayed in Figure 6 for phenyl-benzoquinone. When the intensity of the illuminating light was reduced from  $4 \times 10^7$

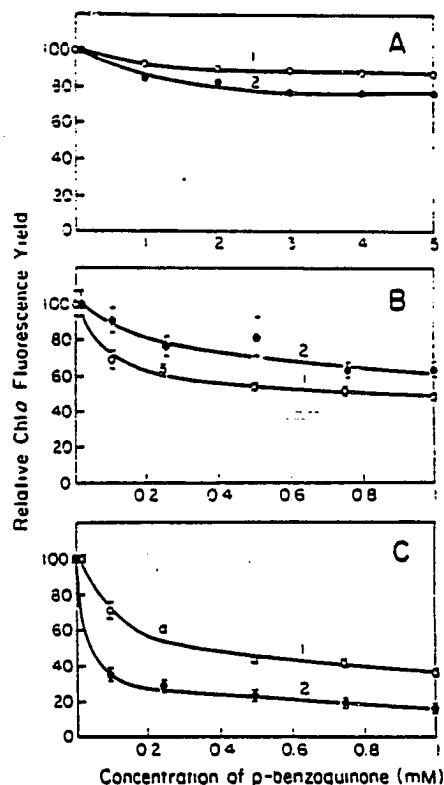


FIG. 5. Para-benzoquinone titration graphs of Chl  $\alpha$  fluorescence intensity under different conditions for spinach thylakoids. Curves 1 and 2 in panel A (flow cytometry) were measured with incident light intensity of  $4 \times 10^7$  or  $4 \times 10^6$  W m $^{-2}$ , respectively. Curves 1 in panels B (initial Chl  $\alpha$  fluorescence, close to  $F_0$ ) and C (Chl  $\alpha$  fluorescence measured at 17 s, close to  $F_{max}$ ) were measured with  $2 \times 10^2$  W m $^{-2}$  light intensity, but curves 2 were measured with  $12$  W m $^{-2}$ . Note the difference in the abscissa scale between panel A and the other two.

(trace 1) to  $4 \times 10^6$  W m $^{-2}$  (trace 2) in panels A and from  $2 \times 10^2$  (trace 1) to  $12$  W m $^{-2}$  (trace 2) in panels B and C, the quenching by the same concentration of quinone on the Chl  $\alpha$  fluorescence increased (see panels A and C). These changes brought about shifts in the quencher titration graphs. In agreement with data in Figure 4B, no shift was found for the titration graphs for the initial fluorescence ( $F_i$ ) in panel B (Fig. 6). The above results also support the conclusion that the fluorescence measured with the flow cytometer is likely to have  $F_{max}$  character. The opposite result on the intensity dependence on  $F_i$  in Figure 5B remains unexplained. Trace 3 in Figure 6A is plotted from Ashcroft et al.'s data for phenylbenzoquinone. The light intensity used in that experiment was  $10$  m mol m $^{-2}$ s $^{-1}$ , at 476 nm.

To confirm the existence of the diffusion equilibrium (29) between the oxidized and the reduced forms of quinone molecules in our experimental system, an experiment changing the viscosity of the suspension medium was designed. Figure 7 displays the p-benzoquinone titration graphs of Chl  $\alpha$  fluorescence measured with

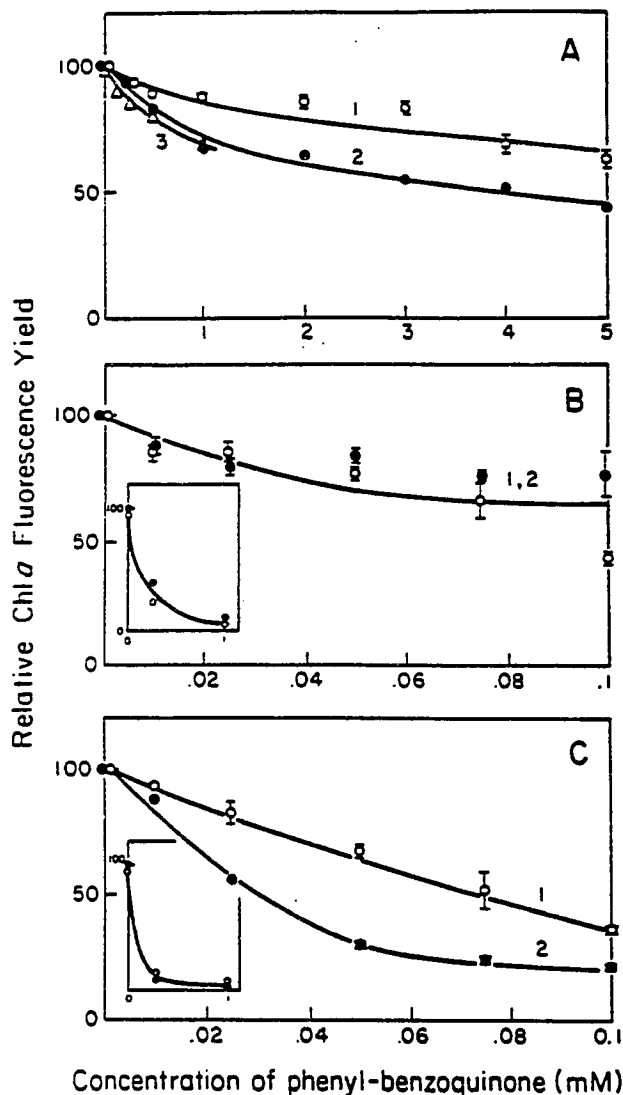


FIG. 6. Phenyl-benzoquinone titration graphs of Chl *a* fluorescence intensity under different conditions for spinach thylakoids. Experimental details are as in Figure 5. Note the difference in the abscissa scale between panel A and the other two. For convenience of comparison with Figure 5, insets in B and C have the same concentration scale as the scales in Figure 5B and 5C.

conventional fluorometry when the viscosity was changed. Panel A is for  $F_i$  and panel B is for  $F_{17a}$ . Increasing the viscosity of the suspension medium (replacing 50% of the suspension medium by glycerol, traces 2) did not affect the trace for  $F_i$  but decreased the quenching activity of the same concentration of the quinone on  $F_{17a}$ . This implies that  $F_{max}$  may be influenced by the diffusion rate of quinones across the thylakoid membranes.

#### DISCUSSION

In conventional fluorescence measurements (21) decreasing the illumination time ( $t$ ) instead of decreasing

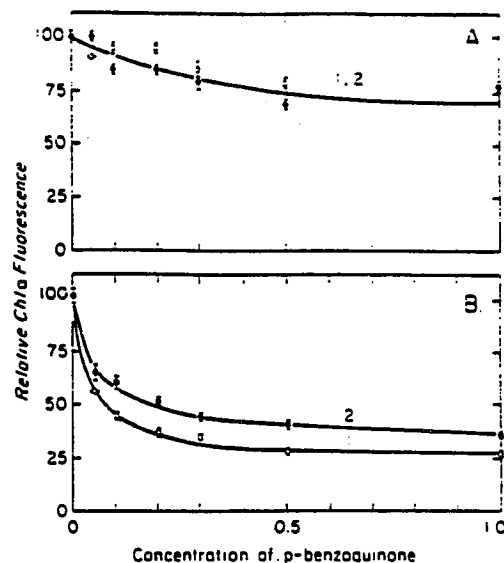


FIG. 7. Effect of changing viscosity on p-benzoquinone titration graphs for Chl *a* fluorescence from spinach thylakoids, measured with conventional fluorometry. Traces 1: control; traces 2: viscosity was increased by the addition of 50% glycerol. Panel A is for fluorescence close to  $F_0$  and panel B is for  $F_{17a}$ . The fluorescence yield has been normalized to 100 when the quinone concentration is zero.

light intensity in the flowing suspension system reduces the photochemical activation in the reaction center. Thus, when the flow is fast and the illumination time short, one measures  $F_0$  in the flow system. Stopping the flow, that is, increasing the time  $t$ , allows one to measure  $F_{max}$ . Since the flow cytometer is a flowing system, it is reasonable to expect that the Chl *a* fluorescence measured by flow cytometer may be  $F_0$ . Mauzerall (24) reported that, in a dark-adapted sample, the fluorescence rise time is 25 ns. This rise was explained later to be due to the reduction of the oxidized form of the reaction center Chl *a* of PS II,  $P_{680}^+$ , another Chl *a* fluorescence quencher of PS II (see, e.g., ref. 30). This rise time is, however, increased to approximately 0.3  $\mu$ s after a second illumination (30). The current picture is that this fast fluorescence rise measures electron flow from the electron donor Z to  $P_{680}^+$ . In our flow cytometer, the time for a 1  $\mu$ m particle to cross a length of the laser spot (16  $\mu$ m) is 1.7  $\mu$ s, which is much longer than 20 ns to 0.3  $\mu$ s for the reduction of  $P_{680}^+$  and for the reduction of  $Q_A$  to  $Q_A^-$  (510 ps) (12,13). Thus, it is reasonable to expect that in a flow cytometer, we will be measuring  $F_{max}$ , not  $F_0$ , especially because the laser light intensity is strong. Estimates based on several assumptions and considerations of energy losses lead us to conclude that about  $10^6$  photons were absorbed per  $10^7$ – $10^8$  chlorophyll molecules present, i.e., about one photon per 10–100 chlorophyll molecules present. Thus, all reaction centers must undergo at least one turnover and the system must reach the  $F_{max}$  state.

At very high intensities, however, multiple hits in a single photosystem unit are commonly observed (see, e.g., ref. 18), leading to exciton-exciton annihilation. Therefore, increasing the intensity of the light source will decrease the relative quantum efficiency for sample fluorescence. Although high light intensity was applied in flow cytometry experiments, our data on light-intensity dependence (Figs. 5A, 6A) display an increase in Chl *a* fluorescence quantum yield when the laser light intensity is increased from  $4 \times 10^5$  to  $4 \times 10^7$  W m<sup>-2</sup>, implying the absence of exciton-exciton annihilation process in spinach thylakoids flowing in the cytometer under our experimental conditions. Furthermore, the same experiment implies the absence of photoinhibitory phenomenon since photoinhibition 1) leads to reduction of variable Chl *a* fluorescence with increasing light intensity and 2) involves long-term (not 2.5  $\mu$ s exposure) chemical and physical changes (see, e.g., a review by Kyle and Ohad (19)).

The conclusion of Ashcroft et al. (3) that the flow cytometry Chl *a* fluorescence is  $F_0$  was not supported. In hypotonically shocked chloroplasts, ferricyanide decreased (3) Chl *a* fluorescence significantly (by 50 to 75%); at  $F_0$ , all  $Q_A$  should have been in the oxidized form and ferricyanide could not have further increased the concentration of  $Q_A$  and, thus, decreased the quantum yield of Chl *a* fluorescence. The absence of the effect of varying [DCMU] on fluorescence intensity cannot prove its  $F_0$  character either (Fig. 3) (3). An independence of the effect of [DCMU] on fluorescence is also expected for  $F_{max}$ . Only when Chl *a* fluorescence is between  $F_0$  and  $F_{max}$  should increasing [DCMU] cause an increase in its yield. High light intensity used in this flow cytometer is not expected to keep the fluorescence at the  $F_0$  level. Thus, the independence of fluorescence yield on [DCMU] is considered consistent with the  $F_{max}$  character of fluorescence. Chl *a* fluorescence in weak light increases with temperature up to 55°C and then decreases (Fig. 2). This character was not observed in the Chl *a* fluorescence with a flow cytometer. Furthermore, a comparison of flow cytometry data with those obtained on  $F_{max}$  showed a similarity between the latter two, suggesting that the flow cytometer measures  $F_{max}$ , and not some level close to  $F_0$  (Fig. 2).

All other experimental results can also be explained by the hypothesis that flow cytometry measures  $F_{max}$ . In our experimental system, there were two sources to quench Chl *a* fluorescence: 1) the oxidized form of  $Q_A$  and 2) the oxidized form of externally added quinone, which may come close to Chl *a* molecules. Due to the high light intensity used in flow cytometry, the rate constants of  $Q_A$  reduction and even that of the reduction of extrinsic quinones increase. High concentrations of  $Q_A^-$  and even reduced quinone analogues must have been created in samples illuminated with such a high-intensity beam. The equilibrium between  $Q_A$  and  $Q_A^-$  is determined by the [ $Q_B$ ] and the equilibrium between the local oxidized form of quinone and the

Table 1  
Quinone Concentrations Causing 50% Quenching of Chl *a* Fluorescence, in Spinach Thylakoids<sup>a</sup>

	Cytometry fluorescence	$F_{17.5}$ ( $I_1$ )	$F_{17.5}$ ( $I_2$ )
p-benzoquinone	>>5mM	0.37mM	60 $\mu$ M
Phenyl-benzoquinone	>5mM	72 $\mu$ M	31 $\mu$ M
DBMIB	0.24mM	8 $\mu$ M	5 $\mu$ M

<sup>a</sup>Data were obtained by flow cytometry (light intensity  $4 \times 10^7$  W m<sup>-2</sup>) and by a home-built fluorometer (5):  $F_{17.5}$  at  $2 \times 10^2$  W m<sup>-2</sup> ( $I_1$ ) and  $F_{17.5}$  at 12 W m<sup>-2</sup> ( $I_2$ ).

bulk quinone. The viscosity experiment in Figure 7 confirmed that the diffusion rate of the quinone molecules has a significant effect on the fluorescence yield. Compared to the reduction rate of  $Q_A$  and quinone strong light, the exchange rate of the reduced quinones with bulk quinone is expected to be rather slow. Therefore, in the flow cytometer used, almost all the  $Q_A$  and the "local" externally added quinone can be considered to exist in the reduced form. Thus, Chl *a* fluorescence yield reaches maximum even at high concentrations of externally added quinone quenchers when measured with a flow cytometer. However, when conventional fluorometers with lower light intensity were used, the equilibration of reduced quinones with bulk quinones allows more oxidized quinones to exist in the vicinity of Chl *a* and to quench fluorescence. Our results, in which decreasing light intensity increases the quenching effect of the same concentration of quinones in flow cytometry (Figs. 5A, 6A) and in conventional fluorometers (Figs. 4C, 5C, and 6C), confirm the above hypothesis. This change only occurs in the fluorescence close to  $F_{max}$ . Therefore, in our cytometry experiment the fluorescence measures  $F_{max}$ , but not  $F_0$  character.

There are two modes of action proposed to describe the quinone-induced fluorescence quenching. One (1,4,15) suggests that the added quinones function to dissipate excitation energy by interaction with either PS II light-harvesting chlorophyll-protein complexes or the PS II reaction center chlorophyll. An alternative mechanism (see, e.g., ref. 17) suggests that the added quinones compete with the intrinsic plastoquinone electron acceptor,  $Q_B$ , for the same or overlapping binding sites in a common binding domain on the D-1 protein, since many substituted quinones act as  $Q_B$  analogs. Data in Table 1 show the quenching capabilities of three quinones. In three different experiments, DBMIB quenched more Chl *a* fluorescence than the other two quinones at the same concentration (data not shown). The concentration of DBMIB, at which 50% quenching of Chl *a* fluorescence occurs, is much lower than that of the other two in all three cases (Table 1), implying that DBMIB is more accessible to Chl *a* or  $Q_B$  than the other two. Although qualitatively similar, quantitatively different results were obtained by Karukstis et al. (15). These differences are due to the unique conditions of flow cytometer data discussed ear-

lier: a larger rate of reduction of quinones as compared to the rate of exchange of these quinones with the bulk quinones.

The flow cytometry experiments are useful for photosynthesis research. Progress in this area potentially depends on the correct analysis of intrinsic Chl *a* fluorescence. Therefore, information in this paper is valuable for further flow cytometry studies on photosynthetic samples related to plant biology or marine biology research. Dual-laser-based flow cytometry may also be useful (see ref. 3 for preliminary observation) since one can change the time interval between two flashes (actinic and measuring) and then measure changes in the fluorescence yield with time, thereby providing information on the time-dependent changes in the photochemical events of photosystem II.

### ACKNOWLEDGMENTS

The authors thank Drs. Gregorio Weber and Jack Widholm for their useful suggestions.

### LITERATURE CITED

1. Amez J, Fork DC: Quenching of chlorophyll fluorescence by quinones in algae and chloroplasts. *Biochim Biophys Acta* 143:97-107, 1967.
2. Arnon DI: Copper enzyme in isolated chloroplasts. Polyphenoloxidase in *Beta vulgaris*. *Plant Physiol* 24:1-15, 1949.
3. Ashcroft RG, Preston C, Cleland RE, Critchley C: Flow cytometry of isolated chloroplasts and thylakoids. *Photobiochem Photobiophys* 13:1-14, 1986.
4. Berens SJ, Scheele J, Butler WJ, Magde D: Time-resolved fluorescence studies of spinach chloroplasts—evidence for the heterogeneous bipartite model. *Photochem Photobiol* 42:51-57, 1985.
5. Blubaugh DJ: The Mechanism of Bicarbonate Activation of Plastoquinone Reduction in Photosystem II of Photosynthesis. Ph.D. Thesis. Biology, University of Illinois at Urbana-Champaign, 1987.
6. Cao J, Govindjee: Chlorophyll *a* fluorescence transient as an indicator of active and inactive photosystem II in thylakoid membranes. *Biochim Biophys Acta*.
7. Duysens LNM: Introduction to (bacterio)chlorophyll emission: A historical perspective. In: *Light Emission by Plants and Bacteria*, Govindjee, Amez J, Fork DC (eds). Academic Press, Orlando, 1986, pp 3-28.
8. Duysens LNM, Sweers HE: Mechanism of two photo-chemical reactions in algae as studied by means of fluorescence. In: *Studies on Microalgae and Photosynthetic Bacteria*, Japanese Society of Plant Physiologists (eds). University of Tokyo Press, Tokyo, 1963, pp 353-372.
9. Dive C, Workman P, Watson JV: Improved methodology for intracellular enzyme reaction and inhibition kinetics by flow cytometry. *Cytometry* 8:552-561, 1987.
10. Eaton-Rye JJ, Govindjee: Electron transfer through the quinone acceptor complex of photosystem II in bicarbonate depleted spinach thylakoid membranes as a function of actinic flash number and frequency. *Biochim Biophys Acta* 935:237-247, 1988.
11. Govindjee, Satoh K: Fluorescence properties of chlorophyll *b*- and chlorophyll *c*-containing algae. In: *Light Emission by Plants and Bacteria*, Govindjee, Amez J, Fork DC (eds). Academic Press, Orlando, 1986, pp 497-538.
12. Govindjee, Wasielewski M: Photosystem II: From a femtosecond to a millisecond. In: *Photosynthesis*, Briggs WR (ed). Alan R. Liss, Inc., New York, 1989, pp 71-103.
13. Schatz GH, Brock H, Holzwarth AR: Picosecond kinetics of fluorescence and absorbance changes in photosystem II excited at low photon density. *Proc Natl Acad Sci USA* 84:3414-3418, 1987.
14. Kitajima M, Butler WL: Quenching of chlorophyll fluorescence and primary photochemistry in chloroplasts by dibromothymoquinone. *Biochim Biophys Acta* 376:105-115, 1975.
15. Karukstis KK, Boegeman SC, Fruetel JA, Gruber SM, Terris MH: Multivariate analysis of photosystem II quenching by substituted benzoquinones and naphthoquinones. *Biochim Biophys Acta* 891:256-264, 1987.
16. Karukstis KK, Gruber SM, Fruetel JA, Boegeman SC: Quenching of chlorophyll fluorescence by substituted anthraquinones. *Biochim Biophys Acta* 932:84-90, 1988.
17. Karukstis KK, Monell CR: Reversal of quinone-induced chlorophyll fluorescence quenching. *Biochim Biophys Acta* 973:124-130, 1989.
18. Knox RS: Photosynthetic efficiency and exciton transfer and trapping. In: *Primary Processes of Photosynthesis*, Barber J (ed). Elsevier, New York, 1977, pp 55-97.
19. Kyle DJ, Ohad I: The mechanism of photoinhibition in higher plants and algae. *Encyclopedia Plant Physiol New Ser* 19:468-475, 1986.
20. Lavorel J: On a relation between fluorescence and luminescence in photosynthetic systems. In: *Progress in Photosynthesis Research*, Vol. 2, Metzner H (ed). H. Laupp, Tubingen, 1969, pp 883-898.
21. Lavorel J: Heterogenéité de la chlorophylle in vivo. I. Spectres d'émission de fluorescence. *Biochim Biophys Acta* 60:510-523, 1962.
22. Lavorel J, Breton J, Lutz M: Methodological principles of measurement of light by photosynthetic systems. In: *Light Emission by Plants and Bacteria*, Govindjee, Amez J, Fork DC (eds). Academic Press, Orlando, 1986, pp 57-98.
23. Marti GE, Magruder L, Schuette WE, Gralnick HR: Flow cytometry analysis of platelet surface antigens. *Cytometry* 9:448-455, 1988.
24. Mauzerall D: Light-induced fluorescence changes in *Chlorella*, and the primary photoreactions for the production of oxygen. *Proc Natl Acad Sci USA* 69:1358-1362, 1972.
25. Murata N, Satoh K: Absorption and fluorescence emission by intact cells, chloroplasts, and chlorophyll-protein complexes. In: *Light Emission by Plants and Bacteria*, Govindjee, Amez J, Fork DC (eds). Academic Press, Orlando, 1986, pp 137-160.
26. Papa S, Capitani S, Matteucci A, Vitale M, Santi P, Martelli AM, Maraldi NM, Manzoli FA: Flow cytometric analysis of isolated rat liver nuclei during growth. *Cytometry* 8:595-601, 1987.
27. Sane PV, Desai TS, Tataka VG, Govindjee: Heat induced reversible increase in photosystem I emission in algae, leaves and chloroplasts: Spectra, activity and relation to state changes. *Photosynthetica* 18:439-444, 1984.
28. Schreiber U, Armond PA: Heat-induced changes of chlorophyll fluorescence in isolated chloroplasts and related heat-damage at the pigment level. *Biochim Biophys Acta* 502:138-151, 1978.
29. Seely GR, Connolly JS: Fluorescence of photosynthetic pigments *in vitro*. In: *Light Emission by Plants and Bacteria*, Govindjee, Amez J, Fork DC (eds). Academic Press, Orlando, 1986, pp 99-133.
30. Sonneveld A, Rademaker H, Duysens LNM: Chlorophyll *a* fluorescence as a monitor of nanosecond reduction of the photooxidized primary donor P-680<sup>+</sup> of photosystem II. *Biochim Biophys Acta* 548:536-551, 1979.
31. Toppari J, Bishop PC, Parker JW, diZerega GS: DNA flow cytometric analysis of mouse seminiferous epithelium. *Cytometry* 9:456-462, 1988.
32. Trebst A, Harth E, Draber W: On a new inhibitor of photosynthetic electron-transport in isolated chloroplasts. *Z Naturforsch* 25:1157-1159, 1970.
33. Velthuis BR: Electron-dependent competition between plastoquinone and inhibitors for binding to photosystem II. *FEBS Lett* 126:277-281, 1981.

## VITA

Chunhe Xu was born on December 27, 1946, in Shanghai, China, where he received his primary and secondary education. In 1970, he graduated from Fudan University. From 1978 to 1981, he did graduate work in Biophysics at the Shanghai Institute of Plant Physiology, Academia Sinica. In 1981 he was awarded the M.S. degree from Academia Sinica. From 1972 to 1978, he worked as a technician in Guizhou Aircraft Ltd. From 1981 to 1986, he did photosynthesis research in the Shanghai Institute of Plant Physiology as an assistant researcher. In 1986, he joined the Biophysics Program as a graduate student, and the Department of Physiology and Biophysics at UIUC as a teaching assistant in Physiology. He received the McKnight Interdisciplinary Research Fellowship from 1987-1991 and held a research assistantship in the Department of Physiology and Biophysics from 1991-1992. He is a coauthor of the following publications:

1. The dynamics of millisecond delayed light emission and its relationship to photophosphorylation. Shen, Y., Xu, C., Wei, J., Li, D., Feng, Y. and Huang, Z. (1984) in: Adv. Photosynth. Res. (C. Sybesma, ed.) Vol. 2, pp. 383-386, Martinus Nijhoff/Dr. W. Junk Publishers, Den Haag.
2. Relationship between the changes of the fast phase of ms delayed light emission and the proton released by the oxidation of water. Xu, C. and Shen, Y. (1984) Science Sinica B. 27, 37-47.
3. Studies on the coupling mechanism of photophosphorylation IX. The uncoupling effect of antibiotic HP-1 on photophospho-

- rylation. Wei, J., Li, D., Xu, C. and Zhang, H. (1985) Acta Phytophysiological Sinica. 11, 42-47.
4. Characteristics of five new photoautotrophic suspension cultures including two *Amaranthus* species and a cotton strain growing on ambient CO<sub>2</sub> levels. Xu, C., Blair, L.C., Rogers, S.M.D., Govindjee and Widholm, J.M. (1988) Plant Physiol. 88, 1297-1302.
  5. Fluorescence characteristics of photoautotrophic soybean cells. Xu, C., Rogers, S.M.D., Goldstein, C., Widholm, J.M. and Govindjee (1989) Photosynth. Res. 21, 93-106.
  6. Stimulatory effect of sodium bisulfite on the cyclic photophosphorylation of chloroplasts under low light intensity. Wei, J., Shen, Y., Li, D. and Xu, C. (1989) Acta Phytophysiological Sinica. 15, 101-104.
  7. Chlorophyll a fluorescence measurements of isolated spinach thylakoids obtained by using single-laser-based flow cytometry. Xu, C., Auger, J. and Govindjee (1990) Cytometry 11, 349-358.
  8. A dual bicarbonate-reversible formate effect in *Chlamydomonas* cells. El-Shintinawy, F., Xu, C. and Govindjee (1990) J. Plant Physiol. 136, 421-428.
  9. Kinetic characteristics of formate/formic acid binding at the plastoquinone reductase site in spinach thylakoids. Xu, C., Taoka, S., Crofts, A.R. and Govindjee (1991) Biochim. Biophys. Acta, 1098, 32-40.
  10. Differential inhibition of Q<sub>A</sub><sup>-</sup> reoxidation by chloroacetates and its relationship with the bicarbonate effect in spinach thylakoids. Xu, C., Zhu, Y. and Govindjee, (1992). submitted to

Biochim. Biophys. Acta.

11. Differential inhibition of  $Q_A^-$  reoxidation by monohalogenated acetates and the bicarbonate-reversible apparent stabilization of  $Q_B^-$  by monochloroacetate in spinach thylakoids. Xu, C., Zhu, Y. and Govindjee, (1992). In preparation.